Transdisciplinary Strategies to Study the Mechanisms of CD4+ T cell Differentiation and Heterogeneity

Adria Carbo Barrios

Dissertation submitted to the Faculty of the
Virginia Polytechnic Institute and State University in
partial fulfillment of the requirements for the degree of

Doctor of Philosophy
in
Genetics, Bioinformatics, and Computational Biology

Josep Bassaganya-Riera, Chair
Raquel Hontecillas-Magarzo
David R. Bevan
Stefan Hoops

June 16th, 2014
Blacksburg, Virginia

Keywords:
CD4+ T cell differentiation, computational immunology, immunoinformatics

Transdisciplinary Strategies to Study the Mechanisms of CD4+ T cell Differentiation and Heterogeneity

Adria Carbo Barrios

Abstract

CD4+ T cells mediate and orchestrate a tremendous panoply of lymphoid cell subsets in the human immune system. CD4+ T cells are able to differentiate into either effector pro-inflammatory or regulatory anti-inflammatory subsets depending on the cytokine milieu in their environment. This complex process is mediated through a variety of cytokines and soluble factors. Yet, the mechanisms of action underlying the process of differentiation and plasticity of this interesting immune subset are incompletely understood. To gain a better understanding of the CD4+ T cell differentiation and function, here we present an array of different strategies to model and validate CD4+ T cell differentiation and heterogeneity. The approaches presented here vary from ordinary-differential equation-based to agent-based simulations, from data-driven to theory-based approaches, and from intracellular mathematical to tissue-level or cellular modeling. The knowledge generated throughout this dissertation exemplifies how a combination of computational modeling with experimental immunology can efficiently advance the scene on CD4+ T cell differentiation. In this thesis I present i) an overview on CD4+ T cell differentiation and an introduction to which computational strategies have been adopted in the field to tackle with this problem, ii) ODE-based modeling and predictions on Th17 plasticity modulated by PPARγ, iii) ODE- and ABM-based cellular level modeling of immune responses towards Helicobacter pylori and the role of CD4+ T cell subsets on it, iv) Intracellular strategies to validate a potential therapeutic target within a CD4+ T cell to treat H. pylori infection, and finally v) data-driven strategies to model Th17 differentiation based on sequencing or microarray data to generate novel predictions on specific components. I present both mathematical and computational work as well as experimental work, *in vitro* and *in vivo* with animal models, to demonstrate how computational immunology and immunoinformatics can help, not only in understanding this complex process, but also in the development of immune therapeutics for infectious, allergic and immune-mediated diseases.

Acknowledgements

When I decided to move to Virginia Tech to pursue my doctoral studies I would have never imagined the series of life changing events that would not only jump-start my professional career, but also build the person I am today. All people listed in this section have made a significant contribution to either my professional or my personal life during these last 4 years.

First and foremost, I would like to thank Dr. Bassaganya-Riera and Dr. Hontecillas. Josep is a synonym of constancy and discipline. When I think of how he has contributed to my professional growth I will always remember a documentary of Xavi Hernandez, a soccer player in Barcelona, who being asked about one of his past coaches and how hard that coach had pushed him, he honestly stated that he will always be thankful to have been pushed up to his limit, because now he realizes what he is capable to do. I feel the same way and I thank Josep for that. I truly thank him for not only giving me great opportunities in research but also for the opportunities given in management and organization. I also thank him for always having his door for any questions I had. On the other hand, I thank Raquel for her constant and her infinite patience. She has coached me all these years with excellent advice. I thank her for her teaching in immunology and for her balanced approach on several aspects. I will use that not only in my professional life but also in my personal one. I would like to thank Dr. Stefan Hoops for his amazing support on COPASI and other computational matters. Especially the first two years where he always answered my questions. I would like to thanks also Dr. David Bevan for his supportive feedback. I am glad I got to see a more academic part of the program with him. Dennie falls in this category and I thank her for all the help she has provided as well. I would like to thank Holly S. Algood, in Vanderbilt University, for showing me how a long-distant collaboration can be run. She helped me understanding some aspects on collaboration-based research that I will surely use in the future. Dr. Yongguo Mei for his great support and his dedication to some of my projects. Such a driven individual. I would like to thank Dr. Barbara Kronsteiner who helped with a lot with my *in vitro* work. I would like to thank Dr. Madhav Marathe for helping me understanding at an early stage that there is another world after ODE modeling. With him, I would like to thank all the NDSSL group (Maksud, Keith, Stephen, Xinwei) that helped me with the HPC computing parts of this thesis. Former student in NDSSL, I would like to thank Kate Wendelsdorf for making me understand that the Ph.D. is a marathon and not a speed race as I used to think.

I had wonderful talks with her in San Francisco and having that experience at that point of my life helped me grow in a personal way.
I would like to truly thank my catalan gang: Monica and Mirs, my two catalan “partners in crime”. I can’t help but to smile when I remember all the moments we have spent together. I will always be thankful for your support in the lab and foremost, outside the lab. I do hope to continue seeing both of them for years and years to come. On that note I would like to thank Kevin, Will, Jeff, Isabel, and Amir, former NIMML members that also helped me at an early stage. Also Pinyi Lu and Casandra Philipson who helped me advance some of my projects. I would like to thank Montse for her support in difficult moments. I wish her every success. To Tricity, Kristen, and Nathan, good luck on your future endeavors and thanks for the help. I would like to thank the business office people who helped and taught me how to deal with business-related items. I will miss the conversations in that office. To the people in the Animal Care Facilities, thanks for providing and helping me with animal related work. I would also like to thank the funding support through the NIH, MIEP and NIMML that allowed me to complete all my work.
Last, this would not have been possible with my personal support: my family who has always supported me in everything I do and taught me that “querer es poder” and that you get everywhere you want with discipline, constancy, and self-esteem. To my friends, thanks for the nights out and keeping me sane during these years. To my friends in Spain, thanks for the long distance support and the long calls on Skype. And last, to John, this would not have been the same without you, so thanks for that.

To all, it’s been an amazing ride, and for that, I thank you!

Attributions

Several authors have been part of the different chapter of this thesis. This section aims to attribute the work of each of them in each chapter.

Chapter 1

Dr. Bassaganya-Riera and Dr. Hontecillas contributed to write the paper and helped designing the sections of the review. Tricity Andrew and Kristin Eden helped delineating the manuscript.

Chapter 2

Dr. Bassaganya-Riera and Dr. Hontecillas contributed to write the paper, design the experiments, and helped designing the sections of the manuscript. Barbara Kronsteiner helped with *in vitro* cultures. Monica Viladomiu, Mireia Pedragosa helped with the *in vivo* animal studies. Stefan Hoops, Madhav Marathe, Stephen Eubank, and Yongguo Mei helped with the computational work.

Chapter 3

Dr. Bassaganya-Riera and Dr. Hontecillas contributed to write the paper, design the experiments, and helped designing the sections of the manuscript. Monica Viladomiu, Mireia Pedragosa, and Barbara Kronsteiner helped with the *in vivo* animal studies. Stefan Hoops, Madhav Marathe, Stephen Eubank, Katherine Wendelsdorf, Maksudul Alam, Keith Bisset, and Yongguo Mei helped with the computational work. Xinwei Dang helped with the statistical analyses.

Chapter 4

Dr. Bassaganya-Riera, Dr. Algood, and Dr. Hontecillas contributed to write the paper, design the experiments, and helped designing the sections of the manuscript. Danyvid Olivares-Villagómez, Rupesh Chatuverdi, Blanca Piazuelo, Alberto Delgado, and M. Kay Washington helped with the *in vivo* animal studies.

Chapter 5

Dr. Bassaganya-Riera and Dr. Hontecillas contributed to write the paper, design the experiments, and helped designing the sections of the manuscript. Tricity Andrew, Kristin Eden, Monica Viladomiu, and Stefan Hoops helped with the computational work.

Table of Contents

Chapter 1

Introduction: Computational Modeling of Heterogeneity and Function of CD4+ T cells

1.1 Summary 1

1.2 Introduction 2

1.3 Mathematical modeling and CD4+ T cell differentiation 4

1.4 Diving into CD4+ T cell lineages: phenotype or function? 7

1.5 Deciphering CD4+ T cell plasticity by using computational modeling approaches 9

1.6 Complementarity of theoretical and data-driven models 11

1.7 Deterministic versus stochastic approaches 13

1.8 Application of multiscale modeling to study CD4+ T cell differentiation 15

1.9 Conclusions 18

Chapter 2

Systems modeling of molecular mechanisms controlling cytokine-driven CD4+ T cell differentiation and phenotype plasticity

2.1 Summary 20

2.2 Introduction 21

2.3 Mathematical modeling of intracellular cytokine pathways controlling CD4+ T cell differentiation 23

2.3.1 T helper 1 cells 25

2.3.2 T helper 2 cells 27

2.3.3 T helper 17 cells 28

2.3.4 Regulatory CD4+ T cells 29

2.3.5 Importance of PPARγ in CD4+ T cell differentiation 31

2.4 The Modeling Process 32

2.4.1 Parameter estimation for dynamics adjustment 33

2.5 PPARγ plays an essential role in modulating CD4+ T cell differentiation and plasticity in a dose-dependent manner 39

2.6 The lack of PPARγ in naïve CD4+ T cells impairs their ability to differentiate into iTreg cells *in vivo* 42

2.7 Pharmacological activation of PPARγ favors a switch of Th17 cells towards an iTreg phenotype *in vivo* 45

2.8 Discussion and Conclusions 50

2.9 Materials and Methods 54

Chapter 3
Predictive computational modeling of the mucosal immune responses during *Helicobacter pylori* infection

3.1 Summary 59

3.2 Introduction 60

3.3 Mathematical modeling of mucosal immune responses to *H. pylori* infection 62

3.4 *H. pylori* modulates CD4+ T cell subsets in the GLN and gastric LP 66

3.5 Myeloid cell-specific PPARγ deletion modulates macrophage, dendritic cell, and T cell differentiation during *H. pylori* infection 68

3.6 Modeling stochasticity in cellular responses during *H. pylori* infection by using ENteric Immunity SImulator (ENISI) 71

3.7 ABM highlights the immunoregulatory role of PPARγ in modulating host responses towards *H. pylori in silico* 74

3.8 Gastric histopathological lesions are formed as a consequence of effector immune activation during the chronic phase of the *H. pylori* infection 75

3.9 Discussion and Conclusions 79

3.10 Materials and Methods 84

Chapter 4

Systems modeling of the role of IL-21 in the maintenance of effector CD4+ T cell responses during chronic *Helicobacter pylori* infection

4.1 Summary 90

4.2 Introduction 91

4.3 IL-21 deficiency leads to increased *H. pylori* colonization in the mouse model 93

4.4 IL-21 deficiency protects *H. pylori* infected mice from chronic gastritis 96

4.5 Chemokine and cytokine expression is abrogated in IL-21 deficient mice 98

4.6 IL-21 deficiency leads to abrogated Th17 and Th1 effector responses 99

4.7 IL-21 contributes to Th17 differentiation and modulates Th1 responses upon infection with *H. pylori* 100

4.8 Experimental validation of model predictions: IL-21 modulates the expression of Th1 and Th17 transcription factors 107

4.9 Expression of markers of T cell regulation (Foxp3 and IL-10) in IL-21 deficient mice 109

4.10 Discussion and Conclusions 110

4.11 Materials and Methods 117

Chapter 5

Modeling the dynamics of T helper 17 induction and differentiation

5.1 Summary 121

5.2 Introduction 122

5.3 Integrated pipeline for data-driven modeling 124

5.4 Microarray data analyses 125

5.5 Network Inference and Analysis 126

5.6 Model implementation 129

5.7 Model calibration using microarray experimental data 129

5.8 *In silico* experimentation and computational modeling predictions 133

5.8.1 IL-24 modulate the production of IL-17A via a FOXP3-dependent RORγt inhibition 133

5.8.2 NLRP3-deficient Th17 cells have an impaired production of IL-17A 135

5.9 Discussion and Conclusions 137

5.10 Materials and Methods 138

Chapter 6

Concluding Remarks 141

Bibliography and References 144

List of figures

Figure 1.1. Main intracellular differentiation pathways of a single CD4+ T cell 06
Figure 1.2. Heterogeneity of CD4+ T cell subsets ……..…….. 08
Figure 1.3. Multiscale modeling of CD4+ T cell differentiation ……..…… 16

Figure 2.1. Iterative systems modeling approaches …… 33
Figure 2.2. Parameter estimation results for the Th17 phenotype …… 36
Figure 2.3. Induction of effector Th1, Th2, Th17, and iTreg phenotype differentiation *in silico* 38
Figure 2.4. Sensitivity analysis on PPARγ by the CD4+ T cell computational model 39
Figure 2.5. Activation of PPARγ regulates differentiation of CD4+ T cells ……..…… 41
Figure 2.6. Effect of PPARγ Th17 and iTreg markers *in vitro* …… 41
Figure 2.7. Activation of PPARγ regulates differentiation of CD4+ T cells ……..…… 43
Figure 2.8. Experimental design to validate PPARγ knockout predictions by the CD4+ T cell computational model …….. 44
Figure 2.9. Effect of PPARγ on Th17 and iTreg markers *in vivo* ……..…….. 44
Figure 2.10. PPARγ suppresses Th17 cell differentiation and upregulates FOXP3 expression *in vivo* ……..…… 45
Figure 2.11. Validation of the modeling prediction regarding the role of PPARγ in regulating the plasticity between Th17 and iTreg ……..…….. 47
Figure 2.12. Improvement in DAI following oral treatment with pioglitazone (PIO) in RAG2-/- mice ……..…….. 48
Figure 2.13. Improvement in mouse body weight following oral treatment with pioglitazone in RAG2-/- mice ……..…… 48

Figure 2.14. Histopathological analysis on colonic tissue from adoptive transfer studies 49
Figure 2.15. Pharmacological activation of PPARγ favors a switch of Th17 cells towards an iTreg phenotype *in vivo* 49

Figure 3.1. Network model of the mucosal immune responses during *Helicobacter pylori* infection 63
Figure 3.2. Effector and regulatory CD4+ T cell subsets modulate the immune responses during *Helicobacter pylori* infection 67
Figure 3.3. Th1 and Th17 responses during *Helicobacter pylori* infection are dose-dependent 68
Figure 3.4. Predicted dynamics of gastric mucosal cell subsets and luminal *Helicobacter pylori* counts following *in silico* infection of wild-type and myeloid-specific PPARγ knockout models 69
Figure 3.5. *In silico* dynamics of gastric mucosal T cell subset in wild-type and T cell-specific PPARγ knockout mice following infection with *Helicobacter pylori* 70
Figure 3.6. ENISI output results after *Helicobacter pylori* infection *in silico* 72
Figure 3.7. ENISI output results and assessment of the role of PPARγ in both the myeloid and T cell subset modulated T cell responses after *Helicobacter pylori* infection *in silico* in the gastric LP and GLN 73
Figure 3.8. Sensitivity analysis of factors involved in gastric inflammatory lesion formation following *Helicobacter pylori* infection 76
Figure 3.9. Experimental design to validate model prediction on main inducers of histopathological changes during *Helicobacter pylori* infection 77
Figure 3.10. Histopathological assessment of the gastric mucosa of mice after *Helicobacter pylori* infection 78

Figure 4.1. IL-21 is required to control *H. pylori* infection in the mouse model 94
Figure 4.2. IL-21 is required for control of bacterial burden, enhances gastritis, Th1 and Th17 cytokine production in C57BL/6 mice 95
Figure 4.3. Inflammation is reduced in *H. pylori* infected IL-21-/- mice compared to *H. pylori* infected wild-type littermates 97

Figure 4.4. *H. pylori* infected IL-21-/- mice express reduced levels of proinflammatory cytokines and chemokines during chronic infection …….…….. 98
Figure 4.5. Th17 and Th1 responses are reduced in *H. pylori* infected IL-21-/- mice compared to *H. pylori* infected wild-type mice ……. 99
Figure 4.6. Calibration process using the CD4+ T cell computational model to adjust dynamics to *H. pylori* specific data ……..…..…… 102
Figure 4.7. Computational fitting of computational model parameters from *H. pylori*-derived RT-PCR and protein data in COPASI ……..……..……103
Figure 4.8. Parameter estimation results and differential reaction on model fluxes after Th17 induction ……..……..…… 104
Figure 4.9. The CD4+ T cell computational model predicts *in silico* modulation of differentiation and maintenance by IL-21 ……..…… 106
Figure 4.10. IL-21 is required for the upregulation of Th1 and Th17 responses and it modulates neutrophil recruitment in the gastric lamina propria during the chronic stages of *H. pylori* infection ……..…….. 107
Figure 4.11. Transcription factors associated with Th1 and Th17 are affected by IL-21 deficiency in the mouse model ……..…… 108
Figure 4.12. IL-21 modulates the expression of IL-10 during *Helicobacter pylori* Infection ……..…… 109
Figure 4.13. Predictive value of the CD4+ T cell differentiation model …..……..…. 113
Figure 4.14 *H. pylori*- specific IgG1 and IgG2a is reduced in IL-21 deficient mice during *H. pylori* infection ……..……..…… 116

Figure 5.1. Integrated data-driven modeling pipeline to generate SBML-compliant, comprehensive, and predictive computational models of Th17 differentiation ……..… 125
Figure 5.2 Network inference and analysis prior to importation into an SBML-compliant environment ……..……..… 128
Figure 5.3 Computational fitting of Th17-related molecules …..……..…… 131
Figure 5.4 Computational fitting of Th17-related molecules (II) ……..…… 132
Figure 5.5. Sensitivity analysis on salt-sensing GSK1 by the Th17 differentiation computational model ……..…… 133
Figure 5.6: *In silico* experimentation: IL-24 modulates IL-17A production through a FOXP3-dependent mechanism ……..…… 135

Figure 5.7: *In silico* experimentation: NLRP3 helps to modulate IL-17A production in Th17 cells …….……..…… 137

List of tables

Table 2.1. Complete assessment of 7 parameter estimations performed by using COPASI's Particle Swarm algorithm with 3000 iterations and a particle size of 50 for reactions number 10, 11, 13 and 14 ……..……. 35

Table 2.2: CD4+ T cell model fitting performed by using COPASI's global parameter estimation …… 35

Table 2.3. Table of assumptions for the representation of activation and inhibition pathways of the CD4+ T cell computational model …….. 36

Table 2.4. Comprehensive summary of stimuli input versus molecule expression Output ……..……. 37

Table 3.1. Immunophenotypic markers used in flow cytometry to characterize immune subsets …… 65

Table 3.2. Evolution of parameter values used in the Agent-Based Model (ABM) and Ordinary Differential Equation (ODE)-based Helicobacter pylori infection models ……. 65

Table 4.1 Reactions involved in IL-21 activation ……..…….. 105

Chapter 1

Introduction: Computational Modeling of Heterogeneity and Function of CD4+ T cells

Adria Carbo, Raquel Hontecillas, Tricity Andrew, Kristin Eden, and Josep Bassaganya-Riera.

Carbo A., Hontecillas R., Andrew T., Eden K., Mei Y., Hoops S., Bassaganya-Riera J. (2014) "Computational modeling of heterogeneity and function of CD4+ T cells" *Frontiers in Cell and Dev Bio*. MBio. 2014 Jul 22;5(4). pii: e01243-14. doi: 10.1128/mBio.01243-14.

1.1 Summary

The immune system is composed of many different cell types and hundreds of intersecting molecular pathways and signals. This large biological complexity requires coordination between distinct pro-inflammatory and regulatory cell subsets to respond to infection while maintaining tissue homeostasis. CD4+ T cells play a central role in orchestrating immune responses and in maintaining a balance between pro- and anti- inflammatory responses. This tight balance between regulatory and effector reactions depends on the ability of CD4+ T cells to modulate distinct pathways within large molecular networks, since dysregulated CD4+ T cell responses may result in chronic inflammatory and

autoimmune diseases. The CD4+ T cell differentiation process comprises an intricate interplay between cytokines, their receptors, adaptor molecules, signaling cascades and transcription factors that help delineate cell fate and function. Computational modeling can help to describe, simulate, analyze, and predict some of the behaviors in this complicated differentiation network. This first chapter provides a comprehensive overview of existing computational immunology methods as well as novel strategies used to model immune responses with a particular focus on CD4+ T cell differentiation.

1.2 Introduction

The human immune system consists of two main behavioral and functional waves: first, the innate immune response provides a first barrier against foreign elements and second, the adaptive immune system builds an effective and specific immune response to combat such elements. The principal function of the adaptive responses is not only the specific recognition to foreign antigens, but also the formation of immunologic memory, and the development of tolerance to self-antigens [1]. Originated in the bone marrow and matured in the thymus, CD4+ T cells are part of the specific adaptive immunity compartment. T cell selection in the thymus allows creating an array of T cell repertoire for antigen recognition, as well as allowing the selection process through MHC-II and the expression of surface markers, such as CD4 or CD8 [2]. Mature CD4+ T cells then translocate into the secondary lymphoid organs, such as the lymph nodes or the spleen, where they are involved in immune surveillance through interaction with MHC-II molecules expressed on the surface of antigen-presenting cells [3]. In this inductive site, naïve CD4+ T cells sample the tissue environment and depending on the cytokine milieu, they differentiate into functionally distinct regulatory and effector subsets.

The central dogma of CD4+ T cell differentiation has evolved over the past decades as new studies have unveiled differentiation pathways and novel mechanisms shaping the CD4+ T cell compartment. The Th1 versus Th2 conceptual framework that Mossman and Coffman provided [4] was largely expanded when novel discoveries on RORgt and IL-17A producing T cells defined the Th17 phenotype [5] and with the identification of

FOXP3 raised as a key transcription factor in charge of driving the regulatory response in CD4+ T cells [6, 7]. Recent in-depth characterization of CD4+ T cell lineages has resulted in the discovery of new phenotypes, positioning the CD4+ T cell population as one of the most heterogeneous immune cell subsets. Furthermore, the latest discoveries are pushing the understanding of CD4+ T cell differentiation from a 4-player game to a multi-pronged interplay of complex networks and common transcription factors and cytokines with highly plastic functionalities. As an example, the production of IL-9 by the transcription factor PU.1 leads to the establishment of the Th9 phenotype [8]. Furthermore, other phenotypes, such as Th17, are now under scrutiny since IL-17 and IL-22 are co-expressed in an IL-23 dependent manner [9, 10]. New studies are pointing out to the aryl hydrocarbon receptor (AhR) as the master transcription factor responsible for IL-22 secretion [11], leading to the designation of a new CD4+ T cell phenotype, Th22. Moreover, FOXP3-independent IL-10 upregulation has been implicated in the activation of the regulatory axis under the regulatory type 1 (Tr1) CD4+ T cells [12]. Lastly, follicular T helper cells (Tfh) have become an object of intense study since they have been described as a very plastic subset that could swift the CD4+ T cell balance. Tfh cells can leave the T cell areas and localize in the B cell follicle, a migration that is facilitated by their concurrent expression of the B cell zone homing chemokine receptor CXCR5 and downregulation of the T cell zone homing chemokine receptor CCR7 [13, 14]. Thus, this close proximity to B cells allows Tfh cells to support their activation, expansion and differentiation. To help promote this crosstalk with B cells, Tfh cells produce IL-21 via activation of the transcription factor BCL-6, thereby promoting a Th1/Th17 profile. Also, IL-2 is emerging as a trigger for Th1 differentiated cells to adopt a Tfh-like phenotype by down-regulating BLIMP1 and interacting with STAT proteins [15]. Since the BCL-6 pathway is linked to STAT factors induced by IL-6 that in turn promotes IL-21 and TNFa production, the study of the role of Tfh is important in the context of infectious, immune-mediated or chronic inflammatory diseases.

Computational modeling has become an indispensable tool to synthesize, organize, and integrate diverse data types and theoretical frameworks to help generate new knowledge and guide *in vivo* experimentation. This chapter highlights how computational modeling has helped advancing the understanding of signaling events controlling CD4+ T

heterogeneity and it also discusses new opportunities in the context of modeling strategies and tools.

1.3 Mathematical modeling and CD4+ T cell differentiation

Initial attempts to apply computational modeling approaches to study CD4+ T cell differentiation only focused on the Th1 and Th2 phenotypes. Indeed the well-established dichotomy between these two phenotypes is supported by extensive information on how T-bet (Th1) and GATA3 (Th2) interact. One of the first published studies extrapolated the Th1/Th2 experimental facts into systemic behavior during an immune response, indicating that suppression and domination of one phenotype over the other could dictate the final differentiation outcome [16]. In this study, the model encompassed not only Th1 and Th2, but also the effect of antigen presentation via APCs. This mathematical model illustrated how the final differentiation of Th1 or Th2 depends in both the competition for antigenic stimulation and the cytokine mediated cross suppression between phenotypes. Subsequent studies applied mathematical modeling to study the Th1 and Th2 phenotypes in the presence of other cytokines such as IL-10 or TGFb [17], antigen availability and instructional intracellular feedbacks [18, 19], upregulation of the master transcription factors T-bet and GATA3 [20, 21] or in the context of cancer and rejection of melanomas [22]. These modeling efforts highlighted the differences between instructive and feedback mechanisms as well as activated pathways in both phenotypes. Other studies solely focused on a single phenotype, such as the work published by Schultz et al. [23] where the computational model revealed that Th1 differentiation is a two-step process in which the early Th1 cell-polarizing phase is followed by a later phase showing expression of T-bet. Hofer at al. [24] published a mathematical model showing that GATA-3 transcriptional activation creates a threshold for autoactivation, resulting in two GATA-3 expression states: one for basal expression and one of high expression sustained by its autoactivation.

As new data became available, the increasing complexity of the CD4+ T cell paradigm became evident and new computational approaches were developed to ascertain the

regulatory mechanisms controlling differentiation, plasticity and heterogeneity. Van den Ham et al. [25] developed an ODE-based model that describes important regulators and allows for stable switches between several different phenotypes. Other studies focused on the interaction of Th17 and iTreg since Betelli et al. [26] described the functional antagonism of Th17 and iTreg. For instance, Hong et al. [27] constructed a mathematical model of Th17/Treg differentiation that exhibited functionally distinct states, including a RORgt+ FOXP3+. While reductionist approaches have improved our ability to understand small components of the system, studying CD4+ T cell heterogeneity often requires implementing systems approaches and computational methods that can help deciphering complexity. Computational models of CD4+ T cell differentiation and heterogeneity are needed to accurately represent how CD4+ T cells are differentiated and accurately predict sensitivities to determine which pathways and molecules can be most critical to switch from one phenotype or another. A major challenge in systems-level models is the calibration process. Estimation of parameters of large-scale CD4+ T cell differentiation models have proven successful [28] by following a "divide-and-conquer approach". This approach is highly useful when parameterizing large models with more than one parameter. First the parameter calibration is divided into smaller parameter estimations: one estimation per phenotype represented in the model. If necessary, other parameter estimations involving specific interactions, such as the Th1/Th2 or the Th17/Treg crosstalk, can be performed. Once parameters are located in a more targeted parameter space, a global parameter estimation is run with all the parameters in the model, allowing us to identify a good global parameter set. These approaches can be easily performed using modeling software such as COPASI [29].

The CD4+ T cell differentiation model described in [28] allows the user to have a global understanding with 4 CD4+ T cell phenotypes represented. The most recent systems biology markup language (SBML)-compliant network [30] provides a structured understanding on different pathways involved in CD4+ T cell differentiation (Figure 1.1). Another example would be the model by Mendoza et al. [31]. In this model, a continuous dynamical system, in the form of a set of coupled ordinary differential equations, was used. Such strategy was then applied to a regulatory network of 36 nodes, representing four CD4+ T cell phenotypes (Th1, Th2, Th17, and Treg). Although this model creates a framework for four phenotypes, the calibration of this larger network, however, was not

conducted with experimental data but with default parameters that enabled the differentiation of the 4 phenotypes, not taking in consideration if reactions occur in a rapid or slow fashion, for example.

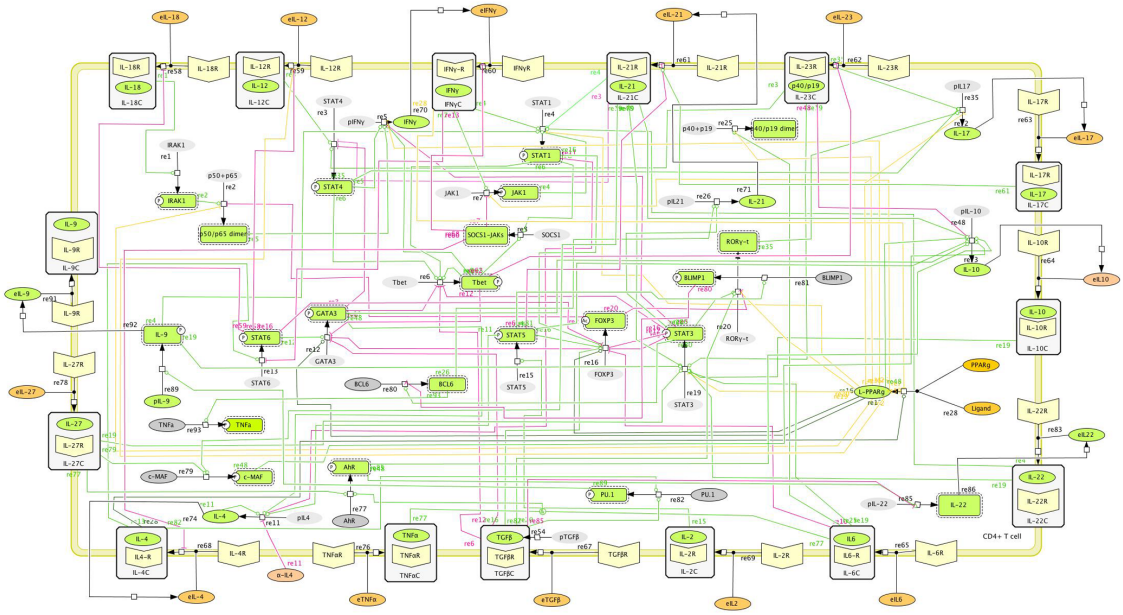

Figure 1.1. Main intracellular differentiation pathways of a single CD4+ T cell. Systems Biology Markup Language (SBML)-compliant network model of CD4+ T cell differentiation, including cytokines, receptors and intracellular signaling pathways controlling CD4+ T cell fate and function Figure 1.

Others have explored the contribution of different CD4+ T cell phenotypes to the modulation of immune responses towards *Helicobacter pylori* infection [32]. This study aimed to provide new mechanistic insights on the dynamics of mucosal Th1, Th17, and Treg cells by using both an ODE and agent based (ABM) cellular model of the mucosal immune responses during *H. pylori* infection. Alternatively, the logical model strategy has also been used to explore CD4+ T cell differentiation. Mendoza et al. applied [33, 34] either continuous or discrete dynamical systems, regulatory networks of Th1/Th2 or of a combination of different transcription factors adding Th17 and iTreg to represent different states. Even though network modeling has shown to be appropriate, as the production of high-dimensional experimental data is increasingly becoming available, other methods, such as ODE-based or agent-based modeling [29, 35, 36], could help understanding the mechanisms of CD4+ T cell differentiation at the systems level.

1.4 Diving into CD4+ T cell lineages: phenotype or function?

CD4+ T cells form a complex and highly specialized network, representing a major population implicated in mediating host protective and homeostatic responses. However, their excessive or uncontrolled accumulation can also represent a feature in different diseases such as Inflammatory Bowel Disease (IBD) [37], Alzheimer's disease [38], multiple sclerosis [39], or allergic disease [40], among many others. Therefore, their function is closely guided by external signals that are captured from the environment. Also, CD4+ T cells orchestrate immune responses by modulating the function of other cell subsets, such as dendritic cells or macrophages, through secretion of an array of soluble factors, cytokines, and chemokines into the environment. The cytokine profile secreted by each CD4+ T cell will directly depend on which intracellular molecular pathways have been activated, which cytokines are released and how the priming of the single CD4+ T cell has occurred. As an example, IL-6 and TGFβ will activate the Th17 transcriptional machinery, composed by RORgt, RORa, and the phosphorylated form of STAT3. These molecules will activate the transcription of IL-21 and IL-17 and will direct the cell into a Th17 phenotype. However, when a CD4+ T cell is located in an environment rich in TGFb, lacking IL-6 or other pro-inflammatory cytokines, TGFb will promote FOXP3 and the phosphorylated STAT5, resulting in the secretion of IL-10 and TGFb that will activate the regulatory axis. This differentiation dichotomy also depends in part on the T-cell receptor (TCR) engagement and a co-stimulatory signal, frequently involving the CD28 receptor: two basic signals required for a full CD4+ differentiation process. Indeed, Miskov-Kizanov et al. showed how the duration of T cell stimulation through the TCR receptor is a critical determinant of cell date and plasticity by constructing a logic circuit model of TCR signaling pathways in CD4+ T cells [41].

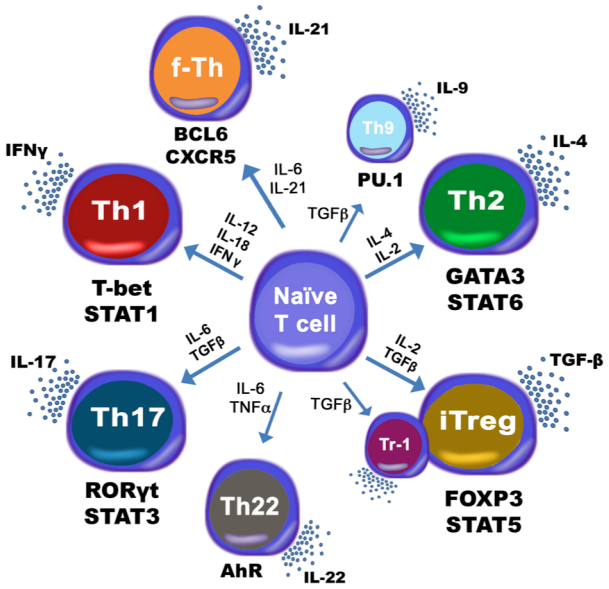

Figure 1.2. Heterogeneity of CD4+ T cell subsets: T helper type 1 (Th1), type 2 (Th2), type 17 (Th17), type 9 (Th9) and type 22 (Th22), Follicular T helper cells (Tfh), and induced regulatory T cells (iTreg) as well as type 1 regulatory T cells (Tr1).

CD4+ T cells have a strong predisposition to certain programming and developmental programs enabled by the cytokine environment. However, in the context of disease, where plasticity between phenotypes appears to be the norm, rather than the exception, double positives, such as IFNg/IL17A often appear in pathological states such as in the context of murine colitis, where the accumulation of IL-17A+ IFNg+ seems to occur in an IL-23 dependent manner [42]. Moreover, several studies showed that IL-17A could potently induce type 2 diabetes [43-45] potentially by modulating the pathogenesis of insulin resistance induced by angiotensin II type 1 receptor [46] hence increasing the production of renal nitric oxide [47]. Th17 also showed a pleiotropic functionality, since intestine IL-17A+ IL-10+ T cells were found in the small intestine following treatment with anti-CD3 antibody, known to induce an immunosuppressive environment [48]. Furthermore, intestinal epithelial lesions were accentuated in IL-17A null mice [49]. These implications support a theory, whereby CD4+ T cells are not defined by its inflammatory status but by the functions they accomplish after being exposed to the cytokine milieu. The CD4+ T cell compartment has been demonstrated to be governed, not only by phenotype, but also by function, therefore forcing the distinction between a stable T cell lineage and a T cell differentiation state. Indeed, the ability of a CD4+ T cell to choose a predetermined differentiation program has been shown to be more complex than expected. This determination seems to now bow down to a more functional approach, where CD4+ T cells are not determined by phenotype, but by function, as needed. The traditional view on the CD4+ T cell dogma has now changed into a more comprehensive vision, where

not only 2 or 4, but 8 known phenotypes are represented and new phenotypes or states are likely to emerge (Figure 1.2).

1.5 Deciphering CD4+ T cell plasticity by using computational modeling approaches

Transcription factors, T-cell receptor, chemokines, surface receptors, and cytokines determine how CD4+ T cells become activated, maintained and how they can mature into distinguishable featured profiles. However, an increasing understanding on how the mechanisms of differentiation work is revealing increased flexibility and plasticity between different CD4+ T cell phenotypes that allow functional heterogeneity. As discussed above, the functional plasticity between Th1 and Th17 cells resulting in IFNg+ IL-17A+ CD4+ T cells [50, 51] has already been investigated. Indeed, Th17 has been shown to be a very unstable phenotype [52]. Functionally, Th17 cells during mucosal inflammation seem significantly different than those Th17 cells involved in regulating homeostasis at the steady state. Whereas IL-17A single positive Th17 cells produce IL-22, which may provide a mechanisms through which Tregs cells reinforce the epithelial barrier [53], this same Th17 population can accumulate and produce additional mediators such as IFNg or GM-CSF during gut inflammatory disorders [42, 54, 55]. CD4+ T cell plasticity is not only initiated by a change within the intracellular compartment, but also by a change in the extracellular environment. Th1 cells have been demonstrated to acquire plasticity towards a follicular T helper (Tfh)-like phenotype when they encounter a cytokine milieu that is not rich in IL-2 [56, 57]. The regulatory phenotype iTreg has also been reported to adopt plasticity mechanisms. Several studies have identified, for example, a double RORgt+ FOXP3+ [58, 59] that can further differentiate into a pathogenic IL-17-expressing CD4+ T cell [60]. These examples illustrate the need for improving our mechanistic understanding at the systems level, where plasticity in the *in vivo* setting needs to be at focus.

Computational methods have also been applied to study the plasticity of CD4+ T cells. Magombedze et al. considered a population plasticity mechanism between Th1 and Th2

during Mycobacterium avium infection by using a reduced ODE-based model where the phenotype change of MAP-specific T cells occurred due to differences in the rates of differentiation, proliferation and death at the site of infection [61]. However, the cellular plasticity involving several intracellular pathways was not represented. In contrast, Pedicini et al. used computational models to analyze the cellular plasticity between Th1 and Th2 cells, extending the regular Tbet/GATA3 plasticity predictions to a broader panel of molecules, involving IRF4, STAT1 and STAT6, MAF, NFAT, and SOCS1 [62]. More comprehensive approaches have also been explored by using extended logical formalisms with Boolean variables to assess the effect of different cytokines in making a CD4+ T cell evolve towards a specific state [63]. As a general rule, validation studies are performed to endorse and corroborate the usefulness of computational models. Whereas computational models may be used for in silico experimentation, in vivo and in vitro validation needs to be performed in order to ensure its predictability and prove that the plasticity described in silico can be translated into an in vivo setting in those cases. To address plasticity in vivo, the modeling cycle needs to be completed; first, the model needs to be created based on either available data and/or theory-driven knowledge. Afterwards, calibration procedures need to ensure that a good parameter value set has been found and quality control needs to be run to check that the computational model fully represents our experimental data. Third, in silico experimentation, using loss-of-function, overexpression or sensitivity analysis strategies need to be performed. Finally, in vivo or in vitro validation studies will authenticate the computational model and serve as future calibration data for model refinement. These new approaches are helping immunologists to target novel experiments that will shed some light to the subjective issue of CD4+ T cell plasticity.

The computational CD4+ T cell differentiation landscape has generated several validated studies. We validated experimentally that activation of the transcription factor peroxisome proliferator activated receptor gamma (PPARg) favored the plasticity of Th17 cells towards iTreg cells, a key prediction of our CD4+ T cell model [28]. This model consisted of 60 differential equations, representing 52 reactions and 93 species, computing the differentiation of a CD4+ T cell into Th1, Th2, Th17, and Treg. The model included cytokines, nuclear receptors and transcription factors that defined fate and function of CD4+ T cells. The first set of computationally derived hypotheses were

centered around PPARγ and its modulatory role between Th17 and iTreg. Time course simulations illustrated how PPARγ can trigger plasticity in IL-17A+ producing Th17 cells, causing the system to become a iTreg CD4+ T cell. To validate this prediction, *in vitro* and *in vivo* experiments in the context of an IBD onset were designed with PPARγ null CD4+ T cells as well as with a treatment with pioglitazone, a PPARγ activator. The study presented in [41] also validated the interaction of FOXP3 and mTOR following TCR activation by purifying and activating DCs and CD4+ T cells and assessing the expression of different intracellular markers using cell staining and flow cytometry. Another example is the validation of the time-dependent, dual T-bet wave during Th1 differentiation validated using gene expression analysis in CD4+ T cells isolated from wild-type and IFNγ null mice [23].

1.6 Complementarity of theoretical and data-driven models

In computational immunology, often times, the available knowledge about a given set of biological events is used to construct a specific mathematical model. This theoretical approach is therefore directly correlated to the amount of information that is publicly available and the model created upon these pieces of data will only represent the processes delineated within. On the other hand, models can be constructed based solely on analyzing data itself. The increasing availability of high-dimensional data to quantify signaling and cellular responses, together with the novel sequencing technology advancements, is opening a new avenue to use these data-rich datasets to build computational models to help understanding CD4+ T cell differentiation responses. This systems-biology approach, however, can be a double-edged sword: generating high-throughput datasets are part of a big-data strategy, and sometimes, without the appropriate tools, can bring more confusion than understanding to the problem [64]. On the other side, this increased availability of data, if used correctly, can streamline the modeling approach, offering a tremendous amount of data for calibration purposes that could allow modelers to build fully calibrated, predictive and extremely comprehensive models that could help generate important hypotheses. These two opposed modeling views can actually be used as a complementary strategy. Theoretical models lack data

either for network architecture construction or for model calibration. Data-driven modeling, however, are sometimes confusing, and lack general rules to guide the user and make sense of such big pieces of data. Combining the organization-based approach from theory-driven models with the amount of data and novelty from the data-driven model, highly predictive, hybrid models can be ultimately constructed. In fact, substantial evidence has been shown to understand that the just and only use of data-driven models can represent a trap. The so called “Big Data Hubris” (the often implicit assumption that big data are a substitute, rather than a supplement to, traditional data collection and analysis) already triggered an overestimation of Google’s overestimation on flu prevalence in 2013 [65]. This is a clear example on how data-based and data-driven results were wrongly generated due to the lack of theory underlying unstructured data integration.

The long-standing traditional theory-driven approach has been proven to provide helpful insights on how CD4+ T cells function, where modeling strategies are based on prior biological understanding of the molecular mechanisms involved [16, 24, 27, 33, 66]. However, often times theory-driven modeling is intimately linked to reductionist approaches, since the availability of calibration data can become an issue if building comprehensive networks. Data-driven modeling emerges as a new and complementary approach for multivariate analysis and systems-level analyses. An example on how to use high-throughput data to construct a CD4+ T cell comprehensive network is the study published by Yosef et al., where they used transcriptional profiling with microarrays at high temporal resolution to build a Th17 induction system [67]. In this study, 1,291 genes were differentially identified and clustered into 20 groups, depending on their temporal profiles. Another advantage highlighted in this study is the use of modules to explain the processes controlling Th17 differentiation. Four regulatory modules were identified: the positive module that increased IL-17 levels, the negative module that downregulated IL-17, the signature of Th17 genes and signature of other CD4+ T cell subtypes. This work supported the finding of 3 novel key regulators of Th17 function: *Mina*, *Fas*, and *Pou2af1*. Another study where data-driven approaches were taken was the work performed by Ciofani et al., where they combined genome-wide transcription factor occupancy, expression profiling of transcription factor mutants, and transcriptional regulatory network [68]. Integration of several datasets allowed the inference of a Th17

network that highlighted some key regulators to Th17 plasticity, such as *Fosl2*. These two approaches have unveiled novel nodes by using a data-driven approach. However, both networks, which represent static pictures, lack dynamics running on the background. By adding dynamics to the system, a whole new dimension can be added. These data-rich models could be used to determine how the system evolves when a node is knocked-out, or how sensitive are reactions and fluxes to change by a special drug or modulator in a more mechanistic manner. A counterfactual example related to the CD4+ T cell differentiation process is the role of IL-17A in chronic inflammation during IBD. Although it has been reported increased expression of IL-17A during IBD [69] and both IL-17R-deficient mice in TNBS-induced colitis model [70] as well as IL-17A-deficient mice in a DSS-induced colitis model [71] were reported to worsen the clinical disease symptoms, some other opposing studies highlighted the protective role of IL-17A production *in vivo* [72]. In this case, where it is clear there are missing pieces in this puzzle, a combined strategy with both theory-driven and data-driven modeling could shed some light by looking at other players in these intricate and complex interactions.

Data-driven modeling nicely complements and synergizes with theory-driven due to the availability of data for calibration purposes, the potential of discovering novel regulators in the network that have never been described before, and the capability to comprehensively and mechanistically understand complex systems. At the same time, hypotheses extracted from modeling need to be validated to become accepted theories by the community. The combination of theory driven models with data-driven approaches is becoming a strong, useful tool to ensure that the basic knowledge is represented, but at the same time, that novelty and higher predictability is reached.

1.7 Deterministic versus stochastic approaches

In complex regulatory schemas, such as the CD4+ T cell differentiation network, gene expression is controlled by transcriptional signals that determine how rapid and how often a specific gene is transcribed. This transcription process, however, depends on

other signals and molecules, such as transcription factors and promoter signals that will trigger cell-to-cell variability. Often times, gene transcription is a result of a combination of other signaling cascades, therefore adding not only complexity and variability due to the differential activation of upstream molecules, but also a time delay while the signal molecule concentration either accumulates or decays.

In CD4+ T cell differentiation, variability is a key component of the process. In fact, not all the cells expressing RORgt exhibit IL-17A production even in the presence of the correct inductors TGFb and IL-6 [58]. Furthermore, Guo et al. showed how IL-4 secreting and non-secreting cells from Th2 cultures have a similar probability of producing IL-4 upon subsequent stimulation, implying that there is stochastic element in IL-4 production by stimulated Th2 cells [73]. Even after assuming that most genes are expressed from both alleles when the transcription machinery is in place, some studies point out that some cytokine genes in T cells are often expressed in a monoallelic manner [74]. Alternatively, the transcription rates also vary if agonistic transcription factors are bound [75]. Given these set of premises, stochastic approaches that add this type of variability within the CD4+ T cell subset can be used to help explain biological variation. In this case, this variability offers a unique way to control regulation, by inducing stimuli but controlling the fraction of cells expressing a specific cytokine.

Deterministic models of CD4+ T cell differentiation are more prevalent than stochastic-based models. Of note, deterministic approaches have unveiled a large amount of findings that relate to single cell behavior. A fraction of these models have focused on the analysis of one phenotype only [23, 76], and other models have focused on more than one phenotype and the interactions between the resulting states [25, 27, 28, 76]. Mariani et al., in contrast, used a stochastic approach to show how an IL-4 stochastic mechanism acting at the chromatin level can be integrated with transcriptional regulation to quantitatively control cell-to-cell variability [77]. Furthermore, Santoni et al. used an agent-based model to assess Th1 versus Th2 fates in the context of hypersensitivity reactions [78]. Recently, Mei et al. assessed the role of the IL-6 receptor in controlling the balance between Th17 and iTreg using a novel, web-based stochastic modeling tool [79]. Other approaches have used the mathematical formulation of a cell population master equation (CPME) that describes population dynamics and takes into account the

major sources of heterogeneity, namely stochasticity in reaction, DNA-duplication, and division, using the Montecarlo algorithm [80]. Manninen et al. [81] developed several approaches to incorporate stochasticity into deterministic differential equation models, obtaining so-called Itô stochastic differential equations, and applied them to neuronal protein kinase C signal transduction pathway modeling. Even though traditional molecular biology research has tended to composite single cell deterministic models, diversification of T cell fate during CD4+ T cell differentiation implies that the fate of any individual cell may also be acquired stochastically. Therefore, stochastic simulations within the CD4+ T cell differentiation process could help to understand the tight regulation between phenotypes as well as help identify key nodes that, when acting at higher variability, can skew the output of differentiation into a specific differentiation program.

1.8 Application of multiscale modeling to study CD4+ T cell differentiation

CD4+ T cell differentiation is a process where a change in the intracellular compartment can tremendously impact the outcome of tissue pathology and clinical disease. Distinct intracellular processes dictate the secretion of chemokines, cytokines, and other soluble factors. These components can, at the same time, modulate other CD4+ T cell nearby by binding to specific receptors. This population effect can modulate other downstream immune subsets that can ultimately affect the formation of lesions at the tissue level. Thus, CD4+ T cell differentiation is not only an intracellular process: population and cellular organization are another major mechanism that may contribute to the change in the dominant phenotype of effector CD4+ T cells during chronic pathologies [82]. Indeed, the mucosal immune system includes hierarchical interactions between cells leading to emerging behaviors with dimensions ranging from nanometers to meters and time scales from nanoseconds to years. The spatiotemporal scales where CD4+ T cells participate can actually range from micro-seconds to months or years and to nanometers to centimeters or meters (Figure 1.3A).

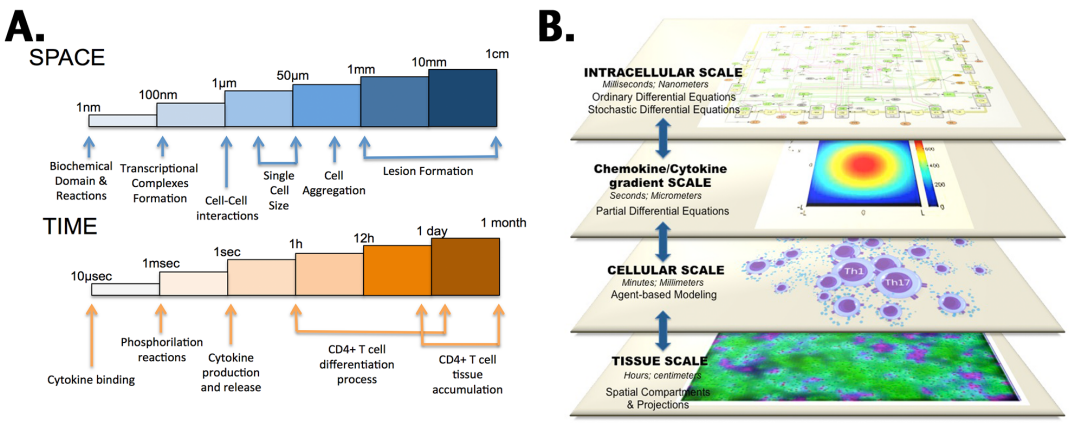

Figure 1.3. Multiscale modeling of CD4+ T cell differentiation. The CD4+ T cell differentiation process comprises different scales (intracellular, gradient, cellular, and tissue-level scale) as well as different spatiotemporal parameters (milliseconds to hours and nanometers to centimeters).

Complex and dynamic information processing networks transfer information across scales in immunity encoding host responses and repair measures. The architecture of such multiscale network also needs to be completely embedded in a comprehensive, integrated system. Because of this flexibility in parameter calibration and sensitivity analyses, Ordinary or Stochastic Differential Equations (ODE or SDE) are ideal candidates to encapsulate and simulate intracellular events. In the multiscale setting, these ODE- or SDE-based models would reproduce intracellular CD4+ T cell activation with a release of cytokines and chemokines as a result of the process of differentiations. Partial Differential Equation (PDE) modeling would be a great way to simulate the diffusion reactions of such cytokines in the environment. Ultimately, an agent-based model, adding randomness to the biological system, which helps to better represent responses at the cellular level, would encompass and organize the ODE/SDE models with the PDE simulations by simulating CD4+ T cells as objects that can change its state depending on the cytokine milieu. As a result of these premises, multiscale models are positioned as a comprehensive tool to understand not only the intracellular events happening within the CD4+ T cell compartment at a single cell level, but also understanding the interactions and sensitivities, at the cellular, population and tissue levels, that contribute to disease chronicity, tolerance, or resolution (Figure 1.3B).

All together, ODE models can calculate the intracellular concentration of different species over time, PDE models could analyze the gradient concentration of cytokines

and chemokines secreted by the ODE model, ABM based models could modulate the cell-cell interactions and spatial compartments could represent the tissue-level scale, including lesion formation. Current experimental techniques are limited in allowing immunologists to quantitatively manipulate immune responses to pathogens in a controlled manner in animal models and to trace events at the tissue level confidently back to specific cellular level interactions and molecular or signaling mechanisms. In a multiscale model, one can test whether mechanisms seen in the experimental context in vivo or in vitro are plausible explanations for phenomena observed at the clinical level. There have been several previous studies on multiscale modeling in the context of immunity: Sloot et al. [83] proposed a multi-scale modeling methodology in computational biomedicine and presented two cases studies. Krinner et al. [84] coupled an agent-based model of hematopoietic stem cells with an ODE model of granulopoiesis. Also, Klinke [66] published a multiscale model of dendritic cell education and trafficking in the lung. Some very recent multiscale approaches to study the CD4+ T cell population have been performed in the context of HIV infection [85] and also in the context of CD4+ T cell migration, signaling, and interaction with the APC compartment [86]. Furthermore, Dwivedi et al. recently developed a multiscale systems model of IL-6–mediated immune regulation in Crohn's disease, by integrating intracellular signaling with organ-level dynamics of pharmacological markers underlying the disease [87]. Despite all these strategies and studies, there is no multiscale model that computes CD4+ T cell differentiation based on the availability of certain factors in the environment and considers more than one scale in the simulation.

Multiscale modeling may also help integrate immune processes and metabolic pathways to build systems-level immunometabolic frameworks. Indeed, T cell metabolism is highly dynamic and has a tremendous impact on the ability of T cells to grow, activate and differentiate [88]. Glucose metabolism is one of the pathways that has been target to explore immunometabolism. One example is the study from Maciver et al. where they found that activation of T cells causes a large increase in glucose transporter 1 (Glut1) expression and surface localization [89]. Furthermore, CD28 appeared to promote Akt-independent up-regulation of Glut1 and Akt-dependent Glut1 cell surface trafficking [90]. Multiscale modeling analyses could also help to differentiate which are the metabolic needs to promote specific developmental programs. In fact, effector and regulatory

phenotypes have distinct glycolytic and lipid oxidative metabolic programs [91]. Pearce et al. reviewed [92] how activated T cells have an anabolic metabolism, whereas non-proliferating T cells had an opposed catabolic metabolism. Furthermore, autophagy has been found to be essential for T cell survival and proliferation [93]. Later the same group described how the same process of autophagy may have a physiologically significant role in the clearance of mithocondria in T cells as part of normal T cell homeostasis [94], creating a clear link between immunometabolism and T cell function. By using a multiscale strategy, these metabolic programs could be integrated in differentiation simulations and more importantly, the processes could be manipulated to control anti- and pro-inflammatory development in the context of inflammatory diseases. Thus, modeling can be used to quantitatively study dynamic processes located at the interface of immunity and metabolism.

Of note, understanding the mechanisms of CD4+ T cell differentiation and plasticity across scales can lead to the identification of novel therapeutic targets for skewing effector cells into regulatory phenotypes that suppress inflammation. Therefore, multiscale modeling can, indeed, increase predictability and systems-wide mechanistic understanding as to how CD4+ T cells are activated, maintained, and transformed.

1.9 Conclusions

T cell immune responses are extremely heterogeneous and complex. This variability is not fully understood and there are still several questions in regards to CD4+ T cell plasticity and function. Indeed, the issue of what criteria to use to characterize distinct T cell subsets is becoming increasingly complicated. Moreover, the idea that CD4+ T cells are governed by function and not by phenotype is clearly emerging as more double positive and plastic behaviors are being unveiled. The possibility that every helper T cell process is a unique combination of molecules, however, cannot be discarded. This review highlighted how CD4+ T cells have a strong predisposition to certain developmental programs, but it also showed how, at certain times with certain environmental signals, this predisposition is skewed towards another program.

Computationally, the plural CD4+ T cell scenario is still a field of interest and active investigation. As new advancements in the understanding of immune responses continue to unfold, computational modeling approaches are likely to be required to comprehensively and systematically investigate mechanisms across spatiotemporal scales and to help integrate diverse data types.

Chapter 2

Systems modeling of molecular mechanisms controlling cytokine-driven CD4+ T cell differentiation and phenotype plasticity

Adria Carbo, Raquel Hontecillas, Barbara Kronsteiner, Monica Viladomiu, Mireia Pedragosa, Pinyi Lu, Stefan Hoops, Madhav Marathe, Stephen Eubank, Yongguo Mei, and Josep Bassaganya-Riera.

Carbo A., Hontecillas R., Kronsteiner B., Viladomiu M., Pedragosa M., et al. (2013) "Systems Modeling of Molecular Mechanisms Controlling Cytokine-driven CD4+ T Cell Differentiation and Phenotype Plasticity". *PLoS Comput Biol* **9(4)**: e1003027. doi:10.1371/journal.pcbi.1003027

2.1 Summary

Differentiation of CD4+ T cells into effector or regulatory phenotypes is tightly controlled by the cytokine milieu, complex intracellular signaling networks and numerous transcriptional regulators. We combined experimental approaches and computational modeling to investigate the mechanisms controlling differentiation and plasticity of CD4+ T cells in the gut of mice. Our computational model encompasses the major intracellular pathways involved in CD4+ T cell

differentiation into T helper 1 (Th1), Th2, Th17 and induced regulatory T cells (iTreg). Our modeling efforts predicted a critical role for peroxisome proliferator-activated receptor gamma (PPARγ) in modulating plasticity between Th17 and iTreg cells. PPARγ regulates differentiation, activation and cytokine production, thereby controlling the induction of effector and regulatory responses, and is a promising therapeutic target for dysregulated immune responses and inflammation. Our modeling efforts predict that following PPARγ activation, Th17 cells undergo phenotype switch and become iTreg cells. This prediction was validated by results of adoptive transfer studies showing an increase of colonic iTreg and a decrease of Th17 cells in the gut mucosa of mice with colitis following pharmacological activation of PPARγ. Deletion of PPARγ in CD4+ T cells impaired mucosal iTreg and enhanced colitogenic Th17 responses in mice with CD4+ T cell-induced colitis. Thus, for the first time we provide novel molecular evidence *in vivo* demonstrating that PPARγ in addition to regulating CD4+ T cell differentiation also plays a major role controlling Th17 and iTreg plasticity in the gut mucosa.

2.2 Introduction

The CD4+ T cell differentiation process activates the transcriptional and secretory cellular machinery that helps orchestrate immune modulation in infectious, allergic and immune-mediated diseases. Upon antigen presentation, naïve CD4+ T cells become activated and undergo a differentiation process controlled by the cytokine milieu in the tissue environment. For instance, interleukin-6 (IL-6) in combination with transforming growing factor β (TGF-β) trigger a naive CD4+ T cell to become a T helper 17 (Th17) cell [26, 95]. In contrast, TGF-β alone can activate regulatory pathways leading to differentiation of naive CD4+ T cells into an induced regulatory CD4+ T cell (iTreg) phenotype, which in turn tightly dampens effector and inflammatory responses.

CD4+ T cell differentiation was once viewed as a rigid process whereby a naive cell differentiated into terminal phenotypes. However, mounting evidence supports the tissue environment-dependent plasticity of CD4+ T cell subsets and suggests the emergence of new phenotypes [9, 96, 97]. At the molecular level, plasticity is achieved by a cytokine-driven reprogramming of signaling pathways and targeted activation of master regulator transcription factors which results in gene expression changes [98]. Antigen

presenting cells (APCs) influence T cell differentiation through antigen presentation, co-stimulation and cytokine secretion [99]. The crosstalk between T cell phenotypes has been fully characterized in terms of classical Th1 versus Th2 differentiation [100-103]. Indeed, a logical network model of CD4+ T cell differentiation process centered around Th1 versus Th2 differentiation was published by Mendoza [33]. However, this logical model did not consider the Th17 or iTreg cell subsets. In the last decade, Th17 has emerged as an extremely plastic phenotype [50, 98, 104, 105] that can acquire regulatory functions following changes in the local cytokine milieu [58, 106-108]. Furthermore, human iTreg cells become interleukin-17 (IL-17)-producing Th17 cells [109], thereby supporting the concept that Th17 plasticity is a two-way process. However, the molecular mechanisms underlying these processes are incompletely understood.

Retinoic acid receptor-related orphan receptor gamma (RORγt) is a master regulator transcription factor required for Th17 differentiation [5, 110] and it has been proposed as a potential therapeutic target to suppress Th17 responses in autoimmune diseases [111, 112]. Similar to RORγt, the peroxisome proliferator-activated receptors (PPARs) are ligand-activated transcription factors and members of the nuclear receptor superfamily. PPARγ is highly expressed in CD4+ T cells and it has been reported to modulate Th1 and natural Treg (nTreg) function [113-115], but limited information is available regarding its role in modulating the Th17 and iTreg phenotypes. The loss of PPARγ in CD4+ T cells enhanced antigen-specific proliferation and overproduction of interferon γ (IFN-γ) in response to IL-12 [116]. In addition, the deficiency of PPARγ in nTreg cells impairs their ability to prevent effector T cell-induced colitis following transfer of naïve CD4+ T cells into SCID recipients [116]. Furthermore, pharmacologic activation of PPARγ prevents removal of the silencing mediator for retinoid and thyroid hormone receptors' co-repressor from the RORγt promoter in T cells, thus interfering with RORγt transcription [117]. While previous studies shed some light on the role of PPARγ in Th17 differentiation, this is the first study to investigate the role of PPARγ in controlling Th17 to iTreg cell plasticity in the gut mucosa.

Computational approaches have become a powerful tool that allows concurrent multiparametric analysis of dynamic biological processes and diseases. The emerging

use of systems modeling in combination with experimental immunology studies *in vivo* can help integrate existing knowledge and provide novel insights on rising trends and behaviors in biological processes such as CD4+ T cell differentiation and function. Of note, bioengineering studies demonstrated the predictive value of a whole-cell computational model of the life cycle of *Mycoplasma genitalium* [118]. These multi-mode calibrated models demonstrate an emerging strategy to answer questions about fundamental cell-based processes *in silico* and help focus experimental designs of animal pre-clinical and human clinical studies.

We combined computational modeling and mouse adoptive transfer studies to gain a better mechanistic understanding of the modulation of CD4+ T cell differentiation and plasticity at the intestinal mucosa of mice. Our sensitivity analyses highlighted the importance of PPARγ in the regulation of Th17 to iTreg plasticity. Indeed, *in vivo* evidence demonstrates that PPARγ is required for the plasticity of Th17 promoting a functional shift towards an iTreg phenotype. More specifically, PPARγ activation is associated with upregulation of FOXP3 and suppression IL-17A and RORγt expression in colonic lamina propria CD4+ T cells. Conversely, the loss of PPARγ in T cells results in colonic immunopathology driven by Th17 cells in adoptive transfer studies.

2.3 Mathematical modeling of intracellular cytokine pathways controlling CD4+ T cell differentiation

The population of CD4+ T cells is functionally and phenotypically heterogeneous consisting of at least four subsets involved in coordinating various aspects of adaptive immunity. Upon antigenic stimulation by antigen-presenting cells, naïve CD4+ T cells (Th0) expand and differentiate into at least three effector cell subsets referred to as Th1, Th2, Th17, and induced regulatory T (iTreg) cells (Figure 1.2). In addition to the four Th phenotypes studied and modeled in this project other CD4+ T cell phenotypes have been characterized, including transforming growing factor β (TGF-β)-producing CD4+ T cells (Th3) [119], IL-10-producing CD4+ T cells (Tr1) [120], IL-9-producing CD4+ T cells (Th9) [121] and T follicular helper (Tfh) cells located in the follicular regions of lymph

nodes and spleen [122, 123]. Signaling pathways controlling fates on these phenotypes are closely connected to the four core subsets (Th1, Th2, Th17 and iTreg). Each of these phenotypes is characterized by distinct effector and regulatory functions, which are regulated by a signature pattern of cytokines and multiple transcription factors. The signaling pathways that lead to these four predominant fates are cross-regulated via feedback loops that facilitate a balanced immune response to pathogens or abnormal cells while avoiding chronic inflammation and autoimmunity. To orchestrate the immune response, CD4+ T cells secrete a series of specific cytokines and other soluble factors. Cytokines are small molecules secreted in response to external stimuli, which are key in cell-to-cell communication. Cytokine signaling is fast and canonical, consisting of 1) binding to cytokine cell surface receptor, 2) activation of receptor-associated kinase, 3) STAT phosphorylation and translocation into the nucleus and 4) activation of gene expression.

We present for the first time a mathematical and computational model built upon the current paradigms of molecular interactions that occur in CD4+ T cells. This model will help us to elucidate the regulatory mechanisms underlying CD4+ T cell differentiation, identify novel putative CD4+ T cell subsets, and study the dynamics of Th cell differentiation. Previous modeling efforts have also focused on the CD4+ T cell. For instance, Mendoza reported a logical network model for controlling the differentiation process in CD4+ T cells [33], however, that model was build upon the Th1 versus Th2 paradigm, without considering Th17 or iTreg subsets. Additional models of immunity are available for predicting the generation of memory cells [124, 125] and determining the role of IL-2 in the interplay between effector and regulatory phenotypes [126]. There is also a comprehensive review on differentiation of effector CD4+ T cell populations by Zhu and colleagues [127]. Recent publications also reported on modeling approaches for specific CD4+ T cell phenotypes, such as the regulation of Th1 by T-bet, IL-12 and interferon-γ (IFN-γ) [23] or the regulation of the crosstalk between Th17 and iTreg by quantifying the master regulators [27]. Other studies have focused on the interaction between more than two phenotypes using logical models [63]. However, our extended ODE-based model is the first to illustrate in a detailed and comprehensive manner the intracellular regulatory networks controlling fate determination for all four phenotypes in a deterministic way (i.e., Th1, Th2, Th17 and iTreg). Specifically, we have extended

previous models by adding some new detailed interactions for the Th1/Th2-related pathways, including new pathways controlling plasticity between Th17 and iTreg cells, as well as the crosstalk among these pathways. In addition, in contrast to previous studies and given the initial results of the sensitivity analysis, our structural network model includes the modulation of this process by the nuclear receptor peroxisome proliferator-activated receptor gamma (PPARγ).

Three distinct signals regulate CD4+ T cell activation and differentiation: a signal from the T cell receptor (TCR) interacting with MHC, a co-stimulatory signal (i.e., CD28 interacting with B7.1 or B7.2 on antigen presenting cells), and a cytokine-driven signal. Other studies have focused on CD4+ T cell proliferation [128], TCR signaling [27] or co-stimulatory signals [129]. In this report, we assemble the knowledge about non-cognate interactions controlling the CD4+ T cell differentiation process (i.e., cytokine milieu, signaling pathways and transcription factors) available in the literature into a comprehensive network model. This is a first step toward a more comprehensive understanding of the dynamics of the CD4+ T cell differentiation process at the systems level. Thus, we are describing activation pathways by phenotype, as well as the inhibitory mechanisms that lead to the induction or suppression of a CD4+ T cell phenotype.

2.3.1 T helper 1 cells

A naïve T cell can differentiate into a Th1 phenotype through two major signaling pathways which have recently been shown to be interconnected and their expression is coordinated by antigen-induced signaling [23, 130, 131]. The first pathway involves antigen recognition through the T cell receptor (TCR) that activates the signaling pathway of IFN-γ, and the transcription factors signal transducer of activation of transcription (STAT)-1 and T-bet. IFN- γ binds to its receptor IFN-γR, on the T cell surface, and activates janus kinase-1 (JAK-1) and STAT-1 [132-134] which leads to the expression of T-bet in Th1 [135, 136]. Furthermore, T-bet can induce its own transcription [137] and is known to induce IFN-γ expression [138], thereby creating a positive feedback loop. Independent of IFN-γ a sustained expression of T-bet in human Th2 cells induces Th1 cytokines and represses Th2 cytokines [138, 139]. T-bet is also

capable of activating suppressor of cytokine signaling (SOCS)-1, which then blocks IL-4R signaling in response to IL-4 stimulation [140], therefore inhibiting the Th2 phenotype and favoring Th1 differentiation. In addition to T-bet, another strong activator of SOCS-1 is STAT-1 which also favors Th1 differentiation [141]. On the other hand, SOCS-1 can inhibit JAK-1 and block the activation of STAT-1 by IFN-γ *in vivo* [142, 143], thereby representing a negative feedback loop that could suppress Th1 differentiation.

The other major pathway for a naïve CD4+ T cell to differentiate into a Th1 phenotype involves the IL-12/STAT-4 axis [138, 144] by the activation of STAT-4 through the signaling of antigen-presenting cell (APC)-derived IL-12 [137, 145], where STAT-4 up-regulates IFN-γ expression [146]. Furthermore, STAT-4 is not only capable of inducing Th1 differentiation independently of T-bet, but it is also essential for Th1 differentiation in the absence of T-bet [144]. Indeed, Furuta et al. (2008) showed that Th1 differentiation was severely impaired in both T-bet$^{-/-}$ CD4^{+} T cells and STAT4$^{-/-}$ CD4^{+} T cells, which suggests that STAT-4 activates T-bet directly or indirectly [144].

Although IL-18 is not required for the development of Th1 cells, it is essential for the effective induction and activation of Th1 cells by IL-12 [147], as it synergizes with IL-12 in the induction of IFN-γ by activating STAT-4 and promoting IFN-γ activation [148]. IL-18 signals through the IL-1 receptor associated kinase (IRAK-1) to induce the accumulation of NF-κB[149] which then leads to the induction of IFN-γ[150]. Indeed, nuclear factor-kappaB (NF-κB) and STAT-4 synergize to induce IFN-γ [151, 152].

Next we describe the underlying mechanisms that inhibit naïve T cells from differentiating into a Th1 phenotype. There is evidence that STAT-6 inhibits the IL-12/STAT-4 pathway [153] and is required for the down-regulation of IL-18Rα [154]. The over-expression of STAT-3 reduces the expression of the trans-acting T cell-specific factor (GATA-3), a transcription factor involved in Th2 differentiation, and T-bet, and hence inhibits the differentiation into Th1 and Th2 [155]. The transcription factor forkhead box P3 (FOXP3), a marker for Treg cells, inhibits the production of IFN-γ by physically binding to and blocking NF-κB from inducing IFN-γ [156]. PPARγ ligands can directly decrease IFN-γ expression [157]. At the same time, however, the inactivation of STAT-3 by PPARγ [158] could activate IFN-γ expression as STAT-3 inhibits IFN-γ. In

macrophages, PPARγ down-regulates the expression of pro-inflammatory cytokines by antagonizing the activities of transcription factors such as activator protein (AP)-1, STAT and NF-κB [159], and in epithelial cells it favors the nucleocytoplasmic shuttling of the activated p65 subunit of NF-κB [160]. It remains unknown whether these mechanisms observed in macrophages and epithelial cells play a role in CD4+ T cell differentiation.

2.3.2 T helper 2 cells

Naïve T helper cells will differentiate into the effector Th2 phenotype, characterized by the expression of IL-4, IL-5 and IL-13, through two apparently independent pathways, namely, the IL-4/STAT-6 and IL-2/STAT-5 axis [161]. GATA-3 is the common link between both pathways[161]. Binding of IL-4 to its receptor leads to the phosphorylation of STAT-6 which induces GATA-3 expression[162]. GATA-3 is known to activate IL-4[163], which creates a positive feedback loop ensuring the stability of Th2 fate.

Enhanced IL-2 signaling by binding to its receptor and inducing STAT-5 is an essential pathway for Th2 differentiation [164, 165]. Neutralization of IL-2 abolishes early IL-4 production without affecting early GATA-3 expression [166], which suggests alternative mechanisms for activating GATA-3. Experimental results in mice indicate that GATA-3 is capable of inducing its own expression [163]. Recently it has been reported that Notch directly regulates GATA-3 expression, and synergistically contributes to Th2 differentiation [167, 168]. These findings may explain Th2 differentiation *in vivo* without the stimulation by IL-4.

PPARγ expression in activated T cells is dependent on IL-4 [169], indicating a link with the Th2 fate. Direct physical interactions between PPARγ and NFAT can result in inhibition of IL-2 production by CD4+ T cells [170]. While IL-4 upregulates PPARγ expression, treatment of $CD4^+$ T cells with PPARγ agonists (i.e., ciglitazone or 15dPGJ2) triggered the physical association between PPARγ and NFATc1, resulting in IL-4 promoter inhibition and decreased IL-4 production [171], suggesting the existence of a regulatory mechanism that prevents excessive differentiation towards the Th2 phenotype. Also, 13-hydroxyoctadecadienoic acid, an endogenously generated PPARγ agonist, down-regulated IL-2 production by human peripheral blood T lymphocytes by

reducing NFAT and NF-κB binding to the IL-2 promoter [172]. Moreover, IL-4 was shown to simultaneously increase the expression of PPARγ and 12-15-lipooxygenase, the enzyme involved in the generation of 13-hydroxyoctadecadienoic acid [173]. Thus, it has been proposed that IL-4 indirectly down-regulates IL-2 production by T cells through a PPARγ -dependent mechanism [172, 173].

The differentiation into Th2 could possibly be inhibited through a variety of mechanisms that have also been incorporated in our network model. For instance, the over-expression of SOCS-1 in Th2 cells represses STAT-6 activation and profoundly inhibits IL-4-induced proliferation [174] and SOCS-1 inhibits IL-4R from phosphorylating STAT-6[175, 176]. Furthermore, STAT-1 is required for the repression of IL-4-induced gene expression by IFN-γ [177]. Also, IFN-γ was shown to inhibit STAT-6 by suppressing its phosphorylation by IL-4R[178]. On the other hand, the iTreg cell-derived cytokine transforming growth factor-β (TGF-β) inhibits GATA-3 expression at the transcriptional level, however, it does not interfere with IL-4 signaling [179]. FOXP3 interacts with NFAT, such that NFAT becomes unable to induce IL-4 expression [156], thereby rearing it unable to activate T cells in response to antigenic stimulation via the TCR [180].

2.3.3 T helper 17 cells

Th17 cells are characterized by their production of the cytokine IL-17. TGF-β, together with pro-inflammatory cytokines IL-6 or IL-21 and IL-23, orchestrate the differentiation of CD4+ T cells into the Th17 phenotype in a concentration-dependent manner [181, 182]. It has been demonstrated that TGF-β synergizes with IL-6 [183] or IL-21 [184, 185] to promote the expression of IL-17. This is achieved through stimulation of retinoid-related orphan receptor (ROR)γt by IL-6 through the transcription of STAT-3 [186, 187], which in turn induces expression of IL-17 [155, 188]. While RORγt is essential for the differentiation of naïve CD4+ T cells into Th17 effector cells, IL-23 is required for maintaining and stabilizing the Th17 phenotype[189], and it acts through the IL-23R [190].

The Th17 differentiation process is very similar in mice and humans [191, 192]. As in mice, TGF-β, IL-23 and pro-inflammatory cytokines (IL-1β and IL-6) were all essential for

human Th17 differentiation [193]. In this regard, TGF-β along with IL-21 and IL-23 stimulate the expression of RORγt, which in turn induces expression of IL-17 [155, 170]. Th17 cells also secrete IL-21 [191]. IL-6, IL-21 but not TGF-β induced IL-23 receptor up-regulation in stimulated naive CD4+ T cells [170].

The differentiation of Th17 cells is antagonized by transcription factors that control the differentiation of other lineages, such as T-bet (Th1), GATA-3 (Th2), and FOXP3 (Treg) [194]. T-bet inhibits IL-23 and hence is critical for the stability of the Th17 phenotype[52, 195]. GATA-3 acts as an inhibitor of Th17 [196], this could be mediated by the inhibition of STAT-4, a promoter of IL-17 expression. FOXP3 inhibits the RORγt-driven transcription of IL-17 by directly suppressing RORγt [182, 197]. Furthermore, the IL-2/STAT-5 axis constrains Th17 [192] in part through a FOXP3-dependent mechanism, since STAT-5 activates FOXP3 [198] as well as through the inhibition of the STAT-3/IL-21 pathway [199]. Double positive FOXP3 RORγt T-helper cells have been identified as an intermediary that displays suppressive function [108]. Of note, the equilibrium of this double positive balance coexist and it is tightly controlled, suggesting that a perturbed equilibrium coming from a change in cytokine milieu might lead to a skewed phenotype [59]. In line with this fact, IL-2 signaling via STAT-5 constrains Th17 generation [200] and IL-2 has been found to regulate the development of Th17 via FOXP3+ regulatory T cells [201].

Another known inhibitor of Th17 differentiation is PPARγ as its activation can inhibit STAT-3 and hence contribute to the down-regulation of IL-17 through the IL-6/STAT-3/RORγt/IL-17 axis [202, 203]. Although TGF-β alone is not capable of inducing IL-17 and hence producing Th17, it is necessary for differentiation into Th17 and its absence induced a shift from a Th17 profile to a Th1-like profile [191, 193]. Moreover, PPARγ is a key negative regulator of human and mouse Th17 differentiation since it reduced RORγt transcription on a single-cell level [204].

2.3.4 Regulatory CD4+ T cells

Induced or adaptive Treg (iTreg) cells can be generated from naïve CD4+ T cells by the stimulation of TCR and in the presence of TGF-β1 [205, 206] and the absence of IL-6

[183]. TGF-β induces the expression of FOXP3, which is the master regulator for Treg [206-208], and the IL-2/STAT-5 pathway is essential for the up-regulation of FOXP3 [209]. The participation of TGF-β in the differentiation of Th17 cells places the Th17 lineage in close relationship with $CD4^+CD25^+FOXP3^+$ iTregs, as TGF-β also induces differentiation of naive T cells into $FOXP3^+$ iTregs in the peripheral immune compartment [191]. The key difference that drives a TGF-β-stimulated CD4+ T cell towards Th17 or iTreg is the presence or absence of IL-6, respectively. Interestingly, iTreg cells can differentiate into pathogenic Th17 in the presence of IL-6 and/or IL-23 [210], indicating plasticity in lineage commitment.

STAT-1 is also critical for the induction of iTreg cells. STAT1-deficient mice developed a functional impairment of iTreg cells [211, 212]. Recently, it was shown that FOXP3 expression is boosted by IFN-γ through the activation of STAT-1 which then directly binds to the FOXP3 promoter [213].

PPARγ ligands enhance the differentiation of CD4+ T cells into iTreg cells [214, 215], although the underlying mechanisms are incompletely understood. Additionally, PPARγ ligands inhibit the production of pro-inflammatory cytokines, including IL-6 [159]. In turn, IL-6 inhibits the expression of FOXP3 and hence favors Th17 over the iTreg phenotype [207, 216]. Thus, in the presence of PPARγ activation there is less IL-6 and a suppressed IL-6 mediated inhibition of FOXP3 that will favor the iTreg phenotype and facilitate anti-inflammatory responses and prevention of autoimmune disease.

Differentiation of CD4+ T cells into iTreg is inhibited through multiple mechanisms, including negative regulation of FOXP3 expression via GATA-3 [217], IL-4-mediated inhibition of FOXP3 through STAT-6 [218], and inhibition of TGF-β-induced FOXP3 by IL-6 and IL-21 [184]. The latter mechanism of inhibition of iTreg differentiation appears to be mediated via STAT-3 activation, since IL-6 fails to inhibit FOXP3 in STAT-3-deficient mice [219].

Interestingly, IFN-γ-deficient-mice had more FOXP3-positive cells than wild-type mice in all secondary lymphoid organs except the thymus [220]. However, T-bet- or IL-4Rα-deficient mice did not show a similar increase. *In vitro* differentiation studies showed that

conversion of naïve CD4+ T cells into FOXP3-positive iTreg cells by TGF-β was significantly inhibited by IFN-γ in a STAT-1-dependent manner. In an earlier study [221], autocrine IFN-γ production regulated TGF-β-driven FOXP3 expression in iTreg and suppressed the conversion of naïve CD4+ T cells into FOXP3^{+} iTreg cells. However, IFN-γ is critically required for the conversion of naïve T cells to iTregs in a mouse model of multiple sclerosis [212]. Furthermore, in human iTreg differentiation, a mechanism by which the STAT-1-activating cytokines IL-27 and IFN-γ amplify TGF-β-induced FOXP3 expression is revealed [213]. Finally, recent reports show that the transcription factors for Th1, Th2, and Th17 cells, T-bet, GATA-3, and RORγt, respectively, can also be co-expressed in some Treg cells [58, 98, 222], thereby indicating the existence of intermediate phenotypes. However, the molecular network leading to these intermediate phenotypes and their function remain largely unknown. The better understanding of the dynamics of iTreg differentiation is important for driving the informed development of possible Treg cell-based therapeutics against immune-mediated diseases.

2.3.5 Importance of PPARγ in CD4+ T cell differentiation

Inflammation is at the core of most human diseases, including chronic, infectious and immune-mediated. Activation of PPARγ, a widely expressed transcription factor, represents a conserved anti-inflammatory mechanism involved in the prevention of cancer [223, 224], diabetes [225-227], atherosclerosis [228], obesity [229], infectious [230-234] and immune-mediated diseases [116, 235-237]. Thus, modeling the mechanisms by which PPARγ regulates CD4+ T cell differentiation and function will facilitate a rational development of anti-inflammatory drugs and immunotherapeutics.

At the cellular level, iTreg express 10-fold greater amounts of PPARγ than Th1 cells [238] and PPARγ is required for naturally occurring Treg-mediated protection from colitis [116]. Moreover, PPARγ has been identified as a key down-regulator of differentiation of CD4+ T cells into Th17 [117] a phenotype associated with inflammation. In macrophages, PPARγ favors a switch from a pro-inflammatory “classically activated” M1 to an M2 “alternatively activated” anti-inflammatory phenotype [239]. Since PPARγ is ubiquitously expressed in the gut, tracing clinical improvements from therapeutic interventions with thiazolidinediones (TZD) and other PPARγ ligands back to concrete

PPARγ-initiated immunological mechanisms has proven extremely challenging. PPARγ activity delineates the susceptibility to intestinal inflammation ranging from highly pro-inflammatory (low expression or activation) to anti-inflammatory (high expression or activation) states. We have developed a multiscale model of the intestine to understand how PPARγ modulates the immune response dynamics, gut pathology and anti-inflammatory responses [240]. The initial level of granularity was cellular (immune and epithelial cells), with multiple tissues and compartments such as lumen, colonic lamina propria (LP) and mesenteric lymph nodes (MLN) [240].

Here we present a higher resolution structural model network with molecular granularity that illustrates the principal pathways controlling the CD4+ T cell differentiation process towards Th1, Th2, Th17 and iTreg. An additional and novel feature of our model is that we describe the role of PPARγ as a central modulator of CD4+ T cell differentiation and function.

2.4 The Modeling Process

Generating a mathematical model usually is comprised of three steps: first, a translation from the literature into a structural network is needed. The architecture of the model has to be assembled based on literature fates. Secondly, data extracted from the literature and data generated by our laboratory is inserted in the model to adjust the dynamics of the model and ensure the correct trends and behaviors of different molecules in the model. This process is known as ‘parameter estimation’. Once the parameters are set, a quality control check is needed to guarantee that signaling pathways are being activated promptly at the correct time with the right signal.
At this point, the model is ready to start running *in silico* experimentation and generating predictions with the right initializations. Ultimately, computational results will be generated, *in vitro* and *in vivo* validation studies are performed and the data generated in those studies is used to re-calibrate the model, using ‘parameter estimation’ again, thus closing and completing the modeling process. This iterative process is outlined in Figure 2.1.

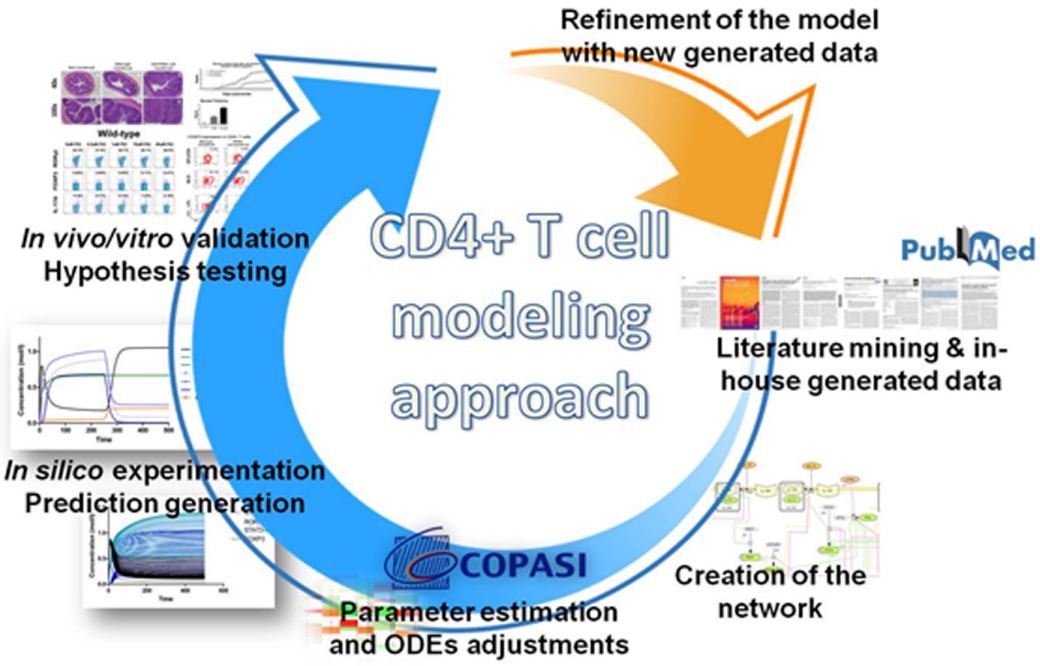

Figure 2.1. Iterative systems modeling approaches. The modeling approaches include fully integrated computational strategies and experimental validation studies. After literature search and generation of calibration data, a comprehensive network is created using CellDesigner. Parameters are then adjusted in the model using the modeling software COmplex PAthway SImulator (COPASI) [29] and quality control analysis is performed. *In silico* experimentation is conducted and several hypotheses are generated. These hypotheses will then be tested using in *vivo* and *in vitro* experimentation. Finally, the new data generated will be used to re-calibrate the model to start the process again.

2.4.1 Parameter estimation for dynamics adjustment

Once all the relationships between molecules were set, they were incorporated in the CellDesigner diagram representing a single CD4+ T cell (Figure 1). This diagram represents the cellular response of one CD4+ T cell activating and inhibiting reaction that take place in three different places: the extracellular environment, the cytoplasm and the nucleus space. Since CellDesigner [241], a software package that enables users to describe molecular interactions using a well-defined and consistent graphical notation, and our MIEP-developed modeling software, the COmplex PAthway SImulator (COPASI) [29] are Systems Biology Markup Language (SBML)-compliant an import was made into COPASI and the rate laws were adjusted to create the ordinary differential equations

(Addendum 1). To model CD4+ T cell differentiation, hill function and mass action equations were used. While Hill Coefficient allowed us to quantify the effect of a ligand binding a macromolecule through cooperative binding, mass action laws can represent dynamic equilibriums for elementary reactions, considering products as a proportion of the participating molecules in the reaction.

The parameter estimation computational approach was used to determine the unknown constants driving the dynamics of the model. Briefly, we used the Particle Swarm Optimization (PSO) [242] algorithm to obtain computational values for our model parameters in order to fit our experimental data (Addendum 2) to the model. PSO is a global search algorithm and thus depends only minimally on the initial guess of each parameter and therefore avoids the subjective estimation caused by initial guesses in local methods as Levenberg-Marquardt. PSO has been used in other publications for the same purpose [243].

Given the complexity of the model, the parameter estimation task was split into different sub-estimations that would run faster. Seven different parameter estimations were run successfully, including a parameter estimation for each phenotype (Th1, Th2, Th17 and iTreg), plus an extra one for PPARγ calibration, one for the Th1/Th2 crosstalk and a last one called 'global parameter estimation' that would include all these last six mentioned. Next, the 'non-zero-gradient' approach was performed. This step consists of assessing all the values with the gradients and check, value per value and parameter per parameter, which of those have the lowest or highest gradient. This approach can inform of which values have to be used for each phenotype and reaction. For instance, if we want to assess the parameter named re10.K1 and this reaction is involved in the Th1 phenotype we want to use the value that has the highest/lowest gradient in our results. In this case, it would coincide with the Th1 parameter estimation. An example is shown in Table S2. As an example, the parameter K1 in reaction number 10 has the lowest gradient in the results of the Th1/Th2 cross-talk parameter estimation. So when uploading these numbers to the model, re10.K1 will have a value of 64.1808, which is the one obtained from the task.

	Treg		Th1/Th2 crosstalk		PPARγ		Th1		Th2		Th17		GLOBAL	
	Value	Gradient	Value	Gradient	Value	Gradient	Value	Gradient	Value	Gradient	Value	Gradient	Value	Gradient
(re10).K1	0.001	0	64.1808	-1.36E-14	0.0001	0	78.9493	0	4.48882	0	0.0001	0	0.125481	0
(re10).K2	0.001	0	0.653062	-3.40E-13	0.000467	0	0.896854	2.26E-05	5.1868	0	0.002558	0	6.68935	0
(re10).K3							0.031433	0.025928	8.8104	0	33.3943	0	68.6086	0
(re10).K4	100	0	0.004751	-1.01E-10	0.001	0	0.033855	0	0.034989	0			66.6168	0
(re11).K	0.001	0	129.053	-1.68E-18	616.482	0	24.2222	0	6.05458	0	72.3554	0	0.263953	-4.13E-08
(re13).K							0.001	0	0.215051	0			1.13527	0
(re13).K1	4.04519	0	0.804264	9.06E-07	4.66657	-8.98E-11	58.6807	0	22.7396	0	1.24514	-0.00012	5.04432	8.11E-05
(re13).K2	20.2244	0	0.264994	2.23E-07	0.020342	0	91.0374	7.62E-17	17.3976	0	3.17239	-2.76E-06	1.65934	4.94562
(re13).K3	63.8744	0	1.84607	3.72E-07	98.0024	0	0.234452	0	0.003972	0	4.4635	0.032907	14.9788	0.017183
(re14).K1	99.8072	0	0.053541	-5.83E-07	0.001036	0.00176	0.11157	0	0.501917	1.13E-08	0.316136	5.10E-05	0.001061	0
(re14).K2	13.7099	0	93.5748	-2.37E-12	1.2029	0	0.004353	0	15.0378	0	0.000103	0.00E+00	0.075552	-0.00094
(re14).K3							0.007358	0	7.06485	0			19.7117	0
(re14).K4	16.1015	0	0.0014	1.32E-06	16.0166	0	0.001477	0.138192	32.6577	0	82.3441	0	70.3556	0
(re14).K5	0.200742	0	0.003127	1.49E-06	99.9928	-8.39E-12	3.59161	3.70E-06	22.2073	0	100	-1.89E-10	0.016858	433.378
(re14).K6	10.2927	0	0.001	0.29453	0.001	4.52E-05	0.230841	9.10E-08	0.001067	1.29E-08	2.59756	-4.22E-06	0.453002	10.6218

Table 2.1. Complete assessment of 7 parameter estimations performed by using COPASI's Particle Swarm algorithm with 3000 iterations and a particle size of 50 for reactions number 10, 11, 13 and 14. This table was used to compare turnover values as well as optimal gradients to choose an effective combination of parameters.

The results on the parameter estimation using Particle Swarm shows a good fitting between the experimental data and the values computationally estimated by COPASI with reduced weighted error (Table 2.2 and Figure 2.2). These values are then implemented in the reactions and rate laws to adjust the dynamics of the model, based on the model assumptions considered for the CD4+ T cell model (Table 2.3).

				Statistical Analysis		
Fitted specie[1]	**No. of Experimental Set**	**Experimental induced phenotype**	**Objective value**[2]	**Root Mean Square**	**Error Mean**	**Error Mean St. Deviation**
IL23R	#1	iTreg	0.02	0.08165	-3.70×10^{-17}	0.08165
FOXP3	#2	iTreg	1.26×10^{-16}	1.12×10^{-8}	1.12×10^{-8}	0
IL17_ratio	#4	Th17	142.396	5.9664	-2.9842	5.16655
IL17	#3	Th17	0.0620155	0.24902	0.24902	0
INFγ	#3	Th17	8.80e-7	0.0009380	-0.0009380	0
FOXP3_ratio	#4	Th17	1.25×10^{-6}	0.00055	0.0004194	0.0003701
IL4	#5	Th2	1.53255	0.505396	0.29067	0.413444
INFγ	#6	Th2	7.41×10^{-17}	8.61×10^{-9}	-8.61×10^{-9}	0
IL2	#7	Th1	1.14711×10^{-7}	0.00023949	-0.0001798	0.0001582
INFγ	#7	Th1	3.572	0.402944	0.37702	0.142195

Table 2.2: CD4+ T cell model fitting performed by using COPASI's global parameter estimation. A species is fitted computationally using experimental data and simulation algorithms. The objective value is the value that COPASI targets based on the experimental data and the computational simulation.

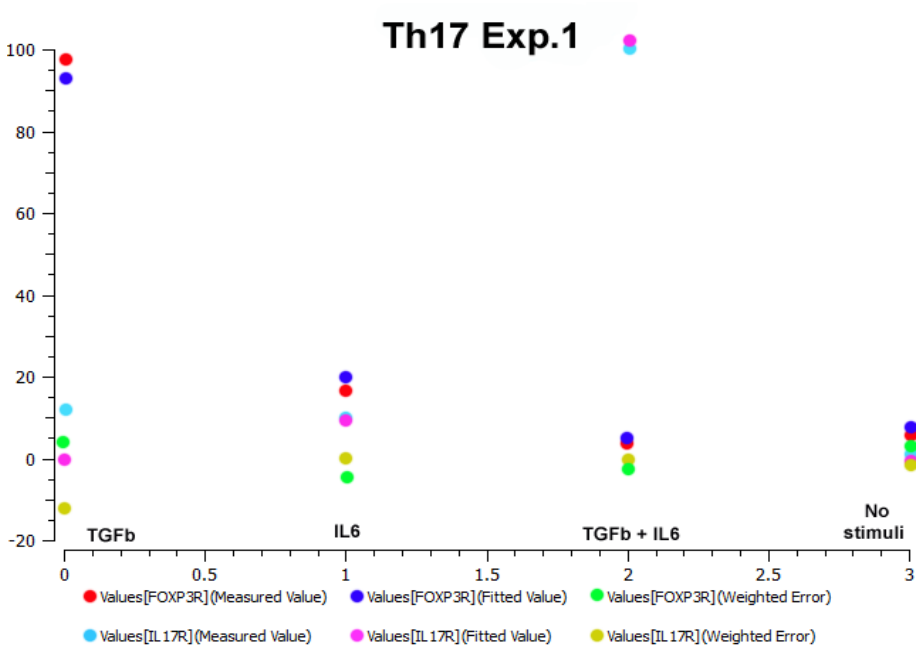

Figure 2.2. Parameter estimation results for the Th17 phenotype. IL-17 and FOXP3 were fitted by COPASI using the ParticleSwarm algorithm. The fitted value (dark blue and pink dots) could reproduce the behavior of the measured value (red and light blue dots). The weighted error (green dots) is around 0, indicating that the fitting has been performed successfully.

No.	Description of the modeling assumptions
1	The volume of the T cell remains constant throughout simulations and inductions
2	Cytokines are externalized as internally produced at different rates determined by parameter estimation and capable to induce and support differentiation
3	Induction of CD4+ T cell phenotypes depends only on external cytokine availability
4	Levels under 0.1 mol/l in simulations are considered undetectable
5	The expression of TCR is considered equal in the induction of the four phenotypes and so, its proliferation as well
6	We assume a co-stimulatory signal through CD28-B7.1 or B7.2 together with the equal expression of TCR and the combination of cytokines
7	The induction of phenotypes is only driven by the cytokine milieu
8	α-IL4 and α-IFNγ are artificial blockers of Th2 and Th1 differentiation respectively
9	Time of differentiation between phenotypes is the same within subsets
10	Species are activated until saturation point in the reaction. At this time, the increase of the preceding species will not affect the concentration of the saturated one
11	PPARγ knock-out creation is based on the idea of the ligand impairment to the molecule, thus abolishing the expression of L-PPARγ, which would elicit modulatory responses.
12	The binding of a protein to its receptor occurs at different rates depending on the receptor. These parameters were assessed with parameter estimation and calibration processes.

Table 2.3. **Table of assumptions for the representation of activation and inhibition pathways of the CD4+ T cell computational model.** Modeling assumptions were made based

on the literature and on experimental observations to be able to properly modulate and calibrate the CD4+ T cell computational model.

Once this step is completed, quality control is performed. Using the proper initialization given by literature and represented in Table 2.4, the system is induced to the four phenotypes and checked to reproduce the correct up- and downregulation of specific molecules.

Phenotype	External stimuli to induce	Upregulation	Downregulation
Th1	eIFNγ eIL-12 eIL-18 αIL-4	IFNγ STAT1-P Tbet-P IL-12 IL-18 IRAK1-P	IL-4 GATA3-P IL-17 aFOXP3 STAT3-P STAT6-P RORγt
Th2	eIL-4 αIFNγ	IL-4 GATA3-P STAT6-P	IL-17 aFOXP3 STAT3-P STAT1-P IFNγ Tbet-P IRAK1-P IL-18 IL-12 RORγt
Th17	eIL-6 eTGF-β	IL-17 RORγt STAT3-P IL6 TGFβ	aFOXP3 STAT1-P IFNγ Tbet-P GATA3-P IL-4 STAT6-P IL-12 IL-18
iTreg	eTGF-β IL-2	aFOXP3 TGF-β	IL-17 RORγt STAT3-P STAT6-P GATA3-P IL-4 IFNγ Tbet-P STAT1-P IL-12 IL-18

Table 2.4. Comprehensive summary of stimuli input versus molecule expression output. The four CD4+ T cell phenotypes by a variety of external stimuli represented in the second

column. These external stimuli cause upregulation of molecules represented in the third column and downregulation of the molecules represented in the fourth column.

These four phenotype checks are the result of our CD4+ T cell modeling efforts after calibration and they provide evidence that our computational and mathematical model is capable of reproducing the behaviors of the four CD4+ T cell phenotypes in terms of cytokines, inductors and transcription. In addition, we demonstrate that the calibration process has been run successfully and the dynamics of the CD4+ T cell differentiation network model are adjusted to mimic immunological behaviors characteristic of each phenotype (Figure 2.3).

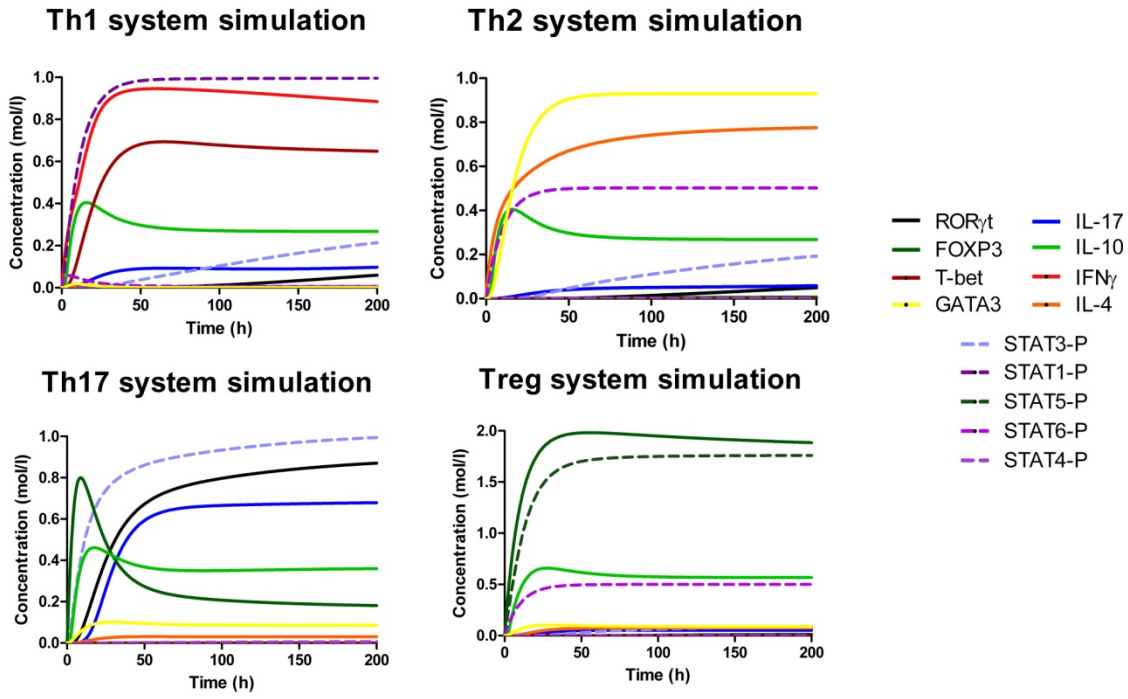

Figure 2.3. Induction of effector Th1, Th2, Th17, and iTreg phenotype differentiation *in silico*. The addition of increasing amounts of IL-12, IL-18 and IFN-γ (Th1), IL-4 (Th2), IL-6 and TGF-β (Th17) or TGF-β alone (iTreg) as external stimuli in the system resulted in increasing amounts of related molecules for each phenotype.

To partially summarize, the CD4+ T cell differentiation model consists of 60 ODEs, 52 reactions and 93 species. The mathematical model was engineered to ensure proper modulation of intracellular pathways and cell phenotypes via external cytokines

representing the cytokine milieu. The Hill Function and mass action equations were used [244]. While the Hill Coefficient allowed us to quantify the effect of a ligand binding a macromolecule through cooperative binding, mass action laws can represent dynamic equilibriums for elementary reactions, considering products as a proportion of the participating molecules in the reaction. Experimental data (Addendum 1) was used to calibrate and adjust model parameters to ensure correct dynamics. Among the four possible phenotypes in this mathematical model, to induce Th17 differentiation from a naïve CD4+ T cell, external IL-6 and external TGF-β were added in combination and demonstrated upregulation of RORγt, IL-17 and STAT-3 (Figure 2.3) as followed by our table of initialization fates (Table 2.4). Sensitivity analyses identified PPARγ as an essential regulator of CD4+ T cell differentiation and plasticity (Figure 2.4).

Species	Correlation to PPARγ
eIL17	2495.8
eIL10	-3295.16
eIL18	0
eIL12	0
eIFNg	-0.236289
eIL2	0
IL6-IL6R	-629.747
IL6R	629.747
TFGb-TGFbR	-629.474
TGFbR	629.747
IL4-IL4R	-124.088
IL4R	124.088
IL4	24.97
IGNg-IFNgR	-0.2797
IFNgR	0.2797
IL21	-17.416
IL21-IL21R	-504.938
IL21R	504.938
IL23R	1084.78
IL23-IL23R	-1084.78

Species	Correlation to PPARγ
IL10R	795.8
IL10-IL10R	-795.8
IRAK1-P	-58.918
STAT4-P	0.0292
IFNgR	0.0429
JAK1-P	-7.22061
IL17	-1623.51
IL10	929.931
RORgt	-1891.48
STAT3-P	-671.498
STAT5-P	-117.822
Tbet-P	0.0322203
GATA3-P	232.791
STAT6-P	-77.6707
PPARg	23.6863
L-PPARg	-22.6862
aFOXP3	1114.7
IL17R	871.93
IL17-IL17R	-871.93

Figure 2.4. Sensitivity analysis on PPARγ by the CD4+ T cell computational model. Sensitivity analysis was run with COPASI on our computational model using a delta factor of 0.0001 and a delta minimum of 1e-12. The subtask run for the analysis was a time-series with t=100h and correlation of all the variables of the model against activated PPARγ was assessed, showing high correlation with key transcription factors that determine phenotype differentiation on Th17 and iTreg.

2.5 PPARγ plays an essential role in modulating CD4+ T cell differentiation and plasticity in a dose-dependent manner

Based on the results of the sensitivity analysis we performed computer simulations aimed to further characterize the role of PPARγ on Th cell differentiation *in silico*. Following induction of the computational model towards a Th17 phenotype by adding external TGF-β and external IL-6 *in silico*, modeling efforts predicted that increasing concentrations of PPARγ in Th17 cells led to downregulation of RORγt and IL-17 and upregulation of FOXP3 (Figure 2.5A), thus, displaying a phenotype switch from Th17 to iTreg. To validate the results of our computational simulations, we first isolated and sorted naïve CD4+ T cells from spleens of wild-type and T cell-specific PPARγ null mice. Deletion of PPARγ via a transgenic expression of Cre under control of the *CD4* promoter ($PPAR\gamma^{fl/fl}$; CD4-Cre+) allowed us to use loss-of-function approaches to characterize the role of PPARγ in Th17 differentiation. Cells were polarized towards a Th17 phenotype with recombinant mouse IL-6 and TGF-β. IFNγ and IL-4 were eliminated to block Th1 and Th2 differentiation respectively with neutralizing antibodies. After 60 hours of culture, cells were treated with increasing amounts of pioglitazone (PIO), a synthetic PPARγ agonist of the thiazolidinedione (TZD) class of anti-diabetic drugs. Before starting pioglitazone treatment, at t=60h, IL-17 and RORγt expression were significantly upregulated in PPARγ null when compared to wild-type cells (Figure 2.5B). Following pioglitazone treatment for 24h., Th17 cells from wild-type mice showed increasing levels of FOXP3 and downregulation of RORγt and IL-17A with increased concentration of the exogenous PPARγ agonist in wild-type (Figure 2.5C), but this effect was not observed in PPARγ null Th17 cells (Figure 2.5D), suggesting the role of PPARγ in the modulation of these molecules. The same study was repeated three times with very similar trends on these behaviors (Figure 2.6). These results provide *in vitro* evidence that PPARγ significantly dampens Th17 differentiation and slightly enhances FOXP3 expression. Interestingly, uncoupling between suppressed Th17 responses and enhanced iTreg cells suggests that a T cell-extrinsic mechanism (i.e., APC-derived signals) might be contributing to this Th17 plasticity *in vivo*.

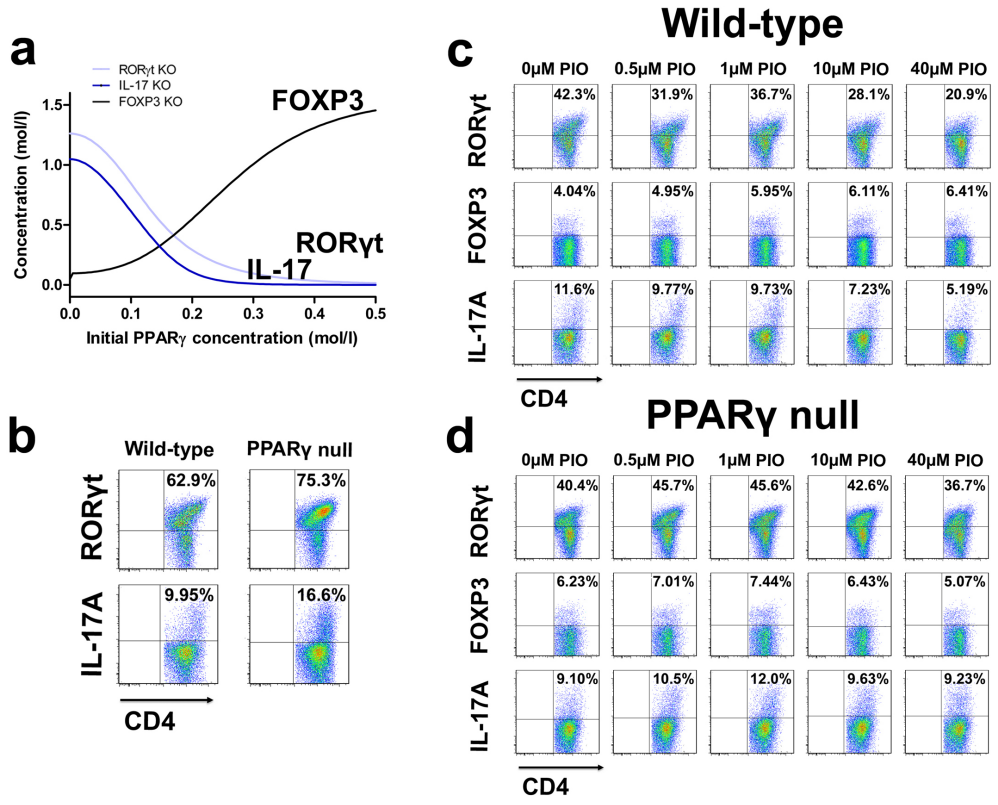

Figure 2.5. Activation of PPARγ regulates differentiation of CD4+ T cells. (A) Computational simulation of the effect of *in silico* activation of PPARγ in a T helper (Th)17 cell on the levels of FOXP3, IL-17 and RORγt. (B) PPARγ inhibits Th17 differentiation. Naïve wild-type CD4+ T cells differentiated with IL-6 in combination with TGF-β *in vitro* for 60h express less RORγt and produce lower levels of IL-17A when compared to T cell-specific PPARγ null Th17 cells. (C) Increasing concentrations of pioglitazone (PIO), a full PPARγ agonist, upregulate FOXP3 in wild-type Th17 differentiated cells following 24h treatment and down-regulate RORγt and IL-17A in wild-type cells. (D) Increasing concentrations of PIO do not have an effect in PPARγ null Th17 cells. The double-positive region can be observed in the upper right part of the flow plots.

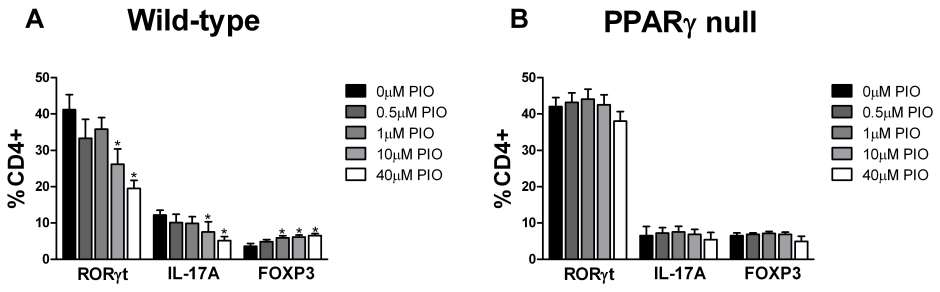

Figure 2.6. Effect of PPARγ on Th17 and iTreg markers *in vitro*. (A) Increasing concentrations of pioglitazone (PIO), a full PPARγ agonist, upregulate FOXP3 in wild-type Th17 differentiated

cells following 24h treatment and down-regulate RORγt and IL-17A in wild-type cells. (B) Increasing concentrations of PIO do not have an effect in PPARγ null Th17 cells. Data are represented as mean ± standard error. Points with an asterisk are significantly different when comparing different PIO treatments with to the non-treated group (P<0.05).

2.6 The lack of PPARγ in naïve CD4+ T cells impairs their ability to differentiate into iTreg cells *in vivo*

To determine whether the loss of T cell PPARγ favors Th17 and impairs iTreg cell differentiation and also to assess whether T cell-extrinsic mechanisms might be affecting iTreg upregulation we conducted computational simulations and *in vivo* studies of PPARγ deletion in T cells. Chronologically, a PPARγ-deficient naïve CD4+ T cell was created *in silico* by blocking PPARγ downstream signaling. The loss of PPARγ *in silico* caused upregulation of RORγt and IL-17 in Th17 cells (Figure 2.7B) and down-regulation of FOXP3 in iTreg cells (Figure 2.7D) compared to wild-type CD4+ T cells (Figure 3A and 2.7C). These results demonstrate that PPARγ exerts a regulatory role in CD4+ T cell differentiation from a naïve state to Th17 or iTreg cells. Next, to validate this computational prediction, we sorted CD4+CD25-CD45RB^{high} naïve T cells from spleens of donor wild-type and T cell-specific PPARγ null mice and adoptively transferred 4 x 10^5 viable cells to SCID recipients (Figure 2.8). Cells isolated from the colonic lamina propria (LP), spleen and mesenteric lymph nodes (MLN) of recipient mice were assayed for expression of FOXP3, RORγt and IL-17A by intracellular flow cytometry. The transfer of CD4+ T cells lacking PPARγ resulted in significantly greater accumulation of IL-17-producing Th17 cells and lower levels of FOXP3+ iTreg cells in spleen, MLN and colonic LP of recipient mice (Figure 2.7E and 2.7F and Figure 2.9).

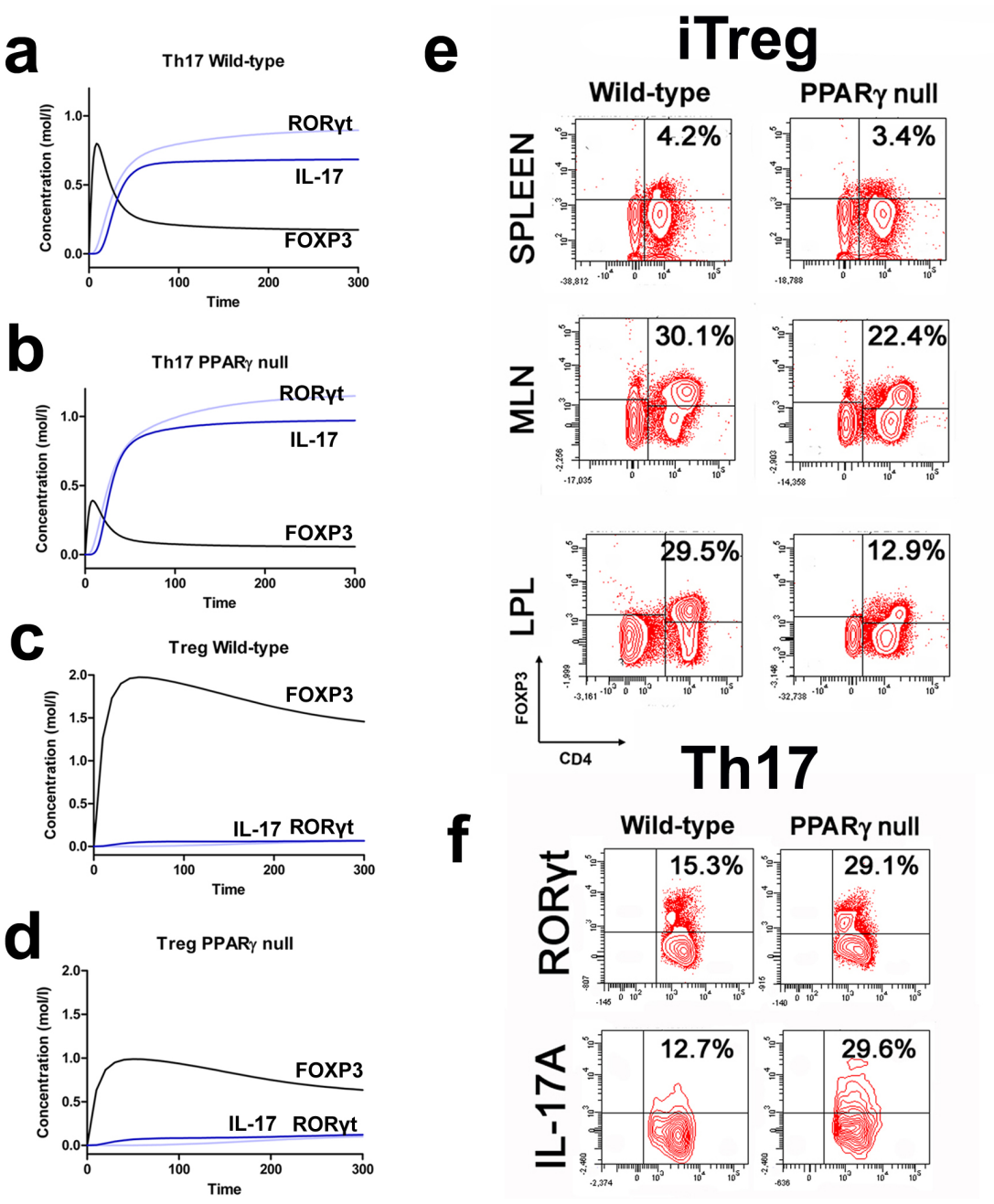

Figure 2.7. Activation of PPARγ regulates differentiation of CD4+ T cells. (A) Computational simulation of the effect of *in silico* activation of PPARγ in a T helper (Th)17 cell on the levels of FOXP3, IL-17 and RORγt. (B) PPARγ inhibits Th17 differentiation. Naïve wild-type CD4+ T cells differentiated with IL-6 in combination with TGF-β *in vitro* for 60h express less RORγt and produce lower levels of IL-17A when compared to T cell-specific PPARγ null Th17 cells. (C) Increasing concentrations of pioglitazone (PIO), a full PPARγ agonist, upregulate FOXP3 in wild-type Th17 differentiated cells following 24h treatment and down-regulate RORγt and IL-17A in wild-type cells. (D) Increasing concentrations of PIO do not have an effect in PPARγ null Th17 cells. The double-positive region can be observed in the upper right part of the flow plots.

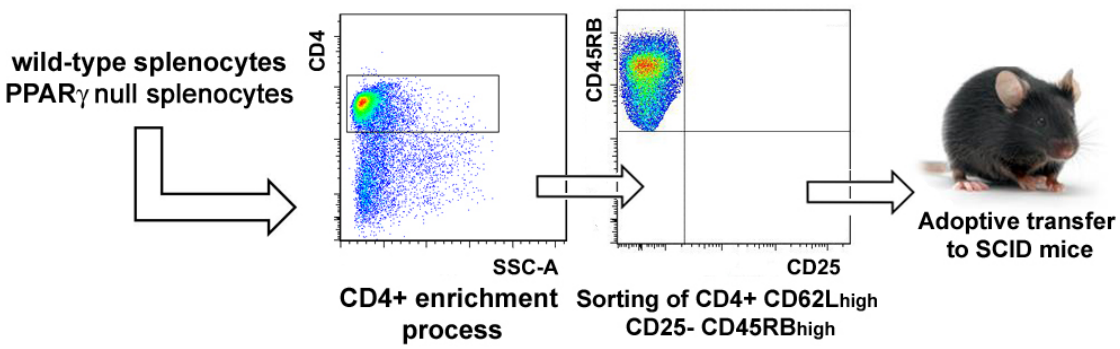

Figure 2.8. Experimental design to validate PPARγ knockout predictions by the CD4+ T cell computational model. Wild-type or PPARγ null splenocytes were isolated and CD4+ enriched to then sort naïve CD4+ T cells and transfer them into a SCID mouse to assess PPARγ-related patterns of differentiation.

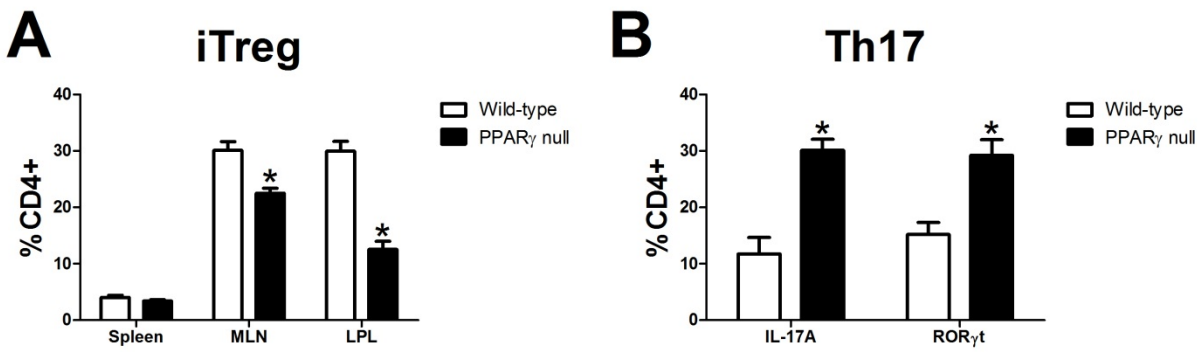

Figure 2.9. Effect of PPARγ on Th17 and iTreg markers *in vivo*. (A) Treg cell accumulation in spleen, mesenteric lymph nodes (MLN) and lamina propria (LP) of SCID recipient mice. (B) Th17 cell accumulation in spleens of recipients of wild-type versus PPARγ null CD4+ T cells. Data are represented as mean ± standard error. Points with an asterisk are significantly different when comparing the PPARγ null group to the wild-type group ($P<0.05$).

Recipients of PPARγ null cells showed a significantly more severe and earlier onset of disease when compared to recipients of wild-type cells (Figure 2.10A). Histological examination demonstrated that colons recovered from recipients of PPARγ null CD4+ T cells had significantly greater lymphocytic infiltration and crypt hyperplasia than those recovered from recipients of wild-type CD4+ T cells (Figure 2.10B).

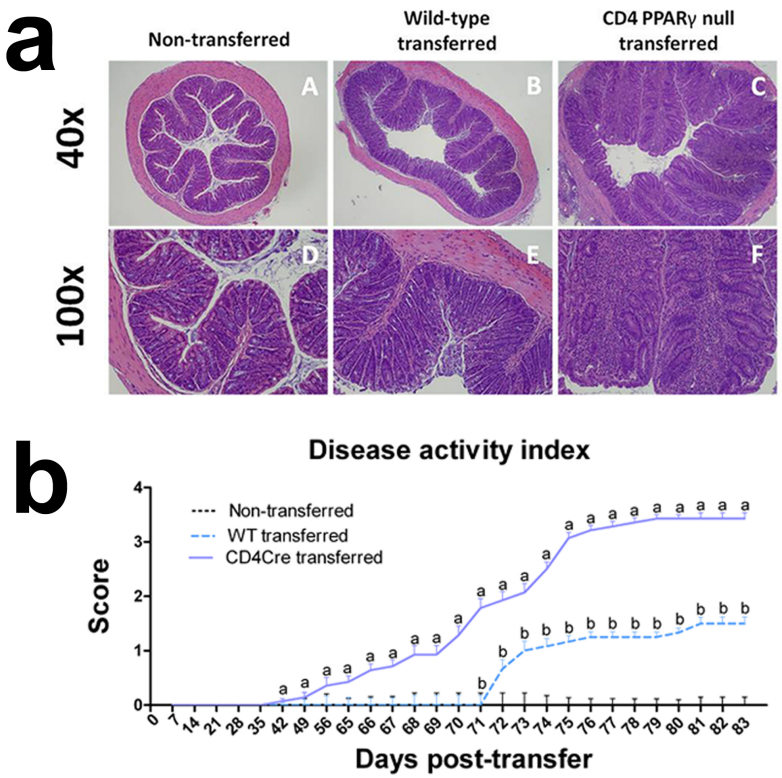

Figure 2.10. PPARγ suppresses Th17 cell differentiation and upregulates FOXP3 expression *in vivo*. (A-D) Computational simulation of the effect of PPARγ deficiency on differentiation from a naïve state into either Th17 or iTreg phenotypes. (E) Th17 cell accumulation in spleens of recipients of wild-type versus PPARγ null CD4+ T cells. (F) Treg cell accumulation in spleen, mesenteric lymph nodes (MLN) and lamina propria (LP) of SCID recipient mice.

2.7 Pharmacological activation of PPARγ favors a switch of Th17 cells towards an iTreg phenotype *in vivo*

To determine whether PPARγ activation played an essential role in converting fully differentiated Th17 cells into iTreg cells, the computational model was induced to Th17 with the addition of IL-6 and TGFβ and PPARγ was activated when the cell was a fully differentiated Th17. Results show that following induction of Th17 and subsequent PPARγ activation, IL-17, STAT-3 and RORγt were dramatically downregulated, whereas FOXP3 was upregulated, thereby demonstrating a phenotypic switch from a Th17 to an iTreg phenotype (Figure 2.11A). To ensure that parameter space scan and time-course were linked and the changes in PPARγ were being observed in a time-dependent

manner, a combination of both was run, reiterating the phenotype switch with increasing concentrations of PPARγ over time observing an upregulation of FOXP3 and a downregulation of IL-17, RORγt and STAT3-P (Figure 2.11B). To address this hypothesis, we sorted CD4+ CD25- CD45RB^{high} naïve T cells from spleens of donor wild-type mice and transferred 4 x 10^5 viable cells to RAG2$^{-/-}$ recipients. When clinical signs of disease and colitis appeared, a subset of mice was sacrificed and spleen, MLN and colons were extracted to examine Th17 and Treg levels (baseline results). After verifying the presence of Th17 cells in colon, MLN and spleen, half of the mice were received a daily treatment of 70 mg/kg of pioglitazone given orally to activate PPARγ (Figure 2.11C). During the treatment period, mice treated with pioglitazone recovered weight (Figure 2.12) and their disease activity scores dropped significantly compared to mice treated with PBS (Figure 2.13). Histopathological examinations also showed that colons from recipient mice treated with pioglitazone had a significantly lower lymphocytic infiltration and crypt hyperplasia than those from non-treated recipients (Figure 2.14).

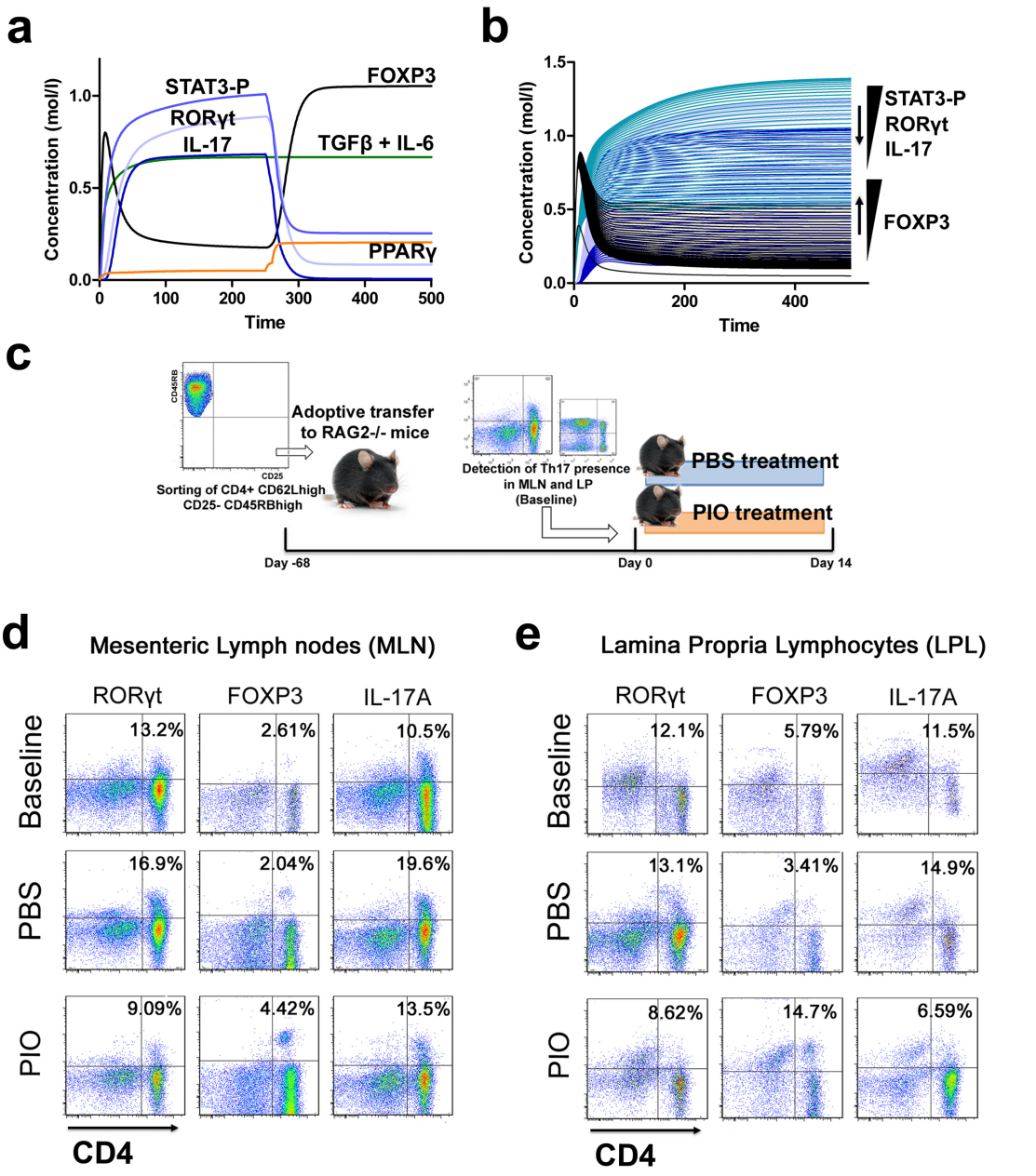

Figure 2.11. Validation of the modeling prediction regarding the role of PPARγ in regulating the plasticity between Th17 and iTreg. (A) Computer simulation illustrating a down-modulation of IL-17, STAT3, RORγt and upregulation of FOXP3 in a differentiated Th17 cell following PPARγ activation. (B) Combination of time-course and PPARγ concentration scan to assess changes of IL-17, STAT3, RORγt and FOXP3 over time. (C) Experimental design for the validation of the model prediction. (D-E) Accumulation of iTreg and Th17 cells in the mesenteric lymph nodes (MLN) and colonic lamina propria (LP) of recipient mice.

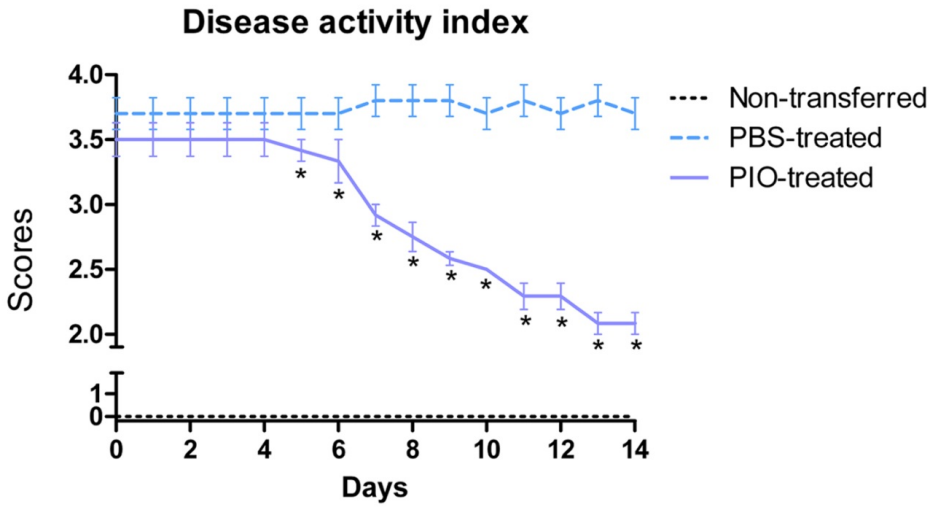

Figure 2.12. Improvement in DAI following oral treatment with pioglitazone (PIO) in RAG2-/- mice. RAG2-/- adoptive transfer recipient mice were treated with either PIO or PBS (control group) and given a composite score reflecting clinical signs of the disease (i.e. perianal soiling, rectal bleeding, diarrhea, and piloerection) for 14 days daily. Data are represented as mean ± standard error. Points with an asterisk are significantly different when comparing the PIO-treated group to the PBS-treated group ($P<0.05$).

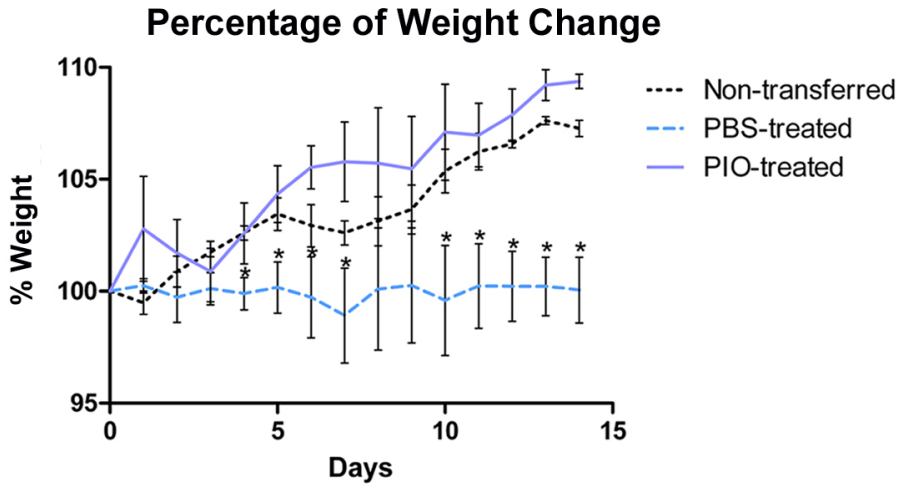

Figure 2.13. Improvement in mouse body weight following oral treatment with pioglitazone in RAG2-/- mice. RAG2-/- adoptive transfer recipient mice were treated with either PIO or PBS (control group) for 14 days and the average daily loss in body weights throughout the 14 day treatment was calculated. Data are represented as mean ± standard error. Points with an asterisk are significantly different when compared to the PBS-treated group ($P<0.05$).

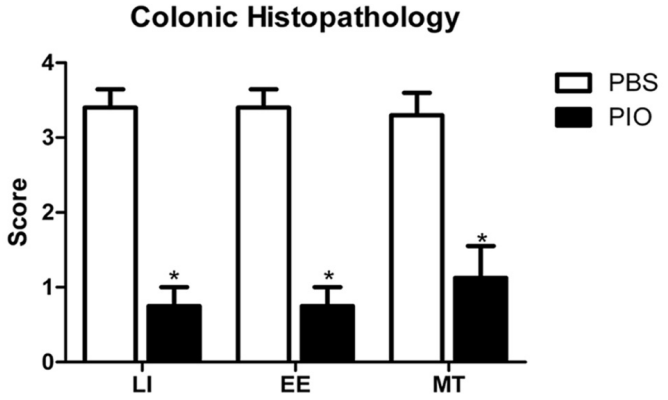

Figure 2.14. Histopathological analysis on colonic tissue from adoptive transfer studies. RAG2-/- adoptive transfer recipient mice were treated with either PIO or PBS (control group) for 14 days and histopathological assessment was performed. All specimens underwent blinded histological examination and were scored (0-4) on leukocyte infiltration (LI), epithelial erosion (EE) and mucosal wall thickening (MT) on day 14 after treatment. Data are represented as mean ± standard error. Points with an asterisk are significantly different at a given time point ($P < 0.05$).

Untreated mice maintained a predominant Th17 response characterized by increased levels of CD4+ T cells expressing RORγt and IL-17A. In contrast, pioglitazone-treated mice not only recovered from colitis and its associated weight loss, but also showed a switch from a predominant Th17 into an iTreg phenotype characterized by increased expression of FOXP3 and decreased IL17-A and RORγt in CD4+ T cells of the colonic LP and MLN (Figure 2.11D and 2.11E and Figure 2.15). This data supports the *in silico* prediction that activation of PPARγ in Th17 cells favors differentiation into iTreg cells, which facilitates colonic tissue reconstitution and recovery from disease.

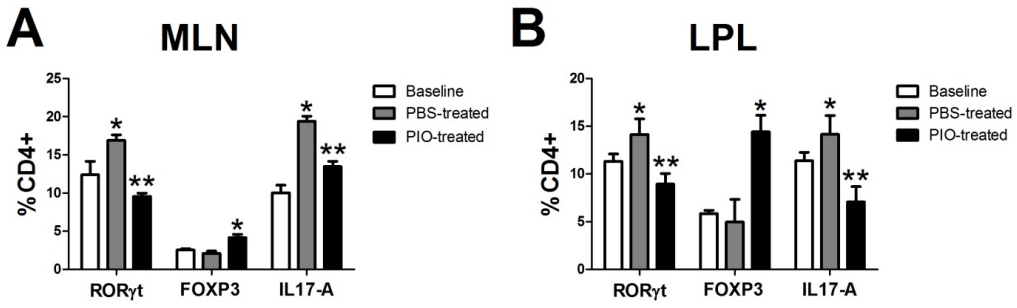

Figure 2.15. Pharmacological activation of PPARγ favors a switch of Th17 cells towards an iTreg phenotype *in vivo.* RAG2-/- mice with induced chronic colitis were treated with either PBS

or PIO for 14 days and flow cytometry were assessed at day 0 (baseline) and at the end of the treatment. (A) Accumulation of iTreg and Th17 cells in the mesenteric lymph nodes (MLN) (B) Accumulation of iTreg and Th17 cells in the colonic lamina propria (LP) of recipient mice. Data are represented as mean ± standard error. Points with an asterisk are significantly different at a given time point ($P < 0.05$).

2.8 Discussion and Conclusions

Computational models can help to synthesize and integrate existing knowledge and narrow the experimental design prior to costly *in vivo* experimentation. To gain a more comprehensive understanding of the mechanisms controlling CD4+ T cell differentiation, we first compiled and integrated existing literature knowledge and data related to the cytokines and intracellular signaling pathways involved in the differentiation of a naïve CD4+ T cell into effector and regulatory cell subsets. To determine whether the model predictions regarding novel mechanisms of immunoregulation in Th17 and Treg cells were sensitive to the model parameters we performed a sensitivity analysis of the signaling pathways controlling Th17 and iTreg phenotypes. Our simulations reproduced known CD4+ T cell differentiation behaviors for Th1, Th2, Th17 and iTreg, and predicted novel mechanisms of T cell-mediated immunoregulation. By simulating the cytokine milieu that surrounds a CD4+ T cell *in silico*, we dissected crucial signaling pathways and their transcriptional regulation programs involved in differentiation and plasticity of CD4+ T cells. While computational predictions carry certain uncertainty given by the topology of the network, computational modeling approaches applied to CD4+ T cell differentiation have proven useful in characterizing the importance of dual waves of expression of T-bet and sequentially acting positive feedback loops of TCR-IFNγ-STAT1-Tbet and IL-12-STAT4-Tbet signaling in Th1 differentiation [23]. A central question in T cell biology involves improving the understanding of instructive versus selective factors that regulate the differentiation process. Selective factors include competition for cytokines by competing clones of CD4+ T cells in an expanding population. For example, regulatory T cells are able to outcompete for IL-2 and deprive effector T cells of this survival signal [245]. While the computational model presented herein comprehensively addresses the instructive factors (i.e., the impact of cytokine combinations on T cell phenotypes), stochastic simulations and multiscale modeling are

needed to adequately model selective factors by linking molecular-level intracellular signaling sub-models and tissue-level cell-cell interaction models. Some studies have addressed selective factors by focusing on the crosstalk in molecular pathways in an expanding Th1 population using *in vitro* data [246] but only one phenotype has been computed and with a limited scope. The study presented here is the first to comprehensively investigate at the systems level the mechanisms controlling CD4+ T cell differentiation and plasticity between Th17 and iTreg cells, presenting a model that computes not only one but four of the CD4+ T cell phenotypes.

Several distinct signals regulate CD4+ T cell activation and differentiation: a signal from the T cell receptor (TCR) interacting with MHC, a co-stimulatory signal (i.e., CD28 interacting with B7.1 or B7.2 on antigen presenting cells), and a cytokine-driven signal. Other studies have focused on CD4+ T cell proliferation [128], TCR signaling [27] or co-stimulatory signals [129]. Our mathematical approach focuses on the non-cognate interactions (i.e., cytokine milieu) and instructive factors controlling CD4+ T cell differentiation. Future studies will leverage the modeling efforts described here to construct multi-scale hybrid models driven by high-performance computing strategies that integrate sub-models of intracellular signaling pathways such as the CD4+ T cell model and tissue-level models that can simulate cell-cell interactions. These integrative approaches will provide an avenue for incorporating stochasticity as well as the modulation of phenotype and function of immune cells at sites of inflammation or infection by selective and instructive factors.

Sensitivity analyses and computational simulations using the CD4+ T cell differentiation model predicted that the nuclear receptor PPARγ modulates the balance between Th17 and iTreg cells, by controlling both the initial differentiation from a naïve CD4+ T cell as well as plasticity between phenotypes. Activation of PPARγ *in silico* favored differentiation of iTreg and antagonized Th17 differentiation by down-modulating RORγt and IL-17. These findings are in line with previous reports demonstrating that the pharmacologic activation of PPARγ selectively controls Th17 differentiation in mice and humans by interfering with RORγt transcription [204]. Furthermore, ciglitazone, a PPARγ agonist, significantly enhanced generation of iTreg cells [114] and PPARγ induced potent and stable FOXP3 expression [115] resulting in the suppression of effector CD4+

T cell responses [116]. Our *in silico* results demonstrate that the upregulation of FOXP3 and downregulation of RORγt and IL-17 in CD4+ T cells is modulated by PPARγ and behaves in a dose-dependent manner. Indeed, our *in vitro* results support the dose-dependent effect in the suppression of Th17, although not accompanied by a similar increase in FOXP3+ iTreg cells. However, our *in vivo* findings further demonstrate that pioglitazone treatment favors a switch of fully differentiated Th17 cells into an iTreg phenotype by increasing activation of PPARγ. Thus, our plasticity modeling efforts are more predictive of *in vivo* than *in vitro* behaviors of CD4+ T cells, suggesting a missing component, possibly provided by APCs in the widely utilized *in vitro* system. For instance, all trans retinoic acid, which *in vivo* is produced by APC-derived, increased and maintained FOXP3 expression [247]. Conclusively, the mechanisms by which T cell extrinsic factors modulate CD4+ T cell plasticity are yet not fully understood. Here, however, we propose PPARγ as a novel candidate for such modulation.

The CD4+ T cell mathematical model predicted an upregulation of RORγt and IL-17 in Th17 cells lacking PPARγ when compared to the wild-type counterparts. In complete correspondence to this modeling prediction, our *in vitro* results show that following Th17 differentiation, CD4+ T cells lacking PPARγ exhibit a more dramatic upregulation of RORγt and IL-17A than wild-type cells. Moreover, we have also observed a marginal upregulation of FOXP3 in wild-type cells. The uncoupling between the dramatic downregulation of RORγt and the more limited upregulation of FOXP3 observed *in vitro* could be attributed to external factors that play an important role in this process, which are not fully mechanistically understood or not included in the *in vitro* system used (i.e., APCs). As opposed to the *in vitro* results, the *in vivo* findings in mice with CD4+ T cell-induced colitis were more consistent with the modeling predictions. Recent studies show that changes in the cytokine environment mediate the conversion of iTreg into Th17 cells [98]. Notably, different subsets of myeloid cells in humans can orchestrate the differentiation of naïve CD4+ T cells into either effector or regulatory phenotypes [99]. Myeloid APCs are essential for the induction of IL-17A+ FOXP3+ T cells from memory CCR6+ T cells or Treg cells [248]. However, the molecular mechanisms controlling CD4+ T cell plasticity remain largely unknown, including the essential versus dispensable regulators of these processes.

Herein, we combined computational and experimental approaches to investigate for the first time the role of PPARγ in the re-programming of fully differentiated Th17 cells into an iTreg phenotype in the gut mucosa. Of note, the presence of FOXP3 RORγt double-positive cells with suppressive actions on effector CD4+ T cell subsets has been associated with the plasticity of Th17 and iTreg [108]. TGF-β is a common inductor of Th17 and iTreg that can upregulate FOXP3, but in combination with IL-6, it upregulates IL-17 and dramatically downregulates FOXP3 expression [26]. Other cytokines, such as IL-23, modulate plasticity by restraining FOXP3+ Treg activity [105]. Clinically, inhibition of IL-17 promotes differentiation of stable iTreg cells in patients with autoimmune hepatitis [249]. However, IL-17+FOXP3+ cells were identified in inflamed intestinal mucosa of patients with Crohn's disease (CD), but not in patients with ulcerative colitis (UC) [250], the two clinical manifestations of inflammatory bowel disease. Furthermore, in line with our sensitivity analysis and computer simulations, results of our adoptive transfer studies in mice indicate that activation of PPARγ by oral pioglitazone administration favors a switch from Th17 to iTreg in MLN and colonic LP of mice with CD4+ T cell-induced colitis, thereby demonstrating that PPARγ is implicated in the modulation of CD4+ T cell plasticity *in vivo*.

The loss of PPARγ favored Th17 differentiation and reduced the conversion of IL-17A-producing Th17 cells into CD4+FOXP3+ T cells *in vivo*. Adoptive transfer studies using T cell-specific PPARγ null naïve T cells demonstrate that PPARγ is needed for suppressing effector responses at sites of inflammation such as the colonic LP in a mouse model of chronic colitis. Interestingly, FOXP3 inhibits Th17 by antagonizing the function of the transcription factors RORγt and RORα [58, 98]. This suggests a potential interaction of RORγt with FOXP3 in larger transcriptional complexes, which could explain why RORγt is more rapidly down-regulated than FOXP3 is increased. More specifically, the decrease of RORγt could result from a synergism between the inhibition exerted by PPARγ and the parallel inhibition caused by FOXP3, which in turn is enhanced when PPARγ is activated. The observation that PPARγ may interact with FOXP3 and RORγt suggests a cross-talk between transcriptional programs of crucial importance to the regulation of immune responses and clinical outcomes during infectious and immune-mediated diseases.

In summary, we demonstrate for the first time that activation of PPARγ results in reprogramming of the CD4+ T cell molecular pathways that control the Th17 phenotype, leading to the induction of an iTreg phenotype. This phenotype switch is associated with protection from CD4+ T cell-induced colitis during adoptive transfer experiments in mice. Thus, the balance between Th17 and Treg cells helps delineate the outcome of immunological processes from effector inflammation to regulatory tolerance. Our modeling approaches allowed us to narrow the design of experiments and to better understand the molecular mechanisms of action controlling CD4+ differentiation. This new mechanistic knowledge is broadly applicable to the development of immune therapeutics for infectious, allergic and immune-mediated diseases. More specifically, we propose that PPARγ is a promising therapeutic target for chronic inflammatory and infectious diseases where Th17 cells contribute to the gut immunopathogenesis.

2.9 Materials and Methods

Ethics statement

All experimental protocols were approved by the Virginia Tech institutional animal care and use committee (IACUC) (Protocol Number: 10-087VBI) and met or exceeded guidelines of the National Institutes of Health Office of Laboratory Animal Welfare and Public Health Service policy. Animals were under strict monitoring throughout the duration of the project and all efforts were made to minimize unnecessary pain and distress. Mice were euthanized by carbon dioxide narcosis followed by secondary cervical dislocation.

Mathematical modeling

To facilitate a comprehensive representation of the dynamics associated with the major non-cognate pathways controlling CD4+ T cell differentiation and plasticity, we constructed an ordinary differential equation (ODE)-based computational model of the cytokines, receptors and transcription factors controlling CD4+ T cell differentiation and plasticity. The mathematical model was engineered to ensure proper modulation of intracellular pathways and cell phenotypes via external cytokines representing the

cytokine milieu. The mathematical model constructed was based on experimental findings and illustrates intracellular pathways controlling a naïve T cell differentiation into Th1, Th2, Th17 or iTreg phenotypes. The model comprises 60 differential equations representing 52 reactions and 93 species. The COmplex PAthway SImulator software [251] (COPASI; http://www.modelingimmunity.org/) was used for model development, sensitivity analysis, and calibration. Sensitivities of the steady-state fluxes of reactions were derived with respect to the reaction rates in the system. These sensitivities were normalized and represented flux control coefficients according to Metabolic Control Analysis (MCA) [252, 253]. In this case, sensitivities were performed with respect to PPARγ pathway-controlling parameters and levels of different species were assessed. The model was calibrated to experimental data, which varied external concentration of cytokines and resulted in different phenotypes described by varying levels of transcription factors and proteins. We used the ParticleSwarm algorithm implemented in COPASI to determine unknown model parameter values and fully calibrate the model. The resulting model adequately computes the differentiation of CD4+ T cells into the four phenotypes: Th1 with external IFNγ, IL-12, IL-18 and αIL-4 addition, Th2 with IL-4 and αIFNγ addition and iTreg with IL-2 and external TGFβ addition. Also, to induce Th17 differentiation from a naïve CD4+ T cell, external IL-6 and external TGF-β were added in combination and demonstrated upregulation of RORγt, IL-17 and STAT-3. *In silico* simulation consisted of time-courses or parameter scans. Also, the combination of both was performed. In this last case, each plotted line has an incremented concentration of the parameter being scanned. Thus, differential patterns of expression of molecules, either upregulated or downregulation, over time can be observed by looking at the arrows in each molecule. This model is available at www.modelingimmunity.org and extensive information of it has been uploaded.

Mice

B6.CB17-Prkdcscid/SzJ (SCID), B6.129P2(Cg)-Rorctm2Litt/J, C57BL/6J and B6(Cg)-Rag2tm1.1Cgn/J were purchased from The Jackson Laboratory and housed under specific pathogen-free conditions in ventilated racks. The mice were maintained in the animal facilities at Virginia Tech. All experimental protocols were approved by the institutional animal care and use committee at Virginia Tech and met or exceeded

guidelines of the National Institutes of Health Office of Laboratory Animal Welfare and Public Health Service policy.

Cell isolation

Spleens and mesenteric lymph nodes (MLN) were excised and crushed in 1xPBS/5% FBS using the frosted ends of two sterile microscope slides. Single cell suspensions were centrifuged at 300 × g for 10 min and washed once with 1xPBS. Red blood cells were removed by osmotic lysis prior to the washing step. All cell pellets were resuspended in FACS buffer (1×PBS supplemented with 5% FBS and 0.09% sodium azide) and subjected to flow cytometric analysis. Paralelly, colons were excised and lamina propria leukocytes (LPL) were isolated. Tissue pieces were washed in CMF (1× HBSS/10% FBS/ 25mM Hepes), and tissue was incubated twice with CMF/5 mM EDTA for 15 min at 37°C while stirring. After washing with 1×PBS, tissue was further digested in CMF supplemented with 300 U/ml type VIII collagenase and 50 U/ml DNAse I (both Sigma-Aldrich) for 1.5 hs at 37°C while stirring. After filtering the supernatants, cells were washed once in 1x PBS, pellets were resuspended in FACS buffer and subjected to flow cytometric analysis.

Immunophenotyping and cytokine analysis by flow cytometry

For fluorescent staining of immune cell subsets 4-6x10^5 cells were incubated for 20 min with fluorochrome-conjugated primary mouse specific antibodies: anti-CD3 PE-Cy5 clone 145-2C11 (eBioscience), anti-CD4 PE-Cy7 clone GK1.5 (eBioscience), anti-CD4 APC clone RM4-5 and anti-CD25 Biotin clone 7D4 (BD Biosciences). Cells were washed with FACS buffer (1×PBS supplemented with 5% FBS and 0.09% sodium azide). For intracellular staining of transcription factors and cytokines, cells were fixed and permeabilized using a commercial kit according to the manufacturer's instructions (eBioscience). Briefly, cells were fixed and permeabilized for 20 minutes, Fc receptors were blocked with mouse anti-CD16/CD32 FcBlock (BD Biosciences) and cells were stained with fluorochrome-conjugated antibodies towards anti-mouse, FOXP3 FITC clone FJK-16s, anti-mouse ROR gamma (t) PE, clone B2B and anti-mouse IL17-A APC, clone eBio17B7 (eBioscience). All samples were stored fixed at 4°C in the dark until acquisition on a LSR II flow cytometer (BD Biosciences). A live cell gate (FSC-A, SSC-A) was applied to all samples followed by single cell gating (FSC-H, FSC-W) before cells

were analyzed for the expression of specific markers. Data analysis was performed with FACS Diva (BD Biosciences) and Flow Jo (Tree Star Inc.).

Adoptive transfer studies in mice

Six-week-old SCID and RAG2-/- mice were administered intraperitoneally (i.p.) 4 x 10^5 CD4+ CD45RB^{high} CD25- from either CD4 null PPAR γ fl/fl or C57BL/6J (wild-type), or B6.129P2(Cg)-Rorctm2Litt/J mice. Mice were weighed on a weekly basis and clinical signs of disease were recorded daily for 14 wk. Mice that developed severe signs of wasting disease were sacrificed. Otherwise, mice were sacrificed 90 days after transfer.

CD4+ T cell subset sorting

Splenocytes obtained from CD4 null PPAR-γ fl/fl or C57BL/6J (wild-type) mice were enriched in CD4+ T cells by magnetic negative sorting using the I-Mag cell separation system (BD Pharmingen). Cells were incubated with a mixture of biotinylated Abs followed by a second incubation with streptavidin particles and exposed to a magnet to remove unwanted cells. The purity of the CD4+-enriched cell suspension was between 93 and 96%. CD4-enriched cells were used for adoptive transfer, or further purified by FACS. For FACS sorting, cells were labeled with CD45RB, CD4, and CD25 and separated into CD4+ CD45RB^{high} CD25- cells (i.e., effector T cells) in a FACSAria cell sorter (BD Biosciences). The purity of the FACS-sorted CD4+ subsets was ≥98%.

In vitro CD4+ T cell differentiation studies

CD4+CD62L+ cells from either wild-type or T PPARγ null (CD4Cre+) mice were sorted using magnetic activated cell sorting (MACS, Miltenyi Biotec) and stimulated with plate bound anti-CD3 (5μg/ml, BD Biosciences) under Th17 conditions with 2.5 ng/ml hTGF-β1 (R&D Systems), 25 ng/ml IL-6 (Peprotech), 10 μg/ml anti-IL-4 (clone 11B11, R&D Systems), and 10 μg/ml anti-IFN-γ (clone XMG1.2, R&D Systems). 60 hours after activation, an aliquot was obtained to check purity and DMSO-diluted pioglitazone (PIO, Cayman Chemicals) was added to the media at 0, 0.1, 1, 10, 40 or 80 μM. Control (0 μM PIO) was treated with DMSO only. 24 hours after treatment Th17 cells were restimulated with PMA (50 ng/mL, Acros Organics) and ionomycin (500 ng/mL, Sigma) in the presence of BD GolgiStop (BD Biosciences) for 6 h, after which intracellular staining was performed. The experiment was repeated three times for consistency. Co-stimulation of

with CD28 has been described to downregulate Th17 development [129, 254]. We also performed optimization studies for Th17 differentiation using CD28 as a co-stimulatory signal and the addition of recombinant IL-23 in the cytokine cocktail, however, no differences were observed. Co-stimulation signaling optimization studies were run adding either 0 or 2.5μg/mL of αCD28 in the media. No differences were found. Thus, the data presented are with αCD3 stimulation only.

Histopathology

Colonic sections were fixed in 10% buffered neutral formalin, later embedded in paraffin and then sectioned (5μm) and stained with H&E stain for histological examination. Colons were graded with a compounded histological score including the extent of (1) leukocyte infiltration, (2) mucosal thickening and (3) epithelial cell erosion. The sections were graded with a score of 0–4 for each of the previous categories, and data were analyzed as a normalized compounded score.

Statistical analysis

Parametric data were analyzed using the ANOVA followed by Scheffe's multiple comparison method. Nonparametric data were analyzed by using the Mann-Whitney's *U* test followed by a Dunn's multiple comparisons test. ANOVA was performed by using the general linear model procedure of SAS, release 6.0.3 (SAS Institute). Statistical significance was assessed at a $P \leq 0.05$.

Chapter 3

Predictive computational modeling of the mucosal immune responses during *Helicobacter pylori* infection

Adria Carbo, Josep Bassaganya-Riera, Monica Viladomiu, Mireia Pedragosa, Madhav Marathe, Stephen Eubank, Katherine Wendelsdorf, Keith Bisset, Stefan Hoops, Xinwei Dang, Maksudul Alam, Barbara Kronsteiner, Yongguo Mei, and Raquel Hontecillas.

Carbo A., Bassaganya-Riera J., Pedragosa M., Viladomiu M., Marathe M., et al. (2013) "Predictive Computational Modeling of the Mucosal Immune Responses during *Helicobacter pylori* Infection". *PLoS ONE* **8(9)**: e73365. doi:10.1371/journal.pone.0073365

3.1 Summary

T helper (Th) cells play a major role in the immune response and pathology at the gastric mucosa during *Helicobacter pylori* infection. There is a limited mechanistic understanding regarding the contributions of CD4+ T cell subsets to gastritis development during *H. pylori* colonization. We used two computational approaches: ordinary differential equation (ODE)-based and agent-based modeling (ABM) to study the mechanisms underlying cellular immune responses to *H. pylori* and how CD4+ T cell subsets influenced initiation, progression and outcome of disease. To calibrate the model, *in vivo* experimentation was

performed by infecting C57BL/6 mice intragastrically with *H. pylori* and assaying immune cell subsets in the stomach and gastric lymph nodes (GLN) on days 0, 7, 14, 30 and 60 post-infection. Our computational model reproduced the dynamics of effector and regulatory pathways in the gastric lamina propria (LP) *in silico*. Simulation results show the induction of a Th17 response and a dominant Th1 response, together with a regulatory response characterized by high levels of mucosal Treg) cells. We also investigated the potential role of peroxisome proliferator-activated receptor γ (PPARγ) activation on the modulation of host responses to *H. pylori* by using loss-of-function approaches. Specifically, *in silico* results showed a predominance of Th1 and Th17 cells in the stomach of the cell-specific PPARγ knockout system when compared to the wild-type simulation. Spatio-temporal, object-oriented ABM approaches suggested similar dynamics in induction of host responses showing analogous T cell distributions to ODE modeling and facilitated tracking lesion formation. In addition, sensitivity analysis predicted a crucial contribution of Th1 and Th17 effector responses as mediators of histopathological changes in the gastric mucosa during chronic stages of infection, which were experimentally validated in mice. These integrated immunoinformatics approaches characterized the induction of mucosal effector and regulatory pathways controlled by PPARγ during *H. pylori* infection affecting disease outcomes.

3.2 Introduction

Helicobacter pylori is a Gram-negative, microaerophilic bacterium of the Epsilonproteobacteria that colonizes the stomach of nearly a half of the world's population. The presence of *H. pylori* in the stomach has been associated with various gastric diseases: gastritis, peptic ulcer disease, gastric adenocarcinoma, and gastric mucosa-associated lymphoma [255]. CD4+ T helper cells (Th) are recognized as a key component of the adaptive immune response to extracellular bacteria and a dominant component of immune responses to *H. pylori* [256-259]. However, the mechanisms by which CD4+ T cells control *H. pylori* infection, disease and the associated gastric immunopathology are incompletely understood.

Th1 cells are induced by IL-18, IL-12 and IFNγ and express T-bet and STAT1 [135], which delineate their effector function. IFNγ secreted by Th1 cells activates effector

functions of macrophages and dendritic cells (DC) in the gastric LP. IL-17-producing Th17 cells promote effector and inflammatory responses that can aid in fighting infections but can also be implicated in tissue damage. Their induction is determined by the combination of IL-6 and TGF-β in the tissue environment, which activate STAT3 and RORγt, two transcription factors involved in Th17 differentiation [26]. IL-17-producing cells enhance epithelial and neutrophil-derived antimicrobial activity and bacterial clearance during early infection with enteroaggregative *Escherichia coli* (EAEC) [260]. Th17 cells can also produce IL-22, which alone or in combination with IL-17 induces the production of antimicrobial peptides involved in bacterial clearance [261]. In contrast to Th17 cells, regulatory T cells (Tregs) are the main anti-inflammatory CD4+ T cell phenotype and their primary role is to down-modulate effector or inflammatory responses, thus facilitating mucosal homeostasis [262].

The genetic makeup of the host and its interaction with *H. pylori* predispose to clinical outcomes during infection [263]. The nuclear receptor peroxisome proliferator activated receptor gamma, (PPARγ) is a crucial regulator of immune responses [116]. We recently demonstrated that gastric colonization with *H. pylori* ameliorates glucose homeostasis in mice through a PPARγ-dependent mechanism involving the modulation of macrophage and Treg cell infiltration into the abdominal white adipose tissue and neuroendocrine changes in the stomach [264]. Interestingly, two recent clinical studies suggest an association between PPARγ and *H. pylori*-related gastric carcinoma [265, 266]. Also, PPARγ is upregulated during *H. pylori* infection [267, 268]. Furthermore, disruption of the PPARγ pathway by microRNA-146b may be implicated in the regulation of Th17 responses and colitis in *Clostridium difficile*-infected mice [269], and PPARγ tightly controls the plasticity of Th17 cells towards an iTreg phenotype [28]. Despite these advances in understanding the role of PPARγ in mucosal immunoregulation, the mechanisms underlying the modulation of gastric mucosal effector and regulatory pathways during *H. pylori* infection are not completely understood.

Results of human studies support the theory that pathogenic subsets of T cells are instrumental in inducing *H. pylori*-associated gastritis and ulcers [256, 270]. More, specifically, patients with peptic ulcer disease exhibit stronger Th1 and Th2 responses to *H. pylori* infection than asymptomatic carriers, whereas the latter exhibit a Treg-

predominant response during infection [256], suggesting that Treg cells might contribute to the persistence of *H. pylori* in the stomach as a harmless commensal organism. Indeed, IL-10-producing Treg cells were particularly abundant in the gastric mucosa of healthy carriers compared to peptic ulcer disease patients [256]. Thus, CD4+ T cells play a decisive role in initiating and shaping the progression of disease and pathological outcomes in *H. pylori* infected individuals.

Mathematical modeling provides novel means of synthesizing cellular, molecular and tissue-level data into a common systems-level framework. Herein, we used two complementary types of modeling to study the impact of *H. pylori* infection in effector and regulatory pathways at the gastric mucosa. In ODE-based modeling, the variables of the equations represent average concentrations of the various components of the mathematical model whereas ABM takes into consideration the rules and mechanisms of behavior of the individual components of the system and spatiotemporal distribution of agents within the system. In contrast to ODE models that have fully developed, mature and automated systems of parameter estimation, a key limitation of ABM is that sensitivity analysis and parameter estimation methods are immature. To investigate how the interplay between CD4+ T cells and other immune and epithelial cell subsets in the gastric mucosa contributes to driving gastric pathology, we formalized a computational model of *H. pylori* infection using ODE and ABM approaches sequentially. We show that *H. pylori* infection triggers a predominant infectious dose-dependent Th1 response that is paralleled by a concurrent Treg response at the gastric mucosa. We also provide evidence in support of a role for increased effector T cell responses and the loss of PPARγ as key contributors to gastric immunopathology during *Helicobacter* infection. Furthermore, our simulations predict that the main cause of gastric damage in the chronic phase of the infection is the pro-inflammatory and effector immune response driven predominantly by effector T cells.

3.3 Mathematical modeling of mucosal immune responses to *H. pylori* infection

Given the complexity, nonlinearity and abundance of feedback loops in mucosal immune responses to *H. pylori* and to facilitate a better understanding of the mechanisms underlying such immune responses at the systems level, we constructed a SBML network model depicting the major effector and regulatory pathways evoked during *H. pylori* infection [271] (Figure 3.1). The model is comprised of four distinct compartments: the lumen, epithelium, gastric LP, and gastric lymph nodes (GLN). The same network was used for ODE and ABM efforts. The ODE model is comprised of 24 species and 43 reactions in both gastric mucosa and GLN, and encompasses immune networks, which lead to 19 ordinary ODE (Addendum #).

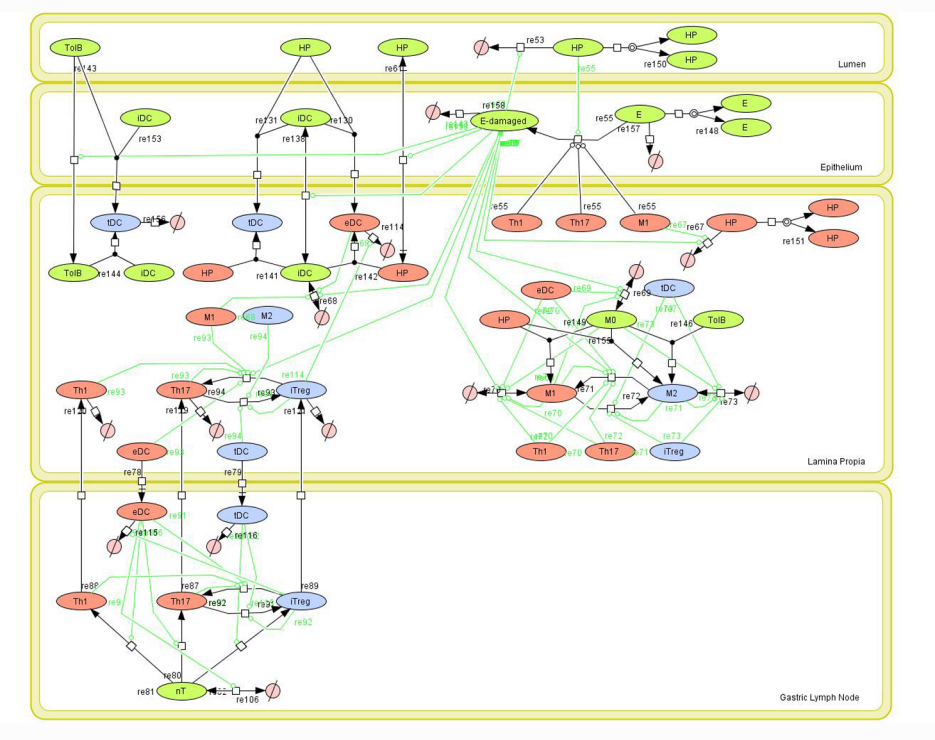

Figure 3.1. Network model of the mucosal immune responses during *Helicobacter pylori* infection. Systems Biology Markup Language (SBML)-compliant network of the interactions between *H. pylori* and cells participating in the innate and adaptive immune response such as macrophages (M1 and M2), dendritic cells (tDC and eDC), epithelial cells (E) and CD4+ T cell subsets (Th1, Th17, iTreg) in the gastric lumen, the epithelium, lamina propria (LP) and the gastric lymph nodes (GLN).

In both ABM and ODE models, effector cell types such as M1 macrophages, Th1, Th17, and pro-inflammatory epithelial cells secrete cytokines and chemokines that i) recruit immune cells, ii) promote activation and differentiation to inflammatory phenotypes, and iii) secrete effector molecules that destroy bacteria and may cause tissue damage.

Regulatory hematopoietic cells such as M2 macrophages, tolerogenic DCs, and Treg cells act antagonistically to their inflammatory/effector counterparts through various contact- and cytokine-dependent mechanisms [272-274].

Immune cell populations are categorized by immunological state (resting, active inflammatory, regulatory), epithelial cells are sub-divided in healthy and damaged subtypes. All populations are further compartmentalized by location in one of four tissue sites (GLN, gastric LP, epithelium and lumen). Computational variables are the absolute number of cells in each compartment over time. Cell differentiation is represented as a flow from one cell-type to another, and migration as a flow from one location compartment to another. In the ABM, individual cells are represented as state-defined agents with concrete spatiotemporal features that follow the model paradigm, changing their state and triggering different reactions as time progresses. This set of agents encapsulates the behaviors of the various individuals that form the system and execution consists of emulating these behaviors after *H. pylori* infection.

Our ABM represents the migration of *H. pylori* from the mucous layer of the gastric lumen towards the epithelium and invasion of the LP. However, upon contact of the bacterium with a healthy epithelial cell, represented as E, bacterial infection is initiated and this epithelial cell starts secreting inflammatory mediators, represented as E_damaged in the network model, thus triggering an inflammatory response that affects macrophages and DCs locally in the LP, which can adopt effector (M1 and effector dendritic cell or eDC) or regulatory (M2 and tolerogenic dendritic cell or tDC) phenotypes. Tolerogenic bacteria (TolB) are also represented, highlighting how commensalism helps to maintain a regulatory phenotype at the gut mucosa.

The ODE model was calibrated using a Particle Swarm algorithm [275] implemented in COPASI [276] with *in vivo* flow cytometry data (Addendum X). Calibration datasets were obtained by intragastrically infecting C57BL/6 mice with *H. pylori* strain 26695 and assaying immune cell subsets (Table 3.1) in the stomach and gastric lymph nodes (GLN) on days 0, 7, 14, 30 and 60 post-infection.

State	Description	Experimental Marker
Th1{LP}	CD4+ T helper 1	CD4+ CD3+ IFNg+ Tbet+
Th17{LP}	CD4+ T helper 17	CD4+ CD3+ RORgt+ IL-17+
iTreg{LP}	Regulatory T cell	CD4+ CD3+ CD25+ FOXP3+
Th1{GLN}	CD4+ T helper 1	CD4+ CD3+ IFNg+ Tbet+
Th17{GLN}	CD4+ T helper 17	CD4+ CD3+ RORgt+ IL-17+
iTreg{GLN}	Regulatory T cell	CD4+ CD3+ CD25+ FOXP3+
eDC{LP}	Effector dendritic cell	CD11c+ MHCII+ IL-12+
tDC{LP}	Tolerogenic dendritic cell	CD11c+ MHCII+ IL-10+
eDC{GLN}	Effector dendritic cell	CD11c+ MHCII+ IL-12+
tDC{GLN}	Tolerogenic dendritic cell	CD11c+ MHCII+ IL-10+
M1	Classically Activated Macrophage	F4/80+ CD11b+ IL-12+
M2	Alternatively Activated Macrophage	F4/80+ CD11b+ IL-10+

Table 3.1. Immunophenotypic markers used in flow cytometry to characterize immune subsets. Different immune cell markers were used to characterize Th1, Th17, Treg, M1, M2 and effector and tolerogenic dendritic cells in both gastric lamina propria and gastric lymph nodes.

In the case of the ABM model, ODE-based model parameter values were used to provide initial values and to narrow the search for parameter values in the estimation. Since parameter estimation techniques in stochastic agent-based processes are not as mature as in ODE tools, starting the parameter value search near the ODE solution facilitates the subsequent trial-error experimentation to find the right parameter that will represent best the experimental data. For this reason, we use ODE-based parameters as a first step in the parameterization process in the ABM-based model. This parameter evolution from the initial ODE values to the final ABM parameter set is represented in Table 3.2.

Parameter	Parameter Description	*Parameter value*									
		ODE	Iteration 1	Iteration 2	Iteration 3	Iteration 4	Iteration 5	Iteration 6	Iteration 7	Iteration 8	Final ABM
aT	Probability of resting T cell stimulation	0.001	0.01	0.1	1	1	1	0.75	0.5	0.5	0.5
p17	Probability of resting T cell stimulation to Th17 vs. Th1 by eDC or M1	0.0001	0.01	0.1	0	0.1	0.1	0.25	0.25	0.25	0.25
anTreg	Probability of resting nTreg stimulation	0.001	0.01	0.1	1	1	1	0.5	0.5	0.5	0.5
vT	fraction of active T cells that become memory T cells	0.005	0.05	0.01	0.1	0.1	0.1	0.25	0.25	0.5	0.5
a1	co-efficient of M1 → M2 activators	0.1	0.5	0.5	1	1	1	1	5	5	5
i1	co-efficient of M1 → M2 inhibitors	0.1	0.5	0.75	1	1	1	1	1	1	1
y1	exponent of M1 → M2	0.1	1	2	4	4	4	4	4	2	2
a2	co-efficient of M2 → M1 activators	0.1	0.3	0.5	1	1	1	1	1	1	1
i2	co-efficient of M2 → M1 inhibitors	0.1	0.1	0.5	1	1	1	1	1	1	1
y2	exponent of M2 → M1	0.1	0.5	0.75	4	4	4	4	4	2	2
ar	co-efficient of iTreg → Th17 activators	0.0001	0.01	0.1	0.1	1	1	1	5	5	5
ir	co-efficient of iTreg → Th17 inhibitors	0.0001	0.01	0.1	1	1	1	1	1	1	1
yr	exponent of iTreg → Th17	0.0001	0.01	0.1	4	4	4	4	4	2	1
a17	co-efficient of Th17 → iTreg activators	0.0001	0.002	0.1	1	1	1	1	1	1	1
i17	co-efficient of Th17 → iTreg inhibitors	0.0001	0.001	0.1	0.1	1	1	1	5	5	5
y17	exponent of Th17 → iTreg	NA	4	4	4	4	4	4	4	2	1
vBM	probability that commensal bacteria induces inflammatory phenotype in macrophages	0.5	0	0	0.9	0.5	0.05	0.25	0.25	0.5	0.5
vBD	probability that commensal bacteria induces inflammatory phenotype in dendritic cells	0.5	0	0	0.9	0.5	0.05	0.25	0.25	0.5	0.25
vBs	probability that commensal bacteria induces inflammatory phenotype in 'sampling' dendritic cells	0.5	0	0	0.9	0.5	0.05	0.25	0.25	0.5	0.5
vEC	Probability that EC transitions to pEcell upon contact within flammatory factors	0.1	0.1	0.01	0.01	0.01	0.1	0.1	0.1	0.25	0.25
vEB	Probability that EC is damaged by microbial toxins	0.1	0.5	0.5	1	1	1	0.5	0.5	0.5	0.5
br	Ability of commensal or inflammatory bacteria to induce chemoattractant expression in epithelial cells	0.00001	0.001	0.1	1	1	1	0.5	0.5	0.5	0.25
uCE	Probability that pEcell is killed by inflammatory factors	0.001	0.01	0.1	1	1	1	0.5	0.5	0.5	0.25
bd	Relative amount of microbicide secreted by pECell, pEC noR in response to commensal or inflammatory bacteria	0.0001	0.0001	0.1	1	1	1	0.5	0.5	0.5	0.25
uM1	Ability of M1 to eliminate bacteria	0.1	0.3	0.5	1	1	1	0.5	0.5	0.5	0.5

Table 3.2. Evolution of parameter values used in the Agent-Based Model (ABM) and Ordinary Differential Equation (ODE)-based *Helicobacter pylori* infection models. Model parameters in the ODE model were obtained from experimental data in mice by running a Particle Swarm algorithm embedded in COPASI. These values were the starting point for optimization methods that would generate the parameter values for the ABM in ENISI. Given that most parameter optimization methods are localized, the starting point is important and can have a

significant impact on the chosen estimated parameter value. Thus, narrowing the search using the parameters of the ODE model represents an efficient way to obtain values for ABM models. Furthermore, the semantics of the ABM are slightly different from the ODE model, in part due to inherent assumptions of the ODE model and also how the ENISI software is set up, making the parameter sets different as well.

3.4 *H. pylori* modulates CD4+ T cell subsets in the GLN and gastric LP

Since CD4+ T cells play a crucial role in determining the outcome of disease during *H. pylori* infection, we sought to determine the relative contributions of effector and regulatory CD4+ T cell subsets in the gastric mucosa during infection. Our ODE modeling approaches showed a distinct time-dependent behavior in Th1, Th17 and iTreg cells represented in the mathematical model during *H. pylori* infection. Th17 cells slightly increased at day 10 post-infection, but as time progressed, they arrived to a plateau at lower levels than Th1 and iTreg cells. In contrast, iTreg cells increased, reaching a stable steady state around day 35 that persisted until day 60 post-infection (Figure 3.2A). Th1 cells chronically populated the gastric LP throughout the infection period, thereby contributing to the overall inflammation of the gastric LP. T cell responses at the gut mucosa were partially controlled by the balance between effector and tolerogenic DCs (eDC and tDC respectively) and the equilibrium constants in our computational model (Figure 3.2B). Flow cytometry analysis of tissues recovered from C57BL/6 wild-type mice infected with *H. pylori* strain 26695 demonstrated that Treg cells were present in both spleen (Figure 3.2C) and GLN (Figure 3.2D), and their numbers were increased starting at day 7 post-infection, reaching a peak around day 30 and persisting throughout the entire infection period. Moreover, we observed the presence of significantly increased percentages of Th1 cells in spleens of *H. pylori*-infected mice on day 30 post-infection (Figure 3.2E). Histopathological analysis of gastric specimens showed mild leukocytic infiltration on the gastric LP (Figure 3.2F) and a slight but significant increase of gastric mucosal hyperplasia (Figure 3.2G).

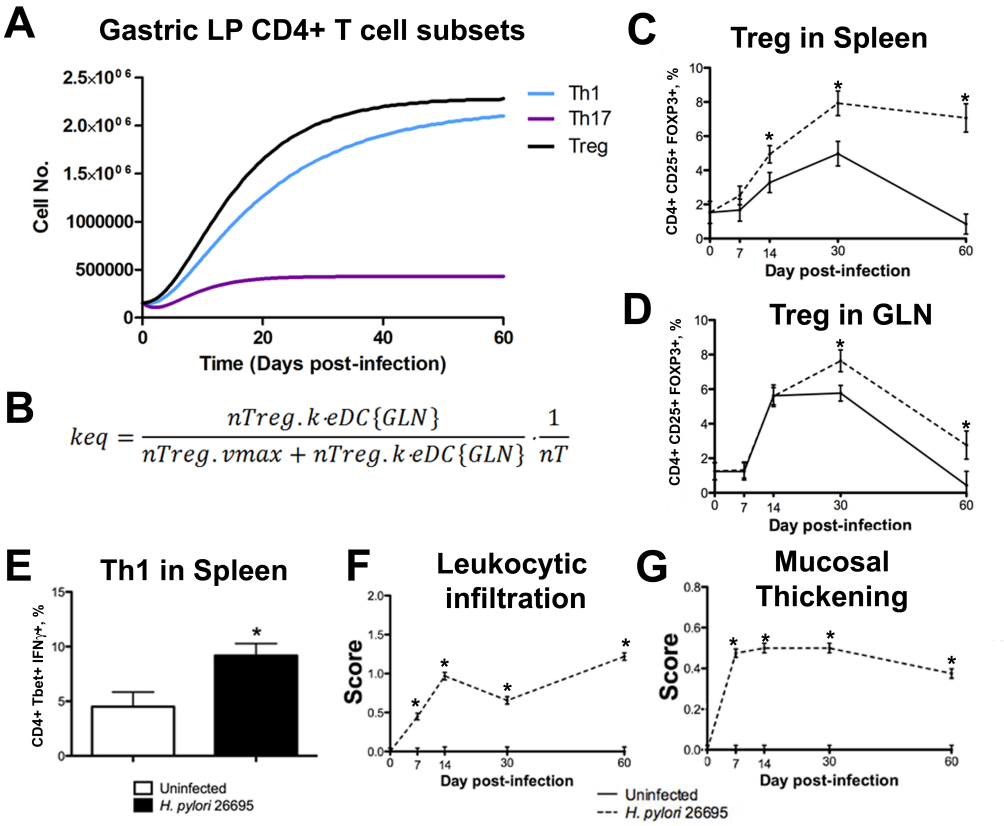

Figure 3.2. Effector and regulatory CD4+ T cell subsets modulate the immune responses during *Helicobacter pylori* infection. (A) *In silico* time-course experiment performed with a challenge of 5x10^7 colony forming units of initial *H. pylori* injected in the mathematical model, showing differences in numbers of gastric lamina propria (LP) CD4+ T cell subsets over time. (B) Equilibrium constant regulating CD4+ T cell gastric lymph nodes (GLN) differentiation in our computational model. (C, D) Flow cytometry analysis results showing differences in the percentages of regulatory T (Treg) cells in spleen and GLN. (E) Flow cytometric analysis showing differences in the expression of IFNγ+ Tbet+ CD4+ T (Th1) cells in the spleen at day 30 post-infection. (F, G) Histopathological analysis on the gastric mucosa showed lesions consistent with *H. pylori* infection. Mouse stomachs had increased leukocyte infiltration in the LP and gastric mucosal thickening due to epithelial cell proliferation.

Additionally, increasing infectious doses of *H. pylori* innoculation elicited a dose-response behavior for Th1 (Figure 3.3A) and Th17 cells in the gastric LP (Figure 3.3B). To validate this model prediction, we performed a dose-response study where mice were inoculated with 0, 10^8, 10^9 or 10^{10} CFU/mL *H. pylori* strain 26695. *In vivo* results demonstrated that the expression of T-bet and RORγt, as well as the production of IFNγ, all within the CD4+ T cell compartment, is dependent on the initial inoculation dose of *H. pylori* (Figure 3.3C-3.3E).

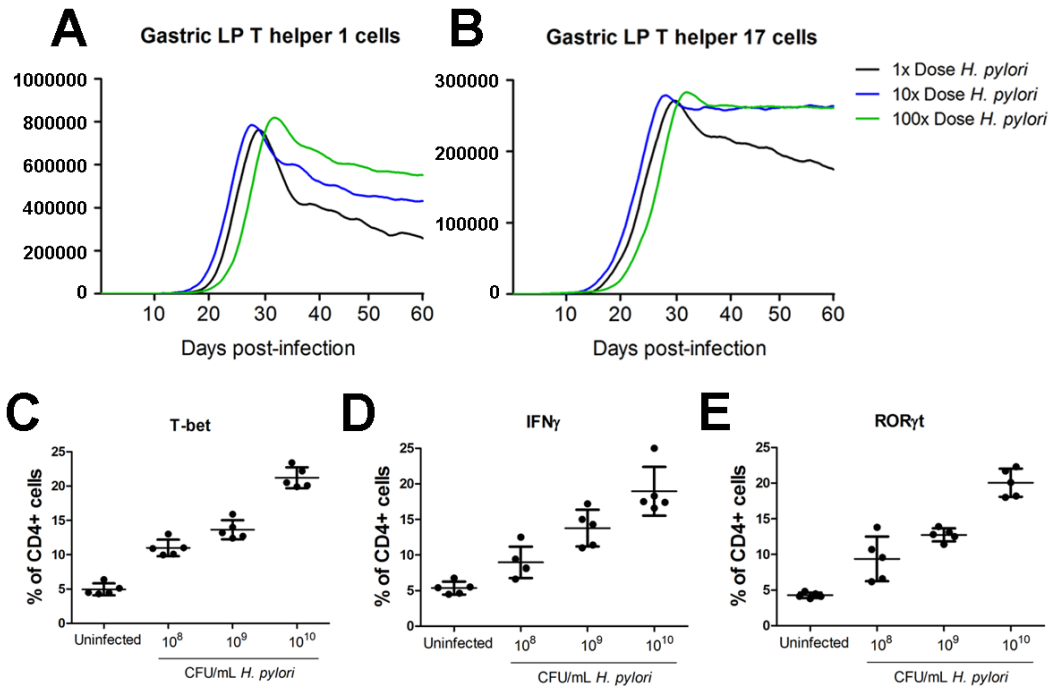

Figure 3.3. Th1 and Th17 responses during *Helicobacter pylori* infection are dose-dependent. Computational simulations with the *H. pylori* model demonstrating a dose-response effect with the initial dose of *H. pylori* in (A) Th1 and (B) Th17. *In vivo* experimentation validating this prediction by observing increased levels of splenic (A) T-bet, (B) IFNγ and (C) RORγt with increasing concentrations in the initial dose of *H. pylori*.

3.5 Myeloid cell-specific PPARγ deletion modulates macrophage, dendritic cell, and T cell differentiation during *H. pylori* infection

PPARγ is recognized as an important immunoregulatory molecule in the gastrointestinal mucosa. To elucidate the role of PPARγ in both myeloid and T cell subsets during *H. pylori* infection, we created cell-specific knockout models. First, to simulate the myeloid-specific PPARγ knockout system we reduced the maximum rate of undifferentiated macrophage M0 transitioning to alternatively-activated M2 macrophages, reduced the maximum rate of M1 conversion to M2 macrophages [204, 277], and reduced the rate of iDC switching to tDC by cytokines [278]. In the case of the T cell-specific PPARγ knockout, we lowered the rate of naïve CD4+ T cells becoming iTreg [114], the maximum rate of Th17 differentiation to iTreg [204] and the rate of constitutive iTreg

stimulation [114, 279]. Simulation results showed a marked impact of the loss of PPARγ on myeloid cell populations following infection. Specifically, when compared to the wild type model, there was an increase in eDC and decreased tDC in both the gastric LP and the GLN (Figure 3.4A and 3.4B). Similarly, elevated M1 and reduced M2 macrophage numbers in the LP were observed (Figure 3.4C and 3.4D). Along with the elevated inflammatory response in the myeloid cell populations we found a decline in *H. pylori* in the gastric lumen indicating more efficient clearance (Figure 3.4E) and a slightly elevated epithelial cell death (Figure 3.4F) in the myeloid-specific PPARγ knockout model when compared to the wild-type system.

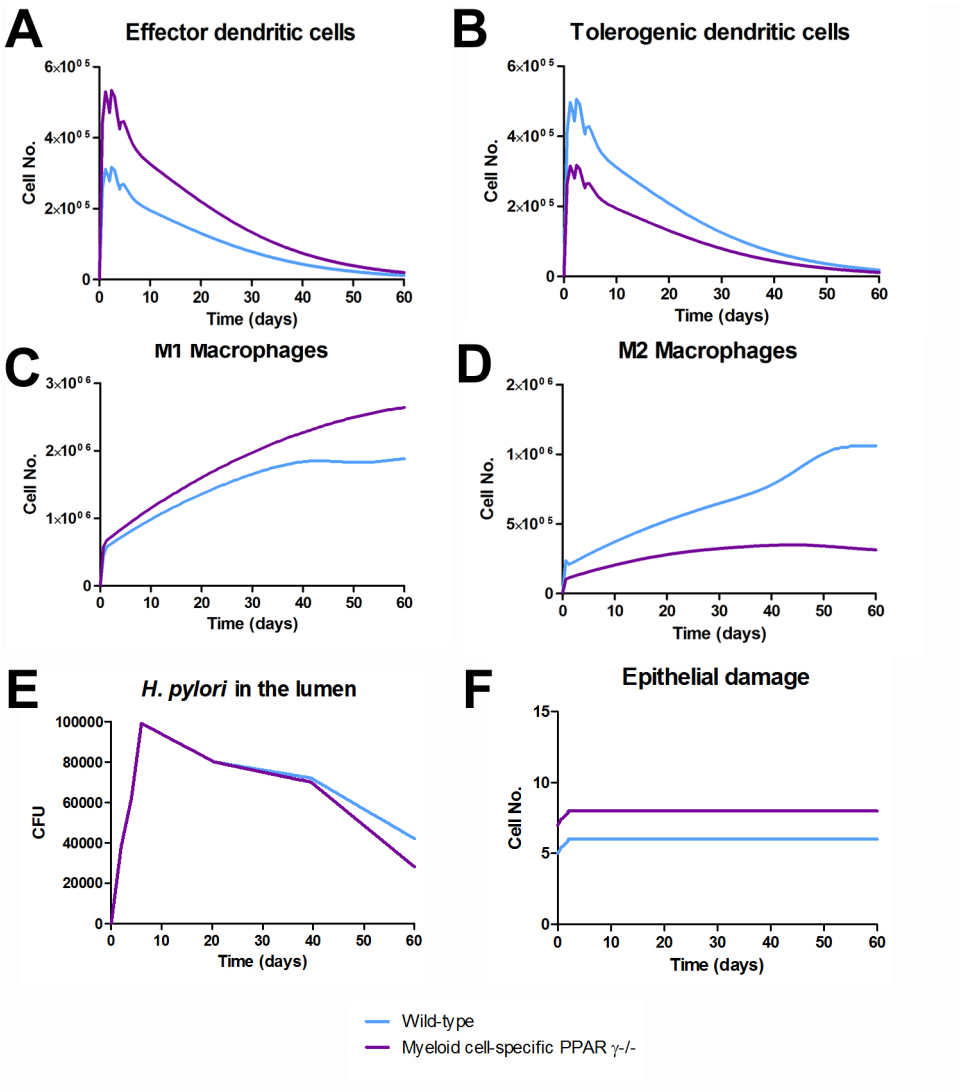

Figure 3.4. Predicted dynamics of gastric mucosal cell subsets and luminal *Helicobacter pylori* counts following *in silico* infection of wild-type and myeloid-specific PPARγ

knockout models. Time-courses were run *in silico* with infections using $5x10^7$ colony forming units (CFU) of *H. pylori* to determine myeloid subsets dynamics. The blue lines represent the wild-type model whereas violet lines represent the PPARγ knockout model in (A) gastric lamina propria (LP) effector dendritic cells, (B) LP tolerogenic dendritic cells, (C) LP M1 macrophages, (D) LP M2 macrophages, (E) *H. pylori* loads in the stomach lumen and (F) epithelial cell damage following infection with *H. pylori.*

The T cell-specific PPAR γ knockout model showed elevated Th1 and Th17 (Figure 3.5A and 3.5B) when compared to the wild-type model, whereas iTreg cell levels in the LP were dramatically decreased (Figure 3.5C). Interestingly, no differences in the numbers of effector or tolerogenic DC were observed (Figure 3.5D and 3.5E). However, a lack of PPARγ in T cells had a mild effect on macrophage populations, increasing the expansion of M1 macrophages (Figure 3.5F) and decreasing the numbers in the M2 alternatively activated macrophage subset (Figure 3.5G).

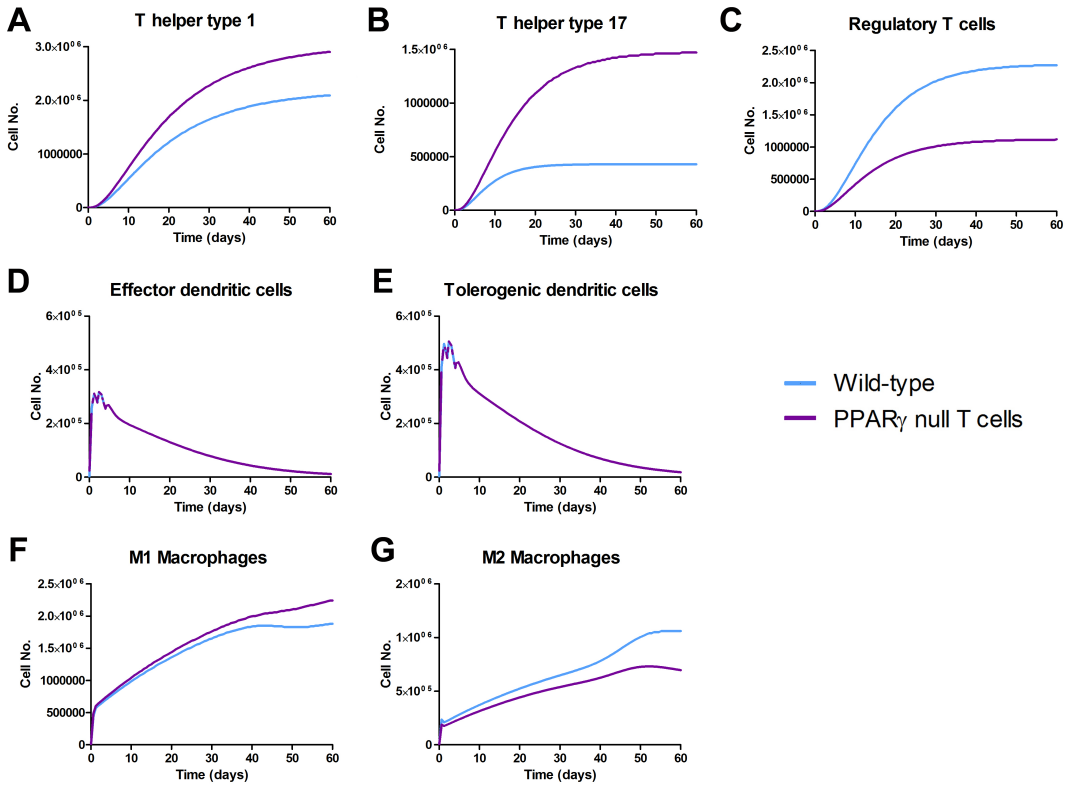

Figure 3.5. *In silico* dynamics of gastric mucosal T cell subset in wild-type and T cell-specific PPARγ knockout mice following infection with *Helicobacter pylori*. Time-course experiments following infection with $5x10^7$ colony-forming units (CFU) of *H. pylori* to determine dynamics on CD4+ T cell phenotypes. Blue lines represent wild type mice and violet lines represent T cell-specific PPARγ knockout mice. T helper (Th) 1 (A), Th17 (B), induced regulatory

T cell (iTreg) (C), effector dendritic cells (D), tolerogenic dendritic cells (E), M1 macrophages (F) and M2 macrophages (G) are illustrated.

3.6 Modeling stochasticity in cellular responses during *H. pylori* infection by using ENteric Immunity SImulator (ENISI)

To further characterize the immunological mechanisms underlying mucosal immune responses to *H. pylori* in a stochastic system, we used ABM based on parameter values derived from refinement on our initial ODE model parameters (Table 3.2). When probabilistic approaches are used, the complex immunological processes can be better represented. We adopted the ABM tool ENteric Immune Simulator (ENISI) developed by us and available at www.modelingimmunity.org [280]. To calibrate the ABM we used a set of parameters derived from our ODE-based modeling approaches as initial values before refinement. After implementing the model specification as well as the initial concentrations as previously described [281], we ran simulations up to 60 days post-infection and analyzed the changes in cell concentrations in both LP and GLN. Results expressed in heat map concentrations show a significant increase in the concentration of CD4+ T cells in both the gastric LP and the GLN (Figure 3.6).

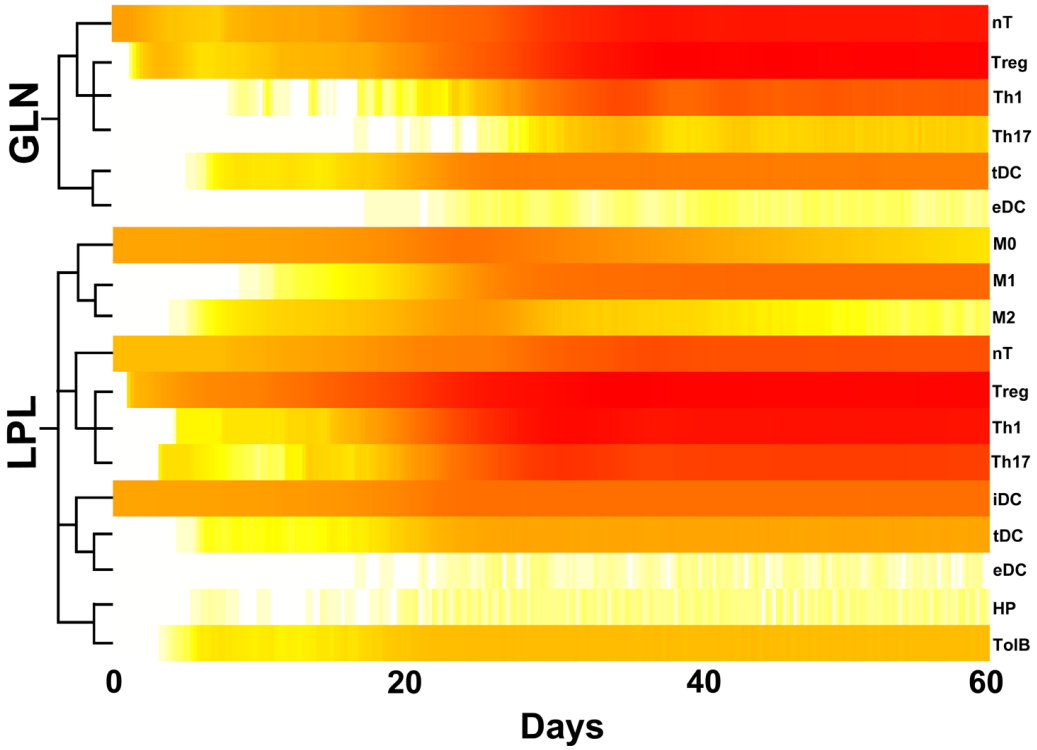

Figure 3.6. ENISI output results after *Helicobacter pylori* infection *in silico*. The *H.pylori*-implemented agent-based model was run as a time-course for 60 days. Heatmap representation of cell concentrations being modulated over time in the gastric Lamina Propria (LPL) and in the Gastric Lymph Nodes (GLN). Cell types are grouped by function and effector vs. regulatory mechanisms.

Taking a closer look at CD4+ T cell subsets following infection in the wild-type model, we observed that in the GLN, Th1 cells peaked on day 30 post infection and remained at high levels with fairly constant values throughout the rest of the infection period (Figure 3.7A, 3.7G). Th17 responses were induced in the GLN and later detected in the LP, together with a Treg cell response that persisted over time in both gastric LP (Figure 3.7B, 3.7C) and GLN (Figure 3.7H, 3.7I).

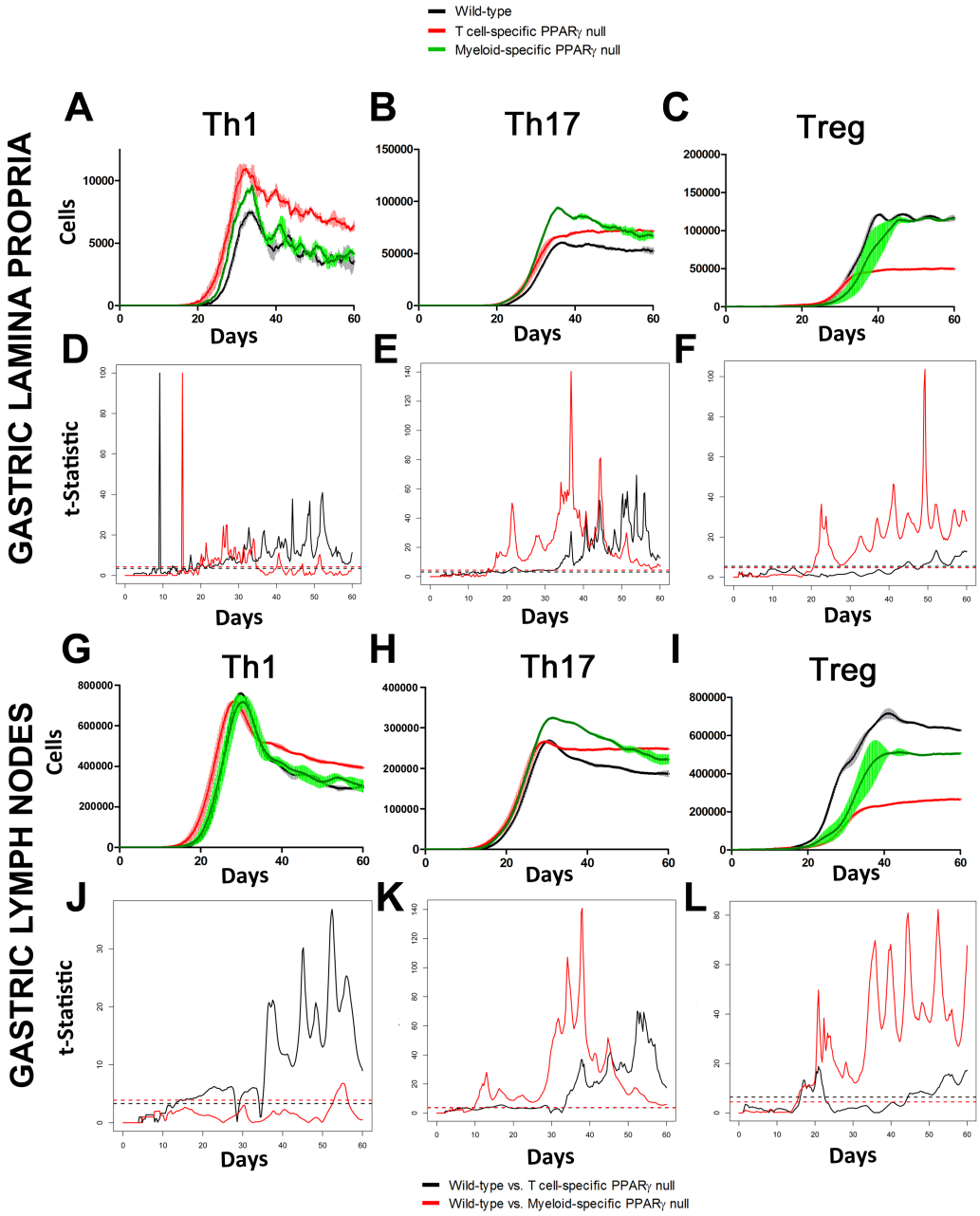

Figure 3.7. ENISI output results and assessment of the role of PPARγ in both the myeloid and T cell subset modulated T cell responses after *Helicobacter pylori* infection *in silico* in the gastric LP and GLN. The *H. pylori* ABM was run as a time-course for 60 days. Model parameters were changed to simulate myeloid or T cell-specific PPARγ knockout systems as described in Table S2. Dynamical variation of Th1 (Figure 6A, 6G) as well as Th17 (Figure 6B, 6H) and regulatory T cells (Figure 6C, 6I) changing over time were plotted. A functional T-test was used with 95% confidence interval to create statistics assessing differences in the myeloid and T cell specific PPARγ knock-out for Th1 (Figure 6D, 6J), Th17 (Figure 6E, 6K) and Treg (Figure 6F, 6L). A threshold value representing the critical value of significance vertically divides the plot into two parts, showing significant differences above the threshold. Data were obtained in 15 runs of the simulation for each different genotype.

3.7 ABM highlights the immunoregulatory role of PPARγ in modulating host responses towards *H. pylori in silico*

In order to investigate the role of PPARγ in mucosal immune responses to *H. pylori in silico*, we engineered T cell-specific and myeloid cell specific PPARγ knockout models. Specifically, to create an *in silico* cell-specific knockout model, rates of regulatory phenotype differentiation were lowered and rates controlling effector response in both LP and GLN were increased. A side-by-side comparison on the parameter changes implemented in the T cell- and myeloid cell-specific PPARγ knockout systems can be found in Table S6. We used a functional T-test to visualize statistically significant differences over time when comparing wild-type and the knockout models. Our results showed a statistically significant expansion of Th1 in the T cell-specific PPARγ null system when compared to the wild-type starting around day 35 and increasing the difference throughout the infection up to day 60 in the gastric LP (Figure 3.7A and 3.7D). In the GLN, significant differences were first detected around day 50 and peaked throughout the rest of infection (Figure 3.7G and 3.7J). No statistically significant differences in Th1 cell numbers were found between the wild-type and the myeloid cell-specific PPARγ knockout system (Figure 3.7A, 3.7D, 3.7G and 3.7J). Regarding Th17 cells, these simulations depicted the immunoregulatory role of PPARγ in the myeloid subset since we observed significant differences in enhanced Th17 responses in the myeloid cell-specific PPARγ knockout model when compared to the wild-type. More specifically, there was a statistically significant effect starting at day 30 and remaining significant until day 60 in the gastric LP (3.7B and 3.7E) and the GLN (3.7H and 3.7K). Th17 cell numbers were also significantly higher in the T cell-specific PPARγ knockout model when compared to the wild-type model in both LP (Figure 3.7B and 3.7E) and the GLN (Figure 3.7H and 3.7K). T cell-specific PPARγ deficiency significantly impaired the expansion of the iTreg cell compartment starting at day 30 and showed an oscillatory behavior and significant differences until day 60 in the gastric LP (Figure 3.7C and 3.7F). In the GLN, the differences between the T cell specific PPARγ knockout and the wild-type were significantly noticeable during the whole period of infection (Figure 3.7I and 3.7L). The myeloid cell-specific PPARγ knockout showed similar differences. In the case of the GLN, the myeloid cell-specific PPARγ knockout model showed significant

differences when compared to the wild type up to day 30 post-infection (Figure 3.7I and 3.7L).

3.8 Gastric histopathological lesions are formed as a consequence of effector immune activation during the chronic phase of the *H. pylori* infection

Sensitivity analysis shows whether the model predictions are sensitive to model parameters and concentrations. It also helps to understand complex relationships between distinct model variables. We extended our modeling approaches to determine which are the main factors involved in gastric lesion development during *H. pylori* infection by using sensitivity analysis. Our sensitivity analysis results using ABM showed how at the early stage of infection (up to week 2 post-challenge), the epithelial cell damage is mainly caused by the bacterium (Figure 3.8A). Interestingly, as the infection progresses, we observed a trend towards Th1 and Th17 cells triggering epithelial cell damage starting 3 weeks post-infection. At the chronic phase of the infection (i.e., around 6-8 weeks post-infection), our results showed a dominant role of Th1 and Th17 effector cells in inducing epithelial cell damage (Figure 3.8A). *H. pylori* induced epithelial cell damage throughout the infection. However, at a later infection stage, the induction of damaged epithelial cells by the effector Th1 and Th17 phenotypes overshadowed the effect of *H. pylori* itself. Of note, sensitivity analysis performed in the deterministic model at day 60 post-infection also showed how Th1 and Th17 cells in both LP and GLN were contributing to the epithelial cell damage as well as M1 macrophage differentiation, whereas *H. pylori* had a more limited impact on the formation of such lesions (Figure 3.8B). This sensitivity analysis data suggested that the main contributors of histopathological damage in the gastric mucosa at a chronic stage of infection are Th1 and Th17 effector responses. Going one step further from the model prediction, we hypothesized that the effector T cell response and not the bacterium itself is the main cause of epithelial cell damage during the chronic phase of *H. pylori* infection.

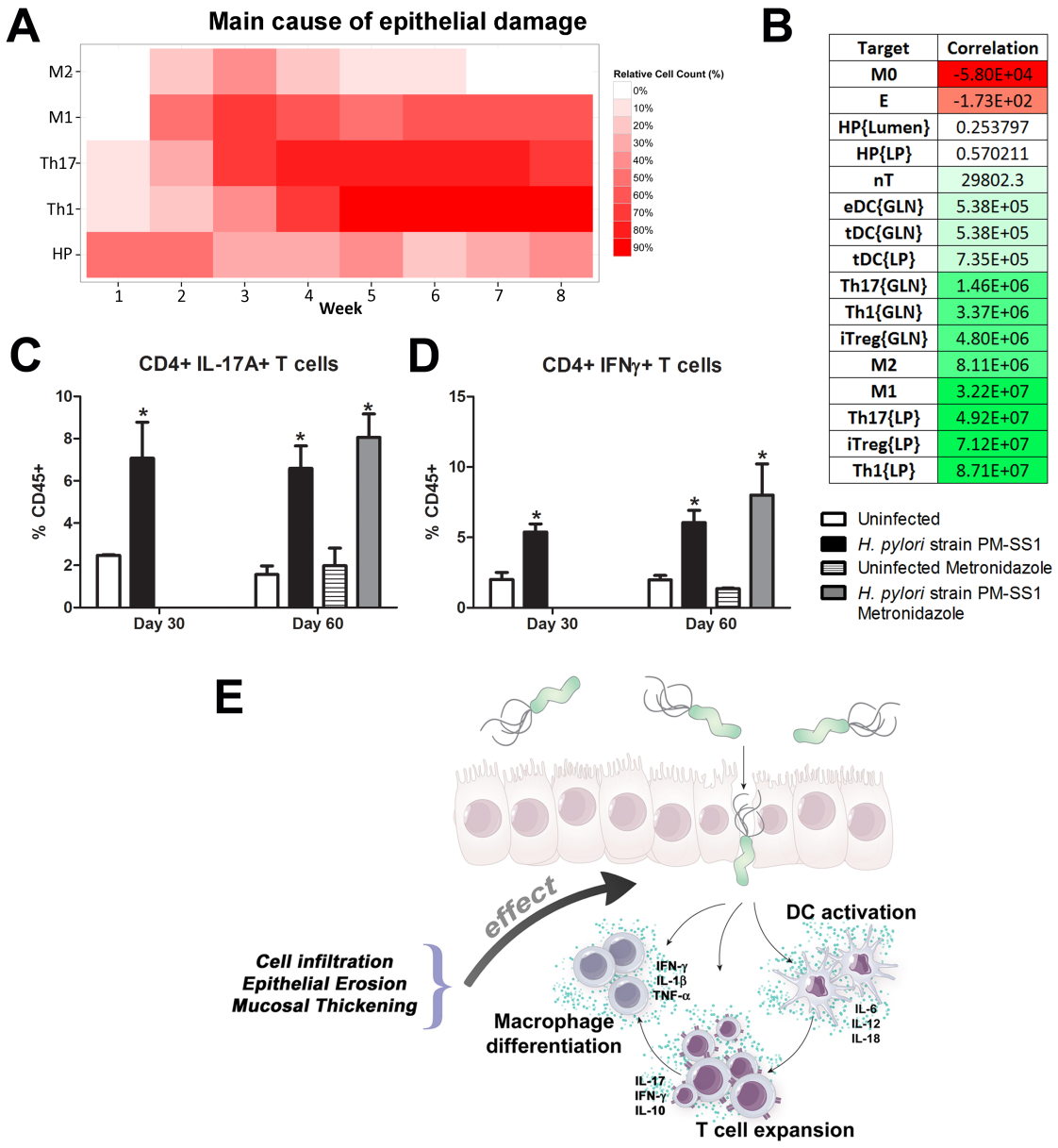

Figure 3.8. Sensitivity analysis of factors involved in gastric inflammatory lesion formation following *Helicobacter pylori* infection. Healthy epithelial cells changing state into pro-inflammatory epithelial cells, thereby contributing to the formation of gastric lesions. (A) Differential time-dependent patterns of lesion formation in the early, meridian and chronic-late stage of infection. (B) ODE-based deterministic sensitivity analysis on pro-inflammatory epithelial cells, as variables, and its formation at day 60 post-infection using a delta factor of 0.001 with a delta minimum of $1x10^{-12}$. (C) Flow cytometric analysis showing differences in the expression of CD4+ IL-17A+ cells in the gastric lamina propria after *H. pylori* infection. (D) Flow cytometric analysis showing differences in the expression of CD4+ IFNγ+ cells in the gastric lamina propria after *H. pylori* infection. (E) Cartoon model representation of the effect of DC activation, T cell expansion and macrophage differentiation on the formation of histopathological lesions in the gastric lamina propria (LP) during *H. pylori* infection.

To validate this hypothesis, C57BL/6 wild-type mice were infected with *H. pylori* strain PM-SS1 to characterize mucosal immune responses and to assess contributors to epithelial cell damage. In this study, a group of mice was treated with metronidazole, an antibiotic shown to effectively clear *H. pylori* from the stomach [282]. This experimental design (Figure 3.9) allows us to begin dissecting the effects of the dynamics of the host response versus the bacterium in the chronic phase of disease.

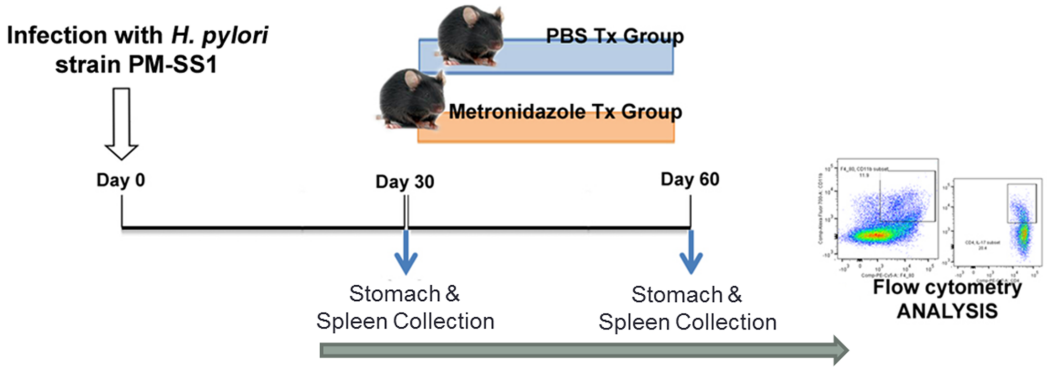

Figure 3.9. Experimental design to validate model prediction on main inducers of histopathologcal changes during *Helicobacter pylori* infection. Wild-type mice were infected with *H. pylori* strain PM-SS1 for 30 and 60 days to monitor cell infiltration and gastric histopathological changes. On day 30 post-infection, a group of mice were euthanized for baseline immunological measurements and the rest were divided into two groups: one treated with metronidazole and one treated with sterile PBS as a control. These groups were euthanized at day 60 post infection.

On day 30 post-infection, a group of mice were euthanized for baseline immunological measurements and the rest were divided into two groups: one treated with metronidazole and one treated with sterile PBS as a control. At day 60 post-infection the remaining mice were euthanized for histological and immunological analyses. Immunophenotyping results showed a pronounced increase of IL-17A- (Figure 3.8C) and IFNγ-producing cells (Figure 3.8D) in the gastric LP after 30 and 60 days post-infection. Metronidazole treatment did not affect effector cytokine expression. These results suggested that effector T cell responses are implicated in lesion development during infection as showed in a cartoon model representation, highlighting the involvement of DC, T cells and macrophages on the formation of gastric lesions in the LP is shown in Figure 3.8E. To determine the presence of gastric mucosal lesions we examined H&E-stained gastric samples. The results show an increased mucosal thickness and mild

infiltration of inflammatory cells, which were more accentuated on day 60 compared to day 30 post-challenge (Figure 3.10).

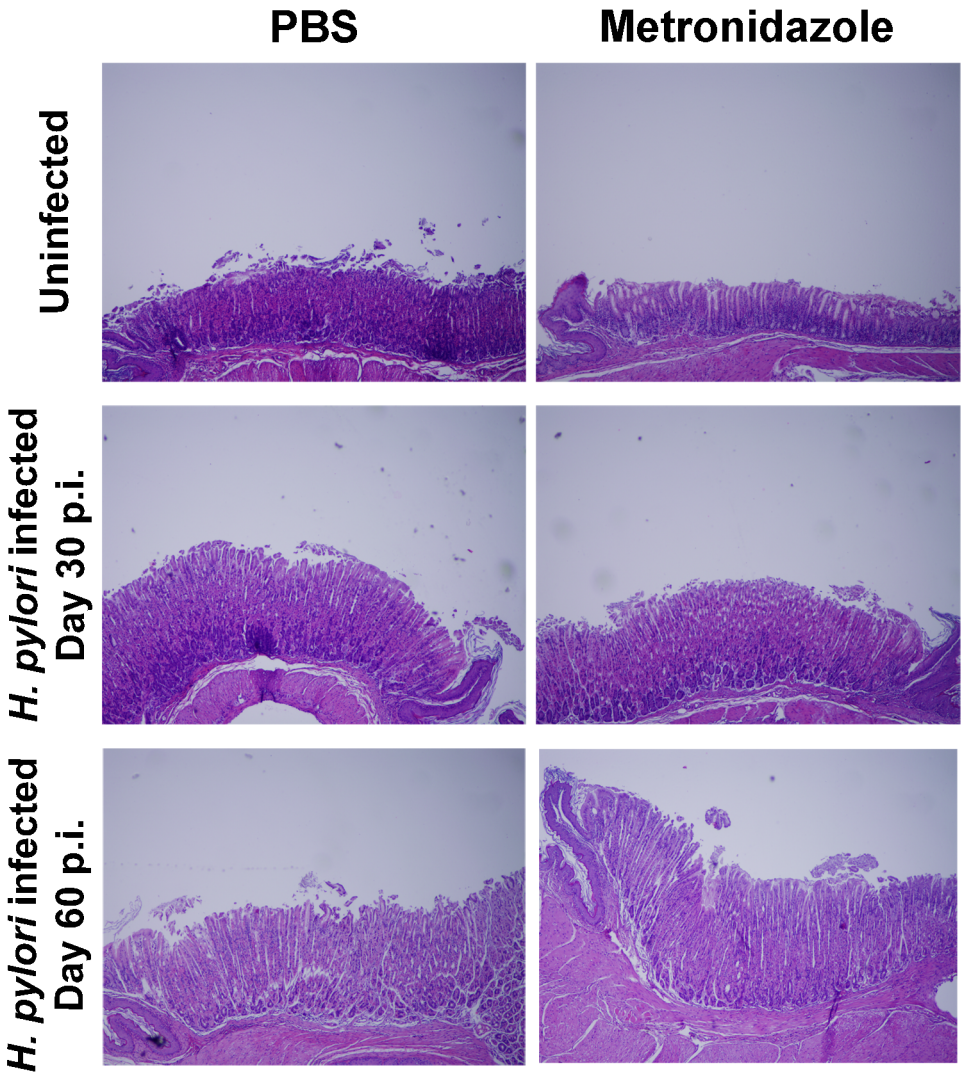

Figure 3.10. Histopathological assessment of the gastric mucosa of mice after *Helicobacter pylori* infection. Representative photomicrographs of stomachs from either non infected or *H. pylori*-infected mice following administration of PBS or metronidazole treatment. Original magnification 40x.

At day 60, no differences were found between mice that received antimicrobial therapy to eradicate *H. pylori* and those that remained untreated. In both groups, we observed a significant increase in the thickness of the gastric mucosa characterized by the

elongation of the gastric pits and moderate depletion of chief cells at the base of glands (Figure 3.10).

3.9 Discussion and Conclusions

Helicobacter pylori infection is associated with an increased risk for developing gastric and duodenal ulcers, gastric mucosa-associated lymphoid tissue lymphoma and gastric adenocarcinoma [283-285]. There is also increasing evidence of *H. pylori* providing protection against esophageal and cardial pathologies [286-289], childhood asthma [290-292], childhood allergies [291, 293], obesity and diabetes [264]. The immunological mechanisms underlying this protective effect of *H. pylori* acting as a commensal bacterium versus a pathogenic organism are incompletely understood.

Here, we combined computational modeling and animal experimentation approaches in an iterative cycle aimed at investigating immunological mechanisms underlying the modulation of mucosal immune responses to *H. pylori*. Overall, our modeling results demonstrate that CD4+ T cells are implicated in *H. pylori* clearance from the gastric LP. Previous studies have shown that *H. pylori*-specific CD4+ T cells preferentially home and accumulate in the infected stomach and L-selectin, C-C chemokine receptor type 4 (CCR4) and macrophages derived chemokines (MDC) play a critical role in Th cell recruitment and trafficking [270]. Indeed, our immunophenotyping results show an increased expression of CD4+ T cell specific IL-17A and IFNγ in the gastric LP following *H. pylori* infection.

Chronologically, we have demonstrated that *H. pylori* evokes a weaker Th17 response, followed by a dominant and more persistent Th1 response that is paralleled by an immunoregulatory CD4+ T cell response characterized by Treg cells slowly accumulating at the beginning of the infection, reaching the highest levels at 30 days post-infection that is sustained over time. Our *in vivo* data matches the simulation results in splenic and GLN Treg cells. Not surprisingly, Treg cell responses suppress inflammation and ulceration caused by the excessive host response to the bacterium [285, 294] and their

balance with other subsets is critical for preventing gastric and duodenal ulcers [295]. Treg cell numbers were significantly decreased in the GLN at day 60, suggesting a potential migration from inductive to effector mucosal sites. We have also observed a downregulation of Th17 responses *in silico* after the first stage of infection, suggesting that effector Th1 cells might be implicated in the chronicity of infection and mucosal lesion development. The plasticity between Th17 and Treg cells, and the mechanisms controlling such phenotypic re-programming are under investigation. Interestingly, pro-inflammatory Th17 cells can acquire a regulatory phenotype with *in vivo* immunosuppresive properties [48]. We recently characterized PPARγ as a key modulator of Th17 plasticity towards an iTreg phenotype by using a combination of systems modeling of CD4+ T cell signaling and *in vivo* validation [279]. Gastric mucosal IL-17-producing cells can also contribute to development of gastric lesions [296, 297]. IL-17 also plays an important role in promoting B cell crosstalk and decreasing inflammation, therefore accentuating regulatory responses [298]. Hence, Th17 cells can exert dual functions as effectors of pathogenic tissue-damaging responses, but also as immunoregulatory responses driven by the secretion of IL-17 and IL-22 [299].

CD8+ T cells are crucial in *H. pylori* infection in humans and pigs [300, 301]. However, our experimental data in mice did not show any differential behavior in CD8+ T cells. Therefore, given the focus of our experimental questions on CD4+ T cells and our initial CD8+ T cell data we decided not to include CD8+ T cells and focus modeling work in the potential involvement of Th1 and Th17 effector responses in the induction of gastric lesions during the chronic phase of *H. pylori* infection. Of note, our sensitivity analysis highlighted the important role of Th1 and Th17 effector cells in the induction of gastric mucosal lesions in the chronic phase of the infection, even overshadowing the role of *H. pylori* itself. Consistent with our computational simulations, our in vivo studies validated the hypothesis that the role of *H. pylori* in tissue damage during the chronic phase of the infection is dramatically reduced.

To study the mucosal immune responses to *H. pylori* at the systems level locally in the gastric mucosa, we used ODE and ABM sequentially. First, our deterministic ODE model shed some new light on CD4+ T cell distribution after infection as well as the role of PPARγ during infection. Secondly, and because strategies for parameter estimation are

neither fully developed nor automated in ABM, the ODE model provided a set of parameter values that were after used as a starting point for our ABM modeling. Since the ABM model uses a probabilistic approach, in comparison to the constant-based ODE model, further refinement on the parameter values was needed and trial-error simulations were performed. Despite of this additional step, having an initial parameter range based on the ODE model has narrowed the range and improved efficiency in the parameter estimation process for ABM. Furthermore, ABM adds randomness to the biological systems, which can help to better represent complex cellular responses and to take into account the individual and emerging behaviors of cells as well as the role spatiotemporal features. Thus, stochastic models can provide novel insights into the effect of cognate and non-cognate interactions, representing entire systems with a greater granularity and capturing cell-cell interactions. By simulating individual behaviors of agents, ABM better represents cross-linked, complex and nonlinear processes with multiple feedback loops and, provides a more comprehensive and interactive modeling of mucosal immune responses to *H. pylori*. The ability of ABM to encompass multiple scales of biological processes and incorporate spatiotemporal considerations, coupled with an intuitive modeling paradigm, underscores the added value of this modeling framework in translational systems immunology and immunoinformatics research. Our combined modeling ODE and ABM approaches provided evidence suggesting that the cause for gastric lesions during the chronic stage of the infection were effector Th1 and Th17 cell subsets as well as inflammatory macrophages. Furthermore, both ODE and ABM based models could generate several predictions that were validated *in vivo*, such as detecting *H. pylori* dose-response dynamics in Th1 and Th17, showcasing the predictive power of the *H. pylori* model. Future studies will investigate the spatiotemporal progression of lesions in relation to immune cell trafficking in the tissue space.

Instructive and selective factors play important roles in shaping the immune responses in the gut. CD4+ T cell and macrophage differentiation highly depends on the cytokine environment, an instructive factor, and the competition of cells for phenotype-changing cytokines (i.e., selective factors). However, secretion of cytokines and chemokines into the tissue environment by cells depends upon intracellular signaling pathways. Multi-scale modeling approaches that combine intracellular signaling pathways and tissue level modeling of cell-cell, cell-bacteria, and cell-molecule interactions will be necessary

to fully represent the mechanisms underlying the actions of selective and instructive factors in mucosal immune responses.

PPARγ is a transcription that tightly controls many aspects of mucosal immune responses. For instance, PPARγ is a negative regulator of macrophage activation [159] and its inhibition contributes to systemic inflammation [302]. Myeloid cell-specific loss of PPARγ has been reported to enhance chemokine and adhesion molecule expression leading to improve recruitment of inflammatory Ly6C^{hi} monocytes to sites of inflammation and infection [303]. Indeed, our results show that PPARγ modulated effector and regulatory responses also during *H. pylori* infection. With the ability to create computational models and extensive *in silico* knockout systems, where expression of the molecule of interest is ablated, we demonstrated a suppression of M2 macrophages and tolerogenic DC, and an increase of M1 macrophages and effector DC in our myeloid cell-specific PPARγ knockout model. A decline in *H. pylori* in the lumen was also observed in the knockout model, indicating more efficient bacterial clearance in the PPARγ knockout model. This coincides with elevated epithelial cell damage, indicating that *H. pylori* could be removed at the expense of elevated gastric lesions. Thus, our results demonstrate that PPARγ in the myeloid subset has a major role in modulating and controlling pro-inflammatory versus anti-inflammatory cell profile and consequently, a central role on bacterial clearance. These findings are in line with a recent report indicating that the lack of PPARγ in myeloid cells confers resistance to *Listeria monocytogenes* infection [303], suggesting that a regulatory network in myeloid cells that is governed by PPARγ restrains bacteriocidal activity and recruitment of inflammatory/effector cell subsets to the mucosal sites.

In CD4+ T cells, PPARγ partially drives differentiation and plasticity between phenotypes [115, 204, 279, 304-306]. Our *in silico* knockout studies in CD4+ T cells highlight the anti-inflammatory properties of PPARγ by observing a suppression of Treg cell numbers and enhancement of effector phenotypes such as Th1 and Th17 in the knockout when compared to the wild-type models. Interestingly, our simulations with the myeloid cell-specific PPARγ knockout system promoted Th17 differentiation and suppressed Treg expansion. Considering that CD4+ T cells have a pivotal role and crosstalk with different

subsets of DC, our findings are in line with other studies suggesting that DC subsets affect Th17 differentiation and plasticity in humans, where CD14+ HLA-DR-/low myeloid derived suppressor cells (MDSC) induced FOXP3+ regulatory T cells whereas CD14+ HLA-DR+ MDSCs promoted the generation of IL-17 secreting CD4+ T cells [99]. Furthermore, myeloid APCs are essential for the induction of IL-17A+ FOXP3+ T cells from memory CCR6+ T cells or Treg cells [248]. These results point out for the first time that PPARγ in myeloid cells plays a central role in Th17 differentiation. In addition, the deletion of PPARγ in T cells had a milder effect in the expression of differentiated macrophages, increasing the numbers of the M1 population and decreasing M2 macrophages. These findings are in line with the importance between innate and adaptive immunity and how CD4+ T cell-derived cytokines can affect the differentiation into pro- versus anti-inflammatory phenotypes. Therefore, CD4+ T cells are necessary and sufficient for gastritis induction in the *H. pylori* infection model. We also observed an oscillatory behavior in the wild type Th1 cell population as well as the knock-out models in the gastric LP using our ABM approach. This phenomena observed in the continuum of interest may be related to biological feedback loops in mucosal immune responses that contribute to maintain homeostasis and priming. One possible explanation could be the iterative process by which dendritic cells enter the GLN and expose the antigen to CD4+ T cells, incrementing its concentration as the subpopulation expands, and decreasing it when chemotactic strategies make CD4+ T cells to leave the lymphatic compartment. Of note, our modeling work highlights CD4+ T cell priming in the GLN. Some studies also point that CD4+ T cells are also likely primers with *H. pylori* antigens captured in the small intestines, where the coccoid form of *H. pylori* is taken up by DCs in the Peyer's Patches [307]. Future studies using multi-scale modeling will elucidate the relationship between the intracellular differentiation pathways, the link to different subsets in the innate immune system and the potential relationships that can rise oscillatory trends in the system.

In summary, we combined computational modeling approaches and mouse challenge studies to investigate how CD4+ T cells and other immune cell subsets are distributed in the gut mucosa during *H. pylori* infection. Our model simulated T cell responses to *H. pylori* by using both platforms: ODE and ABM. Our modeling efforts predicted higher

levels of effector responses in both the LP and the GLN when deleting PPARγ, thus highlighting the role of PPARγ activation as a potential mechanism for modulating CD4+ T cell responses during bacterial infection and positioning PPARγ as a candidate for immunotherapeutics development. Future studies will more fully realize the potential of multiscale modeling to understand mucosal immunity.

3.10 Materials and Methods

Ethics statement

All experimental protocols were approved by the Virginia Tech institutional animal care and use committee (IACUC) (Protocol Numbers: 10-087-VBI & 11-189-VBI) and met or exceeded guidelines of the National Institutes of Health Office of Laboratory Animal Welfare and Public Health Service policy. Animals were under strict monitoring throughout the duration of the project and all efforts were made to minimize unnecessary pain and distress. Mice were euthanized by carbon dioxide narcosis followed by secondary cervical dislocation.

Computational modeling

The computational model of the mucosal immune responses to *H. pylori* was developed in the following steps: first, the structure model as shown in Figure 3.1 was developed using CellDesigner, a widely used Systems Biology Markup Language (SBML)-compliant network structure model development tool. Immune responses to *H. pylori* represented in the model were based on a comprehensive and thorough literature review as well as time-course data generated by us. The inflammatory network portrayed is encoded as follows: Inflammation is initiated when *H. pylori* is innoculated in the gastric lumen. *H. pylori* lives in close proximity to the epithelial lining (i.e., floating on the mucus barrier) and can adhere directly to the host cell membrane and deliver toxins. The virulence factor CagA is injected directly into host cells by the bacteria through a type IV secretion system. CagA's ability to perturb cell polarity is important for the efficient survival and growth of *H. pylori* on the apical surface of the host cell, therefore, being able to replicate in the lumen [308]. Epithelial cells in contact with *H. pylori* initiate a pro-inflammatory

response characterized by production of chemokines, activation of DCs, macrophages and T cells [309]. *H. pylori* can also translocate and migrate into the gastric LP, thus attracting effector DCs [310], directing tolerogenic programming of DCs [311] and enhancing M1 polarization [312]. As expected, APCs engulfing *H. pylori* will display *H. pylori* antigenic determinants associated with MHC and will activate effector and regulatory CD4+ T cell differentiation. The regulation of DCs can restrict different phenotypes, such as Th1 [313]. The secretion of different factors such as IFNγ, IL-17 or IL-1β will activate macrophage differentiation [314] and these differentiated macrophages will help to clear *H. pylori* in the gastric LP. At the same time, *H. pylori*-infected macrophages can induce Th17 cell responses as a positive feedback loop [315]. During this literature search, a database used for model calibrations was also created. Secondly, we implemented the model in both COPASI and ENISI with dynamics of species and reactions defined. COPASI [29] is a widely used tool for ODE-based modeling; ENISI [280] a short name for Enteric Immunity Simulator, is an agent-based modeling tool, which has been developed by the Center for Modeling Immunity to Enteric Pathogens. The averaged-based ODE-based approach can provide mature and computationally efficient numerical algorithms especially for model calibration for modeling average behavior, while the agent-based approach can provide modeling capabilities of individual based behavior, stochasticity, and cell movements easily. The COPASI modeling tool can run in both local machines and condor clusters through an online job submission system. The agent-based modeling tool, ENISI, is high-performance computing (HPC)-based and it runs on our super computer system Shadowfax, a hybrid cluster with 912 processor cores, 5.4 TB of RAM, 40Gb/s InfiniBand network and 80TB parallel storage. An online job submission system of ENISI has been developed for submitting *in silico* experiments through a web interface. These two approaches complement each other. Third, the model was calibrated using the calibration database including time-course data and assuming some biological facts regarding the behavior of specific cell types in the system.

Sensitivity analysis and parameter estimation have been performed in COPASI using a Particle Swarm algorithm and in ENISI using statistical data mining and variance-based analysis techniques, such as local sensitivity analysis using partial factorial experiments

and sparse designs. In parallel with the computational modeling effort, we identified key experiments in mice to validate model predictions. The iterative computer modeling and experimentation cycle has provided a more complete systems-level understanding of the cellular mechanisms underlying immune responses to *H. pylori*. Novel ideas and hypotheses can be easily generated and tested in silico with significant time and cost savings. Therefore, the model was able to predict trends in the behavior of distinct cell types and these computational predictions were validated with experimental data. The model developed in this study is published through the MIEP web portal at www.modelingimmunity.org and available at Biomodels.net (MODEL1307130000). More specifically, in the MIEP website, a tool called CellPublisher is used to publish the annotated model on the web portal that can allow users to navigate the network model in Google-map way and the annotations including the protein structure are presented as tags and 3-D animations.

Mice and H. pylori challenge

Eight to twelve week-old wild-type C57BL/6 mice were fasted for 8 hours and challenged via orogastric gavage with either PBS or 500μL of $5x10^7$, 10^8, 10^9 or 10^{10} CFU/mL of *H. pylori* strains 26695, SS1 or PM-SS1, on days 0, 2 and 4. Urea was added to the drinking water at a concentration of 5% w/v to facilitate bacterial colonization. Mice were checked daily for signs of disease. At day 7, 14, 30 and 60 post infection mice were euthanized and spleen, gastric lymph nodes (GLN) as well as the stomach were excised for further analysis. Mice were housed under a 12:12 light-dark ratio at the animal facilities at Virginia Tech. All experimental procedures were approved by the Institutional Animal Care and Use Committee of Virginia Tech and met or exceeded the requirements of the Public Health Service/National Institutes of Health, the Animal Welfare Act and Public Health Service policy. Animal experimentation was performed under IACUC protocols 10-087 VBI and 11-189 VBI.

H. pylori culture

H. pylori strain 26695 (ATCC), SS1 and PM-SS1 were grown on plates prepared with Difco Columbia blood agar base (BD Biosciences) supplemented with 7% of horse blood (Lampire) and antibiotics at 37°C under microaerophilic conditions. To prepare whole cell (WC) bacterial antigens, bacteria were inactivated with 4% formaldehyde for 26 hours

followed by two washing steps with PBS. Inactivated WC *H. pylori* antigen preparations were resuspended in PBS, quantified and stored at -20°C until further use. Bacterial inactivation was confirmed by culturing formaldehyde treated *H. pylori* for at least 4 days as described above.

Preparation and processing of single cell suspensions

Spleens and GLN were excised and crushed in PBS/5% FBS using the frosted ends of two sterile microscope slides and a syringe plunger, respectively. Single cell suspensions were centrifuged at 300 x g for 10 min and washed once with PBS. In case of splenocytes, red blood cells were removed by osmotic lysis prior to the washing step. For LPL isolation, stomachs were cut open and rinsed with PBS prior to 10 min treatment with 5% Acetylcysteine (Sigma) in HBSS with 2.5% Hepes and 10% FBS, at room temperature for 10min. After treatment, stomachs were digested with 300U/mL of collagenase (Sigma) and 50U/mL of DNAse (Sigma) for 90min at 37C under constant agitation and the cell suspension was filtered with a 100μm strainer. Single cell suspensions from GLN and spleen were either freshly stained for flow cytometry or stimulated with 5 µg/mL of plate-bound anti-mouse CD3 (BD Biosciences) for 6 hours. To inhibit protein secretion from cells, GolgiStopTM (BD Biosciences) was added for the last 4 hours of incubation according to the manufacturer's instructions. Lymphocytes from LPL extraction were enriched using a 44/67% Percoll gradient, washed in PBS and resuspended in FACS buffer. Flow cytometric analysis of *ex vivo*-stimulated cells was performed to assess phenotype and function different immune cell populations.

Immunophenotyping and cytokine analysis by flow cytometry

For fluorescent staining of immune cell subsets 4-6x10^5 cells were incubated for 20 min with fluorochrome-conjugated primary mouse specific antibodies: anti-CD3 PE-Cy5 clone 145-2C11 (eBioscience), anti-CD4 PE-Cy7 clone GK1.5 (eBioscience), anti-CD4 APC clone RM4-5, anti-CD45 APC-eFluor780 clone 30-F11 (eBioscience) and anti-CD25 Biotin clone 7D4 (BD Biosciences). Cells were washed with FACS buffer (PBS supplemented with 5% FBS and 0.09% sodium azide) and incubated for another 20 min with PE-Texas Red-conjugated streptavidin (BD Biosciences). For intracellular staining of transcription factors and cytokines, cells were fixed and permeabilized using a commercial kit according to the manufacturer's instructions (eBioscience). Briefly, cells

were fixed and permeabilized for 20 minutes, Fc receptors were blocked with mouse anti-CD16/CD32 FcBlock (BD Biosciences) and cells were stained with fluorochrome-conjugated antibodies towards anti-mouse/human Tbet PerCP-Cy5.5 clone 4-B10, anti-mouse, FOXP3 FITC clone FJK-16s, IL-17A APC clone eBio17B7 and IFN-γ PE-Cy7 clone XMG1.2 (eBioscience). All samples were stored fixed at 4°C in the dark until acquisition on a LSR II flow cytometer (BD Biosciences). A live cell gate (FSC-A, SSC-A) was applied to all samples followed by single cell gating (FSC-H, FSC-W) before cells were analyzed for the expression of specific markers. Data analysis was performed with FACS Diva (BD Biosciences) and Flow Jo (Tree Star Inc.).

Statistical analysis

Parametric data were analyzed by using the ANOVA followed by Scheffe's multiple comparison method. Nonparametric data were analyzed by using the Mann-Whitney's *U* test followed by a Dunn's multiple comparisons test. The ANOVA was performed by using the general linear model procedure of SAS, release 6.0.3 (SAS Institute). Statistical significance was assessed at a *p-value* ≤ 0.05. To assess the significance in the knock-out models when compared to the wild-type we used a functional T-test approach. The objective of the functional T-test is to evaluate whether two groups of functional curves are statistically different. Specifically, we defined $x_{1i}(t), i = 1, \dots, n_1$ as the functional curves of the first group and $x_{2j}(t), j = 1, \dots, n_2$ as the function curves for the second. To evaluate the difference between two groups of curves, we considered the absolute value of a t-statistic at each point:

$$T_{stat}(t) = \frac{|\bar{x}_1(t) - \bar{x}_2(t)|}{\sqrt{\frac{s_1^2(t)}{n_1} + \frac{s_2^2(t)}{n_2}}}$$

where $\bar{x}_k(t) = \frac{1}{n_k}\sum_{i=1}^{n_k} x_{ki}(t), k = 1,2$, and $s_k^2(t)$ is the sample variance of $x_{ki}(t)$ at the time point t. The values of $T_{stat}(t)$ can provide the relative difference of the two groups of curves, For the test statistic, we considered the maximum value of $T_{stat}(t)$. To find a critical value of this statistic, we use a permutation test by first performing a randomly shuffle of the labels of the curves and then recalculating the maximum of $T_{stat}(t)$ with the

new labels. Repeating this procedure many times can provide an empirical null distribution of $T_{stat}(t)$. Therefore, we can calculate the critical point as a reference for evaluating the values of observed $T_{stat}t$. The values over the calculated threshold will be viewed as statistically significant. To evaluate the effect of epithelial cell damage in the ABM model, preliminary analysis for model sensitivity was conducted. Specifically, we collected the values for number of cells that modulate epithelial cell damage from the ABM model output datasets and grouped them by genotypes. The maximum value of cell counts was used to make 10 cell count range uniformly. Such range was then used to construct heat maps showing the relative significance of different immune subsets over the epithelial cell damage.

Chapter 4

Systems modeling of the role of IL-21 in the maintenance of effector CD4+ T cell responses during chronic *Helicobacter pylori* infection

Adria Carbo, Josep Bassaganya-Riera, Raquel Hontecillas, Danyvid Olivares-Villagómez, Rupesh Chatuverdi, M. Blanca Piazuelo, Alberto Delgado, M. Kay Washington, Holly M. Scott Algood.

Carbo A., Olivares-Villagómez D., Hontecillas R., Bassaganya-Riera J., Chaturvedi R., et al. (2014). "Systems modeling of the role of IL-21 in the maintenance of effector CD4+ T cell responses during chronic *Helicobacter pylori* infection". *mBio* **5():**e01243-14. doi:10.1128/mBio.01243-14

4.1 Summary

The development of gastritis during *Helicobacter pylori* infection is dependent on an activated adaptive immune response orchestrated by T helper (Th) cells. However, the relative contributions of Th1 and Th17 subsets to gastritis and control of infection are still under investigation. To investigate the role of IL-21 in the gastric mucosa during *H. pylori* infection, we combined CD4+ T cell differentiation mathematical modeling with *in vivo* mechanistic studies. We infected IL-21-deficient and wild-type mice with *H. pylori* strain SS1, and assessed colonization, gastric inflammation, cellular infiltration, and cytokine profiles. Chronically *H. pylori*-infected, IL-21-deficient mice had higher *H. pylori* colonization, significantly less gastritis, and reduced expression of proinflammatory cytokines and chemokines compared to infected wild-type littermates. These *in vivo* data were used to calibrate an *H. pylori*-infection dependent, CD4+ T cell- specific

computational model, which then described the mechanism by which IL-21 activates the production of IFNγ and IL-17 during chronic *H. pylori* infection. The model predicted activated expression of Tbet and RORγt, the phosphorylation of STAT3 and STAT1, and suggested a potential role of IL-21 in the modulation of IL-10. Driven by our modeling-derived predictions, we found reduced levels of CD4+ splenocyte-specific *tbx21* and *rorc* expression, reduced phosphorylation of STAT1 and STAT3, and an increase in CD4+ T cell-specific IL-10 expression in *H. pylori*-infected, IL-21-deficient mice. Our results indicate that IL-21 regulates Th1 and Th17 effector responses during chronic *H. pylori* infection in a STAT1 and STAT3 dependent manner, therefore playing a major role controlling *H. pylori* infection and gastritis.

4.2 Introduction

Helicobacter pylori is a Gram-negative microaerophilic bacterium and a dominant member of the gastric microbiota harbored by approximately 50% of the world's population. A hallmark of *H. pylori* infection is a gastric mucosal inflammatory response, termed superficial gastritis [316]. The presence of *H. pylori* increases the risk for development of duodenal ulcer disease, gastric ulcer disease, non-cardia gastric adenocarcinoma, and B-cell malignancies such as gastric mucosa associated lymphoid tumors (MALT lymphomas) and high-grade lymphomas [reviewed in [317, 318]]. Conversely, there is also increasing evidence that *H. pylori* colonization protects against esophageal and cardial pathologies [286-288, 319], childhood asthma [292, 320, 321] and childhood allergies [293, 321]. The gastritis associated with *H. pylori* infection reflects the recruitment and activation of immune cells representing both innate and adaptive immunity [[322] and reviewed in [323]]. Actual treatment for *H. pylori* involves an aggressive triple-antibiotic treatment that unbalances the gastric microbiota. Furthermore, recent studies suggest that *H. pylori* is finding strategies to by-pass the treatment by developing resistance to clarithromycin [324]. Other studies have pointed out that during chronic *H. pylori* infection, the exacerbated immune response in the gastric lamina propria is driving more epithelial cell damage than the bacterium itself [32]. Therefore, new strategies to treat chronic *H. pylori* infections are needed. *H. pylori* infection of humans and experimental infection of rodents typically results in a mixed T helper 1 (Th1)/T helper 17 (Th17)-mediated immune response [257, 322, 325-334]. The long-term chronic inflammatory response to *H. pylori* is believed to drive or initiate the pathways which lead to the adverse outcomes of colonization including chronic gastritis,

intestinal metaplasia, and gastric cancer. Our mouse model of *H. pylori* infection is set up to investigate this critical pathway during chronic infection focusing on the outcome of gastritis.

T cells play a decisive role in initiating and shaping pathological and protective responses in tissues. Classical examples of T cell-mediated diseases are inflammatory bowel disease, type 1 diabetes, psoriasis, rheumatoid arthritis and multiple sclerosis. Relevant to this study, IL-21 is a cytokine produced mostly by activated CD4+ T cells, especially Th17 cells, Tfh cells and NKT cells. IL-21 induces proliferation and increases cell survival and cytokine synthesis in many immune cells [reviewed in [335]]. *H. pylori* also upregulates IL-21 during infection, correlating the IL-21 expression with levels of gastritis in the mouse model [298]. Moreover, IL-21 was associated with *H. pylori* infection in a study of infected humans [336].

Immunoinformatic approaches cannot replace traditional experimentation, however, they can be used to synthesize, organize and integrate diverse datatypes and theoretical frameworks to help generate new knowledge and target *in vivo* experimentation. Indeed, computer simulations of immunological processes can predict novel experimental behaviors, correlations and interactions between components of a complex system such as the signaling pathways controlling differentiation and function of Th cells [260, 269]. A CD4+ T cell computational model was built, calibrated and validated to investigate interactions of external cytokines and transcription factors within a CD4+ T cell in the absence of infection [279]. Our initial CD4+ T cell modeling studies investigated the importance of the peroxisome proliferator activated receptor gamma (PPARγ) in regulating the plasticity between Th17 and iTreg [32]. To not only observe intracellular events, but also to have a cellular understanding of the immune response towards *H. pylori*, we also used a published tissue-level model to study how CD4+ T cell subsets influenced initiation, progression and outcome of disease [32].

This study leverages our published CD4+ T cell model [279] and cellular *H. pylori* model [32] to establish a chronic *H. pylori*- specific CD4+ T cell differentiation model which allowed us to investigate the role of IL-21 in the maintenance of the T cell-mediated gastric mucosal responses to chronic *H. pylori* infection. Thus, we combined

computational modeling and mechanistic experimental studies in mice to dissect the effect of *H. pylori* infection on the intracellular pathways by which IL-21 modulates CD4+ T cell responses during chronic infection. Our *in silico* and *in vivo* data suggest that IL-21 is a key cytokine for maintenance of both the Th1 and Th17 response during *H. pylori* infection. Furthermore, we provide novel evidence that IL-21 is required for the development of gastritis and control of *H. pylori* bacterial burden, as well as for the modulation of T cell-derived IL-10 and phosphorylation of both STAT1 and STAT3. These data together represents key knowledge that could help in the development of novel IL-21-centered, immunotherapeutics for controlling infectious and immune-mediated diseases.

4.3 IL-21 deficiency leads to increased *H. pylori* colonization in the mouse model

The first step to evaluate the role of IL-21 during *H. pylori* infection *in vivo* was to determine any effects on *H. pylori* burden in the mouse stomach. IL-21-/- mice and their wild-type littermates were infected with *H. pylori* SS1. At time points up to 3 months post-infection, mice were sacrificed and *H. pylori* colonization was measured by culture using serial dilution colony counting. At 1 month post-infection there was no significant difference in colonization of IL-21-/- mice compared to wild-type mice (data not shown). However, at later time-points as chronicity develops, IL-21-/- mice had significantly higher levels of *H. pylori* colonization compared to wild-type littermates on both the B6;129 background at 2 months (Figure 4.1A) and 3 months post-infection (Figure 4.1B).

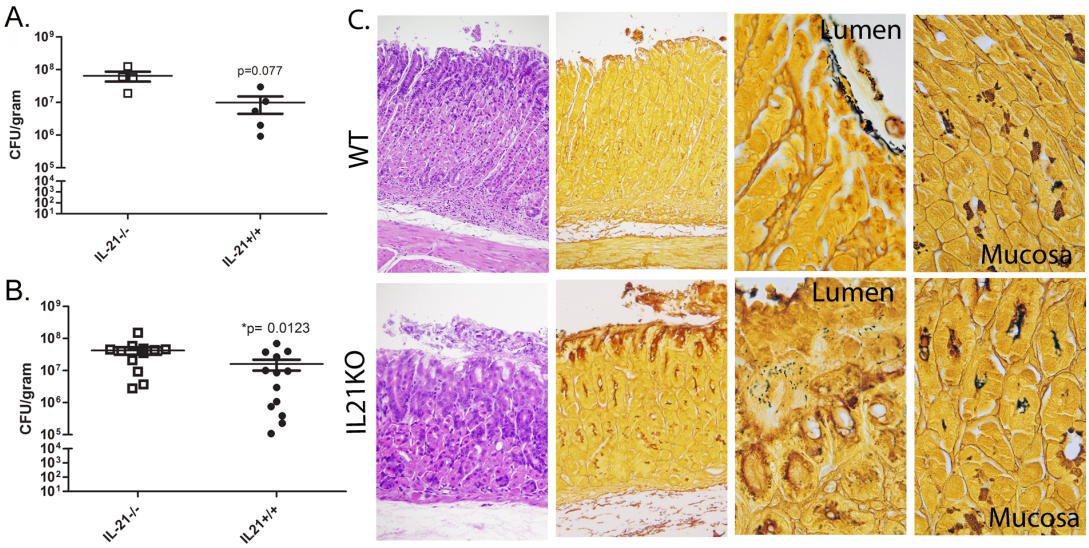

Figure 4.1. IL-21 is required to control *H. pylori* infection in the mouse model. IL-21-/- mice and wild-type littermates were infected with *H. pylori* strain SS1 for up to 3 months. Levels of colonization were measured by plating serial dilutions of stomach homogenates. The number of colony forming units (CFU) was then calibrated to the weight of the tissue and log (CFU/gram) are presented on the graphs for 2 months post-infection (A) and 3 months post-infection (B). Error bar represents SEM. Results are representative of 3 independent experiments. (C) Steiner and H&E stains were performed in both *H. pylori* infected wild-type and IL-21 -/- gastric mucosa sections (sections are at 200x, 200x, 1000x and 1000x, respectively). Sections are representative of 10 wild-type and 10 IL-21-/- mice at 3 months post infection.

We also observed this increase in bacterial burden in IL-21-/- infected mice from the C57BL/6 background (Fig. 4.2A), suggesting that IL-21 modulates the immune response resulting in higher *H. pylori* clearance in the gastric mucosa of wild-type mice. In order to localize *H. pylori* presence in the gastric tissue, a modified Steiner stain was performed on sections from the gastric tissue at 3 months post infection.

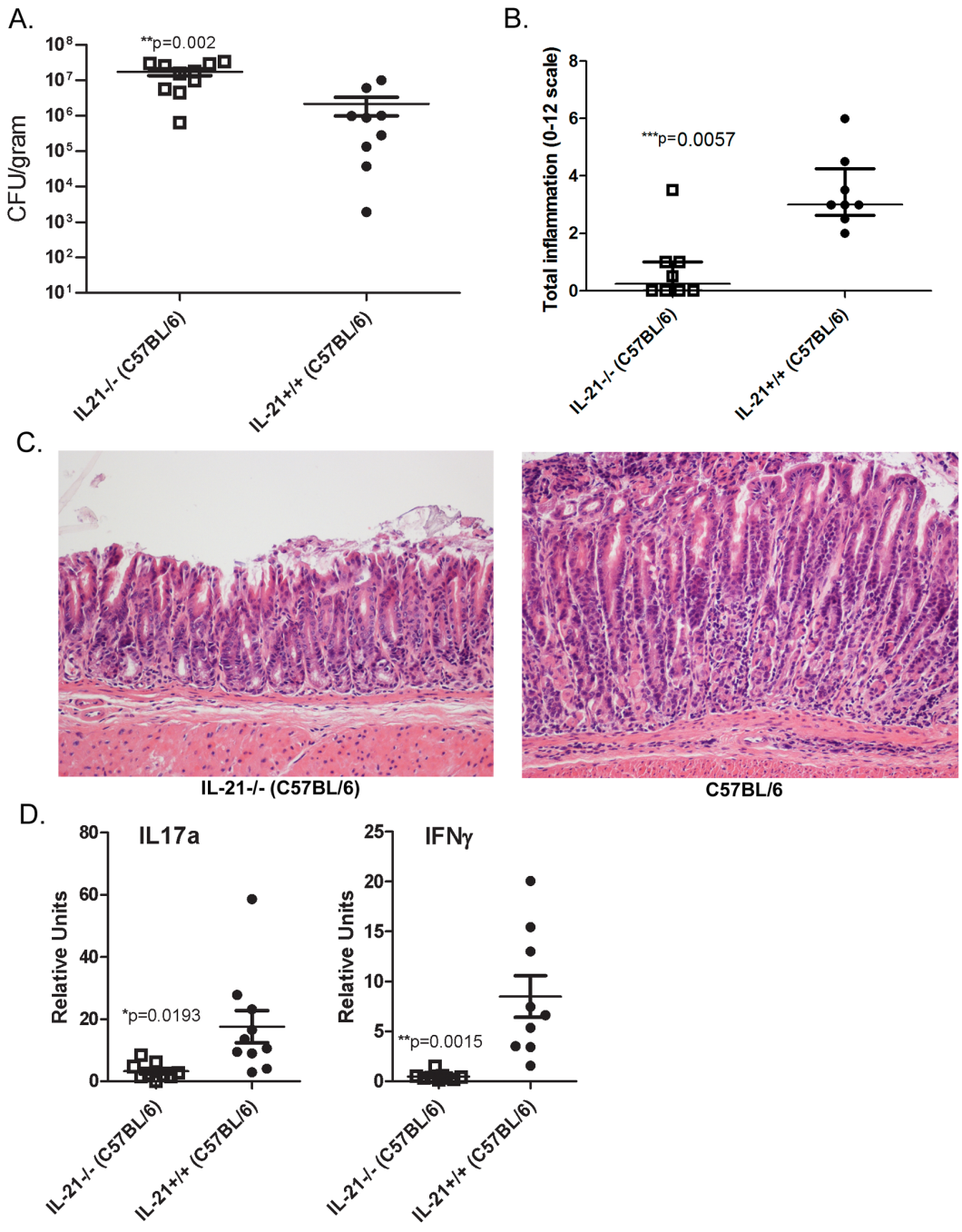

Figure 4.2. IL-21 is required for control of bacterial burden, enhances gastritis, Th1 and Th17 cytokine production in C57BL/6 mice. (A) The number of colony forming units (CFU) was then calibrated to the weight of the tissue and CFU/gram are presented from mice harvested between 2 and 3 months post-infection. Levels of acute and chronic inflammation were scored on stomach tissue (in the corpus and antrum) harvested between 2 and 3 months post infection. (B) Total inflammation was scored on a scale of 0-12. Representative sections of the gastric mucosa are presented (200x, C). (D) Real time rtPCR was performed on stomach tissue of *H. pylori* infected mice. Relative units of IL-17A and IFNγ were measured. Relative units are normalized

using the relative expression calibrated to uninfected wild-type with GAPDH as the endogenous control. Graphs are representative of 2 independent experiments. *p<0.05, **p<0.01.

When inflammation was present in the *H. pylori* infected wild-type mice (representative section, Figure 4.1C), bacteria localized to the mucus on the lumen side of the tissue and were rarely observed deeper in the tissue. Whereas, in the *H. pylori* infected IL-21-/-, where there was minimal inflammation as well as in areas of stomach in wild-type mice where inflammation was low, bacteria were present both in the mucus and in the glands, and also deeper in the tissue (Figure 4.1C).

4.4 IL-21 deficiency protects *H. pylori* infected mice from chronic gastritis

We next sought to evaluate the level of gastritis following *H. pylori* infection, and tissues were scored for inflammation. Scoring the tissue for acute and chronic inflammation in both the antrum and the corpus provided a quantitative method for assessing the presence of the neutrophils (acute inflammation) and lymphocytes (chronic inflammation). *H. pylori* infected IL-21-/- mice had significantly reduced inflammation compared to *H. pylori* infected wild-type mice on both B6;129 (Figure 4.3A) and C57BL/6 backgrounds (Figure 4.2B). Representative photomicrographs demonstrated the lack of inflammation present in the IL-21-/- mice compared to the wild-type littermates at 3 months post-infection on the B6;129 (Figure 4.3B) and C57BL/6 backgrounds (Figure 4.2C). These data suggest that IL-21 plays a role in controlling chronic *H. pylori* colonization and makes a significant contribution to the generation of chronic gastritis.

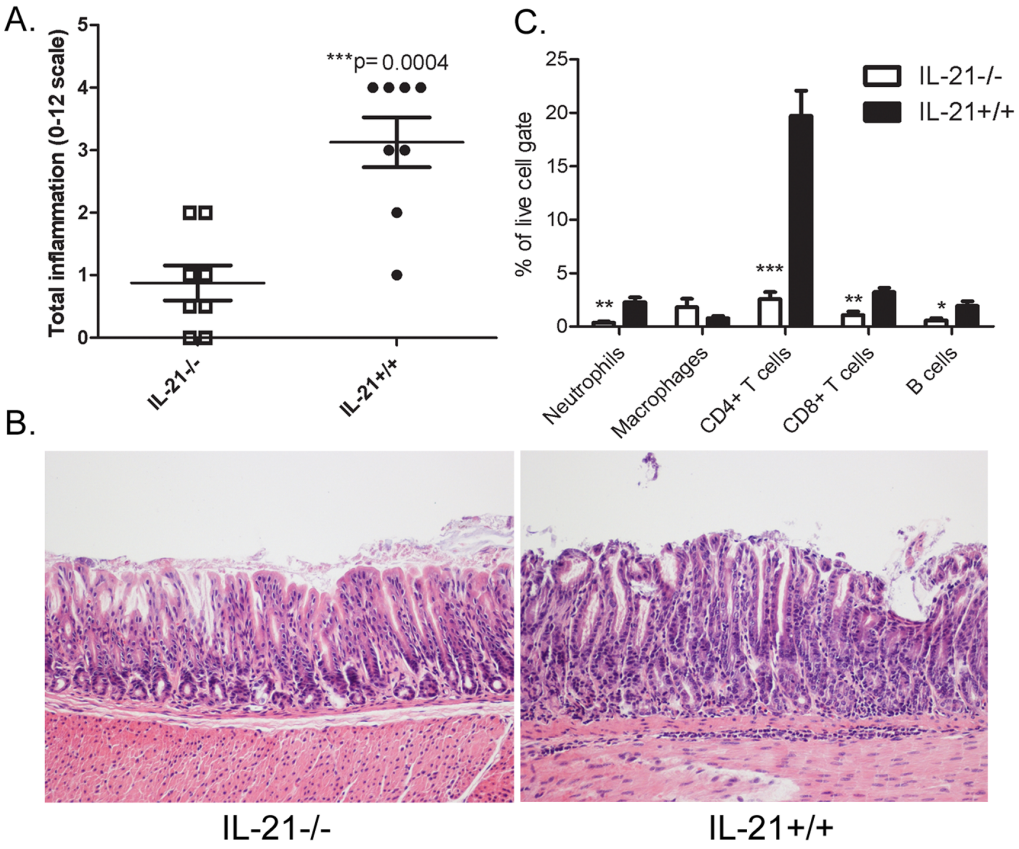

Figure 4.3. Inflammation is reduced in *H. pylori* infected IL-21-/- mice compared to *H. pylori* infected wild-type littermates. Levels of acute and chronic inflammation were scored on stomach tissue (in the corpus and antrum) at 3 months post infection. Total inflammation (A) was scored on a scale of 0-12 (Error bar represents upper and lower interquartile range). Representative sections of the gastric mucosa are presented from 3 months post infection (200x, B). Flow cytometric analysis was performed on dissociated stomach tissue at 3 months post infection (N=8 per genotype). Percentages of neutrophils (Gr1+CD11c+), macrophages (CD11b+Gr1-), CD4+CD3+ T cells, CD8+CD3+ T cells and B cells (B220+) were calculated in the live cell gate from the *H. pylori* infected mice. Error bar represents $\pm$ SEM. *$p \leq 0.05$, **$p \leq 0.01$, *** $p \leq 0.001$. Results are representative of 3 independent experiments.

To evaluate specifically which cell migration to the stomach is affected by the IL-21 deficiency, we immunophenotyped isolated gastric lamina propria cells by flow cytometry. The most striking finding was that IL-21 deficiency significantly affected the numbers of CD4+ T cells in the *H. pylori*-infected stomachs. In addition, reduced numbers of CD8+ T cells, B lymphocytes and neutrophils in the gastric mucosa of *H. pylori*-infected IL-21-/- mice compared to *H. pylori* -infected wild-type littermates were found (Figure 4.3C).

4.5 Chemokine and cytokine expression is abrogated in IL-21 deficient mice

To investigate how levels of chemokines and other inflammatory cytokines were affected by the IL-21 deficiency a multiplex protein assay was performed at 2 and 3 months post-infection. Our data demonstrate that many IFNγ-induced chemokines, including RANTES, IP-10, and MIP1β, were present at significantly lower levels in the *H. pylori*-infected IL-21-/- mice when compared to *H. pylori* infected wild-type littermates (Figure 4.4A). Moreover, the IL-17 induced chemokine, KC (a mouse homologue of IL-8), was significantly lower in the *H. pylori*-infected IL-21-/- mice compared to *H. pylori*-infected wild-type littermates (Figure 4.4B). Pro-inflammatory cytokines, TNFα and IL-1β, which can enhance inflammation or induce further effector T cell differentiation, were significantly lower in the *H. pylori*-infected IL-21-/- mice compared to *H. pylori*-infected wild-type littermates both at the protein (Figure 4.4C) and RNA levels (Figure 4.4D).

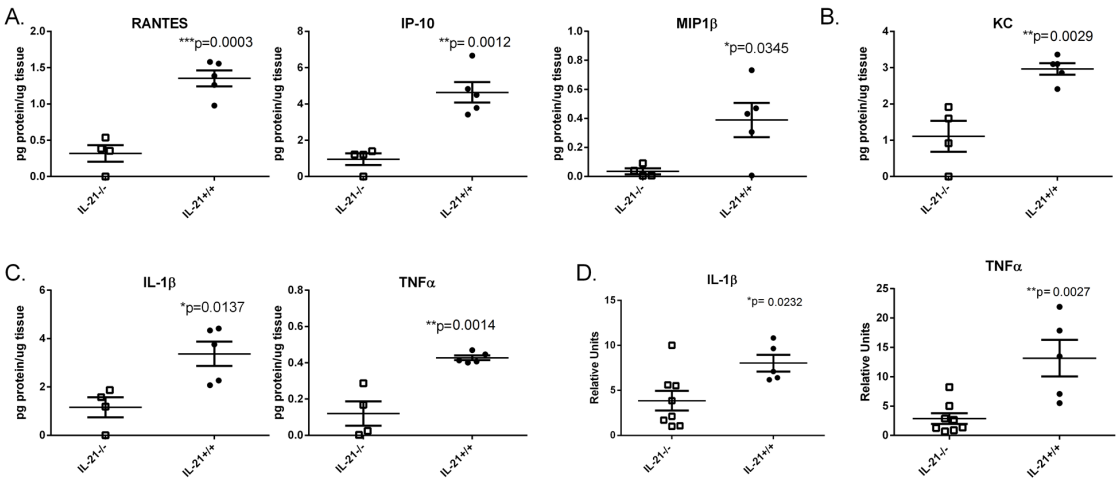

Figure 4.4. *H. pylori* infected IL-21-/- mice express reduced levels of proinflammatory cytokines and chemokines during chronic infection. Gastric protein levels were measured in the stomach tissue using a Milliplex assay at 2 and 3 months post infection. Protein levels are reported as pg of protein per μg of total tissue. (A) Levels of IFNγ induced chemokines (RANTES, IP-10, MIP1β), (B) IL-17A induced chemokine (KC), and proinflammatory cytokines IL-1β and TNFα are reduced in *H. pylori* – infected IL-21-/- mice at the protein level (C) Real time rtPCR was performed on stomach tissue of *H.pylori* infected mice. Relative units of IL-1β and TNFα were measured. Relative units are normalized using the relative expression calibrated to uninfected wild-type with GAPDH as the endogenous control. Graphs are representative of 2 independent experiments. *p<0.05, **p<0.01. (D) Abundance of IL-12p40, G-CSF, GM-CSF and MCP-1 are not affected by IL-21 deficiency during *H. pylori* infection (data not shown). The results are representative of 2 independent experiments. *p≤0.05, **p≤0.01, *** p≤0.001.

4.6 IL-21 deficiency leads to abrogated Th17 and Th1 effector responses

IL-21 plays a role in the maintenance of the Th17 responses [337]. To investigate the role of IL-21 on production of mucosal T cell-derived cytokines in the context of *H. pylori* infection, real time rtPCR was performed on RNA isolated from the stomachs of *H. pylori*-infected IL-21-/- mice and their *H. pylori*-infected wild-type littermates. Expression of both IL-17 (Figure 4.5A) and IFNγ (Figure 4.5B) was significantly reduced in the *H. pylori*-infected IL-21-/- mice compared to *H. pylori*-infected wild-type littermates by 3 months post-infection. We found similar results with our C57BL/6 mice (Fig. 4.2D). These significant differences were confirmed by using a protein-based assay on stomach lysates (Figure 4.5C,D).

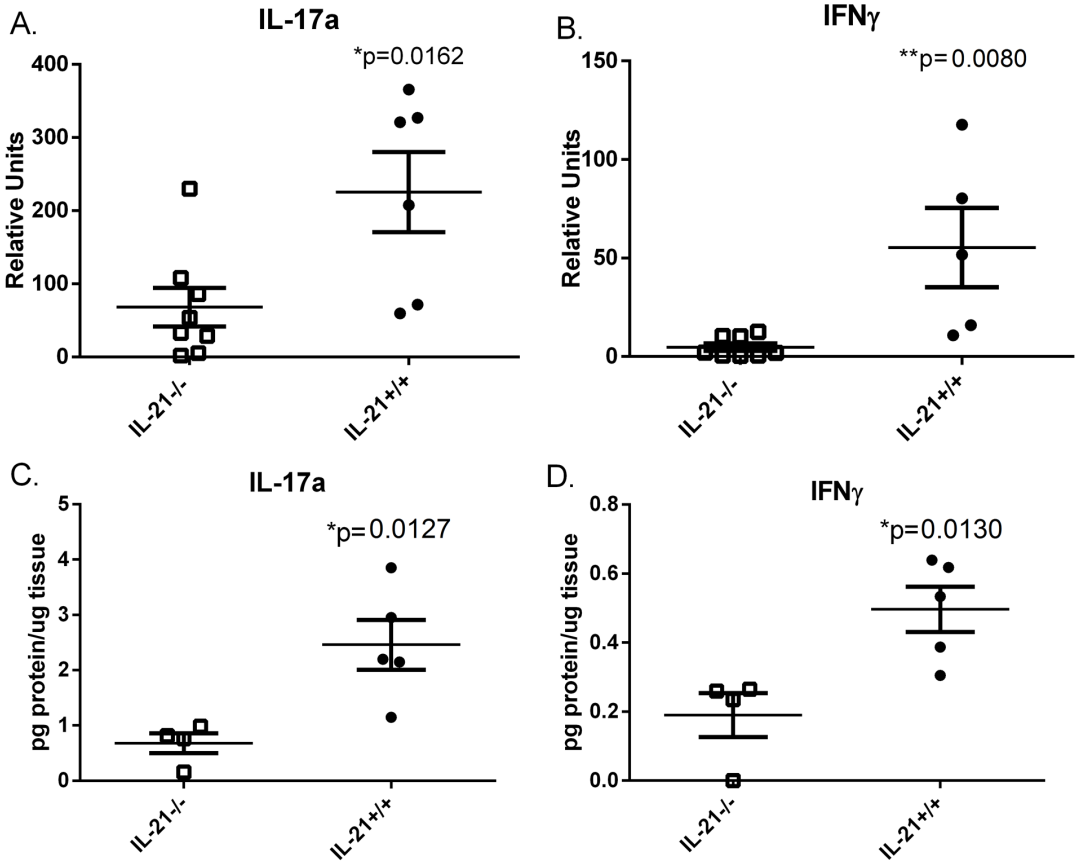

Figure 4.5. Th17 and Th1 responses are reduced in *H. pylori* infected IL-21-/- mice compared to *H. pylori* infected wild-type mice. Real time rtPCR was performed on stomach tissue of *H. pylori* infected mice. Relative units of IL-17A (A) and IFNγ (B) were measured at 3 months post-infection. Relative units are normalized using the relative expression calibrated to uninfected wild-type with GAPDH as the endogenous control. Graphs are representative of 3 independent experiments. Line represents average ± SEM. *p≤0.05, **p≤0.01. Gastric protein

levels were measured in the stomach tissue using a Milliplex assay at 2 and 3 months post infection. Protein levels are reported as pg of protein per μg of total tissue. A. IL-21-/- mice express reduced protein levels of IL-17A (C) and IFNγ (D) during chronic infection. Graphs are representative of 2 independent experiments. Line represents average ± SEM. *$p \leq 0.05$, **$p \leq 0.01$.

4.7 IL-21 contributes to Th17 differentiation and modulates Th1 responses upon infection with *H. pylori*

CD4+ T cells responses are believed to drive chronic inflammation and contribute to long-term damage associated with adverse outcomes of chronic *H. pylori* infection. Based on our experimental data, IL-21 plays a role maintaining the activation of CD4+ T cells since *H. pylori* infected IL-21-/- mice have significantly reduced inflammation in their gastric mucosa compared to wild-type littermates, with the most striking reduction in CD4+ T cells. To gain a more comprehensive mechanistic understanding of why the lack of IL-21 has such an impact on the development and maintenance of CD4+ T cells and their function in the gastric mucosa of *H. pylori*-infected mice, we used our cytokine data to leverage a computational and mathematical model that simulates CD4+ T cell differentiation. Specifically, the original CD4+ T cell differentiation model [28] was calibrated with real-time rtPCR data from wild-type or IL-21 deficient (IL-21-/-) mice infected with *H. pylori* for 3 months (Figure 4.5) to represent the influence of the cytokine environment that a CD4+ T cell encounters during infection. The goal of the study presented here was to investigate the role of IL-21 in the development of the T cell mediated gastric mucosal responses to *H. pylori*. Thus, we combined computational modeling and mechanistic experimental studies in mice to dissect the effect of *H. pylori* infection on the pathways by which IL-21 modulates CD4+ T cell responses. This new mechanistic knowledge could help in the development of novel immunotherapeutic treatments capable of controlling autoimmune diseases such as Crohn's disease, multiple sclerosis, type 1 diabetes and rheumatoid arthritis. Our *in silico* and *in vivo* data suggests that IL-21 is a key cytokine for maintenance of both the Th1 and Th17 response during *H. pylori* infection. Furthermore, the data indicate that IL-21 is therefore required for the development of gastritis and control of *H. pylori* bacterial burden.

As mentioned before, computational modeling and immunoinformatics have been proven to be a powerful tool to understand mechanisms of action underlying immune responses to different pathogens. In this chapter, we used an intracellular model that computes and simulates the process of CD4+ T cell differentiation and a published tissue level model that allow us to look at the contribution of different CD4+ T cell subsets from a cellular scale in the context of a chronic *Helicobacter pylori* infection [32]. These models represent two scenarios at different time and spatial scales. First, the CD4+ T cell model is centered in the intracellular compartment of a CD4+ T cell in the dynamics of its cytokines and transcription factors in the context of *H. pylori* infection. On the other hand, the tissue level model represents the main cell-cell interactions at the tissue level that are triggered after *H. pylori* infection. Future work is directed towards the development of a multiscale platform that can encompass both scales at the same time. Of note, the tissue level model was calibrated in a similar fashion to what is described in this supplementary text but in this case we used cellular data coming from our immunophenotyping studies from IL-21 deficient mice and wild-type littermates (Figure 4.5).

First, to facilitate a comprehensive representation of the dynamics associated with the pathways controlling CD4+ T cell differentiation in the context of *H.pylori*, we used an ordinary differential equation (ODE)-based computational model, which includes 93 species, 46 reactions and 60 ODEs driving activations and inhibition pathways. The equations of the CD4+ T cell differentiation model can be observed in Figure S7. IL-21 plays a semi-central role in our model. When IL-21 is available in the environment, our computational model will bind the external IL-21 to its membrane receptor, IL21R. This will initiate a series of cascade reactions involving the activation of STAT3 and RORγt. At the same time, the formation of the IL-21-IL-21R membrane complex will be inhibited by STAT5 and activated by IL17-IL-17R complex. STAT1 can be also activated after the IL-21-IL-21R complex is formed. Other signals in the computational model, such as STAT3 or BCL6 will activate the internal production of IL-21, which will be externalized to the extracellular space and it will be able to bind to the IL21R if it is available.

As described in [279], on the MIEP website (http://www.modelingimmunity.org/models/cd4-t-cell-model-archive/) and at http://www.ebi.ac.uk/biomodels-main/ (MODEL1303020000), the intracellular CD4+ T cell differentiation model was properly

calibrated using experimental data and validated *in vivo* through a series of mechanistic mouse studies. In order to ensure proper calibration of the CD4+ T cell model and make it predictive to *H. pylori* data, a top-down approach was implemented (Figure 4.6).

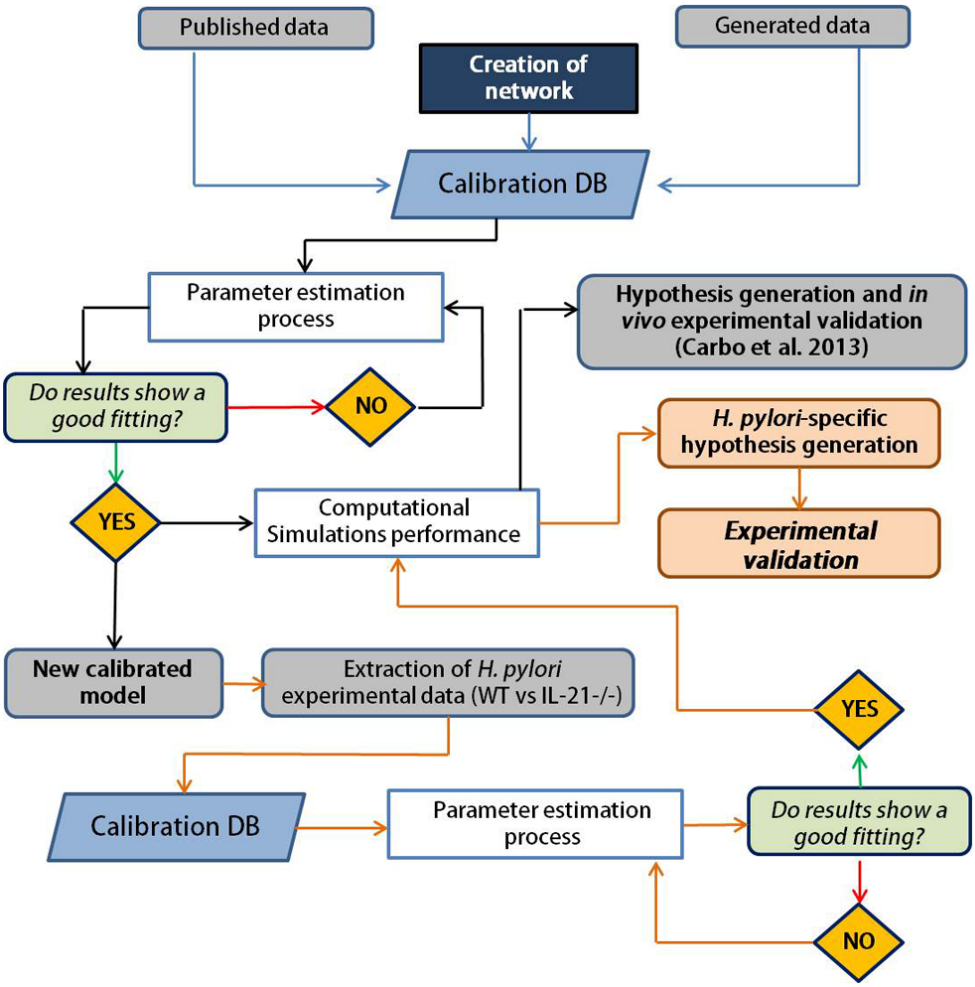

Figure 4.6. Calibration process using the CD4+ T cell computational model to adjust dynamics to *H. pylori* specific data. A top-down approach was used to calibrate IL-21 specific pathways with H. pylori infection data. Briefly, the dynamics of the CD4+ T cell computational model were adjusted by using a calibration database with data obtained from published repositories or in-house generated data. After the parameter estimation process was completed and the model fitted the experimental data, computational simulations were performed. These first sets of simulations are published in [28]. *H. pylori*-specific data regarding the expression of IL-17 and IFNγ was used for further calibration of the model by running parameter estimation iteratively.

To calibrate IL-21-related pathways, *H. pylori*-specific experimental data from wild-type and IL-21 null mice was used and parameters were adjusted using a Particle Swarm algorithm run in the COmplex PAthway SImulator (COPASI) [29] to ensure accurate representation of experimental data. Since the dynamics would result very similar either

using our gene expression (Figure 4.5A) or the protein data (Figure 4.5B), we decided to use the real-time PCR data because the differences in IFNγ where greater. Indeed, calibration results showed appropriate fitting between experimental data and computational predictions (Figure 4.7).

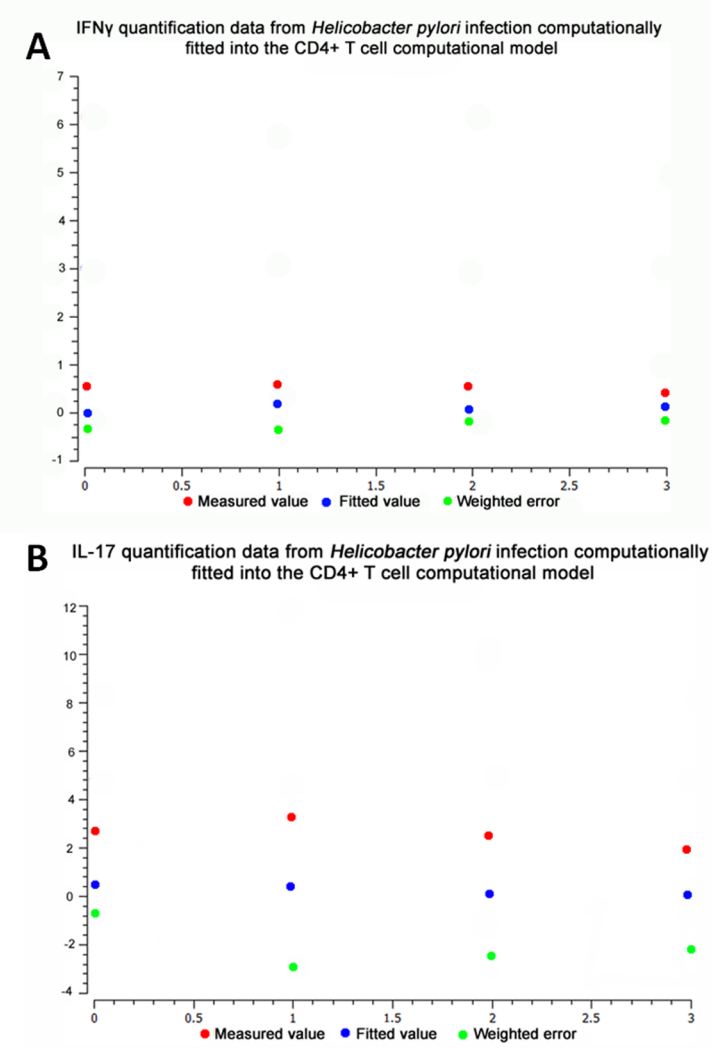

Figure 4.7. Computational fitting of computational model parameters from *H. pylori*-derived RT-PCR and protein data in COPASI. IFNγ (A) and IL-17 (B) were fitted by COPASI using the Particle Swarm algorithm (2000 iterations). The fitted value (dark blue dots) could reproduce the behavior of the measured value (red dots). The weighted error (green dots) is low, indicating that the fitting has been performed successfully. After completion, a new set of hypothesis regarding the role of IL-21 in Th1 and Th17 during *H. pylori* infection were generated and experimental animal studies were run in order to validate such computational predictions.

Other controls demonstrating a good fitting between the model and the experimental data were error mean of estimation results (Figure 4.8A), gradient analysis (Figure 4.8B), and fluxes performance (Figure 4.8C-4.8F).

A.

Experiment	Objective Value	Root Mean Square	Error Mean	Error Mean Std. Deviation
Experiment_2 (IL17)	25.092	2.5046	-2.40693	0.692608
Experiment_3 (IFNg)	1.22178	0.552672	-0.543756	0.0988712

B.

Parameter	Value	Gradient	Parameter	Value	Gradient
(re10).K1	0.15	-9.21E-08	(re33).k1	0.09	0
(re13).K1	5.08738	1.40E-12	(re33).k2	0.09	0.0003437
(re30).K1	97	6.73E-07	(re37).K	0.1	4.84E-05
(re32).K	0.3	-0.0004001	(re38).K3	42.2559	0
(re32).K1	8	3.48E-08			

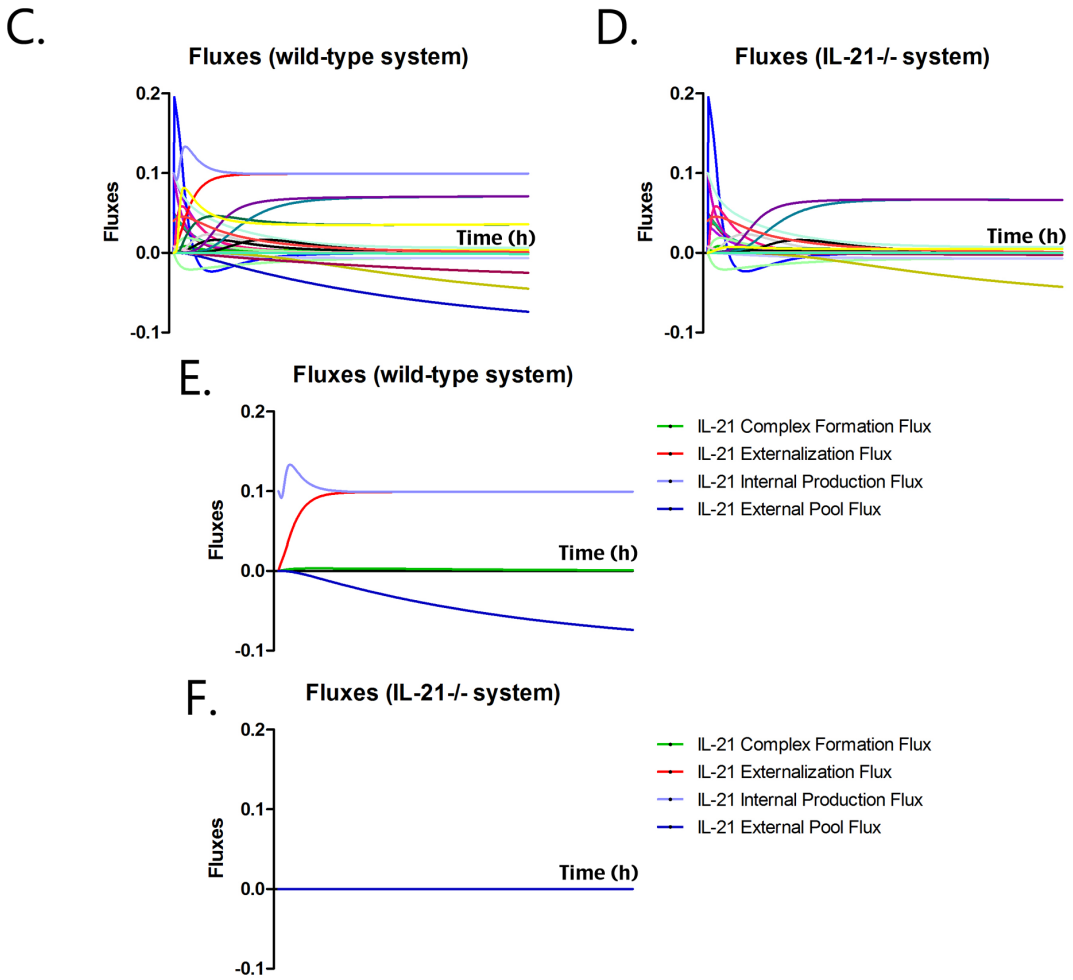

Figure 4.8. Parameter estimation results and differential reaction on model fluxes after Th17 induction. (A) Numerical values on the parameter estimation results showing error means on fitting the experimental data into the computational model. (B) Gradient analysis on parameters related to IL-21 reactions. Fluxes were assessed in COPASI in (C, E) the wild-type model and (D, F) the IL-21 -/- model. Lines in (C) and (D) represent the reaction fluxes of all the reactions in the CD4+ T cell computational model. Fluxes in (E) and (F) have been specified in on the figure's legend.

After completion of the calibration process, time-courses were performed with 600 intervals during 200 hours initializing the model with external IL-12 and IFNγ to induce Th1, and with external IL-6 and TGF-β to induce Th17. iTreg was induced by initializing the model with TGF-β and IL-2. These initial concentrations reproduced the cytokine environment found in the gastric mucosa during the chronic phase of *H. pylori* infection and provided relevant scenarios to study the role of IL-21 in CD4+ T cell differentiation. Furthermore, parameter scans were run on IL-21 comparing key species in the model.

With the rising application of systems biology, sensitivity analysis methods have been widely applied to study the biological systems. Since cell behaviors are not only determined by the characteristics of individual biological components but also by the interactions of such components acting together as a system, we sought to determine which components of the model are either positively or negatively correlated to IL-21. Therefore, sensitivity analyses were run using the correlation analysis task embedded in COPASI using a delta factor of 0.001 and a delta minimum of 10^{-12}.

To evaluate the role of IL-21 in CD4+ T cell differentiation during *H. pylori* infection, we engineered an IL-21-/- CD4+ T cell differentiation model *in silico*. To create the IL-21-/- system, we knocked-out the ability of the model to produce internal IL-21 as well as to exert any effects that are triggered by the binding of IL-21 to its receptor. The reactions that were knocked out to create the in silico IL-21-/- system are described in Table 4.1. As a quality control for the deletion of IL-21 *in silico*, reaction fluxes demonstrated complete inactivation of IL-21 in the knockout system (Fig. 4.8C-4.8F).

Reaction name	Reaction Fundamentals	Type of dynamics	Knocked-out parameter
re32: IL21 Internalization	eIL21 + IL21R = IL21-IL21R	Mass Action and Hill Function	Vf = 0
re33: IL21 externalization	IL21 -> eIL21	Mass Action	K1 = 0
re37: Internal production of IL21	pIL21 = IL21	Mass Action	K1 = 0

Table 4.1 Reactions involved in IL-21 activation. Reactions involved in IL-21 activation were abrogated to simulate a cell specific IL-21 knock-out system.

Modulation of transcription factors is critical for Th cell differentiation and cytokine production [reviewed in [338]]. To broadly investigate the contribution of specific molecules to IL-21, sensitivity analysis was run on internal CD4+ T cell specific IL-21.

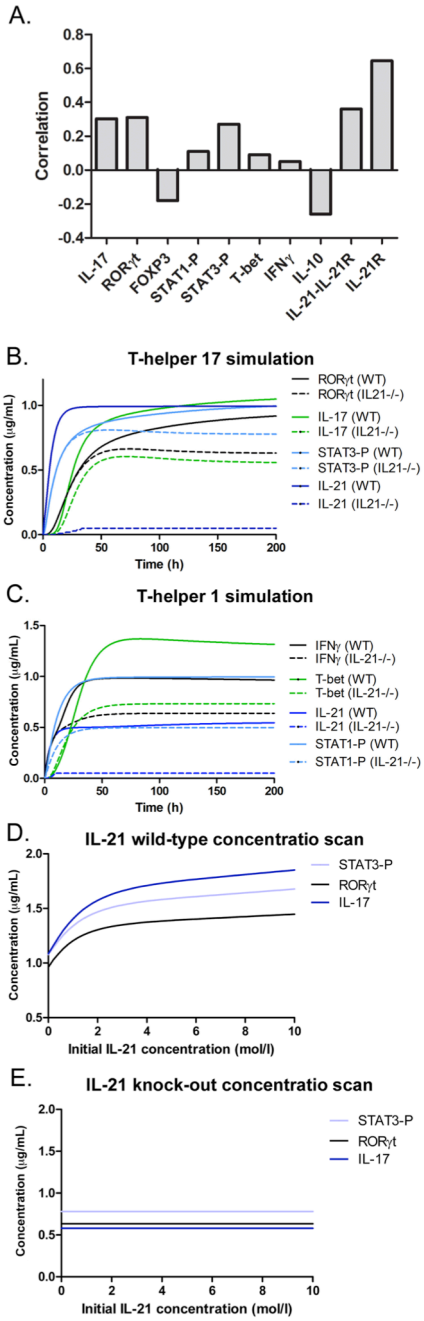

Figure 4.9. The CD4+ T cell computational model predicts *in silico* modulation of differentiation and maintenance by IL-21 (A) Sensitivity analysis on IL-21 over Th1 and Th17 related molecules showing positive or negative correlation to IL-21. (B) RORγt, IL-17, IL-21 and STAT3 in the computed Th17 system. (C) Effect of IL-21 deficiency on modulation of Tbet, and IFNγ in the computed Th1 system. (D, E) Upregulation of RORγt, IL-17 and STAT3-P in a Th17 state with increasing concentrations of IL-21 in the wild-type system, but not in the IL-21-/- during a time-course of 200 hours.

Simulation results showed a positive correlation for Th17 related molecules, such as phosphorylated STAT3 (P-STAT3), IL-17 and RORγt (Figure 4.9A). T-bet, IFNγ and phosphorylated STAT1 (P-STAT1) were also found positively correlated with IL-21 (Figure 4.9A). Interestingly, FOXP3 and IL-10 results on sensitivity analysis showed a negative correlation to IL-21 (Figure 4.9A). *In silico* experimentation indicated that there is a dramatic down-regulation of RORγt, IL-17 and phosphorylation of STAT3 when IL-21 production is deleted during Th17 differentiation (Figure 4.9B). Our results also demonstrated a downregulation of IFNγ and T-bet in the IL-21-deficient model following Th1 differentiation when compared to the wild-type model (Figure 4.9C). Next, we sought to determine the effect of an *in silico* upregulation of IL-21 in Th17-differentiated CD4+ T cells and found that P-STAT3, IL-17 and RORγt were upregulated with increasing doses of IL-21 (Figure 4.9D). These effects were abrogated in the IL-21-deficient system (Figure 4.9E).

Of note, when evaluating Th1 and Th17 populations in our *H. pylori*

tissue level model, we also found reduced numbers of Th1 and Th17 populations in the IL-21 deficient model when compared to the wild-type model during the chronic stage of infection (Figure 4.10). These *in silico* results provided evidence that IL-21 plays a key role in CD4+ T cell modulation during *H. pylori*-induced Th1/Th17 CD4+ T cell responses at chronic time points.

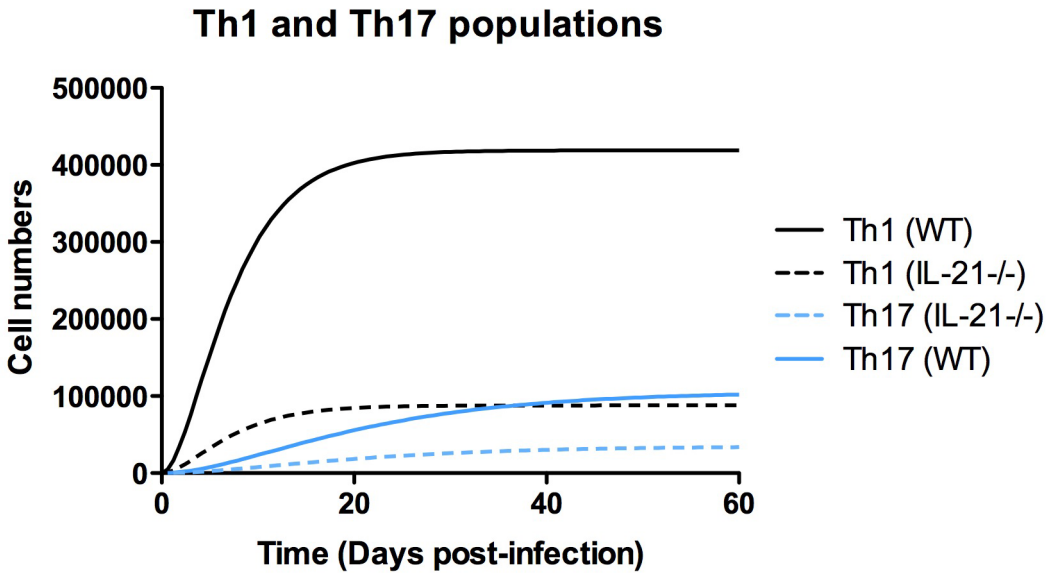

Figure 4.10. IL-21 is required for the upregulation of Th1 and Th17 responses and it modulates neutrophil recruitment in the gastric lamina propria during the chronic stages of *H. pylori* infection. (A) *In silico* time-course experiment performed with a challenge of 5×107 colony forming units of initial *H. pylori* injected in the mathematical model, showing differences in (A) numbers of gastric lamina propria (LP) CD4+ T cell subsets and (B) numbers of gastric lamina propria (LP) neutrophils over time in both the wild-type and the IL-21 deficient model.

4.8 Experimental validation of model predictions: IL-21 modulates the expression of Th1 and Th17 transcription factors

Guided by the model predictions, we sought next to investigate if IL-21 affects gene expression of CD4+ T lymphocyte transcription factors *tbx21* and *rorc* (which translate to Tbet and RORγt) *in vivo*. CD4+ T cells were isolated from spleens of *H. pylori*- infected IL-21-/- mice and wild-type littermates at 3 months post-infection and real time rtPCR

was performed. As predicted, expression of *tbx21* and *rorc* was significantly reduced in the CD4+ cells from *H. pylori* –infected IL-21-/- mice when compared to *H. pylori*-infected wild-type littermates (Figure 4.11A).

Our computational model also predicted that IL-21 positively correlates with phosphorylation of STAT1 and STAT3. Indeed, the *in silico* IL-21-/- model showed a down-regulation of P-STAT3 in Th17 cells (Figure 4.9B) and P-STAT1 in Th1 cells (Figure 4.9C). To test this prediction *in vivo,* the level of P-STAT1 and P-STAT3 was measured in CD4+ splenocytes from *H. pylori*-infected IL-21-/- and *H. pylori*-infected wild-type mice at 3 months post-infection. The data indicate that while total phosphorylation of STAT1 and STAT3 is low when the cells are not restimulated *ex vivo*, the mean fluorescence intensity of the P-STAT1 and P-STAT3 staining is significantly lower in the CD4+ splenocytes from IL-21-/- mice compared to wild-type mice (Figure 4.11B).

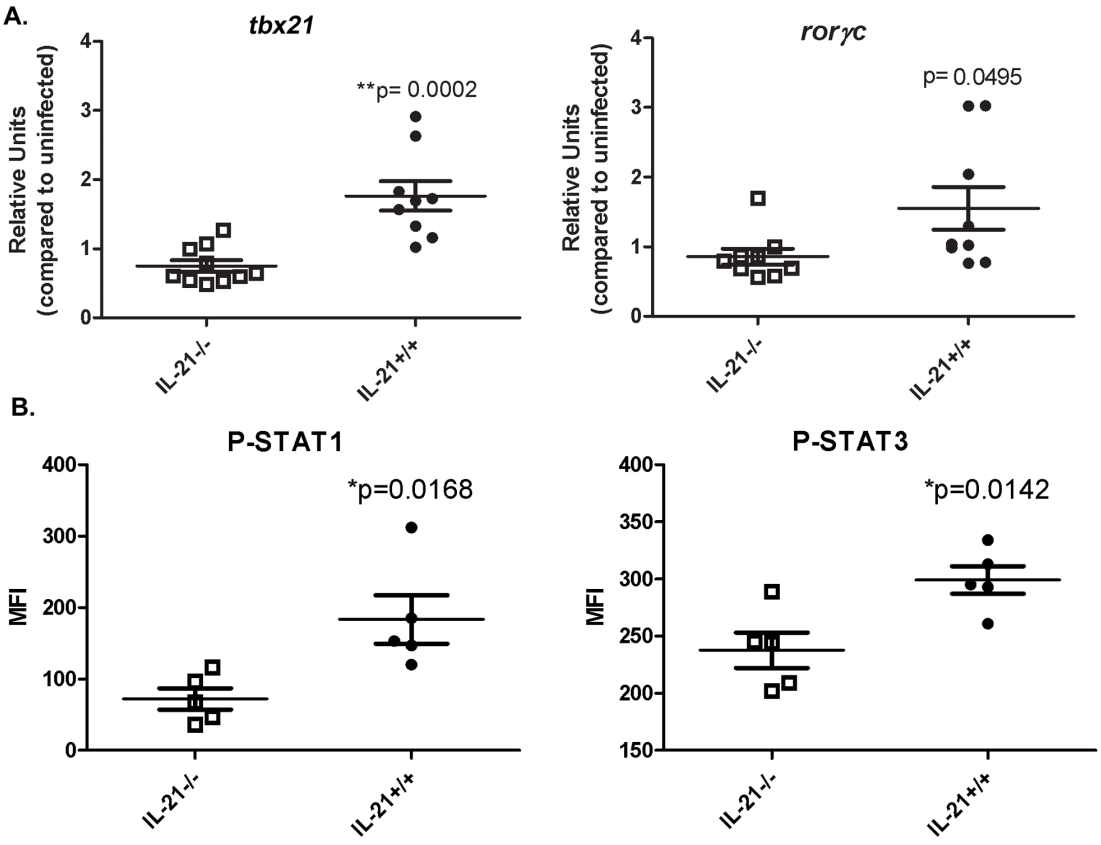

Figure 4.11. Transcription factors associated with Th1 and Th17 are affected by IL-21 deficiency in the mouse model. (A) CD4 lymphocytes isolated from *H. pylori* infected IL-21-/-

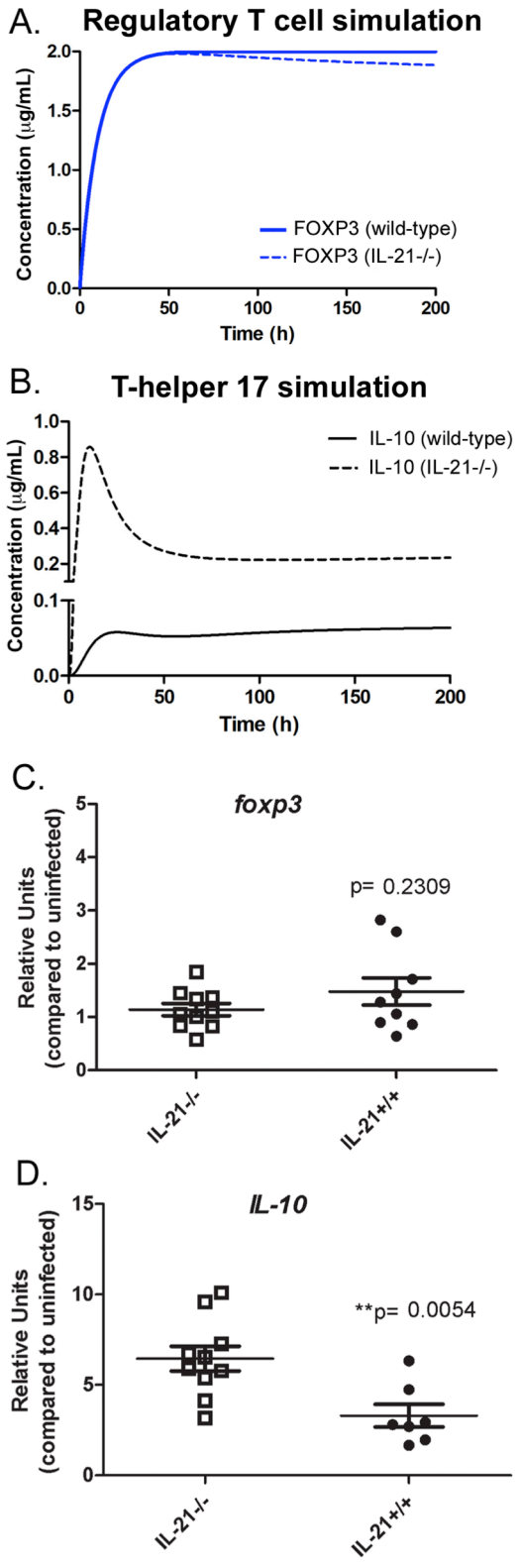

express reduced levels of *tbx21* and *rorc*. Gene expression of transcription factors *tbx21* and *rorc* were measured in CD4+ T cells isolated from the spleens of *H. pylori* infected IL-21-/- and wild-type mice. Relative units are normalized using the relative expression calibrated to expression in CD4+ splenocytes from uninfected mice with GAPDH as the endogenous control. (B) The levels of phospho-STAT1 and phospho-STAT3 in unstimulated cells from infected mice were measured by flow cytometry and the mean fluorescence intensity of the CD4+ splenocytes is reported. Line represents average ± SEM. *p≤0.05, **p≤0.01.

Figure 4.12. IL-21 modulates the expression of IL-10 during *Helicobacter pylori* infection. The CD4+ T cell model predicted (A) a higher production of IL-10 in IL-21-/- mice and (B) no differences in the expression of FOXP3 when comparing wild-type and IL-21-/- mice. To validate those predictions levels of mRNA in CD4+ T cells of spleens of *H. pylori* infected mice were assessed, specifically for (C) *il10* transcripts and (D) *foxp3* transcripts. Line represents average ± SEM.

4.9 Expression of markers of T cell regulation (Foxp3 and IL-10) in IL-21 deficient mice

Since we observed a negative correlation in IL-10 and FOXP3 in relation to IL-21 (Figure 4.9A), we investigated whether there was a change in IL-10 and FOXP3 expression in iTreg cells in the gastric mucosa since major expression of FOXP3 comes from regulatory T cells. To do so, we performed computational simulations in the CD4+ T cell differentiation model and we evaluated the level of IL-10 in Th17 and the level of FOXP3 in iTreg cells. We hypothesized that an increase in Treg cells may explain the decrease in gastritis found in IL-21-/- mice. However, *in silico* results differentiating the mathematical model with TGFβ and IL-2 showed no difference between wild-type and IL-21-/- mice in expression of FOXP3 within the Treg cell subset (Figure 4.12A). Furthermore, when induced with IL-6 and TGFβ together, our mathematical model predicted a dramatic upregulation of IL-10 in the IL-21-deficient system when compared to the wild-type system in Th17 cells (Figure 4.12B). To validate these predictions, we measured *foxp3* transcript levels in CD4+ T cells isolated from the spleens of *H. pylori*-infected IL-21-/- mice and wild-type littermates at 3 months post-infection. Experimental results showed no significant difference in the CD4+ T lymphocytes, validating the model prediction and suggesting that the reduction in Th1 and Th17 effector responses is not mediated through an increase in iTreg cells (Figure 4.12C). We similarly measured IL-10 expression in CD4+ T lymphocytes isolated from the spleens of *H. pylori*-infected IL-21-/- mice and wild-type mice. As the model predicted, IL-10 expression was significantly higher in CD4+ T lymphocytes from *H. pylori*-infected IL-21-/- mice compared to *H. pylori* infected wild-type littermates (Figure 4.12D).

4.10 Discussion and Conclusions

Since the identification of Th17 cells almost a decade ago, we have gained a better understanding of how CD4+ T helper cells help control bacterial colonization beyond providing B cell help and activating macrophage function. Th17 cells play a central role in controlling many bacterial infections through activation of chemokine pathways and antimicrobial responses. They activate these pathways through production of IL-17A, IL-17F and IL-22. In addition, IL-21, which is produced by Th17 cells, plays a role in amplifying the Th17 cell effector response [339]. In this study, we find that IL-21 is not

only required for the maintenance of IL-17 production in the gastric mucosa following *H. pylori* infection, but also that IL-21 plays an important role in the development and maintenance of the IFNγ response. As a result, a deficiency in IL-21 protected *H. pylori* infected mice from chronic gastritis, at the expense of increased bacterial burden. Since IFNg and IL-17 can induce chemokine expression, the lack of Th1 and Th17 responses in the gastric mucosa of the *H. pylori* infected IL-21-/- mice leads to reduced chemokine expression and fewer neutrophils. Since neutrophils are likely controlling the bacterial burden, IL-21-/- mice have more bacterial colonization and interestingly, Steiner stains indicated that the bacteria in the IL-21-/- mice are typically localized not only in the mucus layer but also deeper in the tissues (i.e. in glands, Figure 4.1C). Despite increased bacterial burden and deeper localization of *H. pylori* in the tissue, in our mouse model the infected IL-21-/-, mice do not show any signs of comfort or distress. In wild type mice where inflammation occurs in a localized manner, the *H. pylori* localized to the mucus layer, but the bacteria are not observed in the gland. It is worth noting that there are areas in wild type mice where inflammation is low and in those areas *H. pylori* can also be found deeper in the tissue.

Immunoinformatic approaches are rising as useful tools to provide insight on potential trends through integrating current datasets and knowledge, and detecting behavioral responses at the systems level. In this specific study, after observing how the bacterial burden is significantly higher in the stomachs of IL-21-/- mice (Figure 4.1), we found that these mice have in fact less leukocytic infiltration, including very few CD4+ T cells in the gastric lamina propria (Figure 4.3). One potential explanation is that IL-21 impairs the ability of CD4+ T cells to mount a proper inflammatory response and affects a specific T cell product that would maintain or promote CD4+ T cell recruitment in the gastric lamina propria. This would explain the lack of inflammation in the gastric lamina propria. The ability of the innate immune compartment to clear out the bacteria could then be less effective without the proper effector response driven by CD4+ T cells. As a matter of fact, since CD4+ T cells were our focus, we leveraged the existing CD4+ T cell differentiation model [28] by re-calibrating the model with *H. pylori*-specific data to understand what intracellular events were occurring within the CD4+ T cell compartment to then target experimental studies with predicted hypotheses. Indeed, by using a modeling approach that simulates the time-period of CD4+ T cell differentiation and calibrating with chronic *H. pylori* data, we could determine which are the pathways most affected by the

presence or lack of IL-21. Moreover, we could characterize crosstalk between pathways within the CD4+ T cell differentiation model at the chronic stages of *H. pylori* infection. Previous studies suggest that IL-21 is a key cytokine for Th17 cell maintenance. Indeed, our *in silico* results demonstrate that differences between the wild-type and the IL-21 knockout models are not noticeable at the first stages of differentiation. However, when Th17 is fully differentiated, IL-21 is required for the upregulation of IL-17, RORγt and phosphorylation of STAT3. In fact, results of the tissue level model show a clear difference in Th1 and Th17 populations when comparing the IL-21 deficient system with the wild-type system. Furthermore, our computational simulations show a dramatic downregulation of IL-17, RORγt and the phosphorylation of STAT3 in a fully differentiated Th17 cell. IL-21 also plays an important role in Th1 responses as illustrated by the lower amounts of P-STAT1, T-bet expression and IFNγ. This computational approach allowed us to target experimental studies and be able to confirm and validate all these findings in our *in vivo* model of *H. pylori* infection.

In this regard, IL-10 has long been known to play an important role in the regulation of Th1 cell responses to pathogens [340]. It has also been shown that Th1 effector cells are themselves co-producers of IL-10 and IFNγ, since they use IL-10 as a "self-regulation" mechanism [341, 342], and that TGFβ and IL-6 can induce a CD4+ T cell subset that co-produces IL-17 and IL-10 [95]. These co-producers are considered self-regulatory Th17 cells. Our modeling results predict that IL-21 might be involved in controlling the balance between regulatory and effector responses during *H. pylori* infection through an IL-10 mechanism. Indeed, the CD4+ T cell computational model predicted an upregulation of Th17-specific IL-10 in IL-21-/- mice, supporting the notion that IL-21 modulates negatively the expression of IL-10 in Th17 cells. Taken together, these findings indicate that IL-21 has emerged as a central molecule in CD4+ T cell differentiation that promotes effector responses in Th1 and Th17 cells through P-STAT1 and P-STAT3, respectively, and also downregulates the gene expression of *il10* in Th17 cells (Figure 4.13A). In this study our modeling approaches were predictive of *in vivo* outcomes (Figure 4.13B).

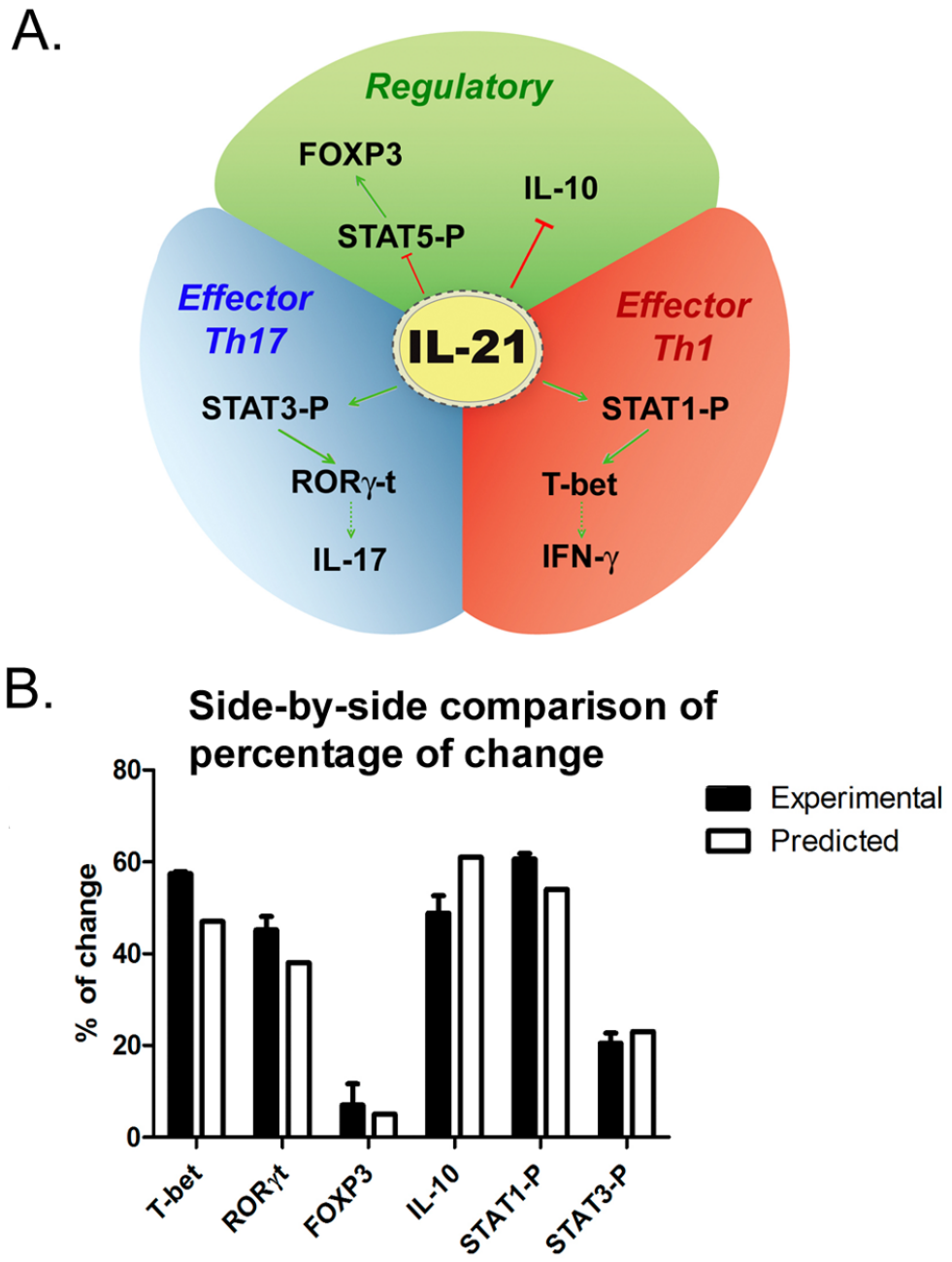

Figure 4.13. Predictive value of the CD4+ T cell differentiation model. (A) Cartoon representation of IL-21 interaction within the CD4+ T cell subset. (B) Side-by-side comparison assessing the differences between the model's predicted percentage of change between the wild-type and the IL-21-/- systems and the experimental results on wild-type and IL-21-/- mice.

While several studies have investigated the role of Th17 versus Th1 cells during control of *H. pylori* infection and the development of gastritis, there does not appear to be a clear indication that one Th subset plays a more important role than the other. Murine studies have shown that Th1 responses are associated with increased gastritis, since

IFNγ-/- mice have decreased levels of gastric inflammation [343]. These studies have also shown that an insufficient Th1 response is associated with increased bacterial colonization [343, 344]. However, there is also evidence that adoptive transfer into SCID mice of $CD4^+$ T cells from T-bet-/- mice, which do not exhibit IFN-γ production and Th1 differentiation, still results in gastritis [345] leaving the door open for a role for Th17 cells or other effector immune cells subsets in gastritis. Some studies have suggested that in the absence of IL-17, there is a decrease in inflammation and an increase in Th1 effector responses, which then drives down bacterial infection. On the other hand, our previously published study suggests that in the absence of IL-17RA (and IL-17 signaling), the Th1 response is not affected and while there is a decrease in acute inflammation driven by neutrophils, the result of loss of IL-17 signaling lead to increased bacterial burden and increased chronic inflammation, especially B lymphocytes [298]. Increased bacterial burden and chronic inflammation were accompanied by an increase in IL-21 expression as well. We hypothesize that IL-21 may drive chronic inflammation in the IL-17RA-/- mice infected with *H. pylori.* Our studies in IL-21-/- mice infected with *H. pylori* presented here demonstrate that IL-21 is required for both Th1 and Th17 responses to be maintained during chronic infection.

A hypothesis for why both Th1 and Th17 responses are suppressed in IL-21-/- mice is that there may be an increase in Treg cells in the absence of IL-21 signaling. Whereas sensitivity analysis performed with our CD4+ T cell computational model indicated that FOXP3 could potentially be negatively correlated to IL-21, the additional time-course, loss-of-function, *in silico* experiments and our data suggest that the number of Tregs is not affected by the deficiency of IL-21. Indeed, the suppression of Th1 and Th17 responses is a more direct effect on the CD4+ T cells as a consequence of the IL-21 deficiency. Our data indicates that at 3 months post-infection there is no increase of Treg cells in the stomachs or in the spleens of the *H. pylori* infected IL-21-/- mice compared to wild-type littermates, but this is not surprising since *H. pylori* IL-21-/- mice have little inflammation in their stomachs and there is an overall decrease in T cells in the stomachs of the IL-21-/- mice. Even in the periphery (spleen) the levels of *foxp3* are not significantly different in the *H. pylori*-infected IL-21-/- mice compared to the *H. pylori* infected wild-type littermates. IL-21 may still affect the efficiency of the Treg response during infection, but our data indicate that it does not affect levels of *foxp3*. But, we

cannot rule out the possibility that Tregs contribute to the higher levels of CD4+-derived IL-10 in the IL-21-/- mice.

IL-21 has been implicated in expanding both Th1 and Th17 cells in our study with *H. pylori,* but it is also a key modulator in intestinal CD4+ T cell populations [346]. These studies suggest IL-21 as a promising therapeutic target for treatment of T cell mediated diseases such as inflammatory bowel disease. IL-21 is upregulated in mouse models of IBD (TNBS-relapsing colitis and DSS-induced colitis) and during chronic bacterial infections like *H. pylori* infection (reviewed in [335]). In models of experimental colitis, IL-21-/- mice were largely protected against both dextran sulfate sodium induced colitis and trinitrobenzene sulfonic acid-relapsing colitis [347]. In these models, the IL-21-/- mice were unable to up-regulate Th17-associated molecules during gut inflammation [347]. Blockade of IL-21 with IL-21R.Fc inhibits disease progression in a lupus prone mouse model [348] and ameliorates disease in a mouse model of rheumatoid arthritis [349]. Recent findings in systemic lupus erythematosus (SLE) patients demonstrates that IL-21 expression correlates with alterations of T cell and B cell subsets, and suggests that targeting IL-21 could provide beneficial effects on both T cell and B cell alterations [350]. In our IL-21-/- model, B cell responses are also affected. We observed that *H. pylori* infected IL-21-/- mice lack an *H. pylori*-specific IgG1 or IgG2a antibody response (measured in the serum, Figure 4.14), but B cells have never been reported to play a pathogenic role during *H. pylori* gastritis. Of note, an anti-IL21 receptor monoclonal antibody is being tested in a phase I clinical trial [324] positioning IL-21 as a promising, host-targeted therapeutic, that could potentially substitute the current aggressive triple-antibiotic treatment in the context of *H. pylori* infection.

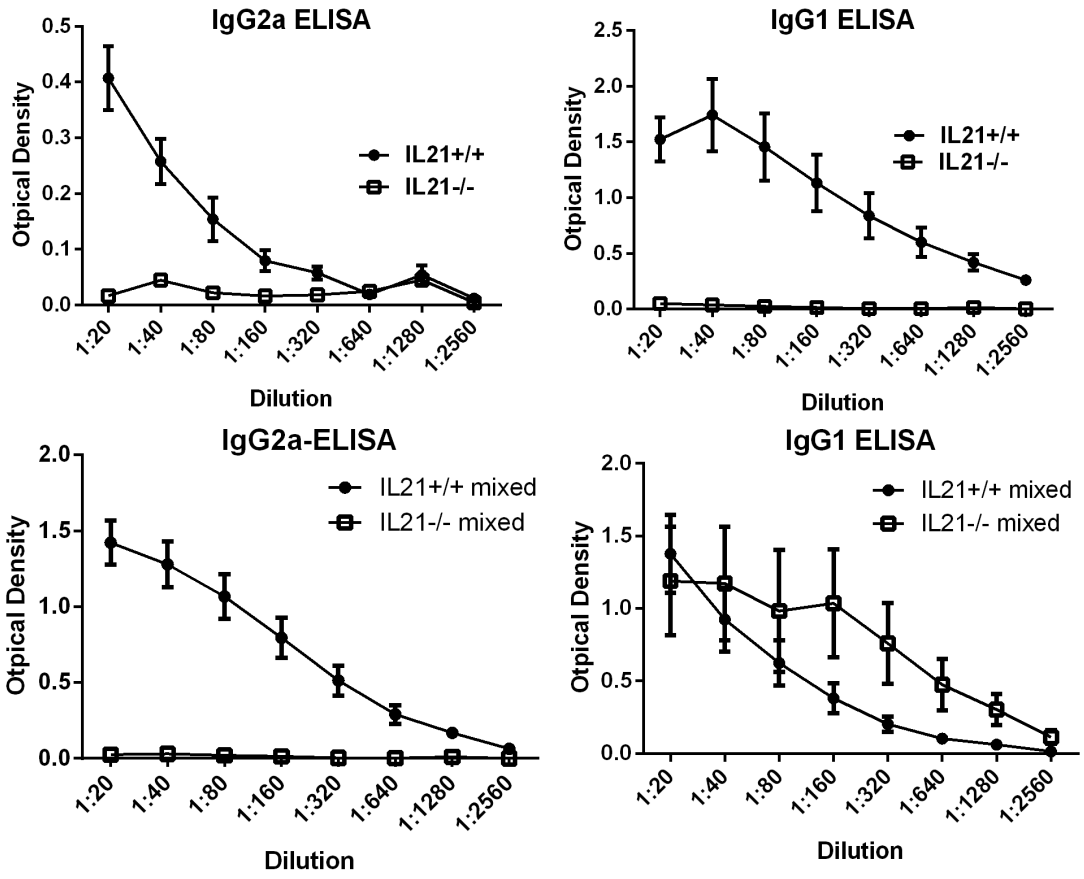

Figure 4.14 *H. pylori*- specific IgG1 and IgG2a is reduced in IL-21 deficient mice during *H. pylori* infection. Isotype antibodies specific for *H. pylori* (strain SS1) were quantitated by enzyme-linked immunosorbent assay (ELISA). Levels of *H. pylori*- specific IgG1 and IgG2a in the serum from SS1 infected mice were measured at 3 months post infection. 9-10 mice (independent serum samples) were used for each mouse group.

In summary, we find that IL-21 deficient mice are protected from *H. pylori*-induced gastritis similar to protection observed in models of chemically induced colitis. Protection from *H. pylori*-induced gastritis was associated with a marked decrease in IL-17 and IFNγ in infected IL-21-deficient mice compared to wild-type mice. Our combined approach utilizing mathematical modeling and *in vivo H. pylori* infections in the mouse model indicate that IL-21 has a role for sustaining both Th1 and Th17 effector cell responses through induction phosphorylation of STAT1 and STAT3 and induced expression of *tbx21* and *rorc*. These data suggest that chronic maintenance of the T cell-mediated inflammation during *H. pylori* infection requires IL-21. Hence, IL-21 may be an

ideal target for the development of immunotherapeutics, although caution should be employed when Th1 and Th17 responses are necessary for controlling more virulent infections.

4.11 Materials and Methods

Mice

Male and female interleukin-21+/- mice (B6;129S5-*Il21*^{tm1Lex}/Mmucd, stock number MMRRC:011723-UCD and backcrossed to C57BL/6, stock number MMRRC: 032800-UCD) were obtained from the NIH Consortium (UC Davis) for the establishment of a breeding colonies. *Helicobacter*-free IL-21-/- and IL-21+/+ (wild-type) male littermates, 8-10 weeks old, were used in all experiments. The IL-21+/- breeding pairs tested negative for intestinal *Helicobacter*. Feces from sentinel mice housed in the same room consistently tested negative for pinworms, mouse parvovirus and several other murine pathogens. Mice were housed and maintained according to the Vanderbilt University Institutional Animal Care and Use Committee (Protocol M/11/055).

Culture of H. pylori

A mouse-passaged derivative of *H. pylori* strain SS1 was used in these experiments. Bacteria were grown on trypticase soy agar (TSA) plates containing 5% sheep blood. Alternatively, bacteria were grown in *Brucella* broth containing 10% heat-inactivated fetal bovine serum (FBS) and 10 μg/ml vancomycin. Plate cultures were grown at 37°C in either room air supplemented with 5% CO_2, or under microaerobic conditions generated by a CampyPak Plus* Hydrogen + CO_2 with Integral Palladium Catalyst (BD). Liquid cultures for infection were grown under microaerobic conditions while shaking at 150 rpm.

Infection of mice with H. pylori

One day prior to infection of mice, *H. pylori* strain SS1 was inoculated into liquid medium and was cultured for 18 hours under microaerobic conditions as described above. Mice

were orogastrically inoculated with a suspension of $5x10^8$ CFU *H. pylori* (in 0.5 ml of *Brucella* broth) twice over 5 days.

Processing of mouse stomachs

The stomach was processed as previously described [351]. In brief, after rinsing in PBS the stomach tissue was cut into longitudinal strips that were used for bacterial culture, RNA analysis, histology and/or protein quantification. For histological analyses, sections were stained with hemotoxylin and eosin to assess inflammation (scoring described below). Moreover, a Steiner stain was performed to localize the *H. pylori* within the gastric tissue as previously described [352].

Mathematical modeling

To assert the dynamics of IL-21-related pathways in CD4+ T cells, an ordinary differential equations (ODE)-based CD4+ T cell differentiation model was used in its wild-type and IL-21-/- set up. Briefly, the model was calibrated with *H. pylori*-specific experimental data and time courses were performed with a Th1, Th17 or iTreg specific initialization to assess the role of IL-21 in these phenotypes.

Culture of H. pylori from mouse stomach

Gastric tissue was homogenized using a Tissue Tearor (Biospec Products Inc.) in Brucella broth with 10% FBS. Serial dilutions of the homogenate were plated as previously described (34). After 5 to 7 days of culture under microaerobic conditions, *H. pylori* colonies were counted.

Stomach Inflammation Scoring

Acute and chronic inflammation in the gastric antrum and corpus were graded on a 0-3 scale [353-355]. Acute inflammation was graded by a blinded pathologist (MKW or MBP) based on density of neutrophils, and chronic inflammation was graded based on the density of lamina propria (LP) mononuclear cell infiltration independent of lymphoid follicles. Total gastric inflammation was calculated as a sum of acute and chronic inflammation in the corpus and the antrum allowing for quantification of total inflammation on a scale of 0-12.

RNA extraction and real-time rtPCR

Total RNA was isolated from the stomach using the TRIZOL isolation protocol (Invitrogen) with slight modifications as previously described (34). CD4+ T cell RNA was isolated using Qiagen's RNeasy kit as directed by the manufacturer. RNA was reverse transcribed using the High Capacity cDNA Reverse Transcription Kit (Life Technology). For real time reverse transcription PCR (rtPCR), we used the relative gene expression method (35). Glyceraldehyde 3-phosphate dehydrogenase (GAPDH) served as the normalizer, and tissue from uninfected mouse stomachs (of same genotype) served as the calibrator sample as previously described (34).

Flow cytometric analysis

To analyze gastric cellular infiltrates, whole mouse glandular stomachs were harvested and processed (with dispase and collagenase) using the Gentle Dissociator (Miltenyi Biotec) as previously described (34). The gastric cells were stained with anti-CD4, anti-CD8, and anti-CD3, anti-Gr1, anti-CD11b and anti-B220 antibodies (BD Biosciences) as previously described (34). Samples were collected and analyzed on a BD LSR II flow cytometer (BD Biosciences).

Analysis of cytokine and chemokine protein levels in gastric tissues

Freshly excised glandular stomach tissues were rinsed in PBS and homogenized in Cell Lytic MT Mammalian Tissue Lysis/Extraction buffer (Sigma). Twenty-five cytokine analytes were measured in tissue lysates using the MILLIPLEX MAP Mouse Cytokine/Chemokine Magnetic Bead Panel kit according to the manufacturer's instructions (Millipore). Standards were also prepared for all 25 cytokine analytes according to the manufacturer's instructions. Protein concentrations were measured using the DC protein assay kit (Bio-Rad Laboratories). The concentration of each cytokine is presented as pg/μg tissue protein.

CD4+ T cell isolations

CD4+ T cells were isolated from the spleens of *H. pylori*–infected IL-21-/- mice and *H. pylori*–infected wild-type littermates between 2 and 3 months post infection. Spleens were harvested and after red blood cell lysis, the cells were magnetically labeled with

CD4 Microbeads (Clone L3T4, Miltenyi Biotec). CD4+ cells were positively selected using the positive selection sensitive program on the autoMACS machine (Miltenyi Biotec) according to the manufacturer's protocol. The resulting population was 92-96% CD4+ by flow cytometry analysis.

STAT1 and STAT3 phosphorylation assays

Levels of STAT phosphorylation were measured by flow cytometry. Briefly, one million splenocytes were either unstimulated or stimulated with 10 ng/mL recombinant IL-6 or recombinant IL-21 (Peprotech) for 15 minutes. After fixation with a final concentration of 1.5% paraformaldehyde, cells were permeabilized with cold methanol. Cells were stained with either phospho-STAT3 (tyr705, D3A7) antibody (Cell Signaling Technology) or phospho-STAT1 (tyr 701, D4A7) antibody for 45 minutes. After several washes, anti-rabbit IgG AlexaFluor 647 was added for 30 minutes. Cells were washed three times and analyzed by flow cytometry.

Statistical analysis

Four to seven mice per group per time point were used for all of the studies. Colonization, inflammation, luminex assays, cytokine real-time rtPCR were all performed as distinct experiments at least 3 times. To compare results obtained with different groups of mice, statistical analysis was performed using one-way Analysis of Variance, followed by a Student-Neuman-Keuls post-hoc test. For analyses of bacterial numbers and cell numbers, the data was normalized by log transformation prior to statistical analysis. For histology scores, the Mann-Whitney U-test was applied to compare results between wild-type and IL-21-/- mice.

Chapter 5

Modeling the dynamics of T helper 17 induction and differentiation

Adria Carbo, Josep Bassaganya-Riera, Tricity Andrew, Kristin Eden, Monica Viladomiu, Stefan Hoops, Raquel Hontecillas.

Carbo A., Bassaganya-Riera J., Andrew T., Eden K., Viladomiu M., et al. (2014). "Modeling the dynamics of T helper 17 induction and differentiation". ***Submitted.***

5.1 Summary

CD4+ T cells play important roles in orchestrating immune responses, maintaining homeostasis, and offering a functional control of immune responses when homeostasis is compromised. Depending on the cytokine milieu, a naïve CD4+ T cell differentiates into different phenotypes such as T helper (Th)1, Th2, Treg, or Th17. The latter, remains a controversial phenotype since it has been identified as a pro-inflammatory and tissue-damaging cell subset in the context of immune-mediated diseases, but it also has been demonstrated that it contributes to regulatory immune responses and pathogen clearance during infection. With the increased availability of high-throughput datasets, modeling that combines theoretical and data-driven approaches become powerful tools to build predictive network models. We used a microarray dataset generated by Yosef et al. to construct a dynamic model of Th17 differentiation. Our modeling pipeline pre-processed the gene expression data to average duplicates and tailor the dataset to 2,000+ genes of interest. By using the Ingenuity Pathway Analysis (IPA) platform, we inferred a static network composed of 67 genes involved in induction, function, and

maintenance of Th17 differentiation. The dynamic network model was built from the IPA network by using CellDesigner and COPASI. *In vitro* time-course mRNA expression data was used to fully calibrate the modeling network using COPASI. Computational simulations highlighted the potential role of IL-24 in shaping effector, IL-17A producing responses, and local sensitivity analysis demonstrated that IL-24 is negatively correlated with FOXP3 expression. In addition, IL-24 was demonstrated to regulate the balance between FOXP3 and RORγt during Th17 differentiation. Moreover, NLRP3 was identified as another potential therapeutic target to treat Th17-driven pathologies, since the ablation of the NLRP3 gene resulted in a dramatic down-regulation of IL-17A production. Local sensitivity analyses on NLRP3 highlighted the positive correlation of NLRP3 with IP-10, GM-CSF, IFNγ, and IL-17A. Summarizing, we established a computational pipeline for constructing and calibrating models of Th17 differentiation based upon gene expression datasets. Our simulation results and sensitivity analyses of the model highlighted the role of IL-24, SGK1, and NLRP3 as key modulators of Th17 differentiation and opened a new avenue of strategies to use publicly available data to generate hypothesis pointing in the direction of immune marker discovery.

5.2 Introduction

The immune system is a highly specialized, hierarchical, and networked system with protective effects against pathogens, injury and disease. The CD4+ T cell subsets are functionally and phenotypically heterogeneous, consisting of distinct populations involved in coordinating various aspects of adaptive immunity. Upon antigen recognition and co-stimulatory signaling, naïve CD4+ T cells will differentiate into a specific phenotype depending on the cytokine milieu. The current understanding of CD4+ T cell differentiation comprises at least nice functionally and phenotypically distinct states: T helper type 1 and 2 (Th1 and Th2) [4], T helper type 9 (Th9) [8], T helper type 17 (Th17) [5], T helper type 22 (Th22) [11], Follicular T helper cells (Tfh) [122, 123], induced regulatory T cells (Treg) [6, 7], and type 1 regulatory cells (Tr1) [120]. In this panicle of CD4+ T cell subsets, the Th17 population is a key player in chronic inflammatory diseases such as Inflammatory Bowel Disease (IBD) [356], type 2 diabetes (T2D) [357], rheumatoid arthritis [358] or in the infectious disease setting such as during *Helicobacter pylori* [32] or *Clostridium difficile* infection [269] and enteroaggregative *Escherichia coli* [260, 359]. Even though Th17 cells have been fully characterized in the context of inflammatory pathologies, they remain elusive and controversial because of their

plasticity and their pleiotropic role in the immune response, functional plasticity and flexibility. For example, intestinal IL-17A+ IL-10+ Th17 cells are known to be immunosuppressive [48], however, in the onset of IBD, increased IL-17A expression has been reported [69] and Th17 cells expressing IFNγ or GM-CSF can accumulate during gut inflammatory disorders [42, 54, 55].

Theoretical models have been used to decipher the mechanisms of the Th17 population by focusing on the reciprocal regulation exerted by the transcription factors RORγt and FOXP3 [27, 34]. We published a computational and mathematical model of CD4+ T cell differentiation that predicted and validated the role of peroxisome proliferator activated receptor gamma (PPARγ) in modulating the plasticity between Th17 and Treg [28]. Due to the increasing availability of high throughput data, combining theoretical and data-driven approaches becomes more feasible. Theory-driven modeling in the context of CD4 + T cell differentiation has been studied by using reductionist approaches, most often based on mutually exclusive concepts, such as Th1 versus Th2 phenotypes with limited consideration towards intermediate or compounded phenotypes. However, combining data-driven and theoretical approaches emerges as a new strategy for multivariate analysis and systems-level hypothesis generation. In this context, network inference is a key step in extracting the information from various datasets in a manner that combines data and theory. An example on how to use high-throughput data to construct a CD4+ T cell comprehensive network is the study published by Yosef et al., where they used transcriptional profiling with microarrays at high temporal resolution to build a Th17 induction system [67]. In this study, 1,291 genes were differentially identified and clustered into 20 groups, depending on their temporal profiles. Another advantage highlighted in this study is the use of modules to explain the processes controlling Th17 differentiation. Four regulatory modules were identified: the positive module that increased IL-17 levels, the negative module that downregulated IL-17, the signature of Th17 genes and signature of other CD4+ T cell subtypes. This work supported the finding of 3 novel key regulators of Th17 function: *Mina*, *Fas*, and *Pou2af1*.

Our current paper describes the creation of a computational model of Th17 induction and differentiation based on Yousef's data [67] that incorporates both dynamics and

sensitivities across 18 time points. To build the dynamic model we analyzed the microarray data and inferred a computational modeling network using the Ingenuity Pathways (IPA) platform, we translated the inferred network into a Systems-Biology Markup Language (SBML)-compliant system, imported the network into COPASI, and calibrated the system with the original microarray datasets used to build the dynamic network model. Our *in silico* predictions about the function of NLRP3 and IL-24 during Th17 differentiation, revealed a modulatory role over IL-17A production. Furthermore, our local sensitivity analysis highlighted the correlations between FOXP3, CEBPB, FOSL1, IRF4, and PPARγ with IL-24, as well as the correlations of IP-10, GM-CSF, IFNγ, and IL-17A with NLRP3.

5.3 Integrated pipeline for data-driven modeling

To streamline the process of model construction from high-dimensional microarray data, we built a semi-automated analysis pipeline that provides a methodological approach for dynamic model construction. Our pipeline efficiently builds a computational model based on experimental data (Figure 5.1) generated in-house or downloaded from publicly available data repositories. A local instance of the Galaxy pipeline, a platform for sequencing analysis, allows us to obtain a list of genes reads which are subjected to trimming algorithms (see next section “Treatment of microarray data”) and used as input in the Ingenuity Pathways Analysis (IPA) platform for creating an initial network model by using IPA’s network inference algorithm. The resulting static network model was implemented into CellDesigner through a CellDesigner plugin (unpublished information) to become an SBML-compliant network model. Next, we imported the SBML-compliant network into the Complex Pathway Simulator (COPASI). COPASI allowed us to perform parameter estimation and local/global sensitivity analysis and obtain a fully calibrated dynamic model of the process of Th17 differentiation. Using time-course and sensitivity analyses, we were able to run *in silico* experimentation with the implemented Th17 differentiation model and come up with a series of predictions in regards to Interleukin-24 (IL-24), and the Noll-Like Receptor Protein 3 (NLRP3).

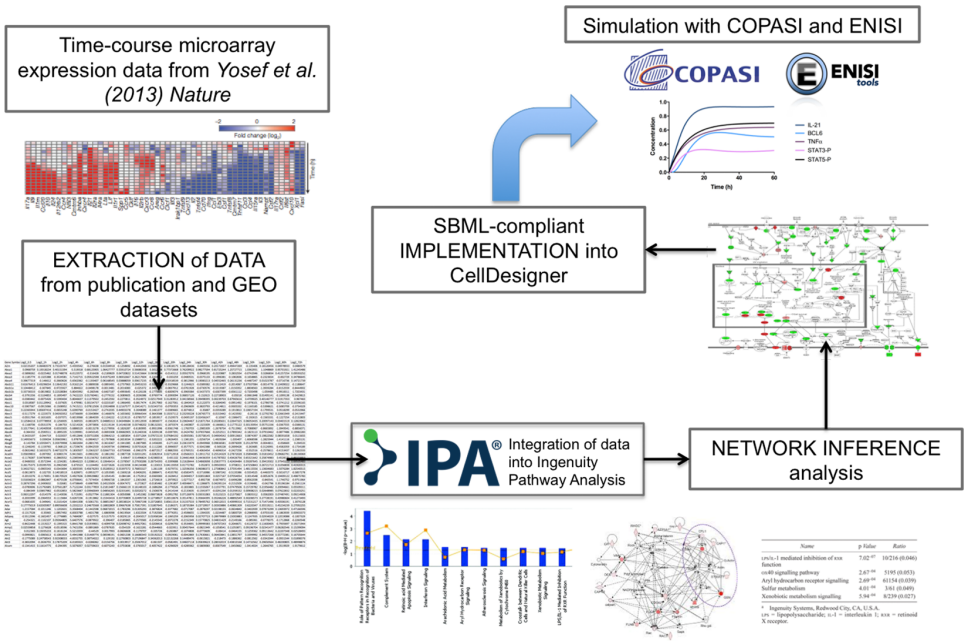

Figure 5.1. Integrated data-driven modeling pipeline to generate SBML-compliant, comprehensive, and predictive computational models of Th17 differentiation. Briefly, publicly available data from GEO was downloaded and treated to represent a tailor input for Ingenuity Pathways (IPA). IPA was used to infer a network that was imported into an SBML-compliant environment. Using the microarray experimental data in COPASI, the computational model was created and used to generate novel predictions.

5.4 Microarray data analyses

The data used for this study was obtained from the Gene Expression Omnibus (GEO) NIH repository with the accession number GSE43955. This dataset contains a microarray expression-profiling array for Th17 differentiation, including a Th0 control. Briefly, Yosef et al. isolated naïve CD4+ T cells from wild-type mice and treated them with IL-6 and TGFβ1. Samples for mRNA analysis were collected at 18 different time points (0, 0.5, 1, 2, 4, 6, 8, 10, 12, 16, 20, 24, 30, 42, 48, 50, 52, 60, and 72 hours). The Th0 control consisted of time- and culture-matched wild-type naïve T cells maintained under Th0 conditions [67]. Furthermore, during microarray or other sequencing analysis strategies, the expression results are often annotated with more than one entry per gene. For this reason, the GEO dataset extracted from [67] contained gene reads that

had entries that were annotated with an unspecified gene name (eg. 1424888_at), and also had different entries for one same gene. At the same time, due to the nature of the experimental design, the data obtained had two different profiles: either non-differentiated or Th17-induced CD4+ T cells. For these variety of reasons, we created a list of genes that contained more than 2,000 genes related to CD4+ T cell differentiation, function, progression, and maintenance, metabolism, inflammatory genetic profiles, and a variety of arrays of transcription factors. We then used the trimming algorithm to trim the microarray gene list to only these 2,000+ genes. Furthermore, the algorithm averaged the value of these genes if it found more than one transcript for each one. Next, we calculated the fold change of each of the genes by dividing the Th17 sample by its corresponding Th0 control at each time point. Finally, in order to limit the value of expression and contain a more meaningful list, we calculated the log2 value of the fold-change of expression as it has been described in other publications [360].

5.5 Network Inference and Analysis

In order to deeply analyze the topologies of microarray gene expression data and infer a network we used the Ingenuity Pathway Analysis (IPA) platform. IPA is a system that transforms a list of genes into a set of relevant networks based on extensive records maintained in the IPA Knowledge base. Furthermore, IPA uses powerful causal analytics that help to build a regulatory picture and a better understanding of the biology underlying a given gene expression dataset. More specifically, we used IPA so that its network inference algorithms could retrieve, not only the experimental validated interactions, but also predicted ones as well as networks that were optimized for triangular connections between genes. With this approach, IPA favors denser networks over more sparsely connected ones. Our treated and modified microarray data, based solely of the gene list and the log2 values, was uploaded into IPA as a list of target genes with expression values. Next, we computed a Core Analysis so IPA could retrieve all regulatory interactions without restricting the search. Moreover, by running a Core Analysis, we mapped the microarray data to IPA's Knowledge Base (IPAKB), created molecular networks (algorithmically generated pathways), divided the data into different

diseases and biological functions, and determined different canonical pathways. Including both experimental and predicted connections, IPA provided a list of upstream activators, where the most up- and down-regulated genes could be observed and the information of such genes could be accessed. Based on the all the genes uploaded into IPA, we created a first inferred network (Figure 5.2A). The expression values of this first network were calculated based on single observations extracted from the microarray dataset. In some cases, time-points were repeated and/or different replicates were given. In those cases, we averaged the values so that the final expression value was representative of three replicates, when available. Given the amount of interactions generated, we selected 67 genes based on fold change expression over time that showed the core of Th17 differentiation (Figure 5.2B). This inferred Th17 interaction network represents the key and indispensable genes for a naïve CD4+ T cell to differentiate into Th17 when the cytokine milieu is rich in IL-6 and TGFβ1. Following modeling reduction we selected 32 genes and their interactions between them and imported them into CellDesigner (Figure 5.2C). To reduce the network by 35 genes, we located IL-6 and TGFβ1 in the IPA network and we built downstream pathways based on the centrality of RORγt and STAT3. Pathways resulting from these interactions were depicted in our SBML-based network in CellDesigner. This SBML-compliant model represents the activating and inhibitory reactions that take place in the cytoplasm and nucleus space and that will ultimately differentiate the cell into a Th17 cell.

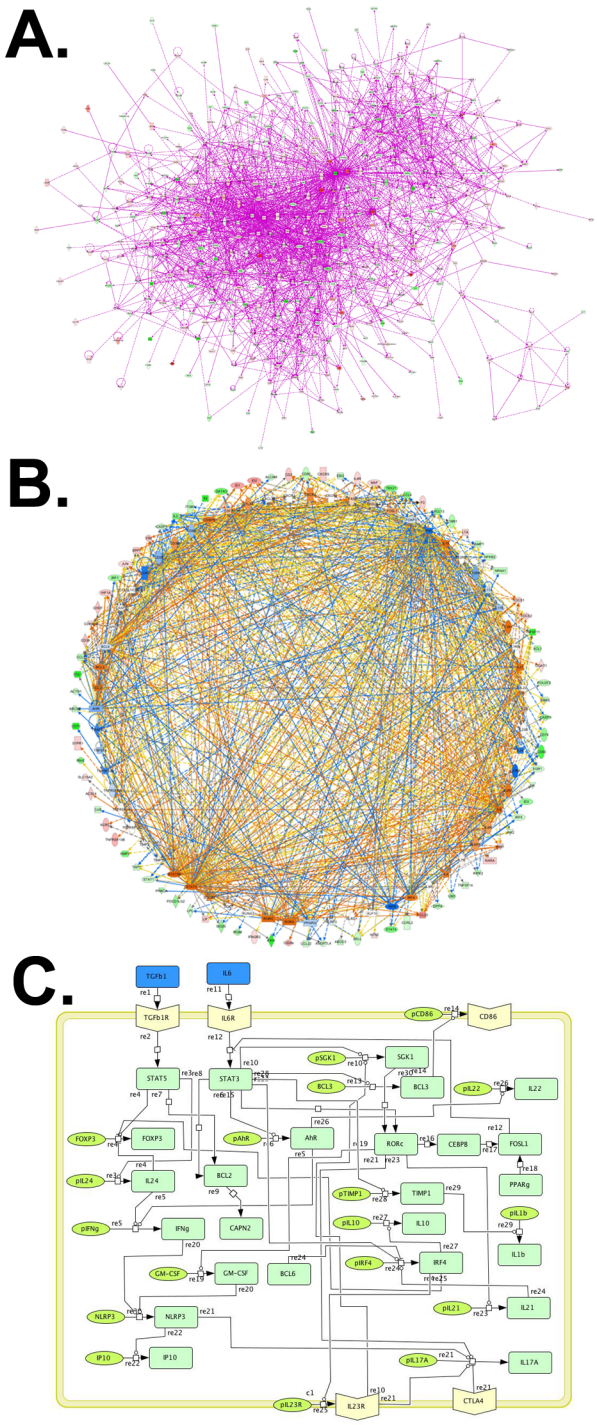

Figure 5.2 Network inference and analysis prior to importation into an SBML-compliant environment. (A) The microarray data was used to generate a comprehensive gene regulatory interaction network in IPA. (B) Out of all the nodes in IPA, 67 genes (up-regulated or down-regulated) were selected based on differences in expression over the Th0 compartment. (C) SBML-compliant Cell designer network with a subset of genes in (B) to import into COPASI.

5.6 Model implementation

The transition from a static interaction diagram into a dynamic model of Th17 differentiation helps to not only understand the connections of the network but also observe how these connections changed mechanistically, in a dynamized manner, over time. Furthermore, the dynamic model allowed us to run *in silico* simulations and detect emerging cellular behaviors that could not be observed by just looking at the static diagram. Thus, adding dynamics to the process increased the predictability of the network. Indeed, other comprehensive models of CD4+ T cell differentiation have been constructed [28]. However, this would be the first model that uses data-driven approaches to construct its network and to calibrate the dynamic model. Using this rationale, we next sought to import the inferred network, built by IPA and translated in CellDesigner, into the COmplex PAthway SImulator (COPASI) [29]. Importing the network into COPASI also allowed us pick-and-choose different reactions and nodes for computational experimentation. After the importation, the name of the species and reactions were annotated, the model was adjusted into COPASI by creating Global Quantities and events, and the rate laws were adjusted to automatically create the ordinary differential equations.

5.7 Model calibration using microarray experimental data

The data used in this study performed by Yosef et al. in [67] consists of a time-course in vitro study where gene expression analysis was performed at 18 different time points (0, 0.5, 1, 2, 4, 6, 8, 10, 12, 16, 20, 24, 30, 42, 48, 50, 52, 60, and 72 hours). CD4+ T cell differentiation is an extremely dynamic process that can vary in a time-window of 1h ranges. Often times, experimental strategies in CD4+ T cell differentiation assess the levels of cytokines and transcription factors once the cell is fully differentiated around 60h post induction. With this approach, we are missing the specific cell dynamics of the process, as well as the subtle details that may open new strategies for therapeutic development. In this case, the 18 time points offer a clear picture of the exact levels of expression of each gene at each time point. Therefore, this dataset represents a perfect

candidate to be used for calibration purposes. To accomplish this goal, we extracted the experimental data from the raw database for the 32 nodes that our computational model is composed of. Using the parameter estimation function in COPASI, we uploaded these 32 curves and used the Genetic Algorithm in combination with a Particle Swarm Optimization (PSO) [242], both embedded in COPASI, to adjust the model parameters. PSO is a global search algorithm and thus depends only minimally on the initial guess of each parameter and therefore avoids the subjective estimation caused by initial guesses in local methods as Levenberg-Marquardt. PSO has been used in other publications for the same purpose [243]. In contrast, the genetic algorithm is an evolutionary algorithm that mimics the process of natural selection by mutating or altering different parts of the system.

The main feature of Th17 cells is their ability to secrete IL-17. This output of IL-17 production is induced by TGFβ1, together with pro-inflammatory cytokines IL-6 or IL-21 and IL-23, in a concentration-dependent manner [181, 182]. It has been demonstrated that TGFβ1 synergizes with IL-6 [183] or IL-21 [184, 185] to promote the expression of IL-17. This is achieved through the activation of retinoid-related orphan receptor (ROR)γt by IL-6 through the transcription of STAT-3 [186, 187], which in turn promotes the transcription of the IL-17 gene [155, 188]. The combination and iterations of the genetic and PSO algorithms resulted in the fitting of these key molecules expression data with the computational model. First, the phosphorylated form of STAT3 controls and plays a central role during Th17 differentiation and function [361]. Our computational model was able to fit the experimental data correctly (Figure 5.3A), which was characterized by an early rise and a constant degradation over time. Next, the related orphan nuclear receptor C gene (RORc) transcribes RORγt, which is central during Th17 differentiation. As our results show, our model was able to fit the bell-shaped expression profile that RORc possesses during differentiation (Figure 5.3B). As a result of Th17 differentiation, IL-21 and IL-17 are produced and secreted by the cell. Our computational model fits IL-17 (Figure 5.3C) and IL-21 (Figure 5.3D).

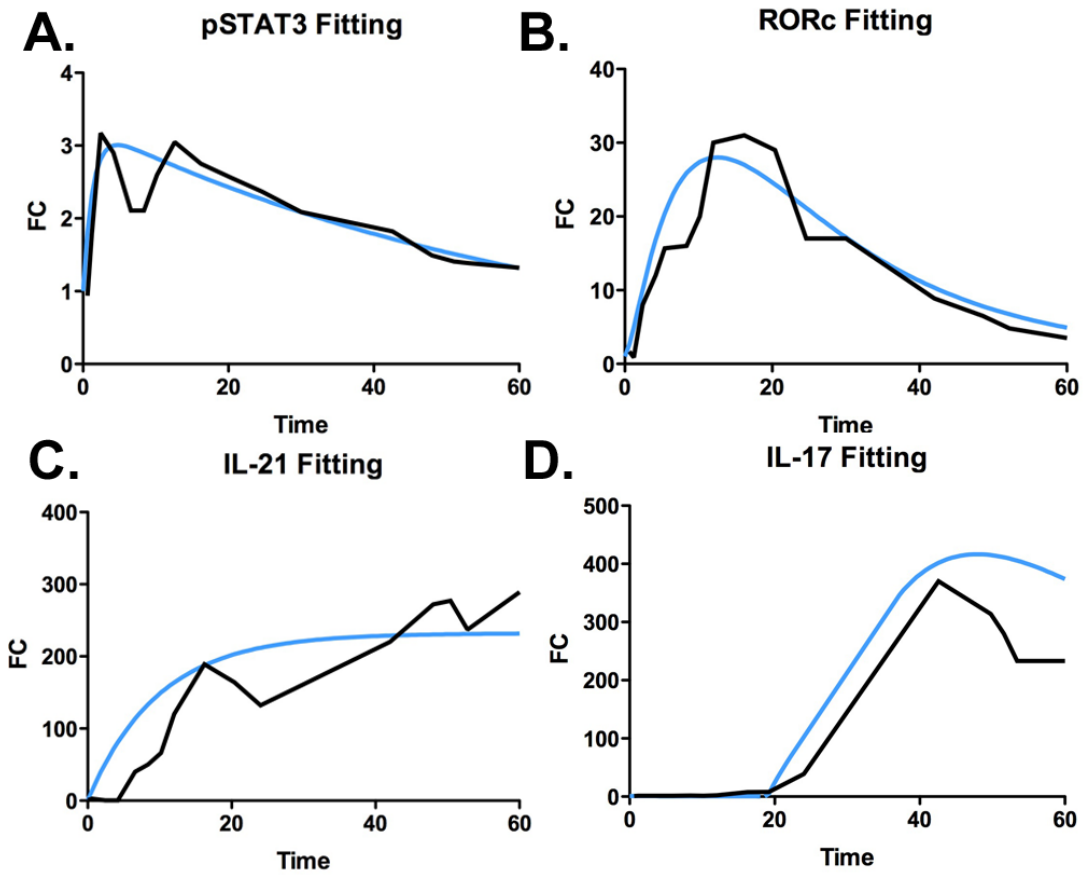

Figure 5.3 Computational fitting of Th17-related molecules. COPASI was used to run parameter estimation based on the microarray experimental data. Using a Genetic Algorithm and PSO, the model fitted (in blue) the experimental data (in black) of (A) phosphorylated STAT3, (B) RORc, (3) Interleukin 21, and (D) Interleukin 17.

Other fitted molecules of the Th17 model are also depicted in Figure 4. IL-10 has usually been considered an anti-inflammatory molecule. Th17 cells produce high levels of IL-10 under certain conditions. In this case, our computational model was able to reproduce the dynamics of this cytokine over time (Figure 5.4A). SGK1 and TIMP1 are two transcription factors that were selected due to their high expression during Th17 differentiation. Although their role during Th17 induction has not been fully elucidated, they remain key players for IL-17 production. Our computational model was able to fit SGK1 (Figure 5.4B) and TIMP1 (Figure 5.4C). Local sensitivity analysis on SGK1, or also known as salt-sensing glucocorticoid kinase 1, showed a strong correlation with RORc, IL-17A, and most notably, the IL-23R (Figure 5.5). Indeed, the relationship between SGK1 and the promotion of pathogenic Th17 cells has already been reported [362]. In this case, Wu et al. demonstrated that SGK1 is an essential node downstream

of the IL-23R pathway and is critical for regulating its expression by de-activating FOXO1. The last example of calibration is represented by FOXP3. FOXP3 inhibits the RORγt-driven transcription of IL-17 by directly suppressing RORγt [182, 197]. Furthermore, the IL-2/STAT-5 axis constrains Th17 [192] in part through a FOXP3-dependent mechanism, since STAT-5 activates FOXP3 [198], as well as through the inhibition of the STAT-3/IL-21 pathway [199]. Indeed, double positive FOXP3 RORγt T-helper cells have been identified as an intermediary that displays suppressive function [108] and are being investigated due to the plasticity of Th17. Our computational model also captures the relationship of FOXP3 and RORγt and it fits the expression data of FOXP3 (Figure 5.4D). These calibration results proved grounds to start *in silico* experimentation with our mathematical and computational model of Th17 differentiation.

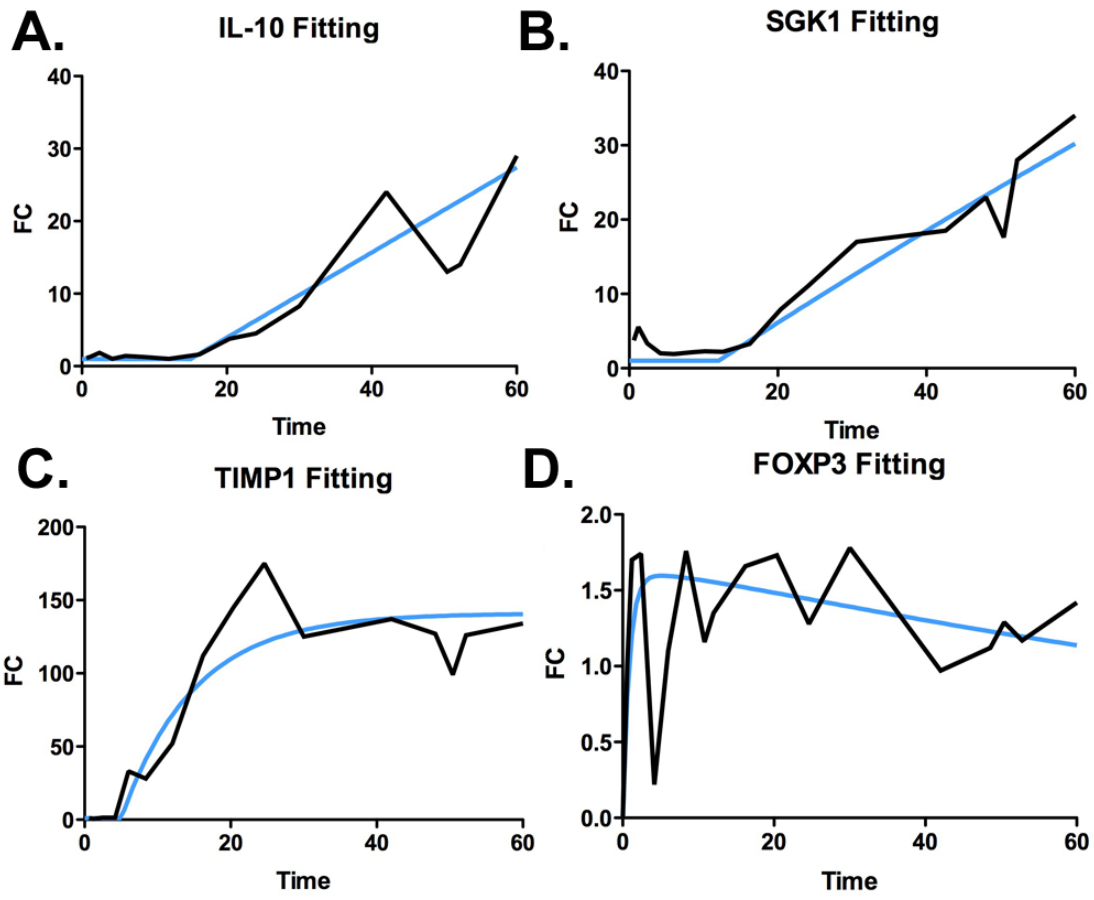

Figure 5.4 Computational fitting of Th17-related molecules (II). COPASI was used to run parameter estimation based on the microarray experimental data. Using a Genetic Algorithm and PSO, the model fitted (in blue) the experimental data (in black) of (A) Interleukin-10, (B) Glucocorticoid Kinase 1 (SGK1), (3) TIMP1, and (D) FOXP3.

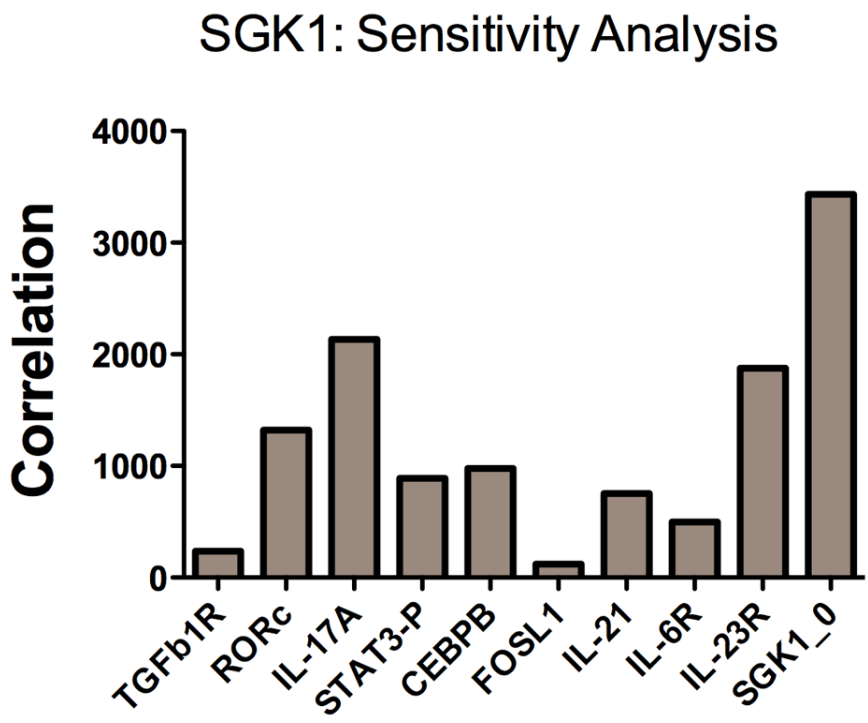

Figure 5.5. Sensitivity analysis on salt-sensing GSK1 by the Th17 differentiation computational model. Sensitivity analysis was run with COPASI on our computational model using a delta factor of 0.0001 and a delta minimum of 1e-12. The subtask run for the analysis was a time-series with t=100h and correlation of all the variables of the model against activated GSK1 was assessed, showing high correlation with key transcription factors that determine phenotype differentiation on Th17.

5.8 *In silico* experimentation and computational modeling predictions

5.8.1 IL-24 modulate the production of IL-17A via a FOXP3-dependent RORγt inhibition

One of the first targets for *in silico* experimentation was Interleukin-24 (IL-24), a member of the IL-10 family of cytokines. Upon binding to its receptors, IL-24 induces rapid activation of STAT1 and STAT3 transcription factors, both of which activate effector profiles in CD4+ T cell differentiation [363]. The role of IL-24 during Th17 differentiation, however, is not well understood and there are no publications explicitly stating how IL-24 fits in the complex Th17 differentiation story. The microarray analysis of the Th17

differentiation datasets used in this study indicates that IL-24 is highly expressed when a naïve CD4+ T cell is induced with TGFβ1 and IL-6. At the same time, our computational model was able to fit such dynamics observed in the experimental data (Figure 5.6A). In order to computationally shed some light on the role of IL-24 during Th17 differentiation, we performed local sensitivity analysis on the IL-24 node. Results showed how IL-24 negatively correlates with FOXP3 and positively correlates with Th17-related molecules such as STAT3, RORc, IL-17A and IL-21 (Figure 5.6B). At first glance, IL-24 seems to promote an effector response by downregulating FOXP3 and minimizing its inhibition towards RORγt. We next sought to determine what would occur if the expression of IL-24 was completely ablated in a Th17 cell. In order to accomplish this goal, we created an IL-24 null system, where the ability of IL-24 to exert its functions to other nodes was completely impaired. Results showed how the expression of FOXP3 in the IL-24 null when compared to the wild-type system remains unchanged during the first, approximately, 10 hours. However, after 10 hours, FOXP3 starts degrading over time. In contrast, in the IL-24 null system, FOXP3 reached a steady-state and it did not undergo degradation (Figure 5.6C). Since FOXP3 and RORγt are regulated with such tight balance, we next sought to determine the effect of this undegraded FOXP3 towards the expression of RORc. Interestingly, the IL-24 null system showed less expression of RORc when compared to the wild-type Th17 model (Figure 5.6D). As a result of this lower expression of RORc, it is not surprising that our results found lower levels of IL-17A production in the IL-24 null system than in the wild-type model (Figure 5.6E). These counterintuitive results generated *in silico* by our Th17 differentiation model in regards to the role of IL-24 during Th17 induction should be validated with specific *in vitro* and *in vivo* experimental studies. If these predictions were validated, IL-24 would arise as an immune-based, powerful, and potential therapeutic target to modulated inflammatory diseases characterized by a Th17 upregulation.

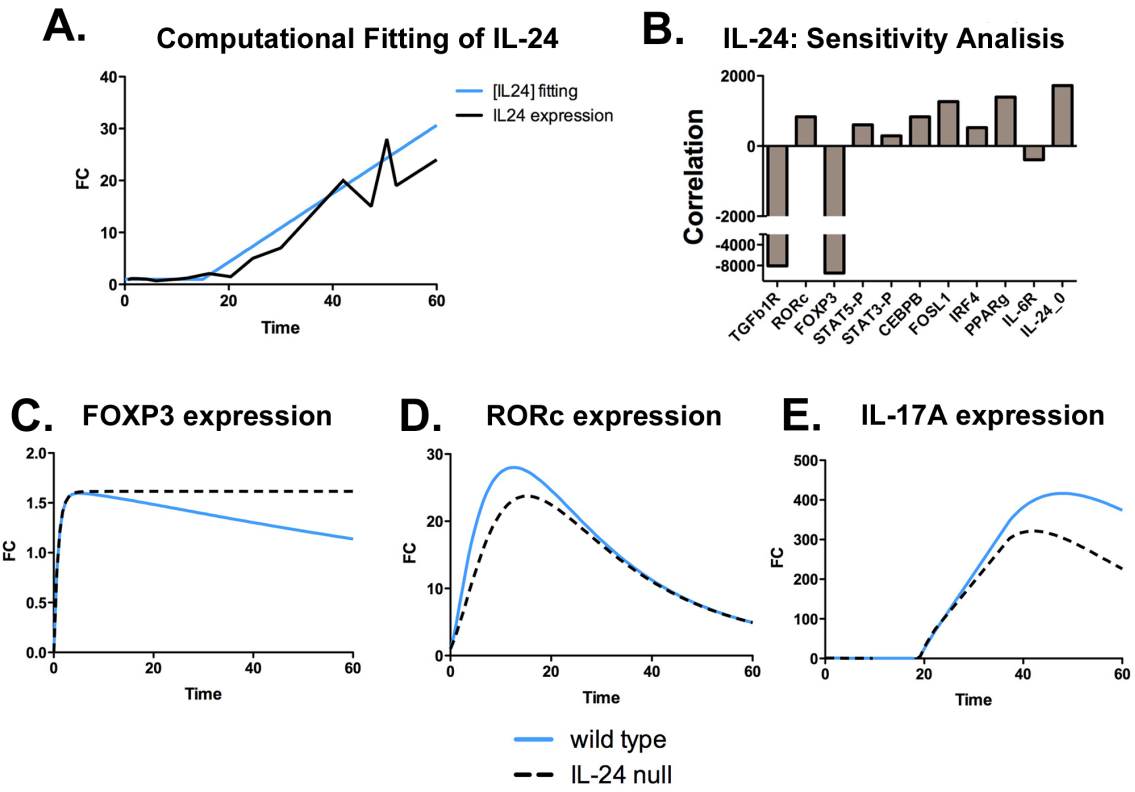

Figure 5.6: *In silico* experimentation: IL-24 modulates IL-17A production through a FOXP3-dependent mechanism. (A) IL-24 computational fitting of the microarray experimental data using Genetic Algorithm and PSO in COPASI. (B) Sensitivity analysis on Interleukin 24. Time-course analysis of (C) FOXP3, (D) RORc, and (E) IL-17A in either a wild-type model, or an IL-24 null Th17 differentiation model.

5.8.2 NLRP3-deficient Th17 cells have an impaired production of IL-17A

Th17 cells stimulate the tissue environment towards an effector profile and orchestrate the function of cell subsets that are part of the innate immune response, such as macrophages, neutrophils, or epithelial cells. Nod-like receptors (NLRs) are a subset of pattern recognition receptors (PRRs) and a key component of innate responses found in the cytosol that are essential for detecting invading pathogens and initiating immune responses. NLRs are molecular platforms activated upon cellular infection or stress that trigger the release of proinflammatory cytokines, such as IL-1β or IL-6 [364]. Within the inflammasome-forming NLRs, NLRP3 has received particular attention since it interacts with the caspase recruitment domain (ASC) and the cytokine protease caspase-1, forming a cytoplasmic complex (NLRP3) [365]. Although it has been recently demonstrated that activation of NLRP3 in other cell subsets promotes Th17

differentiation in the T cell compartment in the context of allogeneic hematopoietic cell transplantation [366] and allergic lung inflammation [367], T cell intrinsic mechanisms by which NLRP3 modulates Th17 function have not been unexplored. In our study, NLRP3 appeared in our list of the genes upregulated by the induction of Th17 over time. In our inferred network, NLRP3 is linked to the activation of GM-CSF and IFNγ (Figure 5.2C), both responsible for the increase of the pathogenic activity of Th17 cells [368]. Our Th17 computational model was able to fit the experimental expression data of NLRP3 (Figure 5.7A). Indeed, our sensitivity analysis confirmed that NLRP3 is linked to the activation of the expression of genes that correlate with tissue-damaging inflammation in Th17 cells, since such as IFNγ, GM-CSF, IP-10, and IL-17A (Figure 5.7B). We next sought to determine the role of NLRP3 over the production of IL-17A. We created an *in silico* NLRP3 null Th17 model. In this system, NLRP3's ability to upregulate its linked genes was completely ablated. Our results show how the lack of NLRP3 in a Th17 cells down-regulates IL-17A (Figure 5.7C). Given the amount of variability of NLRP3 expression in the first time-points of the Th17 induction process, we next sought to determine if a change in the variability of the expression of NLRP3 at the early stages of differentiation would affect the outcome of IL-17A production. To add stochasticity to the NLRP3 node, we used ENISI SDE, a novel web-based stochastic modeling tool [79]. Our results show how that the addition of 5% variability in the expression of the NLRP3 node slightly downregulated the IL-17A production in the Th17 cell (Figure 5.7D). For this reason, we hypothesized that if the variability was higher, the production of IL-17A would be highly affected. Indeed, our results show how when the expression of the NLRP3 node was set at a 30%, the production of IL-17A was dramatically affected (Figure 5.7E). These results highlight the role and T cell intrinsic relationship of NLRP3 and IL-17A. More importantly, NLRP3 could represent a potential therapeutic target to treat Th17-mediated inflammatory diseases. Indeed, NLRP3 is under investigation to evaluate if it can be a good target to treat type 2 diabetes [369, 370].

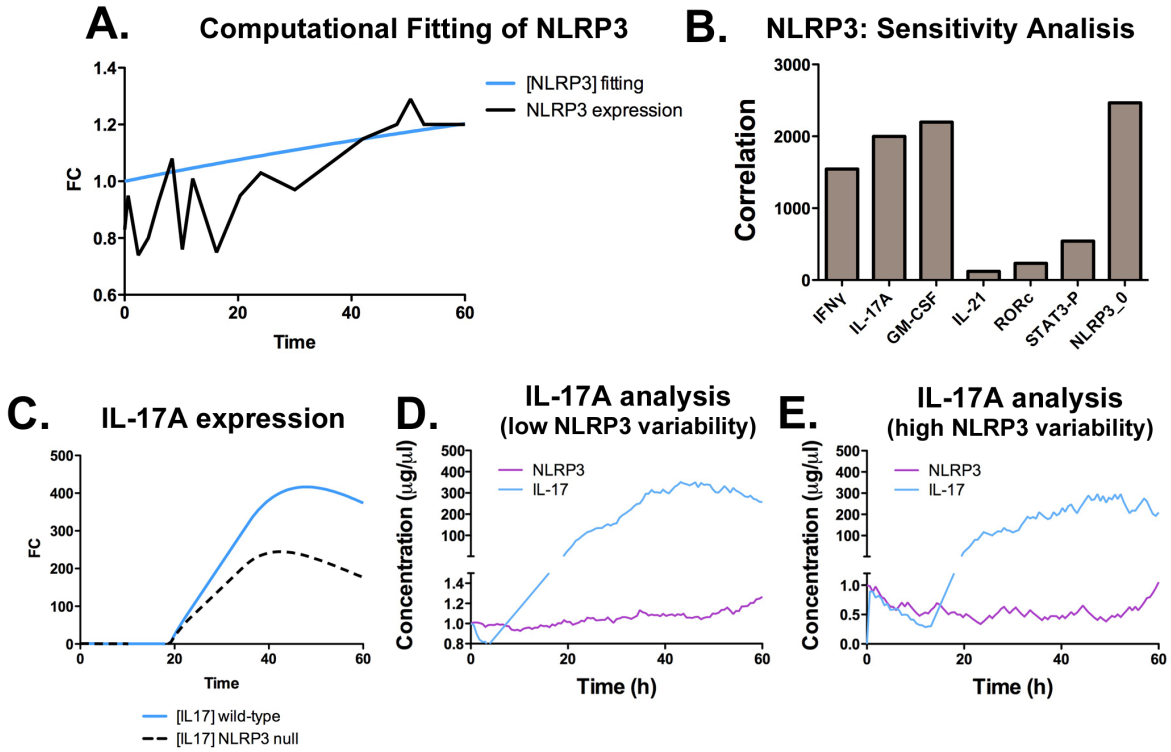

Figure 5.7: *In silico* experimentation: NLRP3 helps to modulate IL-17A production in Th17 cells. (A) NLRP3 computational fitting of the microarray experimental data using Genetic Algorithm and PSO in COPASI. (B) Sensitivity analysis on NLRP3. (C) Time-course analysis of IL-17A in either a wild-type model, or an NLRP3 null Th17 differentiation model. (D) Time course analysis of IL-17A and NLRP3 using a Stochastic Differential Equation Simulatior with a variability on the NLRP node of 5%. (E) Time course analysis of IL-17A and NLRP3 using a Stochastic Differential Equation Simulatior with a variability on the NLRP node of 30%.

5.9 Discussion and Conclusions

As comprehensive transcriptomic and proteomics time-course datasets are becoming increasingly available at lower cost, computational immunology has the potential to convert big data into mathematical problems by constructing predictive models, running hypothesis-generating computational simulations followed by targeted experimental validation. Mathematical modeling of immune responses offers efficient and cost-effective approaches to gain a deeper mechanistic systems-level understanding Th17 differentiation and plasticity, but also on how a Th17 cell can be pharmacologically manipulated to treat diseases. In this study, we presented a computational pipeline that

combines data-driven and theoretical approaches to study a use case on mechanisms of Th17 cell differentiation. Indeed, this paper explores a new potential use of microarray and RNA-seq data to produce predictive dynamic models. In this study, we have identified two genes that are intimately related to Th17 function and induction: IL-24 and NLRP3. Furthermore, the sensitivity analysis confirms the role of SGK1 in modulating Th17 responses via IL-23R [362]. We demonstrated how the computational ablation of both of these genes resulted in a down-regulation of IL-17A production. By using stochastic modeling systems, we also found that intrinsic noise in the NLRP3 gene dramatically affected the expression of IL-17A. Furthermore, we identified a molecular mechanism by which IL-24 exerts its pro-inflammatory effects. By performing sensitivity analysis we found a negative correlation of IL-24 with FOXP3. In the IL-24 null system, we detected that the ablation of IL-24 and the upregulation of FOXP3 *a posteriori*, triggers an unbalanced equilibrium between FOXP3 and RORγt, since both act in an antagonistic manner. More specifically, the subtle FOXP3 upregulation caused by IL-24 led to a downregulation of RORγt. Ultimately, IL-24 ablation down-regulates IL-17A via an upregulation of FOXP3 in meridian time-sections of Th17 induction. Obviously, any prediction generated by the Th17 differentiation model will need to be validated with specific *in vitro* and *in vivo* experiments. The proposed computational modeling pipeline can generate meaningful and counterintuitive predictions by taking advantage of publicly available datasets and apply a computational modeling framework based on network inference and data-mining to create a fully calibrated computational model, in this case, of Th17 differentiation. Altogether, this work serves as a template on how to build a computational models that combine data and theory with deterministic and stochastic features to generate new mechanistic knowledge related to immunological mechanisms and to identify novel therapeutic targets for infectious and immune-mediated diseases.

5.10 Materials and Methods

Algorithms for data treatment

In order to adjust and tailor the input data into Ingenuity Pathways Analysis (IPA) platform we created a python3-based script that trimmed and averaged gene reads. To

run, the script needs a file with a list of genes that the user wants to trim. The script runs as follows: first, the script opens all files and deletes any white spaces at the end of the line. The script then reads and stores the name of the first gene in the list and scans the input microarray dataset. Once found, it transfers the information in another file. If different entries are found, the script averages them and only annotates the averaged value. The script completes once all the genes in the list have been assessed and it creates an output file that will be used as input for IPA.

IPA Analysis

Ingenuity Pathways Analysis (IPA) (Ingenuity Systems, Redwood City, CA, USA) was used for the identification of key nodes in Th17 cells for network inference purposes. The microarray data was uploaded as log2 changes and a Core Analysis was run to map expression data to IPA's Knowledge database. Upstream Activation analysis was performed and selected genes were moved to Pathway Analysis to create the topology interaction network. To specifically characterize the interactions, the IPA's Knowledge database of each interaction was consulted to discern between activation and inhibition reactions.

Model parameter estimation

The parameter estimation task was run in COPASI using the time-course experimental microarray data provided in [67]. Data was uploaded into COPASI using IL-6 and TGFβ as independent initial concentrations. The rest of the nodes were set up as dependent nodes on transient concentration for mapping purposes. The Particle Algorithm with 2000 iterations was used first. Secondly, using Particle Swarm algorithm results as initial values, the Genetic Algorithm was run. Quality control was check on the results of parameter estimation by contra-posing the fitted curves to the experimental data (Figures 5.3 and 5.4).

Sensitivity Analysis

Sensitivity analysis was run with COPASI on our computational model using a delta factor of 0.0001 and a delta minimum of 1e-12. The subtask run for the analysis was a time-series with t=100h and correlation of all the variables of the model against activated

GSK1, NLRP3, and IL-24 were assessed, showing high correlation with key transcription factors that determine phenotype differentiation on Th17.

Creation of an IL-24 and NLRP3 knock-out systems

In order to assess the modulation of NLRP3 and IL-24 over Th17 we created an IL-24 and a NLRP3 knock-out models. In order to do so, we selectively chose the mass action-based reactions that upregulate both nodes and set up their parameters to zero. Therefore, none of these two nodes were able to upregulate its product concentration. Quality control by time-course and scans were run to ensure complete ablation of either NLRP3 concentration in the NLRP3 null model, or IL-24 concentration in the IL-24 null model.

Chapter 6

Concluding Remarks

Immunity is a complex compartment of human function and development. Hundreds of different cell types and an enormous number of different subpopulations regulate the human immune system. In this regard, CD4+ T cells accomplish a key and vital function in immunity: orchestrate not only the adaptive immune response, but also provide effective guidance to innate immune cell subsets. As we have seen in this dissertation, CD4+ T cells differentiate into different subpopulations that are plastic between them at the same time. The process of CD4+ T cell differentiation is a complicated, interconnected, multiplayer, intricate system. The cytokines and transcription factors regulating this network are definitely under scrutiny since, as the field advances, more and more subpopulations are arising.

Given this complexity, computational immunology and mathematical modeling approaches open a great avenue to efficiently answer several questions and understand the system as a whole. Here I present several approaches that have elucidated some of these processes. Chapter 1 describes step-by-step how a comprehensive network of CD4+ T cell differentiation can be built. We published for the first time an ODE-based, systems level, comprehensive CD4+ T cell differentiation network that computed four different phenotypes (Th1, Th2, Th17, and iTreg) based on the cytokine environment concentration. On this regard, parameter estimation approaches were broken down into

different pieces using a divide-and-conquer approach. Using this strategy, we were able to calibrate the CD4+ T cell differentiation model and effectively predict that PPARγ modulates Th17 to Treg plasticity. Validation studies confirmed these novel predictions, adding an extra layer of great value to the mathematical model.

CD4+ T cells are also involved in the cellular scale, where they orchestrate other immune cel subsets. In the context of *H. pylori* infection, we also wanted to observe and evaluate the different contributions of specific subsets. For this purpose, we built a ODE-based, tissue-level model where CD4+ T cells were part of it. After calibration, our data demonstrated that upon infection, Th1 cells predominate over the rest of phenotypes, followed by an iTreg upregulation and a shy increase of Th17 cells over time. Having a tissue-cellular level model also allowed us to use other platforms, such as ENISI. Agent-based simulations confirmed our ODE-based results and allowed us to dig deeper on the role of these CD4+ T cells. We observed by running sensitivity analysis that the production of pro-inflammatory epithelial cell and therefore, the increase in epithelial erosion in the gastric epithelium is caused by *H. pylori* at early stages of infection. However, at meridian and chronic stages of infection, these histopathological features are not being caused by the bacterium anymore, but by the effector immune response triggered by the early infection. Clinically, these results are extremely relevant as chronic patients infected with *H. pylori* are given antibiotic treatment that targets the bacterium, and not the immune response. Our data is highlighting the need of more host-centered, immune-targeted approaches to treat the inflammatory cascade caused by the infection. In this regard, we used the CD4+ T cell differentiation model to target IL-21. Our combined in silico and in vivo results demonstrated that IL-21 could be a potential target to treat *H. pylori* infection. *In vivo* results are in line with in silico predictions, which demonstrate how a lack of IL-21 (or a block in the IL-21 cascade for clinical purposes) can actually prevent the upregulation of the effector immune response.

In this thesis dissertation I also present data-driven strategies to create computational models. One of the main challenges in building robust, comprehensive networks is the amount of data the user needs to calibrate such models. Based on the increasingly availability of sequencing datasets, together with the increased technology advancement to analyze these pieces of data, we developed a novel pipeline which allows a modeler

to extract public available data and turn it into a computational model as shown in Chapter 5. These more advanced strategies could potentially solve on the of biggest problems in mathematical modeling: the calibration step. At the same time, data-driven models, when backed up with theory, have a very high predictability. This power is demonstrated by the detection of nodes such as IL-24 and NLRP3 in the Th17 compartment. These nodes have not been described before.

There are current limitations on computational immunology at the moment. Here I present several strategies to model CD4+ T cell differentiation and function. However, there is room for improvement to link the intracellular compartment with cell-to-cell interactions. This is a research problem itself. Multiscale modeling is actually arising as a key tool to be able to connect these complicated networks. If this was the case, the research questions that one can ask to the model can be more inclusive. For example, one could think that a CD4+ T cell differentiates into Treg with only TGFβ. However, what would happen if a dendritic cell, next to the CD4+ T cell, is secreting IL-6? Much probably, if the environment is rich in not only TGFβ, but also IL-6, this cell would not become a Th17 cell, which has an opposite function to the TGFβ-only differentiated Treg. This problem, as one can see, includes different timescales and spatial compartments. As discussed in Chapter 5, multiscale modeling approaches are now being under investigation and the modeling field will probably advance on that direction.
To finally conclude, CD4+ T cells and its different phenotypes still have a lot to be known. Recent technologies such as single-cell sequencing, will allow to shed some light to the understanding of this interesting subset. In this thesis dissertation, I have shown how we can approach this problem through a combined mathematical, computational, and experimental approach to generate and validate very novel predictions on CD4+ T cell differentiation and function. The modeling approaches presented allowed us to narrow the design of experiments and to better understand the molecular mechanisms of action controlling CD4+ differentiation. These strategies for knowledge generation and discovery open a clinical angle for drug development and discovery. Indeed, this new mechanistic knowledge is broadly applicable to the contribution of the understanding of CD4+ T cell differentiation and heterogeneity, also yet to the development of immune therapeutics for infectious, allergic and immune-mediated diseases.

Bibliography and References

1. Luckheeram RV, Zhou R, Verma AD, Xia B: **CD4(+)T cells: differentiation and functions**. *Clinical & developmental immunology* 2012, **2012**:925135.
2. Klein L, Hinterberger M, Wirnsberger G, Kyewski B: **Antigen presentation in the thymus for positive selection and central tolerance induction**. *Nature reviews Immunology* 2009, **9**(12):833-844.
3. Drayton DL, Liao S, Mounzer RH, Ruddle NH: **Lymphoid organ development: from ontogeny to neogenesis**. *Nature immunology* 2006, **7**(4):344-353.
4. Mosmann TR, Coffman RL: **TH1 and TH2 cells: different patterns of lymphokine secretion lead to different functional properties**. *Annual review of immunology* 1989, **7**:145-173.
5. Ivanov, II, McKenzie BS, Zhou L, Tadokoro CE, Lepelley A, Lafaille JJ, Cua DJ, Littman DR: **The orphan nuclear receptor RORgammat directs the differentiation program of proinflammatory IL-17+ T helper cells**. *Cell* 2006, **126**(6):1121-1133.
6. Hori S, Nomura T, Sakaguchi S: **Control of regulatory T cell development by the transcription factor Foxp3**. *Science* 2003, **299**(5609):1057-1061.
7. Fontenot JD, Gavin MA, Rudensky AY: **Foxp3 programs the development and function of CD4+CD25+ regulatory T cells**. *Nature immunology* 2003, **4**(4):330-336.
8. Ma CS, Tangye SG, Deenick EK: **Human Th9 cells: inflammatory cytokines modulate IL-9 production through the induction of IL-21**. *Immunology and cell biology* 2010, **88**(6):621-623.
9. Trifari S, Spits H: **IL-22-producing CD4+ T cells: middle-men between the immune system and its environment**. *European journal of immunology* 2010, **40**(9):2369-2371.
10. Sonnenberg GF, Fouser LA, Artis D: **Border patrol: regulation of immunity, inflammation and tissue homeostasis at barrier surfaces by IL-22**. *Nature immunology* 2011, **12**(5):383-390.
11. Ramirez JM, Brembilla NC, Sorg O, Chicheportiche R, Matthes T, Dayer JM, Saurat JH, Roosnek E, Chizzolini C: **Activation of the aryl hydrocarbon receptor reveals distinct requirements for IL-22 and IL-17 production by human T helper cells**. *European journal of immunology* 2010, **40**(9):2450-2459.

12. Pot C, Apetoh L, Kuchroo VK: **Type 1 regulatory T cells (Tr1) in autoimmunity**. *Seminars in immunology* 2011, **23**(3):202-208.
13. Ansel KM, McHeyzer-Williams LJ, Ngo VN, McHeyzer-Williams MG, Cyster JG: **In vivo-activated CD4 T cells upregulate CXC chemokine receptor 5 and reprogram their response to lymphoid chemokines**. *The Journal of experimental medicine* 1999, **190**(8):1123-1134.
14. Hardtke S, Ohl L, Forster R: **Balanced expression of CXCR5 and CCR7 on follicular T helper cells determines their transient positioning to lymph node follicles and is essential for efficient B-cell help**. *Blood* 2005, **106**(6):1924-1931.
15. Breitfeld D, Ohl L, Kremmer E, Ellwart J, Sallusto F, Lipp M, Forster R: **Follicular B helper T cells express CXC chemokine receptor 5, localize to B cell follicles, and support immunoglobulin production**. *The Journal of experimental medicine* 2000, **192**(11):1545-1552.
16. Fishman MA, Perelson AS: **Th1/Th2 differentiation and cross-regulation**. *Bulletin of mathematical biology* 1999, **61**(3):403-436.
17. Yates A, Bergmann C, Van Hemmen JL, Stark J, Callard R: **Cytokine-modulated regulation of helper T cell populations**. *Journal of theoretical biology* 2000, **206**(4):539-560.
18. Bergmann C, Van Hemmen JL, Segel LA: **Th1 or Th2: how an appropriate T helper response can be made**. *Bulletin of mathematical biology* 2001, **63**(3):405-430.
19. Bergmann C, van Hemmen JL, Segel LA: **How instruction and feedback can select the appropriate T helper response**. *Bulletin of mathematical biology* 2002, **64**(3):425-446.
20. Yates A, Callard R, Stark J: **Combining cytokine signalling with T-bet and GATA-3 regulation in Th1 and Th2 differentiation: a model for cellular decision-making**. *Journal of theoretical biology* 2004, **231**(2):181-196.
21. Mariani L, Lohning M, Radbruch A, Hofer T: **Transcriptional control networks of cell differentiation: insights from helper T lymphocytes**. *Progress in biophysics and molecular biology* 2004, **86**(1):45-76.
22. Eftimie R, Bramson JL, Earn DJ: **Modeling anti-tumor Th1 and Th2 immunity in the rejection of melanoma**. *Journal of theoretical biology* 2010, **265**(3):467-480.
23. Schulz EG, Mariani L, Radbruch A, Hofer T: **Sequential polarization and imprinting of type 1 T helper lymphocytes by interferon-gamma and interleukin-12**. *Immunity* 2009, **30**(5):673-683.
24. Hofer T, Nathansen H, Lohning M, Radbruch A, Heinrich R: **GATA-3 transcriptional imprinting in Th2 lymphocytes: a mathematical model**. *Proceedings of the National Academy of Sciences of the United States of America* 2002, **99**(14):9364-9368.
25. van den Ham HJ, de Boer RJ: **From the two-dimensional Th1 and Th2 phenotypes to high-dimensional models for gene regulation**. *International immunology* 2008, **20**(10):1269-1277.
26. Bettelli E, Carrier Y, Gao W, Korn T, Strom TB, Oukka M, Weiner HL, Kuchroo VK: **Reciprocal developmental pathways for the generation of pathogenic effector TH17 and regulatory T cells**. *Nature* 2006, **441**(7090):235-238.

27. Hong T, Xing J, Li L, Tyson JJ: **A mathematical model for the reciprocal differentiation of T helper 17 cells and induced regulatory T cells**. *PLoS computational biology* 2011, **7**(7):e1002122.
28. Carbo A, Hontecillas R, Kronsteiner B, Viladomiu M, Pedragosa M, Lu P, Philipson CW, Hoops S, Marathe M, Eubank S *et al*: **Systems modeling of molecular mechanisms controlling cytokine-driven CD4+ T cell differentiation and phenotype plasticity**. *PLoS computational biology* 2013, **9**(4):e1003027.
29. Hoops S, Sahle S, Gauges R, Lee C, Pahle J, Simus N, Singhal M, Xu L, Mendes P, Kummer U: **COPASI--a COmplex PAthway SImulator**. *Bioinformatics* 2006, **22**(24):3067-3074.
30. Hucka M, Finney A, Sauro HM, Bolouri H, Doyle JC, Kitano H, Arkin AP, Bornstein BJ, Bray D, Cornish-Bowden A *et al*: **The systems biology markup language (SBML): a medium for representation and exchange of biochemical network models**. *Bioinformatics* 2003, **19**(4):524-531.
31. Mendoza L, Pardo F: **A robust model to describe the differentiation of T-helper cells**. *Theory in biosciences = Theorie in den Biowissenschaften* 2010, **129**(4):283-293.
32. Carbo A, Bassaganya-Riera J, Pedragosa M, Viladomiu M, Marathe M, Eubank S, Wendelsdorf K, Bisset K, Hoops S, Deng X *et al*: **Predictive computational modeling of the mucosal immune responses during Helicobacter pylori infection**. *PloS one* 2013, **8**(9):e73365.
33. Mendoza L: **A network model for the control of the differentiation process in Th cells**. *Biosystems* 2006, **84**(2):101-114.
34. Mendoza L: **A virtual culture of CD4+ T lymphocytes**. *Bulletin of mathematical biology* 2013, **75**(6):1012-1029.
35. Mei MH, R.; Zhang, X.; Bisset, K.; Eubank, S.; Hoops, S.; Marathe, M.; Bassaganya-Riera, J.; : **ENISI Visual, an Agent-based Simulator for Modeling Gut Immunity**. *IEEE International Conference on Bioinformatics and Biomedicine (BIBM)* 2012.
36. Wendelsdorf KV, Alam M, Bassaganya-Riera J, Bisset K, Eubank S, Hontecillas R, Hoops S, Marathe M: **ENteric Immunity SImulator: a tool for in silico study of gastroenteric infections**. *IEEE transactions on nanobioscience* 2012, **11**(3):273-288.
37. Abraham C, Cho JH: **Inflammatory bowel disease**. *The New England journal of medicine* 2009, **361**(21):2066-2078.
38. Monsonego A, Nemirovsky A, Harpaz I: **CD4 T cells in immunity and immunotherapy of Alzheimer's disease**. *Immunology* 2013, **139**(4):438-446.
39. Chitnis T: **The role of CD4 T cells in the pathogenesis of multiple sclerosis**. *International review of neurobiology* 2007, **79**:43-72.
40. Islam SA, Luster AD: **T cell homing to epithelial barriers in allergic disease**. *Nature medicine* 2012, **18**(5):705-715.
41. Miskov-Zivanov N, Turner MS, Kane LP, Morel PA, Faeder JR: **The duration of T cell stimulation is a critical determinant of cell fate and plasticity**. *Science signaling* 2013, **6**(300):ra97.
42. Ahern PP, Schiering C, Buonocore S, McGeachy MJ, Cua DJ, Maloy KJ, Powrie F: **Interleukin-23 drives intestinal inflammation through direct activity on T cells**. *Immunity* 2010, **33**(2):279-288.

43. Arababadi MK, Nosratabadi R, Hassanshahi G, Yaghini N, Pooladvand V, Shamsizadeh A, Hakimi H, Derakhshan R: **Nephropathic complication of type-2 diabetes is following pattern of autoimmune diseases?** *Diabetes research and clinical practice* 2010, **87**(1):33-37.
44. Zeng C, Shi X, Zhang B, Liu H, Zhang L, Ding W, Zhao Y: **The imbalance of Th17/Th1/Tregs in patients with type 2 diabetes: relationship with metabolic factors and complications**. *Journal of molecular medicine* 2012, **90**(2):175-186.
45. Jagannathan-Bogdan M, McDonnell ME, Shin H, Rehman Q, Hasturk H, Apovian CM, Nikolajczyk BS: **Elevated proinflammatory cytokine production by a skewed T cell compartment requires monocytes and promotes inflammation in type 2 diabetes**. *Journal of immunology* 2011, **186**(2):1162-1172.
46. Ohshima K, Mogi M, Jing F, Iwanami J, Tsukuda K, Min LJ, Higaki J, Horiuchi M: **Roles of interleukin 17 in angiotensin II type 1 receptor-mediated insulin resistance**. *Hypertension* 2012, **59**(2):493-499.
47. Imanishi M, Okada N, Konishi Y, Morikawa T, Maeda I, Kitabayashi C, Masada M, Shirahashi N, Wilcox CS, Nishiyama A: **Angiotensin II receptor blockade reduces salt sensitivity of blood pressure through restoration of renal nitric oxide synthesis in patients with diabetic nephropathy**. *Journal of the renin-angiotensin-aldosterone system : JRAAS* 2013, **14**(1):67-73.
48. Esplugues E, Huber S, Gagliani N, Hauser AE, Town T, Wan YY, O'Connor W, Jr., Rongvaux A, Van Rooijen N, Haberman AM *et al*: **Control of TH17 cells occurs in the small intestine**. *Nature* 2011, **475**(7357):514-518.
49. Yang XO, Chang SH, Park H, Nurieva R, Shah B, Acero L, Wang YH, Schluns KS, Broaddus RR, Zhu Z *et al*: **Regulation of inflammatory responses by IL-17F**. *The Journal of experimental medicine* 2008, **205**(5):1063-1075.
50. Lee YK, Turner H, Maynard CL, Oliver JR, Chen D, Elson CO, Weaver CT: **Late developmental plasticity in the T helper 17 lineage**. *Immunity* 2009, **30**(1):92-107.
51. Kurschus FC, Croxford AL, Heinen AP, Wortge S, Ielo D, Waisman A: **Genetic proof for the transient nature of the Th17 phenotype**. *European journal of immunology* 2010, **40**(12):3336-3346.
52. Mathur AN, Chang HC, Zisoulis DG, Kapur R, Belladonna ML, Kansas GS, Kaplan MH: **T-bet is a critical determinant in the instability of the IL-17-secreting T-helper phenotype**. *Blood* 2006, **108**(5):1595-1601.
53. Lin S, Yang X, Liang D, Zheng SG: **Treg cells: a potential regulator for IL-22 expression?** *International journal of clinical and experimental pathology* 2014, **7**(2):474-480.
54. El-Behi M, Ciric B, Dai H, Yan Y, Cullimore M, Safavi F, Zhang GX, Dittel BN, Rostami A: **The encephalitogenicity of T(H)17 cells is dependent on IL-1- and IL-23-induced production of the cytokine GM-CSF**. *Nature immunology* 2011, **12**(6):568-575.
55. Codarri L, Gyulveszi G, Tosevski V, Hesske L, Fontana A, Magnenat L, Suter T, Becher B: **RORgammat drives production of the cytokine GM-CSF in helper T cells, which is essential for the effector phase of autoimmune neuroinflammation**. *Nature immunology* 2011, **12**(6):560-567.

56. Oestreich KJ, Mohn SE, Weinmann AS: **Molecular mechanisms that control the expression and activity of Bcl-6 in TH1 cells to regulate flexibility with a TFH-like gene profile**. *Nature immunology* 2012, **13**(4):405-411.
57. Liao W, Lin JX, Wang L, Li P, Leonard WJ: **Modulation of cytokine receptors by IL-2 broadly regulates differentiation into helper T cell lineages**. *Nature immunology* 2011, **12**(6):551-559.
58. Zhou L, Lopes JE, Chong MM, Ivanov, II, Min R, Victora GD, Shen Y, Du J, Rubtsov YP, Rudensky AY *et al*: **TGF-beta-induced Foxp3 inhibits T(H)17 cell differentiation by antagonizing RORgammat function**. *Nature* 2008, **453**(7192):236-240.
59. Lochner M, Peduto L, Cherrier M, Sawa S, Langa F, Varona R, Riethmacher D, Si-Tahar M, Di Santo JP, Eberl G: **In vivo equilibrium of proinflammatory IL-17+ and regulatory IL-10+ Foxp3+ RORgamma t+ T cells**. *J Exp Med* 2008, **205**(6):1381-1393.
60. Osorio F, LeibundGut-Landmann S, Lochner M, Lahl K, Sparwasser T, Eberl G, Reis e Sousa C: **DC activated via dectin-1 convert Treg into IL-17 producers**. *European journal of immunology* 2008, **38**(12):3274-3281.
61. Magombedze G, Eda S, Ganusov VV: **Competition for antigen between Th1 and Th2 responses determines the timing of the immune response switch during Mycobaterium avium subspecies paratuberulosis infection in ruminants**. *PLoS computational biology* 2014, **10**(1):e1003414.
62. Pedicini M, Barrenas F, Clancy T, Castiglione F, Hovig E, Kanduri K, Santoni D, Benson M: **Combining network modeling and gene expression microarray analysis to explore the dynamics of Th1 and Th2 cell regulation**. *PLoS computational biology* 2010, **6**(12):e1001032.
63. Naldi A, Carneiro J, Chaouiya C, Thieffry D: **Diversity and plasticity of Th cell types predicted from regulatory network modelling**. *PLoS computational biology* 2010, **6**(9):e1000912.
64. Bray D: **Reasoning for results**. *Nature* 2001, **412**(6850):863.
65. Lazer D, Kennedy R, King G, Vespignani A: **Big data. The parable of Google Flu: traps in big data analysis**. *Science* 2014, **343**(6176):1203-1205.
66. Klinke DJ, 2nd: **A multi-scale model of dendritic cell education and trafficking in the lung: implications for T cell polarization**. *Annals of biomedical engineering* 2007, **35**(6):937-955.
67. Yosef N, Shalek AK, Gaublomme JT, Jin H, Lee Y, Awasthi A, Wu C, Karwacz K, Xiao S, Jorgolli M *et al*: **Dynamic regulatory network controlling TH17 cell differentiation**. *Nature* 2013, **496**(7446):461-468.
68. Ciofani M, Madar A, Galan C, Sellars M, Mace K, Pauli F, Agarwal A, Huang W, Parkurst CN, Muratet M *et al*: **A validated regulatory network for Th17 cell specification**. *Cell* 2012, **151**(2):289-303.
69. Fujino S, Andoh A, Bamba S, Ogawa A, Hata K, Araki Y, Bamba T, Fujiyama Y: **Increased expression of interleukin 17 in inflammatory bowel disease**. *Gut* 2003, **52**(1):65-70.
70. Zhang Z, Zheng M, Bindas J, Schwarzenberger P, Kolls JK: **Critical role of IL-17 receptor signaling in acute TNBS-induced colitis**. *Inflammatory bowel diseases* 2006, **12**(5):382-388.
71. Ito R, Kita M, Shin-Ya M, Kishida T, Urano A, Takada R, Sakagami J, Imanishi J, Iwakura Y, Okanoue T *et al*: **Involvement of IL-17A in the pathogenesis of**

DSS-induced colitis in mice. *Biochemical and biophysical research communications* 2008, **377**(1):12-16.
72. Ogawa A, Andoh A, Araki Y, Bamba T, Fujiyama Y: **Neutralization of interleukin-17 aggravates dextran sulfate sodium-induced colitis in mice**. *Clinical immunology* 2004, **110**(1):55-62.
73. Guo L, Hu-Li J, Paul WE: **Probabilistic regulation of IL-4 production in Th2 cells: accessibility at the Il4 locus**. *Immunity* 2004, **20**(2):193-203.
74. Riviere I, Sunshine MJ, Littman DR: **Regulation of IL-4 expression by activation of individual alleles**. *Immunity* 1998, **9**(2):217-228.
75. Chen Z, Lin F, Gao Y, Li Z, Zhang J, Xing Y, Deng Z, Yao Z, Tsun A, Li B: **FOXP3 and RORgammat: transcriptional regulation of Treg and Th17**. *International immunopharmacology* 2011, **11**(5):536-542.
76. Gross F, Metzner G, Behn U: **Mathematical modeling of allergy and specific immunotherapy: Th1-Th2-Treg interactions**. *Journal of theoretical biology* 2011, **269**(1):70-78.
77. Mariani L, Schulz EG, Lexberg MH, Helmstetter C, Radbruch A, Lohning M, Hofer T: **Short-term memory in gene induction reveals the regulatory principle behind stochastic IL-4 expression**. *Molecular systems biology* 2010, **6**:359.
78. Santoni D, Pedicini M, Castiglione F: **Implementation of a regulatory gene network to simulate the TH1/2 differentiation in an agent-based model of hypersensitivity reactions**. *Bioinformatics* 2008, **24**(11):1374-1380.
79. Mei Y, Carbo, A., Hontecillas, R., Bassaganya-Riera, J. : **ENISI SDE: A novel web-based stochastic modeling tool for computational biology**. *2013 IEEE International Conference on Bioinformatics and Biomedicine* 2013.
80. Stamatakis M, Zygourakis K: **A mathematical and computational approach for integrating the major sources of cell population heterogeneity**. *Journal of theoretical biology* 2010, **266**(1):41-61.
81. Manninen T, Linne ML, Ruohonen K: **Developing Ito stochastic differential equation models for neuronal signal transduction pathways**. *Computational biology and chemistry* 2006, **30**(4):280-291.
82. Magombedze G, Reddy PB, Eda S, Ganusov VV: **Cellular and population plasticity of helper CD4(+) T cell responses**. *Frontiers in physiology* 2013, **4**:206.
83. Sloot PM, Hoekstra AG: **Multi-scale modelling in computational biomedicine**. *Briefings in bioinformatics* 2010, **11**(1):142-152.
84. Krinner A, Roeder I, Loeffler M, Scholz M: **Merging concepts-coupling an agent-based model of hematopoietic stem cells with an ODE model of granulopoiesis**. *BMC systems biology* 2013, **7**(1):117.
85. Yeghiazarian L, Cumberland WG, Yang OO: **A stochastic multi-scale model of HIV-1 transmission for decision-making: application to a MSM population**. *PloS one* 2013, **8**(11):e70578.
86. Huang Z: **Multi-scale models of T cell activation**. *Massachusetts Institute of Technology* 2010.
87. Dwivedi G, Fitz L, Hegen M, Martin SW, Harrold J, Heatherington A, Li C: **A multiscale model of interleukin-6-mediated immune regulation in Crohn's disease and its application in drug discovery and development**. *CPT: pharmacometrics & systems pharmacology* 2014, **3**:e89.

88. Gerriets VA, Rathmell JC: **Metabolic pathways in T cell fate and function**. *Trends in immunology* 2012, **33**(4):168-173.
89. Maciver NJ, Jacobs SR, Wieman HL, Wofford JA, Coloff JL, Rathmell JC: **Glucose metabolism in lymphocytes is a regulated process with significant effects on immune cell function and survival**. *Journal of leukocyte biology* 2008, **84**(4):949-957.
90. Jacobs SR, Herman CE, Maciver NJ, Wofford JA, Wieman HL, Hammen JJ, Rathmell JC: **Glucose uptake is limiting in T cell activation and requires CD28-mediated Akt-dependent and independent pathways**. *Journal of immunology* 2008, **180**(7):4476-4486.
91. Michalek RD, Gerriets VA, Jacobs SR, Macintyre AN, MacIver NJ, Mason EF, Sullivan SA, Nichols AG, Rathmell JC: **Cutting edge: distinct glycolytic and lipid oxidative metabolic programs are essential for effector and regulatory CD4+ T cell subsets**. *Journal of immunology* 2011, **186**(6):3299-3303.
92. Pearce EL: **Metabolism in T cell activation and differentiation**. *Current opinion in immunology* 2010, **22**(3):314-320.
93. Pua HH, Dzhagalov I, Chuck M, Mizushima N, He YW: **A critical role for the autophagy gene Atg5 in T cell survival and proliferation**. *The Journal of experimental medicine* 2007, **204**(1):25-31.
94. Pua HH, Guo J, Komatsu M, He YW: **Autophagy is essential for mitochondrial clearance in mature T lymphocytes**. *Journal of immunology* 2009, **182**(7):4046-4055.
95. McGeachy MJ, Bak-Jensen KS, Chen Y, Tato CM, Blumenschein W, McClanahan T, Cua DJ: **TGF-beta and IL-6 drive the production of IL-17 and IL-10 by T cells and restrain T(H)-17 cell-mediated pathology**. *Nat Immunol* 2007, **8**(12):1390-1397.
96. Li H, Rostami A: **IL-9: basic biology, signaling pathways in CD4+ T cells and implications for autoimmunity**. *Journal of neuroimmune pharmacology : the official journal of the Society on NeuroImmune Pharmacology* 2010, **5**(2):198-209.
97. Levings MK, Roncarolo MG: **T-regulatory 1 cells: a novel subset of CD4 T cells with immunoregulatory properties**. *The Journal of allergy and clinical immunology* 2000, **106**(1 Pt 2):S109-112.
98. Yang XO, Nurieva R, Martinez GJ, Kang HS, Chung Y, Pappu BP, Shah B, Chang SH, Schluns KS, Watowich SS *et al*: **Molecular antagonism and plasticity of regulatory and inflammatory T cell programs**. *Immunity* 2008, **29**(1):44-56.
99. Hoechst B, Gamrekelashvili J, Manns MP, Greten TF, Korangy F: **Plasticity of human Th17 cells and iTregs is orchestrated by different subsets of myeloid cells**. *Blood* 2011, **117**(24):6532-6541.
100. Zhou L, Chong MM, Littman DR: **Plasticity of CD4+ T cell lineage differentiation**. *Immunity* 2009, **30**(5):646-655.
101. Hegazy AN, Peine M, Helmstetter C, Panse I, Frohlich A, Bergthaler A, Flatz L, Pinschewer DD, Radbruch A, Lohning M: **Interferons direct Th2 cell reprogramming to generate a stable GATA-3(+)T-bet(+) cell subset with combined Th2 and Th1 cell functions**. *Immunity* 2010, **32**(1):116-128.
102. Cao W, Chen Y, Alkan S, Subramaniam A, Long F, Liu H, Diao R, Delohery T, McCormick J, Chen R *et al*: **Human T helper (Th) cell lineage commitment is not directly linked to the secretion of IFN-gamma or IL-4: characterization**

of Th cells isolated by FACS based on IFN-gamma and IL-4 secretion. *Eur J Immunol* 2005, **35**(9):2709-2717.
103. Huang Z, Xin J, Coleman J, Huang H: **IFN-gamma suppresses STAT6 phosphorylation by inhibiting its recruitment to the IL-4 receptor**. *J Immunol* 2005, **174**(3):1332-1337.
104. Nistala K, Adams S, Cambrook H, Ursu S, Olivito B, de Jager W, Evans JG, Cimaz R, Bajaj-Elliott M, Wedderburn LR: **Th17 plasticity in human autoimmune arthritis is driven by the inflammatory environment**. *Proc Natl Acad Sci U S A* 2010, **107**(33):14751-14756.
105. Morrison PJ, Ballantyne SJ, Kullberg MC: **Interleukin-23 and T helper 17-type responses in intestinal inflammation: from cytokines to T-cell plasticity**. *Immunology* 2011, **133**(4):397-408.
106. Lopez P, Gonzalez-Rodriguez I, Gueimonde M, Margolles A, Suarez A: **Immune response to Bifidobacterium bifidum strains support Treg/Th17 plasticity**. *PLoS One* 2011, **6**(9):e24776.
107. Ye J, Su X, Hsueh EC, Zhang Y, Koenig JM, Hoft DF, Peng G: **Human tumor-infiltrating Th17 cells have the capacity to differentiate into IFN-gamma+ and FOXP3+ T cells with potent suppressive function**. *Eur J Immunol* 2011, **41**(4):936-951.
108. Tartar DM, VanMorlan AM, Wan X, Guloglu FB, Jain R, Haymaker CL, Ellis JS, Hoeman CM, Cascio JA, Dhakal M *et al*: **FoxP3+RORgammat+ T helper intermediates display suppressive function against autoimmune diabetes**. *J Immunol* 2010, **184**(7):3377-3385.
109. Koenen HJ, Smeets RL, Vink PM, van Rijssen E, Boots AM, Joosten I: **Human CD25highFoxp3pos regulatory T cells differentiate into IL-17-producing cells**. *Blood* 2008, **112**(6):2340-2352.
110. Manel N, Unutmaz D, Littman DR: **The differentiation of human T(H)-17 cells requires transforming growth factor-beta and induction of the nuclear receptor RORgammat**. *Nat Immunol* 2008, **9**(6):641-649.
111. Solt LA, Kumar N, Nuhant P, Wang Y, Lauer JL, Liu J, Istrate MA, Kamenecka TM, Roush WR, Vidovic D *et al*: **Suppression of TH17 differentiation and autoimmunity by a synthetic ROR ligand**. *Nature* 2011, **472**(7344):491-494.
112. Huh JR, Leung MW, Huang P, Ryan DA, Krout MR, Malapaka RR, Chow J, Manel N, Ciofani M, Kim SV *et al*: **Digoxin and its derivatives suppress TH17 cell differentiation by antagonizing RORgammat activity**. *Nature* 2011, **472**(7344):486-490.
113. Clark RB, Bishop-Bailey D, Estrada-Hernandez T, Hla T, Puddington L, Padula SJ: **The nuclear receptor PPAR gamma and immunoregulation: PPAR gamma mediates inhibition of helper T cell responses**. *J Immunol* 2000, **164**(3):1364-1371.
114. Wohlfert EA, Nichols FC, Nevius E, Clark RB: **Peroxisome proliferator-activated receptor gamma (PPARgamma) and immunoregulation: enhancement of regulatory T cells through PPARgamma-dependent and -independent mechanisms**. *J Immunol* 2007, **178**(7):4129-4135.
115. Lei J, Hasegawa H, Matsumoto T, Yasukawa M: **Peroxisome proliferator-activated receptor alpha and gamma agonists together with TGF-beta convert human CD4+CD25- T cells into functional Foxp3+ regulatory T cells**. *J Immunol* 2010, **185**(12):7186-7198.

116. Hontecillas R, Bassaganya-Riera J: **Peroxisome proliferator-activated receptor gamma is required for regulatory CD4+ T cell-mediated protection against colitis**. *J Immunol* 2007, **178**(5):2940-2949.
117. Klotz L, Burgdorf S, Dani I, Saijo K, Flossdorf J, Hucke S, Alferink J, Novak N, Beyer M, Mayer G *et al*: **The nuclear receptor PPAR gamma selectively inhibits Th17 differentiation in a T cell-intrinsic fashion and suppresses CNS autoimmunity**. *J Exp Med* 2009, **206**(10):2079-2089.
118. Karr JR, Sanghvi JC, Macklin DN, Gutschow MV, Jacobs JM, Bolival B, Jr., Assad-Garcia N, Glass JI, Covert MW: **A whole-cell computational model predicts phenotype from genotype**. *Cell* 2012, **150**(2):389-401.
119. Weiner HL: **Induction and mechanism of action of transforming growth factor-beta-secreting Th3 regulatory cells**. *Immunol Rev* 2001, **182**:207-214.
120. Groux H, O'Garra A, Bigler M, Rouleau M, Antonenko S, de Vries JE, Roncarolo MG: **A CD4+ T-cell subset inhibits antigen-specific T-cell responses and prevents colitis**. *Nature* 1997, **389**(6652):737-742.
121. Veldhoen M, Uyttenhove C, van Snick J, Helmby H, Westendorf A, Buer J, Martin B, Wilhelm C, Stockinger B: **Transforming growth factor-beta 'reprograms' the differentiation of T helper 2 cells and promotes an interleukin 9-producing subset**. *Nat Immunol* 2008, **9**(12):1341-1346.
122. Nurieva RI, Chung Y, Hwang D, Yang XO, Kang HS, Ma L, Wang YH, Watowich SS, Jetten AM, Tian Q *et al*: **Generation of T follicular helper cells is mediated by interleukin-21 but independent of T helper 1, 2, or 17 cell lineages**. *Immunity* 2008, **29**(1):138-149.
123. Vogelzang A, McGuire HM, Yu D, Sprent J, Mackay CR, King C: **A fundamental role for interleukin-21 in the generation of T follicular helper cells**. *Immunity* 2008, **29**(1):127-137.
124. Kohler B: **Mathematically modeling dynamics of T cell responses: predictions concerning the generation of memory cells**. *J Theor Biol* 2007, **245**(4):669-676.
125. Zand MS, Briggs BJ, Bose A, Vo T: **Discrete event modeling of CD4+ memory T cell generation**. *J Immunol* 2004, **173**(6):3763-3772.
126. Garcia-Martinez K, Leon K: **Modeling the role of IL-2 in the interplay between CD4+ helper and regulatory T cells: assessing general dynamical properties**. *J Theor Biol* 2010, **262**(4):720-732.
127. Zhu J, Yamane H, Paul WE: **Differentiation of effector CD4 T cell populations (*)**. *Annu Rev Immunol* 2010, **28**:445-489.
128. Graw F, Weber KS, Allen PM, Perelson AS: **Dynamics of CD4+ T Cell Responses against Listeria monocytogenes**. *J Immunol* 2012.
129. Ying H, Yang L, Qiao G, Li Z, Zhang L, Yin F, Xie D, Zhang J: **Cutting edge: CTLA-4--B7 interaction suppresses Th17 cell differentiation**. *J Immunol* 2010, **185**(3):1375-1378.
130. Boothby M: **The calculus of integrating differentiation: timing control of T-bet**. *Immunity* 2009, **30**(5):666-668.
131. Barbulescu K, Becker C, Schlaak JF, Schmitt E, Meyer zum Buschenfelde KH, Neurath MF: **IL-12 and IL-18 differentially regulate the transcriptional activity of the human IFN-gamma promoter in primary CD4+ T lymphocytes**. *J Immunol* 1998, **160**(8):3642-3647.
132. Horvath CM: **The Jak-STAT Pathway Stimulated by Interferon {gamma}**. *Sci STKE* 2004, **2004**(260):tr8-.

133. Jaruga B, Hong F, Kim W-H, Gao B: **IFN-{gamma}/STAT1 acts as a proinflammatory signal in T cell-mediated hepatitis via induction of multiple chemokines and adhesion molecules: a critical role of IRF-1**. *Am J Physiol Gastrointest Liver Physiol* 2004, **287**(5):G1044-1052.
134. Krause CD, He W, Kotenko S, Pestka S: **Modulation of the activation of Stat1 by the interferon-[gamma] receptor complex**. *Cell Res* 2006, **16**(1):113-123.
135. Afkarian M, Sedy JR, Yang J, Jacobson NG, Cereb N, Yang SY, Murphy TL, Murphy KM: **T-bet is a STAT1-induced regulator of IL-12R expression in naive CD4+ T cells**. *Nature immunology* 2002, **3**(6):549-557.
136. Afkarian M, Sedy JR, Yang J, Jacobson NG, Cereb N, Yang SY, Murphy TL, Murphy KM: **T-bet is a STAT1-induced regulator of IL-12R expression in naive CD4+ T cells**. *Nat Immunol* 2002, **3**(6):549-557.
137. Mullen AC, High FA, Hutchins AS, Lee HW, Villarino AV, Livingston DM, Kung AL, Cereb N, Yao T-P, Yang SY *et al*: **Role of T-bet in Commitment of TH1 Cells Before IL-12-Dependent Selection**. *Science* 2001, **292**(5523):1907-1910.
138. Szabo SJ, Kim ST, Costa GL, Zhang X, Fathman CG, Glimcher LH: **A novel transcription factor, T-bet, directs Th1 lineage commitment**. *Cell* 2000, **100**(6):655-669.
139. Gunther L, Tilo B, Christoph Sr, Claudia Gn, Julia K, Sandra F, Sonja H, Nicole C-P, Susanne JS, Laurie HG *et al*: **Sustained T-bet expression confers polarized human TH2 cells with TH1-like cytokine production and migratory capacities**. *The Journal of allergy and clinical immunology* 2004, **113**(5):987-994.
140. Losman J, Chen XP, Jiang H, Pan PY, Kashiwada M, Giallourakis C, Cowan S, Foltenyi K, Rothman P: **IL-4 signaling is regulated through the recruitment of phosphatases, kinases, and SOCS proteins to the receptor complex**. *Cold Spring Harb Symp Quant Biol* 1999, **64**:405-416.
141. Sato T, Saito R, Jinushi T, Tsuji T, Matsuzaki J, Koda T, Nishimura S, Takeshima H, Nishimura T: **IFN-gamma-induced SOCS-1 regulates STAT6-dependent eotaxin production triggered by IL-4 and TNF-alpha**. *Biochem Biophys Res Commun* 2004, **314**(2):468-475.
142. Cooney RN: **Suppressors of cytokine signaling (SOCS): inhibitors of the JAK/STAT pathway**. *Shock* 2002, **17**(2):83-90.
143. Kimura A, Naka T, Nagata S, Kawase I, Kishimoto T: **SOCS-1 suppresses TNF-{alpha}-induced apoptosis through the regulation of Jak activation**. *Int Immunol* 2004, **16**(7):991-999.
144. Furuta S, Kagami S-i, Tamachi T, Ikeda K, Fujiwara M, Suto A, Hirose K, Watanabe N, Saito Y, Iwamoto I *et al*: **Overlapping and Distinct Roles of STAT4 and T-bet in the Regulation of T Cell Differentiation and Allergic Airway Inflammation**. *J Immunol* 2008, **180**(10):6656-6662.
145. Jacobson N, Szabo S, Weber-Nordt R, Zhong Z, Schreiber R, Darnell J, Jr, Murphy K: **Interleukin 12 signaling in T helper type 1 (Th1) cells involves tyrosine phosphorylation of signal transducer and activator of transcription (Stat)3 and Stat4**. *J Exp Med* 1995, **181**(5):1755-1762.
146. Park W-R, Nakahira M, Sugimoto N, Bian Y, Yashiro-Ohtani Y, Zhou X-Y, Yang Y-F, Hamaoka T, Fujiwara H: **A mechanism underlying STAT4-mediated up-regulation of IFN-{gamma} induction inTCR-triggered T cells**. *Int Immunol* 2004, **16**(2):295-302.

147. Okamura H, Kashiwamura S-i, Tsutsui H, Yoshimoto T, Nakanishi K: **Regulation of interferon-[gamma] production by IL-12 and IL-18**. *Current Opinion in Immunology* 1998, **10**(3):259-264.
148. Nakahira M, Ahn H-J, Park W-R, Gao P, Tomura M, Park C-S, Hamaoka T, Ohta T, Kurimoto M, Fujiwara H: **Synergy of IL-12 and IL-18 for IFN-{gamma} Gene Expression: IL-12-Induced STAT4 Contributes to IFN-{gamma} Promoter Activation by Up-Regulating the Binding Activity of IL-18-Induced Activator Protein 1**. *J Immunol* 2002, **168**(3):1146-1153.
149. Robinson D, Shibuya K, Mui A, Zonin F, Murphy E, Sana T, Hartley SB, Menon S, Kastelein R, Bazan F *et al*: **IGIF Does Not Drive Th1 Development but Synergizes with IL-12 for Interferon-[gamma] Production and Activates IRAK and NF[kappa]B**. *Immunity* 1997, **7**(4):571-581.
150. Matsumoto S, Tsuji-Takayama K, Aizawa Y, Koide K, Takeuchi M, Ohta T, Kurimoto M: **Interleukin-18 Activates NF-[kappa]B in Murine T Helper Type 1 Cells**. *Biochemical and Biophysical Research Communications* 1997, **234**(2):454-457.
151. Akira S: **The role of IL-18 in innate immunity**. *Current Opinion in Immunology* 2000, **12**(1):59-63.
152. Yoshimoto T, Takeda K, Tanaka T, Ohkusu K, Kashiwamura S-i, Okamura H, Akira S, Nakanishi K: **IL-12 Up-Regulates IL-18 Receptor Expression on T Cells, Th1 Cells, and B Cells: Synergism with IL-18 for IFN-{gamma} Production**. *J Immunol* 1998, **161**(7):3400-3407.
153. Tamachi T, Takatori H, Fujiwara M, Hirose K, Maezawa Y, Kagami S-i, Suto A, Watanabe N, Iwamoto I, Nakajima H: **STAT6 inhibits T-bet-independent Th1 cell differentiation**. *Biochemical and Biophysical Research Communications* 2009, **382**(4):751-755.
154. Smeltz RB, Chen J, Hu-Li J, Shevach EM: **Regulation of Interleukin (IL)-18 Receptor {alpha} Chain Expression on CD4+ T Cells during T Helper (Th)1/Th2 Differentiation: Critical Downregulatory Role of IL-4**. *J Exp Med* 2001, **194**(2):143-154.
155. Yang XO, Panopoulos AD, Nurieva R, Chang SH, Wang D, Watowich SS, Dong C: **STAT3 Regulates Cytokine-mediated Generation of Inflammatory Helper T Cells**. *J Biol Chem* 2007, **282**(13):9358-9363.
156. Bettelli E, Dastrange M, Oukka M: **Foxp3 interacts with nuclear factor of activated T cells and NF-Î°B to repress cytokine gene expression and effector functions of T helper cells**. *Proceedings of the National Academy of Sciences of the United States of America* 2005, **102**(14):5138-5143.
157. Cunard R, Eto Y, Muljadi JT, Glass CK, Kelly CJ, Ricote M: **Repression of IFN-{gamma} Expression by Peroxisome Proliferator-Activated Receptor {gamma}**. *J Immunol* 2004, **172**(12):7530-7536.
158. Wang LH, Yang XY, Zhang X, Huang J, Hou J, Li J, Xiong H, Mihalic K, Zhu H, Xiao W *et al*: **Transcriptional Inactivation of STAT3 by PPAR³ Suppresses IL-6-Responsive Multiple Myeloma Cells**. 2004, **20**(2):205-218.
159. Ricote M, Li AC, Willson TM, Kelly CJ, Glass CK: **The peroxisome proliferator-activated receptor-gamma is a negative regulator of macrophage activation**. *Nature* 1998, **391**(6662):79-82.
160. Kelly D, Campbell JI, King TP, Grant G, Jansson EA, Coutts AG, Pettersson S, Conway S: **Commensal anaerobic gut bacteria attenuate inflammation by**

regulating nuclear-cytoplasmic shuttling of PPAR-gamma and RelA. *Nat Immunol* 2004, **5**(1):104-112.
161. Zhu J, Yamane H, Cote-Sierra J, Guo L, Paul WE: **GATA-3 promotes Th2 responses through three different mechanisms: induction of Th2 cytokine production, selective growth of Th2 cells and inhibition of Th1 cell-specific factors**. *Cell Res* 2006, **16**(1):3-10.
162. Chen Z, Lund R, Aittokallio T, Kosonen M, Nevalainen O, Lahesmaa R: **Identification of Novel IL-4/Stat6-Regulated Genes in T Lymphocytes**. *J Immunol* 2003, **171**(7):3627-3635.
163. Ouyang W, Löhning M, Gao Z, Assenmacher M, Ranganath S, Radbruch A, Murphy KM: **Stat6-Independent GATA-3 Autoactivation Directs IL-4-Independent Th2 Development and Commitment**. 2000, **12**(1):27-37.
164. Cote-Sierra J, Foucras G, Guo L, Chiodetti L, Young HA, Hu-Li J, Zhu J, Paul WE: **Interleukin 2 plays a central role in Th2 differentiation**. *Proceedings of the National Academy of Sciences of the United States of America* 2004, **101**(11):3880-3885.
165. Zhu J, Cote-Sierra J, Guo L, Paul WE: **Stat5 Activation Plays a Critical Role in Th2 Differentiation**. 2003, **19**(5):739-748.
166. Yamane H, Zhu J, Paul WE: **Independent roles for IL-2 and GATA-3 in stimulating naive CD4+ T cells to generate a Th2-inducing cytokine environment**. *J Exp Med* 2005, **202**(6):793-804.
167. Amsen D, Antov A, Jankovic D, Sher A, Radtke F, Souabni A, Busslinger M, McCright B, Gridley T, Flavell RA: **Direct Regulation of Gata3 Expression Determines the T Helper Differentiation Potential of Notch**. 2007, **27**(1):89-99.
168. Fang TC, Yashiro-Ohtani Y, Del Bianco C, Knoblock DM, Blacklow SC, Pear WS: **Notch Directly Regulates Gata3 Expression during T Helper 2 Cell Differentiation**. *Immunity* 2007, **27**(1):100-110.
169. Cunard R, Ricote M, DiCampli D, Archer DC, Kahn DA, Glass CK, Kelly CJ: **Regulation of Cytokine Expression by Ligands of Peroxisome Proliferator Activated Receptors**. *J Immunol* 2002, **168**(6):2795-2802.
170. Yang L, Anderson DE, Baecher-Allan C, Hastings WD, Bettelli E, Oukka M, Kuchroo VK, Hafler DA: **IL-21 and TGF-[bgr] are required for differentiation of human TH17 cells**. *Nature* 2008, **454**(7202):350-352.
171. Chung SW, Kang BY, Kim TS: **Inhibition of interleukin-4 production in CD4+ T cells by peroxisome proliferator-activated receptor-gamma (PPAR-gamma) ligands: involvement of physical association between PPAR-gamma and the nuclear factor of activated T cells transcription factor**. *Mol Pharmacol* 2003, **64**(5):1169-1179.
172. Yang XY, Wang LH, Mihalic K, Xiao W, Chen T, Li P, Wahl LM, Farrar WL: **Interleukin (IL)-4 indirectly suppresses IL-2 production by human T lymphocytes via peroxisome proliferator-activated receptor gamma activated by macrophage-derived 12/15-lipoxygenase ligands**. *J Biol Chem* 2002, **277**(6):3973-3978.
173. Huang JT, Welch JS, Ricote M, Binder CJ, Willson TM, Kelly C, Witztum JL, Funk CD, Conrad D, Glass CK: **Interleukin-4-dependent production of PPAR-gamma ligands in macrophages by 12/15-lipoxygenase**. *Nature* 1999, **400**(6742):378-382.

174. Yu C-R, Mahdi RM, Ebong S, Vistica BP, Chen J, Guo Y, Gery I, Egwuagu CE: **Cell Proliferation and STAT6 Pathways Are Negatively Regulated in T Cells by STAT1 and Suppressors of Cytokine Signaling**. *J Immunol* 2004, **173**(2):737-746.
175. Hebenstreit D, Luft P, Schmiedlechner A, Duschl A, Horejs-Hoeck J: **SOCS-1 and SOCS-3 inhibit IL-4 and IL-13 induced activation of Eotaxin-3/CCL26 gene expression in HEK293 cells**. *Molecular Immunology* 2005, **42**(3):295-303.
176. Losman JA, Chen XP, Hilton D, Rothman P: **Cutting Edge: SOCS-1 Is a Potent Inhibitor of IL-4 Signal Transduction**. *J Immunol* 1999, **162**(7):3770-3774.
177. Venkataraman C, Leung S, Salvekar A, Mano H, Schindler U: **Repression of IL-4-Induced Gene Expression by IFN-{gamma} Requires Stat1 Activation**. *J Immunol* 1999, **162**(7):4053-4061.
178. Huang Z, Xin J, Coleman J, Huang H: **IFN-{gamma} Suppresses STAT6 Phosphorylation by Inhibiting Its Recruitment to the IL-4 Receptor**. *J Immunol* 2005, **174**(3):1332-1337.
179. Gorelik L, Fields PE, Flavell RA: **Cutting Edge: TGF-{beta} Inhibits Th Type 2 Development Through Inhibition of GATA-3 Expression**. *J Immunol* 2000, **165**(9):4773-4777.
180. Torgerson TR, Genin A, Chen C, Zhang M, Zhou B, Anover-Sombke S, Frank MB, Dozmorov I, Ocheltree E, Kulmala P *et al*: **FOXP3 Inhibits Activation-Induced NFAT2 Expression in T Cells Thereby Limiting Effector Cytokine Expression**. *J Immunol* 2009, **183**(2):907-915.
181. Bettelli E, Korn T, Kuchroo VK: **Th17: the third member of the effector T cell trilogy**. *Current Opinion in Immunology* 2007, **19**(6):652-657.
182. Zhou L, Lopes JE, Chong MMW, Ivanov II, Min R, Victora GD, Shen Y, Du J, Rubtsov YP, Rudensky AY *et al*: **TGF-[bgr]-induced Foxp3 inhibits TH17 cell differentiation by antagonizing ROR[ggr]t function**. *Nature* 2008, **453**(7192):236-240.
183. Bettelli E, Carrier Y, Gao W, Korn T, Strom TB, Oukka M, Weiner HL, Kuchroo VK: **Reciprocal developmental pathways for the generation of pathogenic effector TH17 and regulatory T cells**. *Nature* 2006, **441**(7090):235-238.
184. Korn T, Bettelli E, Gao W, Awasthi A, Jager A, Strom TB, Oukka M, Kuchroo VK: **IL-21 initiates an alternative pathway to induce proinflammatory TH17 cells**. *Nature* 2007, **448**(7152):484-487.
185. Zhou L, Ivanov II, Spolski R, Min R, Shenderov K, Egawa T, Levy DE, Leonard WJ, Littman DR: **IL-6 Programs TH-17 Cell Differentiation by Promoting the Sequential Engagement of the IL-21 and IL-23 Pathways**. *Cytokine* 2007, **39**(1):49-49.
186. Foley JF: **STAT3 Regulates the Generation of Th17 Cells**. *Sci STKE* 2007, **2007**(380):tw113-.
187. Harris TJ, Grosso JF, Yen H-R, Xin H, Kortylewski M, Albesiano E, Hipkiss EL, Getnet D, Goldberg MV, Maris CH *et al*: **Cutting Edge: An In Vivo Requirement for STAT3 Signaling in TH17 Development and TH17-Dependent Autoimmunity**. *J Immunol* 2007, **179**(7):4313-4317.
188. Mathur AN, Chang H-C, Zisoulis DG, Stritesky GL, Yu Q, O'Malley JT, Kapur R, Levy DE, Kansas GS, Kaplan MH: **Stat3 and Stat4 Direct Development of IL-17-Secreting Th Cells**. *J Immunol* 2007, **178**(8):4901-4907.

189. Ivanov II, McKenzie BS, Zhou L, Tadokoro CE, Lepelley A, Lafaille JJ, Cua DJ, Littman DR: **The Orphan Nuclear Receptor RORγt Directs the Differentiation Program of Proinflammatory IL-17+ T Helper Cells**. 2006, **126**(6):1121-1133.
190. McGeachy MJ, Chen Y, Tato CM, Laurence A, Joyce-Shaikh B, Blumenschein WM, McClanahan TK, O'Shea JJ, Cua DJ: **The interleukin 23 receptor is essential for the terminal differentiation of interleukin 17-producing effector T helper cells in vivo**. *Nat Immunol* 2009, **10**(3):314-324.
191. Korn T, Bettelli E, Oukka M, Kuchroo VK: **IL-17 and Th17 Cells**. *Annual Review of Immunology* 2009, **27**(1):485-517.
192. Laurence A, O'Shea JJ: **TH-17 differentiation: of mice and men**. *Nat Immunol* 2007, **8**(9):903-905.
193. Volpe E, Servant N, Zollinger R, Bogiatzi SI, Hupe P, Barillot E, Soumelis V: **A critical function for transforming growth factor-[beta], interleukin 23 and proinflammatory cytokines in driving and modulating human TH-17 responses**. *Nat Immunol* 2008, **9**(6):650-657.
194. Awasthi A, Murugaiyan G, Kuchroo V: **Interplay Between Effector Th17 and Regulatory T Cells**. *Journal of Clinical Immunology* 2008, **28**(6):660-670.
195. Gocke AR, Cravens PD, Ben LH, Hussain RZ, Northrop SC, Racke MK, Lovett-Racke AE: **T-bet regulates the fate of Th1 and Th17 lymphocytes in autoimmunity**. *J Immunol* 2007, **178**(3):1341-1348.
196. van Hamburg JP, de Bruijn MJ, Ribeiro de Almeida C, van Zwam M, van Meurs M, de Haas E, Boon L, Samsom JN, Hendriks RW: **Enforced expression of GATA3 allows differentiation of IL-17-producing cells, but constrains Th17-mediated pathology**. *Eur J Immunol* 2008, **38**(9):2573-2586.
197. Ichiyama K, Yoshida H, Wakabayashi Y, Chinen T, Saeki K, Nakaya M, Takaesu G, Hori S, Yoshimura A, Kobayashi T: **Foxp3 Inhibits ROR{gamma}t-mediated IL-17A mRNA Transcription through Direct Interaction with ROR{gamma}t**. *J Biol Chem* 2008, **283**(25):17003-17008.
198. Passerini L, Allan SE, Battaglia M, Di Nunzio S, Alstad AN, Levings MK, Roncarolo MG, Bacchetta R: **STAT5-signaling cytokines regulate the expression of FOXP3 in CD4+CD25+ regulatory T cells and CD4+CD25- effector T cells**. *Int Immunol* 2008, **20**(3):421-431.
199. Wei L, Laurence A, Elias KM, O'Shea JJ: **IL-21 is produced by Th17 cells and drives IL-17 production in a STAT3-dependent manner**. *J Biol Chem* 2007, **282**(48):34605-34610.
200. Laurence A, Tato CM, Davidson TS, Kanno Y, Chen Z, Yao Z, Blank RB, Meylan F, Siegel R, Hennighausen L *et al*: **Interleukin-2 signaling via STAT5 constrains T helper 17 cell generation**. *Immunity* 2007, **26**(3):371-381.
201. Chen Y, Haines CJ, Gutcher I, Hochweller K, Blumenschein WM, McClanahan T, Hammerling G, Li MO, Cua DJ, McGeachy MJ: **Foxp3(+) regulatory T cells promote T helper 17 cell development in vivo through regulation of interleukin-2**. *Immunity* 2011, **34**(3):409-421.
202. Kimura A, Naka T, Nohara K, Fujii-Kuriyama Y, Kishimoto T: **Aryl hydrocarbon receptor regulates Stat1 activation and participates in the development of Th17 cells**. *Proceedings of the National Academy of Sciences* 2008, **105**(28):9721-9726.
203. Li B, Reynolds JM, Stout RD, Bernlohr DA, Suttles J: **Regulation of Th17 Differentiation by Epidermal Fatty Acid-Binding Protein**. *J Immunol* 2009, **182**(12):7625-7633.

204. Klotz L, Burgdorf S, Dani I, Saijo K, Flossdorf J, Hucke S, Alferink J, Nowak N, Beyer M, Mayer G *et al*: **The nuclear receptor PPAR gamma selectively inhibits Th17 differentiation in a T cell-intrinsic fashion and suppresses CNS autoimmunity**. *The Journal of experimental medicine* 2009, **206**(10):2079-2089.
205. Pyzik M, Piccirillo CA: **TGF-beta1 modulates Foxp3 expression and regulatory activity in distinct CD4+ T cell subsets**. *J Leukoc Biol* 2007, **82**(2):335-346.
206. Chen W, Jin W, Hardegen N, Lei K-j, Li L, Marinos N, McGrady G, Wahl SM: **Conversion of Peripheral CD4+CD25- Naive T Cells to CD4+CD25+ Regulatory T Cells by TGF-{beta} Induction of Transcription Factor Foxp3**. *J Exp Med* 2003, **198**(12):1875-1886.
207. Pyzik M, Piccirillo CA: **TGF-{beta}1 modulates Foxp3 expression and regulatory activity in distinct CD4+ T cell subsets**. *J Leukoc Biol* 2007, **82**(2):335-346.
208. Chen W, Jin W, Hardegen N, Lei KJ, Li L, Marinos N, McGrady G, Wahl SM: **Conversion of peripheral CD4+CD25- naive T cells to CD4+CD25+ regulatory T cells by TGF-beta induction of transcription factor Foxp3**. *J Exp Med* 2003, **198**(12):1875-1886.
209. Murawski MR, Litherland SA, Clare-Salzler MJ, Davoodi-Semiromi A: **Upregulation of Foxp3 expression in mouse and human Treg is IL-2/STAT5 dependent: implications for the NOD STAT5B mutation in diabetes pathogenesis**. *Ann N Y Acad Sci* 2006, **1079**:198-204.
210. Kitani A, Xu L: **Regulatory T cells and the induction of IL-17**. *Mucosal Immunol* 2008, **1 Suppl 1**:S43-46.
211. Nishibori T, Tanabe Y, Su L, David M: **Impaired Development of CD4+ CD25+ Regulatory T Cells in the Absence of STAT1: Increased Susceptibility to Autoimmune Disease**. *J Exp Med* 2004, **199**(1):25-34.
212. Wang Z: **Role of IFN-Î³ in induction of Foxp3 and conversion of CD4+ CD25â€“ T cells to CD4+ Tregs**. *The Journal of Clinical Investigation* 2006, **116**(9):2434-2441.
213. Ouaked N, Mantel P-Y, Bassin C, Burgler S, Siegmund K, Akdis CA, Schmidt-Weber CB: **Regulation of the foxp3 Gene by the Th1 Cytokines: The Role of IL-27-Induced STAT1**. *J Immunol* 2009, **182**(2):1041-1049.
214. Housley WJ, O'Conor CA, Nichols F, Puddington L, Lingenheld EG, Zhu L, Clark RB: **PPAR{gamma} regulates retinoic acid-mediated DC induction of Tregs**. *J Leukoc Biol* 2009:jlb.1208733.
215. Wohlfert EA, Nichols FC, Nevius E, Clark RB: **Peroxisome Proliferator-Activated Receptor {gamma} (PPAR{gamma}) and Immunoregulation: Enhancement of Regulatory T Cells through PPAR{gamma}-Dependent and -Independent Mechanisms**. *J Immunol* 2007, **178**(7):4129-4135.
216. Korn T, Mitsdoerffer M, Croxford AL, Awasthi A, Dardalhon VrA, Galileos G, Vollmar P, Stritesky GL, Kaplan MH, Waisman A *et al*: **IL-6 controls Th17 immunity in vivo by inhibiting the conversion of conventional T cells into Foxp3+ regulatory T cells**. *Proceedings of the National Academy of Sciences* 2008, **105**(47):18460-18465.
217. Mantel P-Y, Kuipers H, Boyman O, Rhyner C, Ouaked N, RÃ¼ckert B, Karagiannidis C, Lambrecht BN, Hendriks RW, Crameri R *et al*: **GATA3-Driven**

Th2 Responses Inhibit TGF-Î²1â€“Induced FOXP3 Expression and the Formation of Regulatory T Cells. *PLoS Biol* 2007, **5**(12):e329.
218. Dardalhon V, Awasthi A, Kwon H, Galileos G, Gao W, Sobel RA, Mitsdoerffer M, Strom TB, Elyaman W, Ho IC *et al*: **IL-4 inhibits TGF-beta-induced Foxp3+ T cells and, together with TGF-beta, generates IL-9+ IL-10+ Foxp3(-) effector T cells**. *Nat Immunol* 2008, **9**(12):1347-1355.
219. Yao Z, Kanno Y, Kerenyi M, Stephens G, Durant L, Watford WT, Laurence A, Robinson GW, Shevach EM, Moriggl R *et al*: **Nonredundant roles for Stat5a/b in directly regulating Foxp3**. *Blood* 2007, **109**(10):4368-4375.
220. Chang JH, Kim YJ, Han SH, Kang CY: **IFN-gamma-STAT1 signal regulates the differentiation of inducible Treg: potential role for ROS-mediated apoptosis**. *Eur J Immunol* 2009, **39**(5):1241-1251.
221. Chang J-H, Kang C-Y: **Autocrine IFN-gamma directly regulates Foxp3 expression in naive CD4+CD25- T cells**. *FASEB J* 2008, **22**(1_MeetingAbstracts):848.816-.
222. Koch MA, Tucker-Heard G, Perdue NR, Killebrew JR, Urdahl KB, Campbell DJ: **The transcription factor T-bet controls regulatory T cell homeostasis and function during type 1 inflammation**. *Nat Immunol* 2009, **10**(6):595-602.
223. Carter AB, Misyak SA, Hontecillas R, Bassaganya-Riera J: **Dietary Modulation of Inflammation-Induced Colorectal Cancer through PPARgamma**. *PPAR Res* 2009, **2009**:498-352.
224. Evans NP, Misyak SA, Schmelz EM, Guri AJ, Hontecillas R, Bassaganya-Riera J: **Conjugated linoleic acid ameliorates inflammation-induced colorectal cancer in mice through PPAR gamma**. *J Nutr* 2010, **In Press**.
225. Guri AJ, Hontecillas R, Bassaganya-Riera J: **Peroxisome proliferator-activated receptors: Bridging metabolic syndrome with molecular nutrition**. *Clin Nutr* 2006, **25**(6):871-885.
226. Guri AJ, Hontecillas R, Ferrer G, Casagran O, Wankhade U, Noble AM, Eizirik DL, Ortis F, Cnop M, Liu D *et al*: **Loss of PPAR gamma in immune cells impairs the ability of abscisic acid to improve insulin sensitivity by suppressing monocyte chemoattractant protein-1 expression and macrophage infiltration into white adipose tissue**. *J Nutr Biochem* 2008, **19**(4):216-228.
227. Guri AJ, Hontecillas R, Si H, Liu D, Bassaganya-Riera J: **Dietary abscisic acid ameliorates glucose tolerance and obesity-related inflammation in db/db mice fed high-fat diets**. *Clin Nutr* 2007, **26**(1):107-116.
228. Guri AJ, Misyak SA, Hontecillas R, Hasty A, Liu D, Si H, Bassaganya-Riera J: **Abscisic acid ameliorates atherosclerosis by suppressing macrophage and CD4+ T cell recruitment into the aortic wall**. *J Nutr Biochem* 2010, **21**(12):1178-1185.
229. Bassaganya-Riera J, Misyak S, Guri AJ, Hontecillas R: **PPAR gamma is highly expressed in F4/80(hi) adipose tissue macrophages and dampens adipose-tissue inflammation**. *Cell Immunol* 2009, **258**(2):138-146.
230. Bassaganya-Riera J, Hontecillas R, Zimmerman DR, Wannemuehler MJ: **Dietary conjugated linoleic acid modulates phenotype and effector functions of porcine cd8(+) lymphocytes**. *J Nutr* 2001, **131**(9):2370-2377.
231. Bassaganya-Riera J, Pogranichniy RM, Jobgen SC, Halbur PG, Yoon KJ, O'Shea M, Mohede I, Hontecillas R: **Conjugated linoleic acid ameliorates viral**

infectivity in a pig model of virally induced immunosuppression. *J Nutr* 2003, **133**(10):3204-3214.
232. Paranavitana C, Pittman PR, Velauthapillai M, Zelazowska E, Dasilva L: **Transcriptional profiling of Francisella tularensis infected peripheral blood mononuclear cells: a predictive tool for tularemia**. *FEMS Immunol Med Microbiol* 2008, **54**(1):92-103.
233. Aldridge JR, Jr., Moseley CE, Boltz DA, Negovetich NJ, Reynolds C, Franks J, Brown SA, Doherty PC, Webster RG, Thomas PG: **TNF/iNOS-producing dendritic cells are the necessary evil of lethal influenza virus infection**. *Proc Natl Acad Sci U S A* 2009, **106**(13):5306-5311.
234. Mohapatra SK, Cole LE, Vogel SN, Evans C, Sobral BW, Bassaganya-Riera J, Hontecillas R, Castra OR: **Murine hepatic gene expression changes during LPS-induced protection of host from infection with Francisella tularensis LVS**. *BMC Infectious Diseases* 2010, **In Press**.
235. Hontecillas R, Wannemeulher MJ, Zimmerman DR, Hutto DL, Wilson JH, Ahn DU, Bassaganya-Riera J: **Nutritional regulation of porcine bacterial-induced colitis by conjugated linoleic acid**. *The Journal of nutrition* 2002, **132**(7):2019-2027.
236. Bassaganya-Riera J, Reynolds K, Martino-Catt S, Cui Y, Hennighausen L, Gonzalez F, Rohrer J, Benninghoff AU, Hontecillas R: **Activation of PPAR gamma and delta by conjugated linoleic acid mediates protection from experimental inflammatory bowel disease**. *Gastroenterology* 2004, **127**(3):777-791.
237. Bassaganya-Riera J, Hontecillas R: **CLA and n-3 PUFA differentially modulate clinical activity and colonic PPAR-responsive gene expression in a pig model of experimental IBD**. *Clin Nutr* 2006, **25**(3):454-465.
238. Wohlfert E, Clark RB: **A novel approach for modulating CD4+CD25+ regulatory T cell generation and function through the nuclear receptor PPAR g**. In: *Immunology 2006: 2006; Boston, MA*. J. Immunol.: S144.
239. Hevener AL, Olefsky JM, Reichart D, Nguyen MT, Bandyopadyhay G, Leung HY, Watt MJ, Benner C, Febbraio MA, Nguyen AK *et al*: **Macrophage PPAR gamma is required for normal skeletal muscle and hepatic insulin sensitivity and full antidiabetic effects of thiazolidinediones**. *J Clin Invest* 2007, **117**(6):1658-1669.
240. Wendelsdorf K, Bassaganya-Riera J, Hontecillas R, Eubank S: **Model of colonic inflammation: immune modulatory mechanisms in inflammatory bowel disease**. *Journal of theoretical biology* 2010, **264**(4):1225-1239.
241. Funahashi A MM, Tanimura N, Kitano H: **CellDesigner: a process diagram editor for gene-regulatory and biochemical networks**. *BioSilico* 2003, **1**:159-162.
242. Kennedy JE, R.: **Particle Swarm Optimization**. *Neural Networks, IEEE International Conference* 1995, **4**:1942-1948.
243. Xu R, Venayagamoorthy GK, Wunsch DC, 2nd: **Modeling of gene regulatory networks with hybrid differential evolution and particle swarm optimization**. *Neural networks : the official journal of the International Neural Network Society* 2007, **20**(8):917-927.
244. Goutelle S, Maurin M, Rougier F, Barbaut X, Bourguignon L, Ducher M, Maire P: **The Hill equation: a review of its capabilities in pharmacological modelling**. *Fundamental & clinical pharmacology* 2008, **22**(6):633-648.

245. Feinerman O, Jentsch G, Tkach KE, Coward JW, Hathorn MM, Sneddon MW, Emonet T, Smith KA, Altan-Bonnet G: **Single-cell quantification of IL-2 response by effector and regulatory T cells reveals critical plasticity in immune response**. *Molecular systems biology* 2010, **6**:437.
246. Klinke DJ, 2nd, Cheng N, Chambers E: **Quantifying crosstalk among interferon-gamma, interleukin-12, and tumor necrosis factor signaling pathways within a TH1 cell model**. *Science signaling* 2012, **5**(220):ra32.
247. Lu L, Ma J, Li Z, Lan Q, Chen M, Liu Y, Xia Z, Wang J, Han Y, Shi W *et al*: **All-trans retinoic acid promotes TGF-beta-induced Tregs via histone modification but not DNA demethylation on Foxp3 gene locus**. *PLoS One* 2011, **6**(9):e24590.
248. Kryczek I, Wu K, Zhao E, Wei S, Vatan L, Szeliga W, Huang E, Greenson J, Chang A, Rolinski J *et al*: **IL-17+ regulatory T cells in the microenvironments of chronic inflammation and cancer**. *J Immunol* 2011, **186**(7):4388-4395.
249. Longhi MS, Liberal R, Holder B, Robson SC, Ma Y, Mieli-Vergani G, Vergani D: **Inhibition of Interleukin-17 Promotes Differentiation of CD25(-) Cells Into Stable T Regulatory Cells in Patients With Autoimmune Hepatitis**. *Gastroenterology* 2012.
250. Hovhannisyan Z, Treatman J, Littman DR, Mayer L: **Characterization of interleukin-17-producing regulatory T cells in inflamed intestinal mucosa from patients with inflammatory bowel diseases**. *Gastroenterology* 2011, **140**(3):957-965.
251. Hoops S, Sahle S, Gauges R, Lee C, Pahle J, Simus N, Singhal M, Xu L, Mendes P, Kummer U: **COPASI- A COmplex PAthway SImulator**. *Bioinformatics* 2006, **22**(24):3067-3074.
252. Heinrich R, Rapoport TA: **A linear steady-state treatment of enzymatic chains. General properties, control and effector strength**. *European journal of biochemistry / FEBS* 1974, **42**(1):89-95.
253. Kacser H, Burns JA: **The control of flux**. *Symposia of the Society for Experimental Biology* 1973, **27**:65-104.
254. Bouguermouh S, Fortin G, Baba N, Rubio M, Sarfati M: **CD28 co-stimulation down regulates Th17 development**. *PloS one* 2009, **4**(3):e5087.
255. Atherton JC, Blaser MJ: **Coadaptation of Helicobacter pylori and humans: ancient history, modern implications**. *The Journal of clinical investigation* 2009, **119**(9):2475-2487.
256. Hitzler I, Kohler E, Engler DB, Yazgan AS, Muller A: **The role of Th cell subsets in the control of Helicobacter infections and in T cell-driven gastric immunopathology**. *Frontiers in immunology* 2012, **3**:142.
257. Karttunen R, Karttunen T, Ekre HP, MacDonald TT: **Interferon gamma and interleukin 4 secreting cells in the gastric antrum in *Helicobacter pylori* positive and negative gastritis**. *Gut* 1995, **36**(3):341-345.
258. Bamford KB, Fan X, Crowe SE, Leary JF, Gourley WK, Luthra GK, Brooks EG, Graham DY, Reyes VE, Ernst PB: **Lymphocytes in the human gastric mucosa during Helicobacter pylori have a T helper cell 1 phenotype**. *Gastroenterology* 1998, **114**(3):482-492.
259. Smythies LE, Waites KB, Lindsey JR, Harris PR, Ghiara P, Smith PD: **Helicobacter pylori-induced mucosal inflammation is Th1 mediated and exacerbated in IL-4, but not IFN-gamma, gene-deficient mice**. *J Immunol* 2000, **165**(2):1022-1029.

260. Philipson CW, Bassaganya-Riera J, Viladomiu M, Pedragosa M, Guerrant RL, Roche JK, Hontecillas R: **The role of peroxisome proliferator-activated receptor gamma in immune responses to enteroaggregative Escherichia coli infection**. *PloS one* 2013, **8**(2):e57812.
261. Liang SC, Tan XY, Luxenberg DP, Karim R, Dunussi-Joannopoulos K, Collins M, Fouser LA: **Interleukin (IL)-22 and IL-17 are coexpressed by Th17 cells and cooperatively enhance expression of antimicrobial peptides**. *The Journal of experimental medicine* 2006, **203**(10):2271-2279.
262. Marson A, Kretschmer K, Frampton GM, Jacobsen ES, Polansky JK, MacIsaac KD, Levine SS, Fraenkel E, von Boehmer H, Young RA: **Foxp3 occupancy and regulation of key target genes during T-cell stimulation**. *Nature* 2007, **445**(7130):931-935.
263. Ando T, Goto Y, Ishiguro K, Maeda O, Watanabe O, Ohmiya N, Niwa Y, Hamajima N, El-Omar E, Goto H: **The interaction of host genetic factors and Helicobacter pylori infection**. *Inflammopharmacology* 2007, **15**(1):10-14.
264. Bassaganya-Riera J, Dominguez-Bello MG, Kronsteiner B, Carbo A, Lu P, Viladomiu M, Pedragosa M, Zhang X, Sobral BW, Mane SP *et al*: **Helicobacter pylori colonization ameliorates glucose homeostasis in mice through a PPAR gamma-dependent mechanism**. *PLoS One* 2012, **In Press**.
265. Bazargani A, Khoramrooz SS, Kamali-Sarvestani E, Taghavi SA, Saberifiroozi M: **Association between peroxisome proliferator-activated receptor-gamma gene polymorphism (Pro12Ala) and Helicobacter pylori infection in gastric carcinogenesis**. *Scand J Gastroenterol* 2010, **45**(10):1162-1167.
266. Yao L, Liu F, Sun L, Wu H, Guo C, Liang S, Liu L, Liu N, Han Z, Zhang H *et al*: **Upregulation of PPARgamma in tissue with gastric carcinoma**. *Hybridoma (Larchmt)* 2010, **29**(4):341-343.
267. Konturek PC, Kania J, Kukharsky V, Raithel M, Ocker M, Rembiasz K, Hahn EG, Konturek SJ: **Implication of peroxisome proliferator-activated receptor gamma and proinflammatory cytokines in gastric carcinogenesis: link to Helicobacter pylori-infection**. *Journal of pharmacological sciences* 2004, **96**(2):134-143.
268. Son SH, Kim HK, Ji JS, Cho YS, Kim SS, Chae HS, Choi MG, Han SW, Choi KY, Chung IS *et al*: **[Expression of peroxisome proliferator-activated receptor (PPAR) gamma in Helicobacter pylori-infected gastric epithelium]**. *The Korean journal of gastroenterology = Taehan Sohwagi Hakhoe chi* 2007, **49**(2):72-78.
269. Viladomiu M, Hontecillas R, Pedragosa M, Carbo A, Hoops S, Michalak P, Michalak K, Guerrant RL, Roche JK, Warren CA *et al*: **Modeling the role of peroxisome proliferator-activated receptor gamma and microRNA-146 in mucosal immune responses to Clostridium difficile**. *PloS one* 2012, **7**(10):e47525.
270. Lundgren A, Trollmo C, Edebo A, Svennerholm AM, Lundin BS: **Helicobacter pylori-specific CD4+ T cells home to and accumulate in the human Helicobacter pylori-infected gastric mucosa**. *Infection and immunity* 2005, **73**(9):5612-5619.
271. Funahashi A, Tanimura, N., Morohashi, M., and Kitano, H: **CellDesigner: a process diagram editor for gene-regulatory and biochemical networks**. *BIOSILICO* 2003, **1**:159-162.

272. Iwasaki A: **Mucosal dendritic cells**. *Annual review of immunology* 2007, **25**:381-418.
273. Ng SC, Kamm MA, Stagg AJ, Knight SC: **Intestinal dendritic cells: their role in bacterial recognition, lymphocyte homing, and intestinal inflammation**. *Inflammatory bowel diseases* 2010, **16**(10):1787-1807.
274. Littman DR, Rudensky AY: **Th17 and regulatory T cells in mediating and restraining inflammation**. *Cell* 2010, **140**(6):845-858.
275. J K: **The particle swarm: social adaptation of knowledge**. *IEEE Congress on Evolutionary Computation* 1997:303-308.
276. Hoops S, Sahle S, Gauges R, Lee C, Pahle J, Simus N, Singhal M, Xu L, Mendes P, Kummer U: **COPASI—a complex pathway simulator**. *Bioinformatics* 2006, **22**(24):3067-3074.
277. Spiegelman BM: **PPARgamma in monocytes: less pain, any gain?** *Cell* 1998, **93**(2):153-155.
278. Mansen A, Guardiola-Diaz H, Rafter J, Branting C, Gustafsson JA: **Expression of the peroxisome proliferator-activated receptor (PPAR) in the mouse colonic mucosa**. *Biochemical and biophysical research communications* 1996, **222**(3):844-851.
279. Adria Carbo RH, Barbara Kronsteiner, Monica Viladomiu, Mireia Pedragosa, Pinyi Lu, Casandra W. Philipson, Stefan Hoops, Madhav Marathe, Stephen Eubank, Keith Bisset, Katherine Wendelsdorf, Abdul Jarrah, Yongguo Mei, Josep Bassaganya-Riera: **Systems modeling of molecular mechanisms controlling cytokine-driven CD4+ T cell differentiation and phenotype plasticity**. *PLoS computational biology* 2013, **In Press**.
280. Wendelsdorf K, Alam M, Bassaganya-Riera J, Bisset K, Eubank S, Hontecillas R, Marathe M: **ENteric Immunity SImulator: A tool for in silico study of gastroenteric infections**. *IEEE Transactions on NanoBioScience* 2012, **11**:273-288.
281. Bisset KR, Alam MM, Bassaganya-Riera J, Carbo A, Eubank S, Hontecillas R, Hoops S, Mei Y, Wendelsdorf KV, Xie D *et al*: **High-Performance Interaction-Based Simulation of Gut Immunopathologies with ENteric Immunity Simulator (ENISI)**. In: *26th IEEE International Parallel and Distributed Processing Symposium, IPDPS 2012: 2012*. IEEE Computer Society: 48-59.
282. Olokoba AB, Obateru OA, Bojuwoye MO: **Helicobacter pylori eradication therapy: A review of current trends**. *Nigerian medical journal : journal of the Nigeria Medical Association* 2013, **54**(1):1-4.
283. Parsonnet J, Hansen S, Rodriguez L, Gelb AB, Warnke RA, Jellum E, Orentreich N, Vogelman JH, Friedman GD: **Helicobacter pylori infection and gastric lymphoma**. *The New England journal of medicine* 1994, **330**(18):1267-1271.
284. Parsonnet J, Isaacson PG: **Bacterial infection and MALT lymphoma**. *The New England journal of medicine* 2004, **350**(3):213-215.
285. Correa P, Houghton J: **Carcinogenesis of Helicobacter pylori**. *Gastroenterology* 2007, **133**(2):659-672.
286. Blaser MJ: **Disappearing microbiota: Helicobacter pylori protection against esophageal adenocarcinoma**. *Cancer Prev Res (Phila Pa)* 2008, **1**(5):308-311.
287. Vieth M, Masoud B, Meining A, Stolte M: ***Helicobacter pylori*** **infection: protection against Barrett's mucosa and neoplasia?** *Digestion* 2000, **62**(4):225-231.

288. Vaezi MF, Falk GW, Peek RM, Vicari JJ, Goldblum JR, Perez-Perez GI, Rice TW, Blaser MJ, Richter JE: **CagA-positive strains of *Helicobacter pylori* may protect against Barrett's esophagus**. *The American journal of gastroenterology* 2000, **95**(9):2206-2211.
289. Chow WH, Blaser MJ, Blot WJ, Gammon MD, Vaughan TL, Risch HA, Perez-Perez GI, Schoenberg JB, Stanford JL, Rotterdam H *et al*: **An inverse relation between cagA+ strains of Helicobacter pylori infection and risk of esophageal and gastric cardia adenocarcinoma**. *Cancer Res* 1998, **58**(4):588-590.
290. Blaser MJ, Chen Y, Reibman J: **Does Helicobacter pylori protect against asthma and allergy?** *Gut* 2008.
291. Chen Y, Blaser MJ: **Inverse associations of Helicobacter pylori with asthma and allergy**. *Arch Intern Med* 2007, **167**(8):821-827.
292. Lang L: **Childhood acquisition of Helicobacter pylori linked to reduced asthma and allergy risk**. *Gastroenterology* 2007, **133**(1):6.
293. McCune A, Lane A, Murray L, Harvey I, Nair P, Donovan J, Harvey R: **Reduced risk of atopic disorders in adults with *Helicobacter pylori* infection**. *European journal of gastroenterology & hepatology* 2003, **15**(6):637-640.
294. Harris PR, Wright SW, Serrano C, Riera F, Duarte I, Torres J, Pena A, Rollan A, Viviani P, Guiraldes E *et al*: **Helicobacter pylori gastritis in children is associated with a regulatory T-cell response**. *Gastroenterology* 2008, **134**(2):491-499.
295. Jang TJ: **The number of Foxp3-positive regulatory T cells is increased in Helicobacter pylori gastritis and gastric cancer**. *Pathology, research and practice* 2010, **206**(1):34-38.
296. Sayi A, Kohler E, Hitzler I, Arnold I, Schwendener R, Rehrauer H, Muller A: **The CD4+ T cell-mediated IFN-gamma response to Helicobacter infection is essential for clearance and determines gastric cancer risk**. *J Immunol* 2009, **182**(11):7085-7101.
297. Shi Y, Liu XF, Zhuang Y, Zhang JY, Liu T, Yin Z, Wu C, Mao XH, Jia KR, Wang FJ *et al*: **Helicobacter pylori-induced Th17 responses modulate Th1 cell responses, benefit bacterial growth, and contribute to pathology in mice**. *J Immunol* 2010, **184**(9):5121-5129.
298. Algood HM, Allen SS, Washington MK, Peek RM, Jr., Miller GG, Cover TL: **Regulation of gastric B cell recruitment is dependent on IL-17 receptor A signaling in a model of chronic bacterial infection**. *J Immunol* 2009, **183**(9):5837-5846.
299. O'Connor W, Jr., Zenewicz LA, Flavell RA: **The dual nature of T(H)17 cells: shifting the focus to function**. *Nature immunology* 2010, **11**(6):471-476.
300. Quiding-Jarbrink M, Lundin BS, Lonroth H, Svennerholm AM: **CD4+ and CD8+ T cell responses in Helicobacter pylori-infected individuals**. *Clinical and experimental immunology* 2001, **123**(1):81-87.
301. Krakowka S, Ringler SS, Eaton KA, Green WB, Leunk R: **Manifestations of the local gastric immune response in gnotobiotic piglets infected with Helicobacter pylori**. *Veterinary immunology and immunopathology* 1996, **52**(3):159-173.
302. Wu L, Yan C, Czader M, Foreman O, Blum JS, Kapur R, Du H: **Inhibition of PPARgamma in myeloid-lineage cells induces systemic inflammation, immunosuppression, and tumorigenesis**. *Blood* 2012, **119**(1):115-126.

303. Abdullah Z, Geiger S, Nino-Castro A, Bottcher JP, Muraliv E, Gaidt M, Schildberg FA, Riethausen K, Flossdorf J, Krebs W *et al*: **Lack of PPARgamma in myeloid cells confers resistance to Listeria monocytogenes infection**. *PloS one* 2012, **7**(5):e37349.
304. Zhang MA, Rego D, Moshkova M, Kebir H, Chruscinski A, Nguyen H, Akkermann R, Stanczyk FZ, Prat A, Steinman L *et al*: **Peroxisome proliferator-activated receptor (PPAR)alpha and -gamma regulate IFNgamma and IL-17A production by human T cells in a sex-specific way**. *Proceedings of the National Academy of Sciences of the United States of America* 2012, **109**(24):9505-9510.
305. Bassaganya-Riera J, Viladomiu M, Pedragosa M, De Simone C, Hontecillas R: **Immunoregulatory mechanisms underlying prevention of colitis-associated colorectal cancer by probiotic bacteria**. *PloS one* 2012, **7**(4):e34676.
306. Klotz L, Knolle P: **Nuclear receptors: TH17 cell control from within**. *FEBS letters* 2011, **585**(23):3764-3769.
307. Nagai S, Mimuro H, Yamada T, Baba Y, Moro K, Nochi T, Kiyono H, Suzuki T, Sasakawa C, Koyasu S: **Role of Peyer's patches in the induction of Helicobacter pylori-induced gastritis**. *Proceedings of the National Academy of Sciences of the United States of America* 2007, **104**(21):8971-8976.
308. Tan S, Tompkins LS, Amieva MR: **Helicobacter pylori usurps cell polarity to turn the cell surface into a replicative niche**. *PLoS pathogens* 2009, **5**(5):e1000407.
309. Naumann M, Crabtree JE: **Helicobacter pylori-induced epithelial cell signalling in gastric carcinogenesis**. *Trends in microbiology* 2004, **12**(1):29-36.
310. Andres S, Schmidt HM, Mitchell H, Rhen M, Maeurer M, Engstrand L: **Helicobacter pylori defines local immune response through interaction with dendritic cells**. *FEMS immunology and medical microbiology* 2011, **61**(2):168-178.
311. Zhang M, Liu M, Luther J, Kao JY: **Helicobacter pylori directs tolerogenic programming of dendritic cells**. *Gut microbes* 2010, **1**(5):325-329.
312. Quiding-Jarbrink M, Raghavan S, Sundquist M: **Enhanced M1 macrophage polarization in human helicobacter pylori-associated atrophic gastritis and in vaccinated mice**. *PloS one* 2010, **5**(11):e15018.
313. Bimczok D, Grams JM, Stahl RD, Waites KB, Smythies LE, Smith PD: **Stromal regulation of human gastric dendritic cells restricts the Th1 response to Helicobacter pylori**. *Gastroenterology* 2011, **141**(3):929-938.
314. Wong BL, Zhu SL, Huang XR, Ma J, Xia HH, Bucala R, Wong BC, Lan HY: **Essential role for macrophage migration inhibitory factor in gastritis induced by Helicobacter pylori**. *The American journal of pathology* 2009, **174**(4):1319-1328.
315. Zhuang Y, Shi Y, Liu XF, Zhang JY, Liu T, Fan X, Luo J, Wu C, Yu S, Chen L *et al*: **Helicobacter pylori-infected macrophages induce Th17 cell differentiation**. *Immunobiology* 2011, **216**(1-2):200-207.
316. Algood HM, Cover TL: ***Helicobacter pylori* persistence: an overview of interactions between *H. pylori* and host immune defenses**. *Clinical microbiology reviews* 2006, **19**(4):597-613.
317. Blaser MJ, Atherton JC: ***Helicobacter pylori* persistence: biology and disease**. *The Journal of clinical investigation* 2004, **113**(3):321-333.

318. Peek RM, Jr., Fiske C, Wilson KT: **Role of innate immunity in *Helicobacter pylori*-induced gastric malignancy**. *Physiological reviews* 2010, **90**(3):831-858.
319. Chow WH, Blaser MJ, Blot WJ, Gammon MD, Vaughan TL, Risch HA, Perez-Perez GI, Schoenberg JB, Stanford JL, Rotterdam H *et al*: **An inverse relation between cagA+ strains of *Helicobacter pylori* infection and risk of esophageal and gastric cardia adenocarcinoma**. *Cancer research* 1998, **58**(4):588-590.
320. Blaser MJ, Chen Y, Reibman J: **Does *Helicobacter pylori* protect against asthma and allergy?** *Gut* 2008, **57**(5):561-567.
321. Chen Y, Blaser MJ: ***Helicobacter pylori* colonization is inversely associated with childhood asthma**. *The Journal of infectious diseases* 2008, **198**(4):553-560.
322. Algood HM, Gallo-Romero J, Wilson KT, Peek RM, Jr., Cover TL: **Host response to *Helicobacter pylori* infection before initiation of the adaptive immune response**. *FEMS immunology and medical microbiology* 2007, **51**(3):577-586.
323. Wilson KT, Crabtree JE: **Immunology of *Helicobacter pylori*: insights into the failure of the immune response and perspectives on vaccine studies**. *Gastroenterology* 2007, **133**(1):288-308.
324. Malfertheiner P, Bazzoli F, Delchier JC, Celinski K, Giguere M, Riviere M, Megraud F, Pylera Study G: **Helicobacter pylori eradication with a capsule containing bismuth subcitrate potassium, metronidazole, and tetracycline given with omeprazole versus clarithromycin-based triple therapy: a randomised, open-label, non-inferiority, phase 3 trial**. *Lancet* 2011, **377**(9769):905-913.
325. Haeberle HA, Kubin M, Bamford KB, Garofalo R, Graham DY, El-Zaatari F, Karttunen R, Crowe SE, Reyes VE, Ernst PB: **Differential stimulation of interleukin-12 (IL-12) and IL-10 by live and killed *Helicobacter pylori* in vitro and association of IL-12 production with gamma interferon-producing T cells in the human gastric mucosa**. *Infection & Immunity* 1997, **65**(10):4229-4235.
326. Bamford KB, Fan X, Crowe SE, Leary JF, Gourley WK, Luthra GK, Brooks EG, Graham DY, Reyes VE, Ernst PB: **Lymphocytes in the human gastric mucosa during *Helicobacter pylori* have a T helper cell 1 phenotype**. *Gastroenterology* 1998, **114**(3):482-492.
327. Lindholm C, Quiding-Jarbrink M, Lonroth H, Hamlet A, Svennerholm AM: **Local cytokine response in *Helicobacter pylori*-infected subjects**. *Infection & Immunity* 1998, **66**(12):5964-5971.
328. Sommer F, Faller G, Konturek P, Kirchner T, Hahn EG, Zeus J, Rollinghoff M, Lohoff M: **Antrum- and corpus mucosa-infiltrating CD4(+) lymphocytes in *Helicobacter pylori* gastritis display a Th1 phenotype**. *Infection & Immunity* 1998, **66**(11):5543-5546.
329. Luzza F, Parrello T, Sebkova L, Pensabene L, Imeneo M, Mancuso M, La Vecchia AM, Monteleone G, Strisciuglio P, Pallone F: **Expression of proinflammatory and Th1 but not Th2 cytokines is enhanced in gastric mucosa of *Helicobacter pylori* infected children.** *Digestive & Liver Disease* 2001, **33**(1):14-20.

330. Itoh T, Yoshida M, Chiba T, Kita T, Wakatsuki Y: **A coordinated cytotoxic effect of IFN-gamma and cross-reactive antibodies in the pathogenesis of *Helicobacter pylori* gastritis**. *Helicobacter* 2003, **8**(4):268-278.
331. Mizuno T, Ando T, Nobata K, Tsuzuki T, Maeda O, Watanabe O, Minami M, Ina K, Kusugami K, Peek RM *et al*: **Interleukin-17 levels in *Helicobacter pylori*-infected gastric mucosa and pathologic sequelae of colonization**. *World journal of gastroenterology : WJG* 2005, **11**(40):6305-6311.
332. Caruso R, Fina D, Paoluzi OA, Del Vecchio Blanco G, Stolfi C, Rizzo A, Caprioli F, Sarra M, Andrei F, Fantini MC *et al*: **IL-23-mediated regulation of IL-17 production in *Helicobacter pylori*-infected gastric mucosa**. *European journal of immunology* 2008, **38**(2):470-478.
333. Sugimoto M, Ohno T, Graham DY, Yamaoka Y: **Gastric mucosal interleukin-17 and -18 mRNA expression in *Helicobacter pylori*-induced Mongolian gerbils**. *Cancer science* 2009, **100**(11):2152-2159.
334. Horvath DJ, Jr., Washington MK, Cope VA, Algood HM: **IL-23 contributes to control of chronic *Helicobacter pylori* infection and the development of T helper responses in a mouse model**. *Frontiers in immunology* 2012, **3**:56.
335. Monteleone G, Pallone F, Macdonald TT: **Interleukin-21 (IL-21)-mediated pathways in T cell-mediated disease**. *Cytokine & growth factor reviews* 2009, **20**(2):185-191.
336. Caruso R, Fina D, Peluso I, Fantini MC, Tosti C, Del Vecchio Blanco G, Paoluzi OA, Caprioli F, Andrei F, Stolfi C *et al*: **IL-21 is highly produced in *Helicobacter pylori*-infected gastric mucosa and promotes gelatinases synthesis**. *J Immunol* 2007, **178**(9):5957-5965.
337. Huber M, Brustle A, Reinhard K, Guralnik A, Walter G, Mahiny A, von Low E, Lohoff M: **IRF4 is essential for IL-21-mediated induction, amplification, and stabilization of the Th17 phenotype**. *Proc Natl Acad Sci U S A* 2008, **105**(52):20846-20851.
338. Zhu J, Paul WE: **Peripheral CD4+ T-cell differentiation regulated by networks of cytokines and transcription factors**. *Immunological reviews* 2010, **238**(1):247-262.
339. Deenick EK, Tangye SG: **Autoimmunity: IL-21: a new player in Th17-cell differentiation**. *Immunology and cell biology* 2007, **85**(7):503-505.
340. Cope A, Le Friec G, Cardone J, Kemper C: **The Th1 life cycle: molecular control of IFN-gamma to IL-10 switching**. *Trends in immunology* 2011, **32**(6):278-286.
341. Anderson CF, Oukka M, Kuchroo VJ, Sacks D: **CD4(+)CD25(-)Foxp3(-) Th1 cells are the source of IL-10-mediated immune suppression in chronic cutaneous leishmaniasis**. *J Exp Med* 2007, **204**(2):285-297.
342. Jankovic D, Kullberg MC, Feng CG, Goldszmid RS, Collazo CM, Wilson M, Wynn TA, Kamanaka M, Flavell RA, Sher A: **Conventional T-bet(+)Foxp3(-) Th1 cells are the major source of host-protective regulatory IL-10 during intracellular protozoan infection**. *J Exp Med* 2007, **204**(2):273-283.
343. Akhiani AA, Pappo J, Kabok Z, Schon K, Gao W, Franzen LE, Lycke N: **Protection against *Helicobacter pylori* infection following immunization is IL-12-dependent and mediated by Th1 cells**. *Journal of Immunology* 2002, **169**(12):6977-6984.

344. Eaton KA, Mefford M, Thevenot T: **The role of T cell subsets and cytokines in the pathogenesis of *Helicobacter pylori* gastritis in mice**. *Journal of Immunology* 2001, **166**(12):7456-7461.
345. Eaton KA, Benson LH, Haeger J, Gray BM: **Role of transcription factor T-bet expression by CD4+ cells in gastritis due to *Helicobacter pylori* in mice**. *Infection and immunity* 2006, **74**(8):4673-4684.
346. Monteleone G, Monteleone I, Fina D, Vavassori P, Del Vecchio Blanco G, Caruso R, Tersigni R, Alessandroni L, Biancone L, Naccari GC *et al*: **Interleukin-21 enhances T-helper cell type I signaling and interferon-gamma production in Crohn's disease**. *Gastroenterology* 2005, **128**(3):687-694.
347. Fina D, Sarra M, Fantini MC, Rizzo A, Caruso R, Caprioli F, Stolfi C, Cardolini I, Dottori M, Boirivant M *et al*: **Regulation of gut inflammation and th17 cell response by interleukin-21**. *Gastroenterology* 2008, **134**(4):1038-1048.
348. Herber D, Brown TP, Liang S, Young DA, Collins M, Dunussi-Joannopoulos K: **IL-21 has a pathogenic role in a lupus-prone mouse model and its blockade with IL-21R.Fc reduces disease progression**. *J Immunol* 2007, **178**(6):3822-3830.
349. Young DA, Hegen M, Ma HL, Whitters MJ, Albert LM, Lowe L, Senices M, Wu PW, Sibley B, Leathurby Y *et al*: **Blockade of the interleukin-21/interleukin-21 receptor pathway ameliorates disease in animal models of rheumatoid arthritis**. *Arthritis Rheum* 2007, **56**(4):1152-1163.
350. Terrier B, Costedoat-Chalumeau N, Garrido M, Geri G, Rosenzwajg M, Musset L, Klatzmann D, Saadoun D, Cacoub P: **Interleukin 21 correlates with T cell and B cell subset alterations in systemic lupus erythematosus**. *The Journal of rheumatology* 2012, **39**(9):1819-1828.
351. Horvath DJ, Jr., Radin JN, Cho SH, Washington MK, Algood HM: **The interleukin-17 receptor B subunit is essential for the Th2 response to *Helicobacter pylori*, but not for control of bacterial burden**. *PloS one* 2013, **8**(3):e60363.
352. Elias JM, Greene C: **Modified Steiner method for the demonstration of spirochetes in tissue**. *American journal of clinical pathology* 1979, **71**(1):109-111.
353. Boivin GP, Washington K, Yang K, Ward JM, Pretlow TP, Russell R, Besselsen DG, Godfrey VL, Doetschman T, Dove WF *et al*: **Pathology of mouse models of intestinal cancer: consensus report and recommendations**. *Gastroenterology* 2003, **124**(3):762-777.
354. Franco AT, Israel DA, Washington MK, Krishna U, Fox JG, Rogers AB, Neish AS, Collier-Hyams L, Perez-Perez GI, Hatakeyama M *et al*: **Activation of beta-catenin by carcinogenic *Helicobacter pylori***. *Proceedings of the National Academy of Sciences of the United States of America* 2005, **102**(30):10646-10651.
355. Romero-Gallo J, Harris EJ, Krishna U, Washington MK, Perez-Perez GI, Peek RM, Jr.: **Effect of *Helicobacter pylori* eradication on gastric carcinogenesis**. *Laboratory investigation; a journal of technical methods and pathology* 2008, **88**(3):328-336.
356. Abraham C, Cho J: **Interleukin-23/Th17 pathways and inflammatory bowel disease**. *Inflammatory bowel diseases* 2009, **15**(7):1090-1100.
357. Wu CC, Sytwu HK, Lu KC, Lin YF: **Role of T cells in type 2 diabetic nephropathy**. *Experimental diabetes research* 2011, **2011**:514738.

358. van Hamburg JP, Asmawidjaja PS, Davelaar N, Mus AM, Colin EM, Hazes JM, Dolhain RJ, Lubberts E: **Th17 cells, but not Th1 cells, from patients with early rheumatoid arthritis are potent inducers of matrix metalloproteinases and proinflammatory cytokines upon synovial fibroblast interaction, including autocrine interleukin-17A production**. *Arthritis and rheumatism* 2011, **63**(1):73-83.
359. Philipson CW, Bassaganya-Riera J, Hontecillas R: **Animal models of enteroaggregative Escherichia coli infection**. *Gut microbes* 2013, **4**(4):281-291.
360. Quackenbush J: **Microarray data normalization and transformation**. *Nature genetics* 2002, **32 Suppl**:496-501.
361. Harris TJ, Grosso JF, Yen HR, Xin H, Kortylewski M, Albesiano E, Hipkiss EL, Getnet D, Goldberg MV, Maris CH *et al*: **Cutting edge: An in vivo requirement for STAT3 signaling in TH17 development and TH17-dependent autoimmunity**. *Journal of immunology* 2007, **179**(7):4313-4317.
362. Wu C, Yosef N, Thalhamer T, Zhu C, Xiao S, Kishi Y, Regev A, Kuchroo VK: **Induction of pathogenic TH17 cells by inducible salt-sensing kinase SGK1**. *Nature* 2013, **496**(7446):513-517.
363. Wang M, Liang P: **Interleukin-24 and its receptors**. *Immunology* 2005, **114**(2):166-170.
364. Schroder K, Tschopp J: **The inflammasomes**. *Cell* 2010, **140**(6):821-832.
365. Westwell-Roper C, Nackiewicz D, Dan M, Ehses JA: **Toll-like receptors and NLRP3 as central regulators of pancreatic islet inflammation in type 2 diabetes**. *Immunology and cell biology* 2014, **92**(4):314-323.
366. Jankovic D, Ganesan J, Bscheider M, Stickel N, Weber FC, Guarda G, Follo M, Pfeifer D, Tardivel A, Ludigs K *et al*: **The Nlrp3 inflammasome regulates acute graft-versus-host disease**. *The Journal of experimental medicine* 2013, **210**(10):1899-1910.
367. Besnard AG, Togbe D, Couillin I, Tan Z, Zheng SG, Erard F, Le Bert M, Quesniaux V, Ryffel B: **Inflammasome-IL-1-Th17 response in allergic lung inflammation**. *Journal of molecular cell biology* 2012, **4**(1):3-10.
368. Duhen R, Glatigny S, Arbelaez CA, Blair TC, Oukka M, Bettelli E: **Cutting edge: the pathogenicity of IFN-gamma-producing Th17 cells is independent of T-bet**. *Journal of immunology* 2013, **190**(9):4478-4482.
369. DeFuria J, Belkina AC, Jagannathan-Bogdan M, Snyder-Cappione J, Carr JD, Nersesova YR, Markham D, Strissel KJ, Watkins AA, Zhu M *et al*: **B cells promote inflammation in obesity and type 2 diabetes through regulation of T-cell function and an inflammatory cytokine profile**. *Proceedings of the National Academy of Sciences of the United States of America* 2013, **110**(13):5133-5138.
370. Liu SS, Ding Y, Lou JQ: **NLRP3, a Potential Therapeutic Target for Type 2 Diabetes?** *Cardiovascular drugs and therapy / sponsored by the International Society of Cardiovascular Pharmacotherapy* 2014.